NATIONAL TECHNICAL UNIVERSITY OF ATHENS
SCHOOL OF NAVAL ARCHITECTURE AND MARINE ENGINEERING
DIVISION OF MARINE ENGINEERING

DIPLOMA THESIS

CHARVALOS GEORGIOS

Investigation of tribological properties of mechanical systems of conventional merchant vessels

Thesis committee:

Supervisor:	**C. Papadopoulos, Associate Professor NTUA**
Members:	**L. Kaiktsis Professor NTUA**
	G. Papalambrou, Assistant Professor NTUA

Athens, July 2020

Acknowledgments

The completion of the present thesis marks the end of my studies in the School of Naval Architecture and Marine Engineering of the National Technical University of Athens. For this memorable period of learning, I would like to express my gratitude to my colleagues, friends and professors with whom I shared this experience.

First of all, I would like to express my gratitude and respect to my thesis supervisor, Associate Professor Christos Papadopoulos, for the trust, the motivation, his continuous assistance on the subject and his valuable advice during my studies.

I am also thankful to Associate Professor Nikolaos Ventikos, who provided important resources necessary for the completion of this study. Also, I would like to thank Mr. Michalis Foteinos for the helpful information he offered for the used literature.

Special thanks to my friend Mr. Eleftherios Koukoulopoulos for his recommendations, ideas and support that contributed to finishing this thesis.

For her contribution, remarks and ideas on this study, I would also like to thank my colleague Ms. Maria Iosifidi and wish her a bright career.

I would also like to thank my friends who stand by my side all these years.

Finally, from the bottom of my heart I want to express my love and deepest gratitude to my parents, for their care, their belief in me and their teachings that made me develop to the individual I am today. To them, I owe everything.

Abstract

The majority of the trading activities worldwide is seaborne, a trend that constantly increases over the last four decades. Currently, 50000 vessels operate globally, being capable of servicing 90% of the transportations of the global trading market and accounting for 1% of the total energy consumption between all economic sectors. A modern merchant vessel has to comply with three very important, often colliding, requirements; reliability, successful time of delivery and minimal operational expenses. A main parameter determining whether a merchant vessel is competitive is the operation of her propulsion system. The majority of cargo vessels are equipped with a two-stroke, slow-speed Diesel engine to cover the propulsion requirements. Marine Diesel engines combine high efficiency and power output in respect to weight of installation, fuel consumption and maintenance costs.

The marine Diesel engine is subjected to various regulations regarding limitation of emissions during operation. Due to these ongoing regulations, research focuses on the design of more efficient vessels, with low fuel oil consumption. Reduced fuel oil consumption leads to reduced gaseous emissions and less operational expenses. An approach to this, is the effort of reducing the frictional losses of the vessel. Currently a marine two-stroke Diesel engine bears frictional energy losses of the magnitude of 3-6% of the total brake power.

Scope of the present work is to **study the behavior of friction losses of the propulsion train of bulk carriers,** including main engine losses and loses of the intermediate and stern tube bearings. In order to perform the necessary calculations, in house software has been developed. The key feature of the software is the ability to create a virtual vessel through the basic steps of preliminary ship design, which exhibits similarities to the existing fleet. This is achieved by exploiting the SeaWeb database which provides principal data of the bulk carrier fleet. With empirical relations and methods proposed in the abundant literature, the software is capable of calculating geometrical parameters, the total resistance of a vessel and select a proper engine from a valid industry catalogue as propulsion installation. Then, engine friction is calculated by empirical relations based on the data of the obtained engine. Friction at the shafting system is dealt separately; the software calculates the shafting weight and by proper method found in literature provides the relevant estimation of tribological losses. Following the explanation of workflow, a single-vessel example is performed, as a demonstration of the workflow.

Afterwards, a parametric study is done, in order to investigate the dependence of frictional losses on vessel size. In particular, 100 vessels have been selected, 20 from each bulk carrier class; the dependence of losses on vessel size, resistance, draft and speed has been computed and analyzed. Based on the results, a regression model has been extrapolated, relating friction power loss to geometrical, propulsion and operational parameters of the vessel. Engine friction losses were found to lie between **4 and 6%** of the total brake power, while shafting friction losses varied in the range of **0.1-0.25%,** proving that the literature estimate of 0.5-1% to be an overestimate.

The final act on this work was the execution of nine simulations on the whole bulk-carrier fleet. The vessels from SeaWeb database were used, with each one having assigned a specific engine operational point. Power and revolutions at each point were defined by resistance and draft values. At each simulation, a different fraction of the fleet was considered to apply 10% or 20% speed reduction, due to slow steaming. Through each simulation, the annual energy losses and amount of fuel consumed due to friction were estimated. The study showed that, on average, only from operation of the main engine, **62602 TJ** of energy are lost due to frictional forces, which lead to an annual fuel consumption due to friction of **3012 thousand tones**. Finally, the regression friction model was performed on the database vessels and the results were compared to the simulation results of the calculation procedure.

Σύνοψη

Η πλειοψηφία των εμπορικών δραστηριοτήτων παγκοσμίως επιτυγχάνεται μέσω των θαλάσσιων μεταφορών, μια τάση η οποία παρουσιάζει αυξητική τάση τις τελευταίες τέσσερις δεκαετίες. Σήμερα, υπάρχουν 50000 περίπου πλοία, τα οποία με τους διεθνείς πλόες τους, εξυπηρετούν σχεδόν το 90% των μεταφορών της παγκόσμιας αγοράς του εμπορίου και αντιστοιχούν στο 1% της κατανάλωσης ενέργειας σε σχέση με τους υπόλοιπους τομείς της οικονομίας. Ένα σύγχρονο εμπορικό πλοίο καλείται να συμμορφωθεί με τρεις σημαντικές, συχνά αντικρουόμενες, προδιαγραφές: την αξιοπιστία, τον επιτυχή χρόνο παράδοσης και την ελαχιστοποίηση των λειτουργικών εξόδων. Η κύρια παράμετρος που καθορίζει την ανταγωνιστικότητα ενός εμπορικού πλοίου, είναι η λειτουργία της εγκατάστασης πρόωσης. Η πλειοψηφία των εμπορικών πλοίων φέρει δίχρονη, αργόστροφη μηχανή Diesel. Η ναυτική αυτή μηχανή Diesel συνδυάζει υψηλή απόδοση και ισχύ με χαμηλό βάρος εγκατάστασης, μειωμένη ειδική κατανάλωση καυσίμου και κόστος συντήρησης.

Η ναυτική μηχανή Diesel είναι αποδέκτης ποικίλων κανονισμών επιβολής ορίων ρυπογόνων ουσιών. Καθώς οι κανονισμοί εξελίσσονται, οι έρευνες εστιάζουν στο σχεδιασμό ενεργειακά αποδοτικότερων πλοίων με χαμηλή ειδική κατανάλωση καυσίμου. Μείωση στη κατανάλωση καυσίμου οδηγεί στη μείωση αέριων εκπομπών και στην ελαχιστοποίηση των λειτουργικών εξόδων του πλοίου. Μια προσέγγιση στο σχεδιασμό αποδοτικότερων πλοίων είναι η μελέτη των απωλειών τριβής. Για μια ναυτική δίχρονη μηχανή, οι απώλειες λόγω τριβών αποτελούν το 3-6% της ισχύς πέδης.

Στόχος της παρούσας εργασίας είναι η μελέτη της συμπεριφοράς των απωλειών τριβής των φορτηγών πλοίων χύδην λόγω λειτουργίας της κύριας μηχανής. Για την επίτευξη των απαραίτητων υπολογισμών, σχεδιάστηκε κατάλληλο λογισμικό. Κύριο χαρακτηριστικό του λογισμικού είναι η δυνατότητα δημιουργίας ψηφιακού πλοίου, με γνώμονα τη διαδικασία σχεδιασμού προμελέτης, το οποίο παρουσιάζει ομοιότητες με πλοίο του πραγματικού στόλου. Αυτό επιτυγχάνεται με χρήση της βάσης SeaWeb, η οποία περιέχει πληροφορίες για τις διαστάσεις και τα μεγέθη του στόλου των φορτηγών πλοίων χύδην. Με χρήση εμπειρικών σχέσεων και μεθόδων που βρέθηκαν στη βιβλιογραφία, το λογισμικό υπολογίζει τις γεωμετρικές παραμέτρους του πλοίου, την ολική του αντίσταση για την οποία επιλέγει κατάλληλη δίχρονη μηχανή πρόωσης από έγκυρο βιομηχανικό κατάλογο. Έπειτα, οι απώλειες τριβής της μηχανής υπολογίζονται από τις εμπειρικές σχέσεις για τη δεδομένη μηχανή. Οι απώλειες τριβής του αξονικού συστήματος μελετώνται ξεχωριστά, καθώς το πρόγραμμα εκτιμά το βάρος του αξονικού και βαίνει στον υπολογισμό των απωλειών με κατάλληλη μέθοδο που προσφέρει η βιβλιογραφία. Αφού γίνει επεξήγηση της υπολογιστικής διαδικασίας, πραγματοποιείται παράδειγμα υπολογισμών ενός πλοίου.

Στη συνέχεια, πραγματοποιείται μια παραμετρική μελέτη, με στόχο τη διερεύνηση της σχέσης των απωλειών τριβής με το μέγεθος του πλοίου. Προσομοιώνοντας 100 πλοία, 20 από κάθε τάξη φορτηγών πλοίων, η συμπεριφορά των απωλειών έναντι του μεγέθους πλοίου, της αντίστασης, του βυθίσματος και της ταχύτητας μελετάται. Από τα αποτελέσματα της προσομοίωσης παράγεται παλινδρομικό μοντέλου υπολογισμού της ισχύος απωλειών λόγω τριβής την οποία συνδέει με γεωμετρικές παραμέτρους και παραμέτρους πρόωσης του πλοίου. Οι τριβολογικές απώλειες της μηχανής βρέθηκαν να κυμαίνονται από 4-6% της συνολικής ισχύς πέδης, ενώ οι απώλειες στο αξονικό εντοπίστηκαν στο διάστημα 0.1-0.25%, υποστηρίζοντας πως η εκτίμηση 0,5-1% που συναντάται συνήθως στη βιβλιογραφία τις υπερεκτιμά.

Το τελικό στάδιο της εργασίας είναι η πραγματοποίηση 9 προσομοιώσεων σε όλο το στόλο. Χρησιμοποιήθηκαν τα πλοία της βάσης SeaWeb και στο κάθε ένα προσδόθηκε ένα συγκεκριμένο σημείο λειτουργίας. Η ισχύς και οι στροφές του σημείου καθορίστηκαν από τη δεδομένη αντίσταση και βύθισμα του πλοίου. Σε κάθε προσομοίωση διαφορετικό ποσοστό του στόλου θεωρείται πως εφαρμόζει 10 ή 20% μείωση στην ταχύτητα υπηρεσίας. Για κάθε προσομοίωση, υπολογίστηκαν οι απώλειες τριβής και η αντίστοιχη ποσότητα καυσίμου που καταναλώθηκε σε διάρκεια ενός έτους. Η μελέτη έδειξε πως 62853 TJ καταναλώνονται σε ένα έτος κατά μέσο όρο, λόγω λειτουργίας της κύριας μηχανής, τα οποία αντιστοιχούν σε 3012 χιλιάδες τόνους καυσίμου. Τέλος, το παλινδρομικό μοντέλο εφαρμόζεται στα πλοία των προσομοιώσεων και τα αποτελέσματά του συγκρίνονται με αυτά που προέκυψαν από τη διαδικασία.

Table of contents

1 Literature review

1.1 Introduction

The scope of the present study is to investigate frictional losses in the propulsion system of bulk carriers and provide a fleet scale estimation of energy losses during an annual period. Effects of ship size, operational service point, age and loading condition of the vessel are taken into account. For achieving this purpose, specific software was developed. Starting with the prediction of bulk carrier resistance at the preliminary design stage with the use of empirical and analytical relations found in current literature, a relevant two stroke Diesel engine from a valid industry catalogue, is assumed as the main propulsion unit. Afterwards, estimation of frictional losses at the different parts of the propulsion system (engine, intermediate and tail shaft bearings) occurs. Following the friction estimation, energy losses in one-year period are depicted and conclusions on the behavior of losses are drawn.

1.2 Review

1.2.1 The automobile energy consumption

Holmberg [1] presents calculations of the global energy consumption used to overcome friction in passenger cars, taking into account effects of engine, transmission, tires and brakes. The study was performed on an "average car "of a certain age, brake power installation, engine volumetric capacity and cylinder number, specific total weight, fuel type and average fuel consumption. This average vehicle was supposed to operate on a mean 60 km/h speed on a straight-line direction in the absence of road roughness. The fuel efficiency, emissions and mileage of the vehicle were specified for the installed engine; every measure was verified by industry figures and statistical data. The study indicated that approximately **33%** of the combustion energy is lost in the form of exhaust gases, 29% of the power is lost in the cooling system and the rest 38% is the produced mechanical energy. On average, 5% of the mechanical energy is lost due to air drag, 15% is consumed to overcome brake contact, 70% to overcome tire-road contact and the friction in the engine system and finally 15% to overcome friction in the transmission system. Overall, **21,5%** of the total fuel energy is the beneficial mechanical energy used to move the car.

The same author, expanded this study for heavy duty vehicles (trucks and buses) [2]. Following a similar strategy, **34%** of the total fuel energy was estimated to be the energy used to move the vehicle. Later on, the author, in an effort to describe the impact of tribological research in global economy [3], states that road vehicles account for more than **75%** of the global energy consumption by the energy economic sector.

1.2.2 The global energy consumption by economic sectors

According to Holmberg[3], from the total annual energy production, **34%** is consumed in the **residential** economic sector, **29%** in the **global industry** and **28%** is used in the **transportation** sector. As an illustration, for the year 2016, from the 575 EJ produced from all global energy sources, 161 EJ were consumed only in the transportation economic sector. Transportation accounts for **30%** of total energy use in order to overcome friction, followed by industry and energy industry (each accounting for 20%) and the residential economic sector which consumes 10% of total energy.

In the transportation sector, **road vehicles** (buses, trucks, vans and passenger cars) account for **21%** of the energy consumed, **railway transportation** for **1%** while **air** and **marine transportation for 3%** each. It is obvious that the marine sector accounts for the minority of the total energy consumption.

1.2.3 Environmental legislation

In order to reduce pollution of sea water and atmospheric environment, IMO has adopted a strategy of reducing Greenhouse gas emissions from ships. MARPOL ANNEX VI regulation is the first genuine effort of the global shipping industry in setting the limits for pollution of air from activity in the marine environment. After a ten-year effort to reduce Sulphur emissions, as of 1st January 2020, all vessels sailing under a state flag member of IMO, must comply with this regulation, which imposes a limit on the Sulphur emission from fuel combustion. Specifically, when sailing to a coastal area, the amount of Sulphur in the fuel burnt must be no more than 0.1%, while for open sea 0.5%.

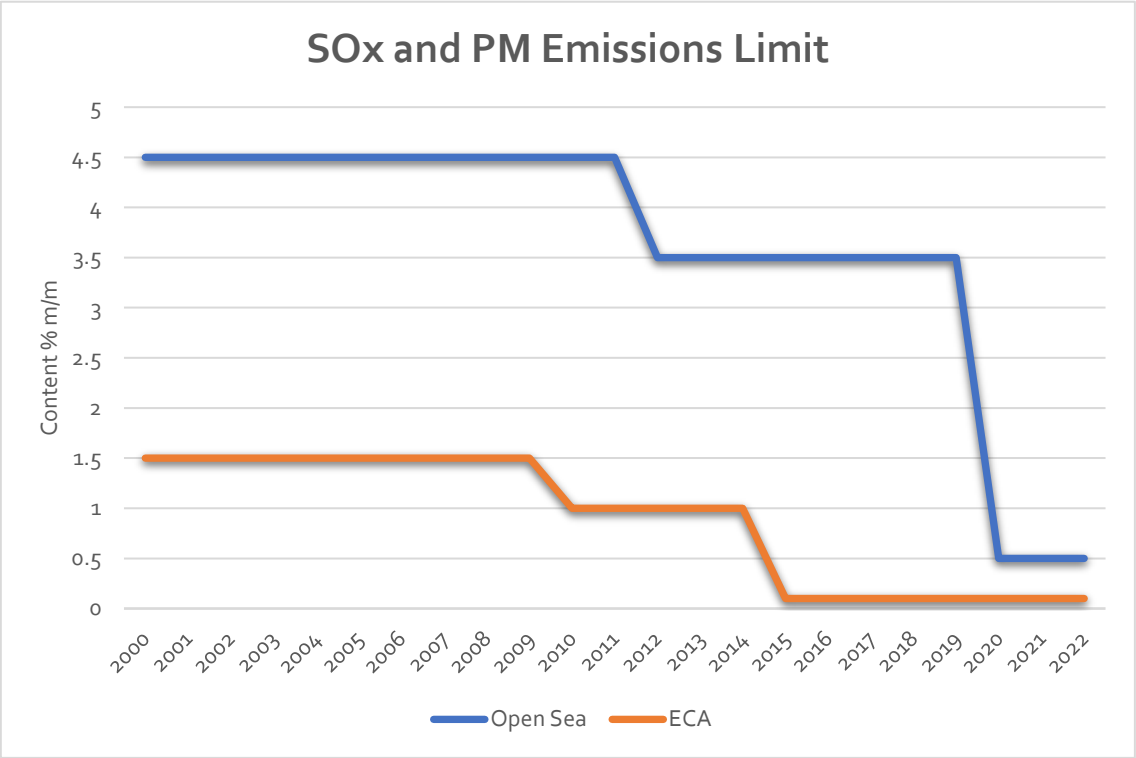

Figure 1.1 Fuel Sulphur content limit

Moreover, starting from January 1st 2000, IMO focused environmental legislation also on NOx emissions, with three tier levels regarding marine Diesel engine nitrogen emissions so far. **Tier I** regulation considered Diesel engines for vessels constructed earlier than 2000. The certified engines under TIER I were valid until 2011. Currently, ships with a marine Diesel engine with power output more than 130 kw are subject to either Tier II regulation (vessels constructed after 2011 and outside ECA areas) or tier III level (vessels constructed after 1st January 2000 and operating inside an ECA area with NOx limitation).

Table 1.1- IMO NO_x limits

Tier	Ship construction date on or after	Total weighted cycle emission limit ($\frac{gr}{kWh}$) for n rpm		
		$n \leq 130$	$130 <= n <= 2000$	$n \geq 2000$
I	1 January 2000	17.0	$45n^{-0.2}$	9.8
II	1 January 2011	14.4	$44n^{-0.23}$	7.7
III	1 January 2016	3.4	$9n^{-0.2}$	2.0

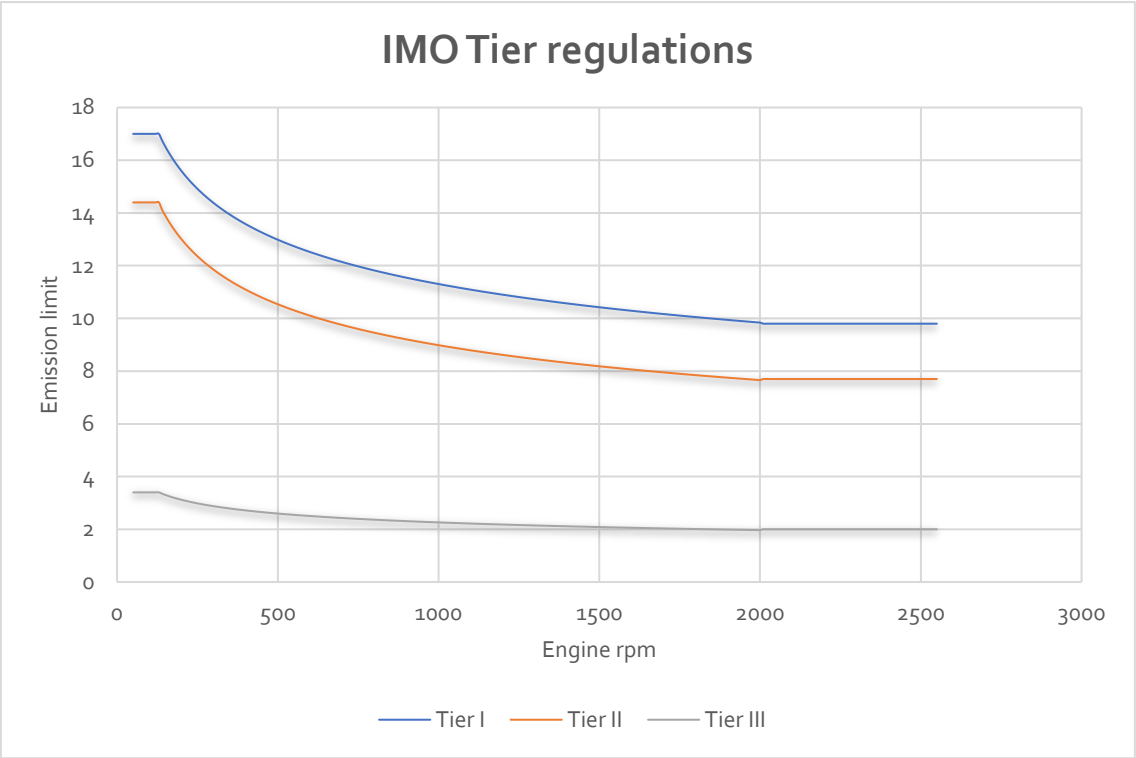

Figure 1.2 IMO N_{ox} emission limit curves

For example, the limitation for a ship built in 2021, according to the tier III level curve, with a specific engine power output at 100 revolutions per minute is $\mathbf{3.4}\ \frac{gr}{kWh}$.

Exhaust gas emissions always have been destructive agents of the natural environment and looming threat for all species inhibiting this planet. The effect of the marine industry is one of the smallest factors contributing to this universal degradation; however, the benefits from controlling its pollutants are quite significant in terms of environmental protection and in becoming a pioneer "green" industry sector.

As of 2050, IMO aims at least at the reduction of carbon emissions by 50%, with the ultimate aim being the elimination of carbon footprint. So, industrial and academic research have already begun their focus on the design of totally environmentally friendly ships.

Bulk carrier vessels, represent the majority of vessels of the global merchant fleet, since they carry an important fraction of the global gross tonnage. Therefore, in order to cover the largest front of the global fleet, the calculation procedure and results of this study, focus on bulk carriers.

1.2.4 Energy Efficiency Index

The first action against reducing CO2 emissions was the implementation from IMO of the Energy Efficiency Index. This index is a measure of how environmentally friendly a vessel has been designed to be. It expresses the total emissions in grams of CO2 per capacity-mile of the ship; in other words, it provides the minimum energy efficiency requirement per capacity-mile. The EEDI is unique for each vessel and the calculation formula is based on the technical design and aspects of the particular vessel. The lower the EEDI, the more efficient the vessel is.

Currently, and up to 2024, the minimum required EEDI is increased each year by 20%. Afterwards, the increment becomes stricter, since the increase rate will be set to 30% for every year. The purpose of this requirement, is for the shipping industry to provide cost-effective solutions from technical and

operational view of the vessel, by incorporating energy efficient systems and innovative, optimal-design concepts.

The general definition is: $EEDI = \frac{CO_2 Consumption}{DWT.V}$.

Triggered by the international legislation for emissions and pollution and inspired by the work of Holmberg [1,2,3], the study focuses on estimating energy loss in the bulk carrier fleet, due to friction in the propulsion system.

1.2.5 Friction literature

Friction is defined as the power loss in the form of heat between two surfaces **in relative motion**. Contact between moving objects or bodies, generate a force (and/or a moment for the case of rotation), opposed to the direction of movement. The power loss resulting from the work of friction force, leads to an amount of energy wasted, which can be neither ignored, nor eliminated.

Although in every mechanical system friction loss is a small proportion of the total energy losses, it binds an important fraction of output power. Reduction in mechanical losses, lead to reduced fuel oil consumption and stalls the effects of wear. Thus, economic benefits arise from the postponement of parts replacement and maintenance costs from wear and material failure, while by cutting down fuel oil consumption, gaseous emissions are reduced [3].

Friction force is expressed through the friction coefficient μ_f, as introduced by Coulomb, $\mu_f = \frac{Friction\ Force}{Vertical\ load}$. All friction models that have been developed throughout the past decades are based on this relation; however, it is well known that the friction coefficient depends on surface topography, material of the bodies, the nature of the relative motion and of course the operating load which render friction dependent on multiple, different parameters.

Although there are applications where friction generation is beneficial, at most cases the friction force has a destructive nature which leads to wear of the material and eventually loss of operating equipment. One commonly applied way of controlling friction coefficient is to lubricate the contact surfaces with a proper fluid, reducing the coefficient by several orders of magnitude. This is the case for an engine of a vessel, where lubrication is the main friction control method used.

When surfaces are separated in this way, lubrication is characterized as hydrodynamic, boundary or mixed. These three states of friction are well described by the Stribeck curve and are defined by the oil film thickness.

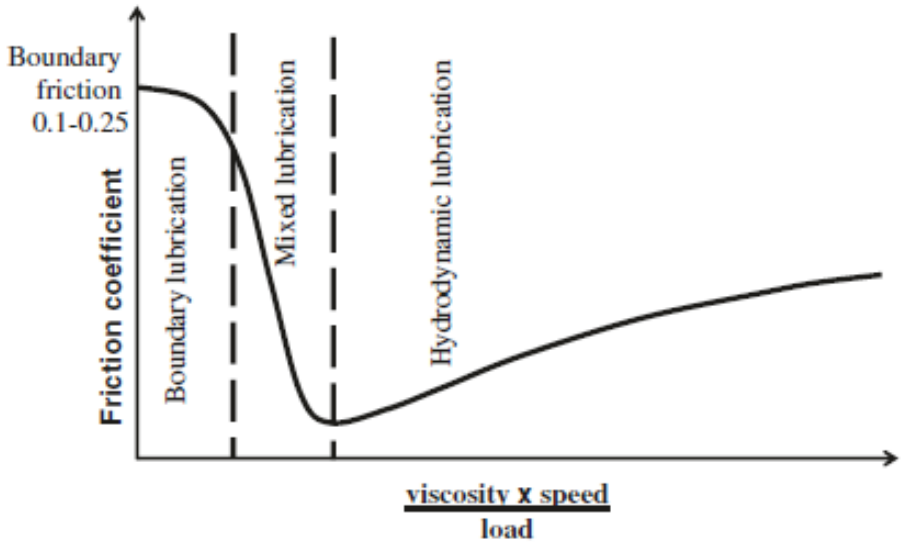

Figure 1.3 Stribeck curve

When the film is too thin, boundary lubrication prevails and the moving surfaces cannot be properly separated. Asperities on sliding surfaces collide with each other, producing heat and leading to high friction coefficient values. Boundary lubrication can happen due to the combination of low speed and high load.

In the mixed lubrication regime, both boundary and hydrodynamic lubrication occur. The film thickness is increased but still asperity contact exists. The type of the friction mechanism in this is defined by the load, speed, viscosity, temperature and surface roughness.

When the speed is increased and even if the load decreases, separation of contact surfaces by the fluid begins. The fluid film gradually thickens until its maximum possible value, when the friction coefficient reaches its minimum value. Then, hydrodynamic lubrication prevails, allowing the sliding surfaces to be totally separated and the load is supported exclusively by the lubricant film. Increase in friction in the hydrodynamic region is due to the increased drag, produced by the fluid and the high operational speed levels.

In steady state condition, the dominating type of friction coefficient in the shafting system of the vessel is hydrodynamic lubrication, where the shaft and the bearing inner surface are separated by proper fluid film thickness, which depends on the bearing clearance and the eccentricity of the two surfaces. In the Diesel engine, hydrodynamic lubrication prevails during the movement of the piston, however, near the TDC, lubrication is actually boundary due to the starvation of the contact areas.

Throughout a ship, friction is encountered at different locations under different mechanisms. Two major categories can be defined. The first refers to the vessel hull which is the frictional part of the total resistance of the vessel, while the second refers to the mechanical systems (mainly met in the engine room):

- Friction in main engine components
- Friction in main shafting system.
- Friction in auxiliary engines (i.e., Diesel generators)
- Friction in auxiliary engine room machinery (bushes, bearings…)

- Friction at pipelines, due to circulation of fluids

From all the above cases, objects of the present study are friction in the main engine and friction in the shafting system of the vessel. The goal is to provide an estimation on power loss due to friction, or otherwise, what fraction of the released fuel energy is lost due to friction. Friction at auxiliary engines and other auxiliary machinery are not included in the present study, since the majority of fuel oil quantity is consumed at the propulsion system. By default, the last category, regarding friction due to fluid motion, is excluded since it is both negligent and irrelevant to the subject.

Frictional resistance is dealt in an indirect manner. It is a major component of the total resistance of a vessel [34], which is overcome by adequate installed engine power. Resistance is a function of draft, wetted surface, vessel geometry and service speed. Thus, a change in resistance leads to different power demand at the propeller, affecting fuel oil consumption of engine. However, it is not considered as a loss in the propulsion system.

Friction loss is mainly occurring at the piston ring package and the guide shoe bearing, which account for more than **65%** of the engine mechanical losses. Anders [4], by both theoretical and numerical investigation concluded that guide shoe friction loss is almost **1.1 %** of the total generated engine power, while piston ring friction is up to **0.9%** of the total brake power. Both these components contribute as much as **5%** of 80% of total mechanical losses or **5%** of the total generated power.

Ciulli [5] performs a review on theoretical and experimental methods of calculating friction of internal combustion engines. The author distinguishes two different approaches of the friction losses; average and instantaneous friction losses evaluation. The first group consists of formulae that provide friction estimation in a complete engine cycle, while the second calculates losses as the sum of friction of engine components as a function of crankshaft angle.

Formulae studied by Ciulli are ideal for preliminary engine study and simulation procedures. Parameters on which mean pressure of friction loss depends on are shown. Mainly crankshaft rotation speed, stroke, bore, cylinders number and mean effective pressure are the common parameters that affect the magnitude of frictional losses. This is concluded by numerous studies and references. Ullman's empirical formula [6] states that f_{mep} depends strongly on the mean piston speed, rather than on load (m_{ip}/m_{ep}) or revolutions of crankshaft. For this reason, a two-stroke engine is subject to fewer losses than that of a four-stroke engine. The same is proposed at by Livanos and Kyrtatos [7] where they propose a model of calculating friction losses at the piston ring package of a four-stroke medium marine Diesel engine. The increase of f_{mep} was found to be much more intense with increasing speed rather than increasing load (at constant speed level).

A drawback on empirical friction models is illustrated by Rakopoulos and Giakoumis [8]. According to the authors, average f_{mep}, although it can provide accurate estimates for steady state conditions on an engine cycle, usually underestimates friction torque around the TDC. Moreover, empirical formulae often need a lot of input data, which are not always available of known afore and sometimes the calibration of certain parameters is difficult. The majority of empirical formulae on friction losses are mainly focused on four-stroke engines, since such studies are found in abundance in literature. Studies with a two-stroke marine engine are much fewer, which limit the capabilities of estimating an average pressure friction loss.

The largest proportion of mechanical losses is met at the piston ring assembly, with losses of the magnitude **25-45%.** In the case of the four-stroke engine, losses apart from piston ring are found at crankshaft, main bearings, valvetrain and at the rest auxiliaries. Studies have mainly focused on the piston assembly system, since an improvement there can have a significant reduction of mechanical

losses. Takata [9] studies the effect of surface geometry, (shape, grooves) and viscosity of lubricating oil on piston ring friction, predicting a potential reduction of 50%, encouraging the adding of texturing. This was also confirmed by Koukoulopoulos [10], who measured 23% and 25% reduction in friction coefficient when applying to the piston ring surface hydrophobicity and texturing respectively. Delprete [11], after a long piston assembly studies review, summarizes all the technical aspects that are taken into account prior to performing a piston ring study.

A marine two-stroke engine is the most advanced form of the Diesel engine. These engines are designed as the prime movers of a ship (which combines the need for increased power and reliability of operation), because they are able to generate the demanded power output in respect to the weight of installation and the low fuel oil consumption. The efficiency of such an engine is controlled by the following parameters, as illustrated by Clausen [12]:

- Increased maximum pressure to mean effective pressure ratio.
- Increased stroke to bore ratio.
- Use of electronically controlled engine (improved control of NO_x emissions, since more parameters can be adjusted during engine operation).

According to Clausen, friction is met at the following components:

- Guide shoe **31**%
- Piston **26**%
- Main bearing **23**%
- Connecting rod **10** %
- Stuffing box **5** %
- Thrust bearing **5** %

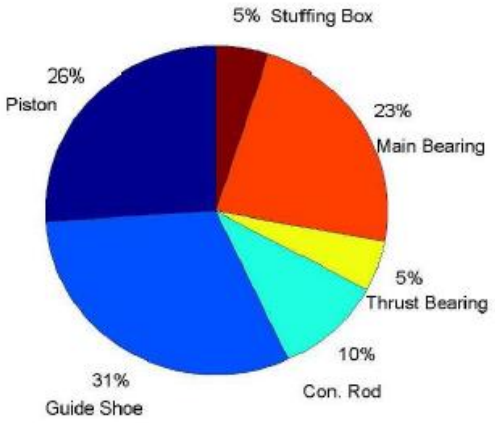

Figure 1.4 Main engine components frictional losses distribution

Mrzljak [13], by performing experimental testing of an estimation model on a two-stroke marine Diesel engine, concluded that indicated power and brake power deviate as much as 1.5% and that friction power losses vary from **5.7÷10.4%** of the total mechanical power. As the load increases, the mean pressure of mechanical losses increases while the percentage value decreases. This happens due to uneven increase of mechanical losses pressure and effective pressure; with the latter being highest at 100% engine load. The author proposed an empirical model of estimating mean pressure of mechanical losses, according to which, pressure depends on cylinder number, bore diameter, mean effective pressure and mean piston speed:

$$p_{f,mr} = 0.0384\left(1 + \frac{1}{Z_{cyl}}\right) + \frac{3}{D_{cl}} + 0.018mep + 0.004c_s.$$

Petrovsky [14] proposes the following breakdown for mechanical losses:

- Friction of engine parts
- Losses due to the ventilating action of rotating parts
- Power absorbed by engine-driven auxiliaries

The author suggests the following form of "propeller law" as an estimation tool for the power of mechanical losses of the engine: $\boldsymbol{P_{fr,pt} = AN^b}$, where A is a constant coefficient and b is a constant depending on engine size.

Apart from engine friction, power is further absorbed at the shafting system, before it reaches the propeller. The shafting system has also been an interesting field for tribology researchers; the shafting is a stiff construction that cannot adapt to external weather and sea applied variations, despite that a vessel is subject to hull deformations.

Shafting losses are dependent on revolutions and weight of the system. It is very important that the shaft and bearings are aligned properly, because misalignment leads to loss of load carrying capacity and increased friction coefficient. This frictional loss keeps escalating as the misalignment angle keeps increasing [15]. It is rather trivial that increased load and improper lubrication accelerate wear rates and material failure. Potential loss of the shafting system is extremely dangerous for the crew since the vessel cannot travel and needs to be towed, while the cost of shafting system damage can easily overcome 1M $.

The estimate of 1-3% loss of power at the shafting system is commonly used in literature. However, recent studies on the field indicate that this fraction is an overestimation; instead, a **0.5%** measure is a more realistic consideration. Vlachos [16], by studying the shafting losses of a VLCC and incorporating the effects of elastic deformations, showed that the estimate of 0.5% is correct and that, in many cases, losses can be even **ten times smaller**.

The shafting losses are further investigated by Siamantas [17]. By taking into consideration oil film thickness, elastic deformations and bearing stiffness on a FEM model of a 10000 TEU, shafting friction losses were estimated as **3%** of the brake horse power.

Brake power is the power output of the engine, to which addition of engine friction losses, yield the total mechanical energy. Values of engine components' losses, especially for the preliminary stage of vessel design are proposed by Fragkopoulos [20]. According to the author, after the flywheel of the engine there is extra power loss, caused by friction in certain rotating components of the shafting system. Gearboxes, hydraulic clutches, reverses and the thrust bearing contribute to further power losses. Clutches and gearboxes are able to reduce brake power by almost 4%, while the thrust bearing is assumed to absorb 0.5% of this mechanical energy [20]. Furthermore, if the engine is running on partial load, then the net power transferred to the shaft (shaft horse power) must be corrected with a partial load coefficient.

For the case of a vessel propelled with a two-stroke Diesel engine, friction at shafting system is lost mainly on the following components:

- Intermediate bearing(s)
- Thrust bearing, if it is separate from the main engine components
- Aft and forward stern tube bearings

Due to the low rotative speed that a two-stroke engine operates, there is no need for clutches or gearboxes and the propeller is directly connected to the engine through the shaft. The absence of these components, in combination with the lower mean piston speeds, lead to the expectation of less power losses than the case of a four-stroke engine.

Booser [18], illustrates a method of calculating the friction coefficient of a journal bearing. By solving the Reynolds equation with both Full and Half Sommerfeld boundary conditions, the author provides a method of calculating the friction force at journal bearings with the use of dimensionless, tabulated data, which is adopted in this study for the estimation of friction shafting losses.

1.2.6 Engine heat losses

The two-stroke marine Diesel engine is the most efficient Diesel engine currently operating in industry. The mechanical output power of the engine can be over 50% of the fuel combustion energy and if waste heat recovery system exists, the gain is almost 5% more [19,21]. Heat losses in a two-stroke Diesel engine occur due to:

- Heat lost in the form of exhaust gases, (22%-30%)
- Cooling losses, (24%-30%)
    - Engine air cooler losses (~67%)
    - Lubricant oil cooler losses (~12%)
    - Water cooler losses (~21%)
- Radiation, (0.5%-1.5%)
- Mechanical power (45%-51%)

Thermal losses of an engine depend on various parameters. Figures provided by the engine maker is often for ISO conditions and low operating temperatures. Heat waste is affected by: calorific value of the fuel, the maximum exhaust gas temperature, the air to fuel ratio, the engine room temperature (air inlet temperature), the sea water inlet temperature, the inlet temperature of lubricating oil and the load of the engine [20].

During combustion in the cycle of engine, the chemical energy of fuel is released. According to the heat balance of the engine, fuel energy is divided into exhaust losses, cooling losses, radiation losses and mechanical power. The produced mechanical power is divided into engine friction and net brake power. The brake power (shaft horse power) is not completely delivered to the propeller due to the shafting losses. From the power delivered to the propeller (dead horse power), the propulsion losses by subtracting the propulsion losses, the remaining proportion is the towing power, which is the power needed for the vessel to overcome the total resistance in order to move at constant speed.

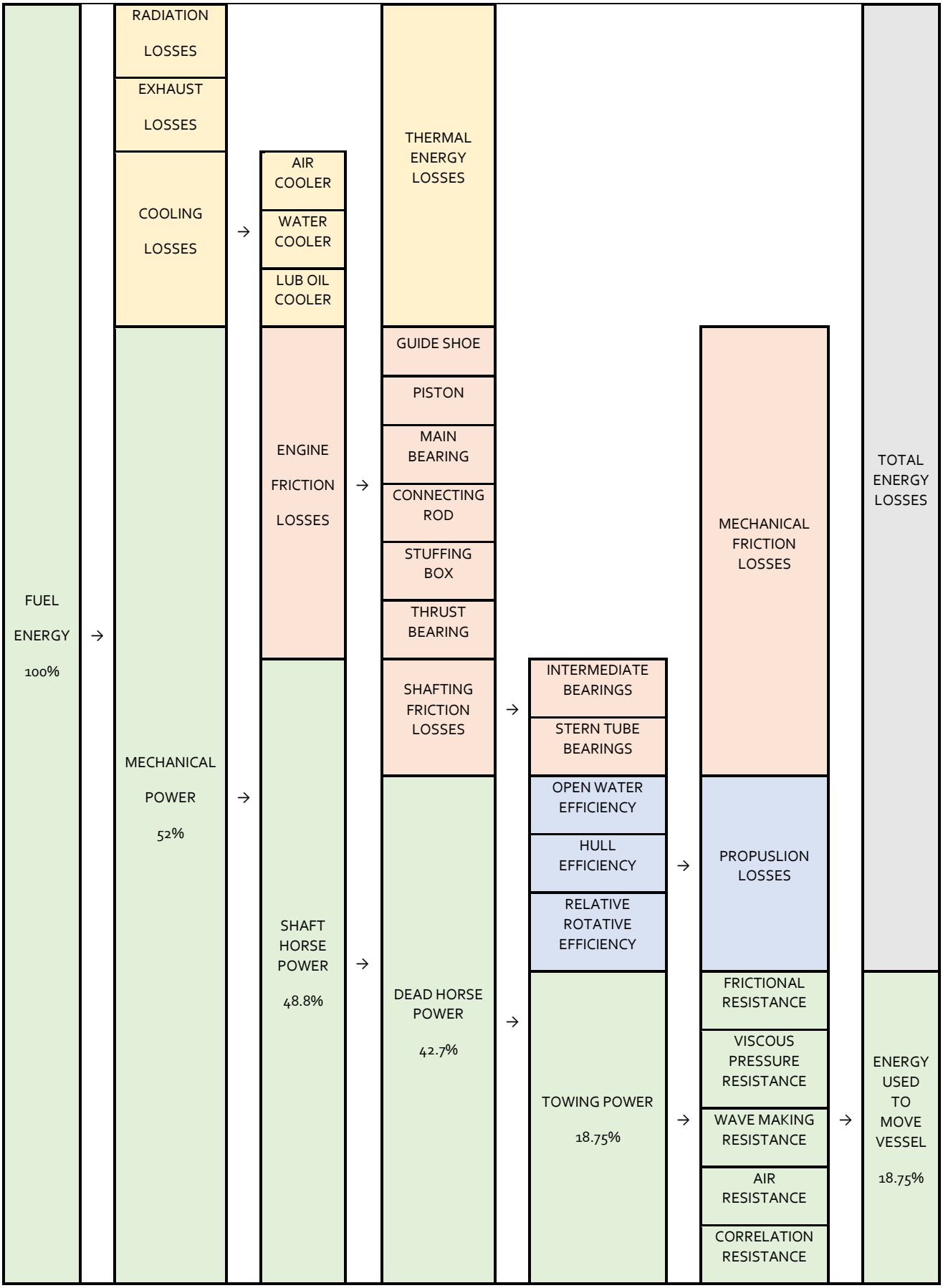

Figure 1.5 Energy breakdown of a merchant vessel

1.2.7 Bulk carriers

A vessel is defined as a bulk carrier if the cargo that is carries, is stored directly in its holds, in bulk form (iron, cotton, wheat, coal, etc.). This vessel type was introduced in the 50's and was an innovation for global trade since it contributed to cut down transportation costs. The intense economic development of Southeastern countries with the enormous demand of raw materials, led to important developments in the ship building industry and the global market rendered the bulk carriers as a profitable investment. Together with tankers and containerships, they represent the majority of the global fleet in terms of total tonnage.

After the economic crisis of 2008, the freight rate dropped for the bulk carrier fleet, currently remaining at low levels, resulting in cancelation of new building orders a reduction in the number of effective vessels. Nowadays, the global bulk carrier fleet accounts for more than 11,219 vessels, comprising almost 43% of the world fleet tonnage [22].

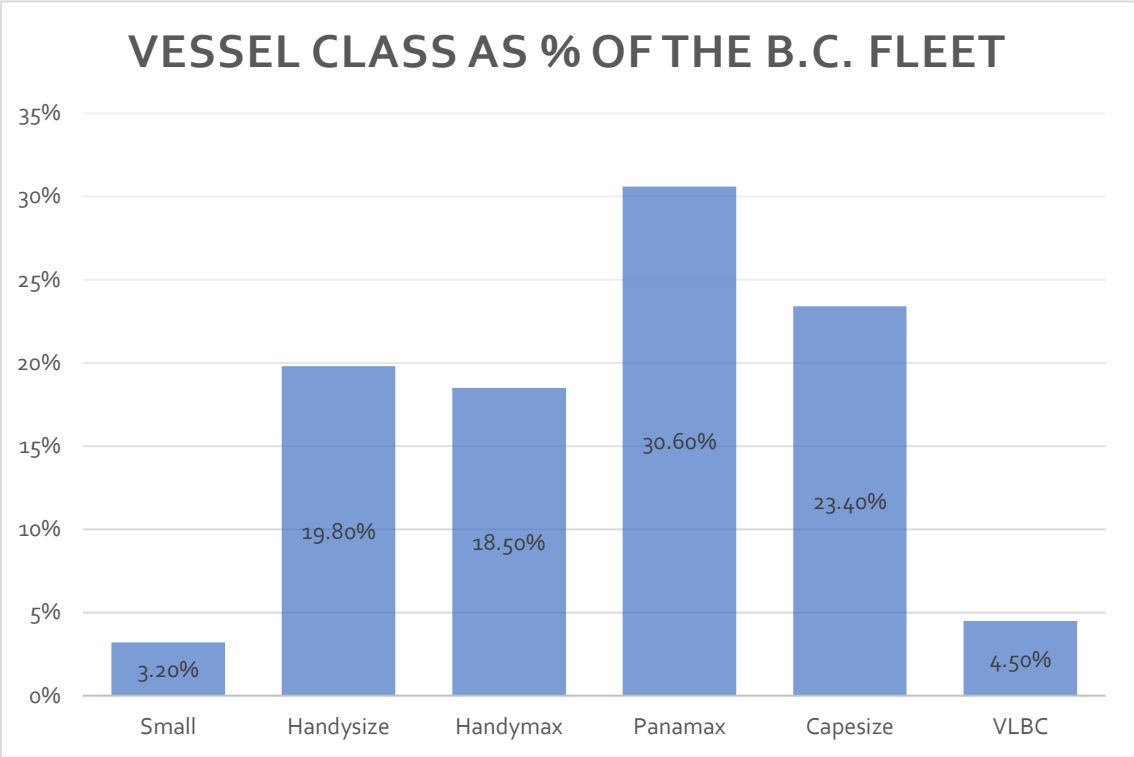

Figure 1.6 Number of bulk carrier vessels [23]

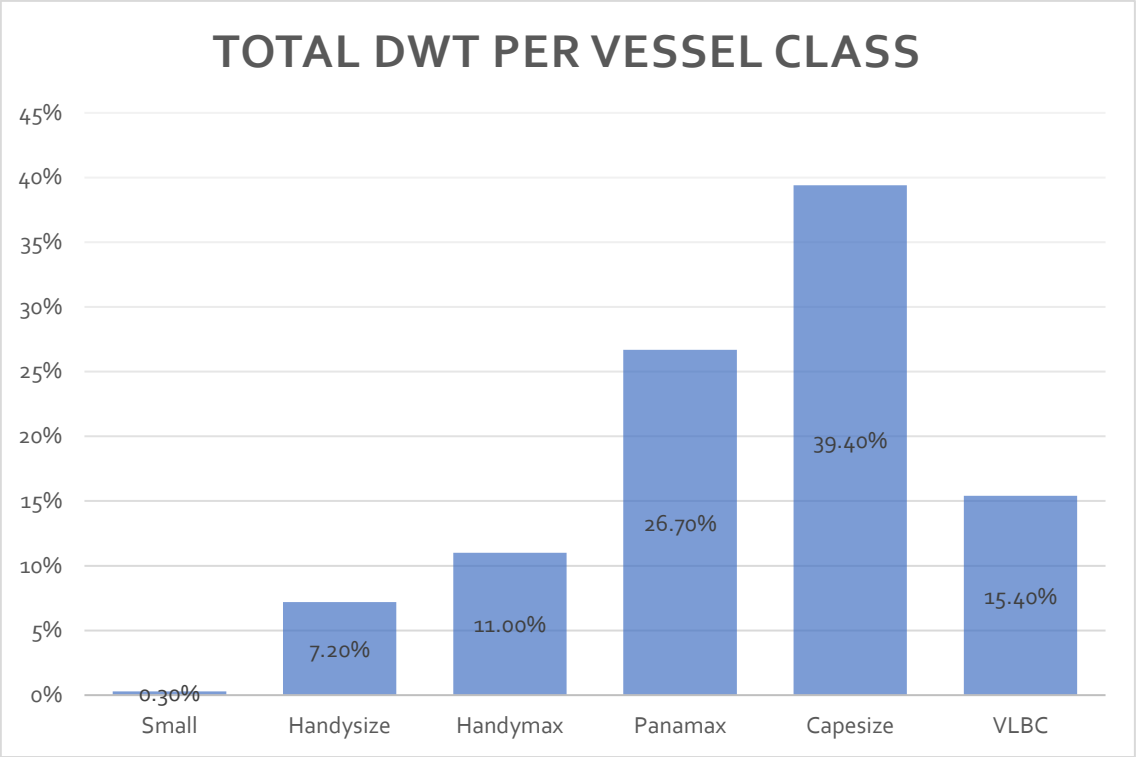

Figure 1.7 Total tonnage of bulk carrier vessels [23]

Bulk carriers are distinguished in the following categories, according to their deadweight, dimensions and certain voyage passages where a dimension restriction is possible.

Table 1.2 Dimensions and classes for bulk carriers [23]

Vessel Class/Subclass	Deadweight [t]	L_{OA} [m]	Max. Breadth [m]	Max. draught [m]
Small	10000	~115	~18	<10
Handysize	10-35000	130-150	~26	~10
Handymax	35-55000	150-200	32,2	10-12
Panamax	55-80000	190-225	28-32,2	12-14
• **Supramax**	60000	180-200	32,2	11-13
Capesize	80-200000	230-270	43-45	17
• **Kamsarmax**	~84000	229	32,2	14,4
• **Dunkirkmax**	~175000	289	45	~16
Very Large Bulk Carrier	>200000	>270	45-60	15-20
• **Newcastlemax**	~205000	299.9	47-50	16,1
• **Chinamax**	~400000	~360	~65	22-23

Bulk carriers are normally single hulled vessels with a double bottom, since there is no mandatory requirement for double hull design as in the case of tanker vessels. Double hull designs are offered by shipyards with the lightship weight increased by little since the steel plates are thinner.

Installed propulsion power for bulk carriers varies from 2500 kW to 25000 kW for a certain design speed. The speed, varies from 11 to 15 knots, depending on the class of ship, as shown in the next figure from MAN technical paper [23]. In this study, this proposed speed model is used as a calculation method of service speed.

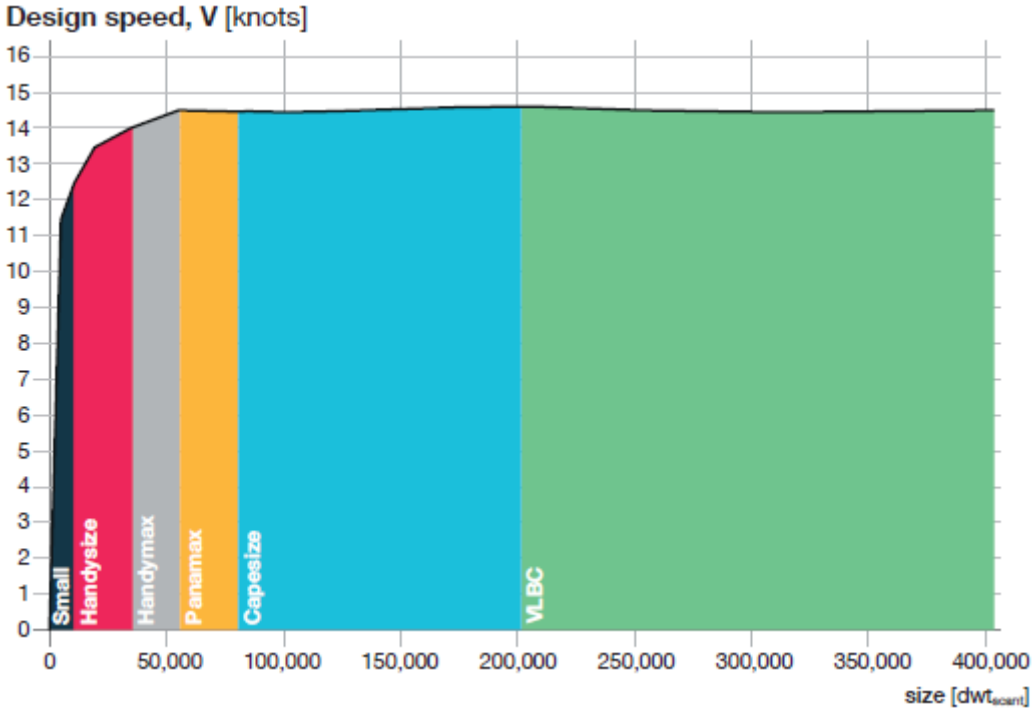

Figure 1. 8 Design speed for according to bulk carrier size [23]

Based on MAN technical papers [(23)], the global fleet of active and ordered bulk carriers as of 2018 is:

Table 1.3 Number of vessels per bulk carrier class 23

BULK CARRIER VESSEL CLASSES	
Small	371
Handysize	2272
Handymax	2195
Panamax	3696
Capesize	2971
VLBC	660

The impact on Greenhouse emissions from the majority of the global merchant fleet is investigated by Lyridis [(35)]. This is achieved with the establishment of the emission index, which is a measure of CO_2 emissions per DWT and nautical mile. Containerships, bulk carriers, tankers and LPG vessels are considered, since they comprise the largest part of the fleet, both in terms of capacity (DWT) and number of vessels in operation. Emission footprint was studied under the different filters installed power and significance in fleet, flag registry, vessel classification society and ship domicile. Containerships and bulk carriers have proven to be the most pollutive vessels. Specifically, **containers** are responsible for the **38.42%** of greenhouse gas emissions, followed by the **bulk carriers** which emissions are of the order of **35.48%.** The bulk carrier class with the **largest** greenhouse footprint was the **Handysize** class, accounting for 40% of the bulk carrier fleet emissions. Handymax accounted for 27%, Panamax vessels for 20% while the rest covered for 13%. A very important result from this study is that as the vessel size grows, the ship is proven to be more efficient, since the emission index drops due to increased geometry and optimum ship design.

2. Calculation of vessel parameters

2.1 Introduction

The main target of the study is to estimate the fuel lost due to friction in the propulsion installation for the bulk carrier fleet, at a designated period and state of operation. So, in order to initiate the estimation effort, calculation procedure is performed on a single vessel, prior to proceeding to fleet-scale measurements. For this reason, a "virtual" vessel is created by the steps of preliminary ship design. At first, the **geometrical parameters** of a vessel are calculated. Next, **hydrodynamic parameters** are calculated in order to provide an estimation for the resistance of the vessel and as a result for the propulsion power. Afterwards, a two-stroke **Diesel engine** is selected from a valid industry catalogue, according to the calculated resistance and predicted power. A **25% margin** is considered as the **maximum increase** in vessel resistance. Then, an operation profile is set, at a **cargo loading condition** (full load, full ballast, partially laden), at a certain **service speed level** (slow-steaming or full speed) and at a certain **hull condition** (newly dry-docked vessel or vessel prior to special survey when fouling effects on hull are maximized). Finally, **friction losses** are calculated; for shafting system and for main engine components separately.

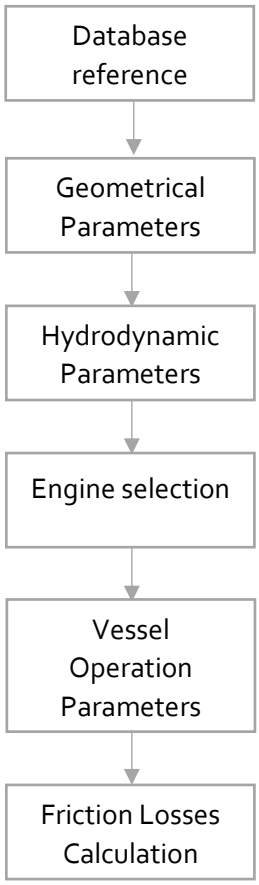

For the purpose of the study, proper software was designed. The software, by exploiting actual data of the SeaWeb database, is able to create a virtual fleet, different that the actual; nevertheless, described by similar characteristics. In this manner, global scale measures can be achieved. Calculation of frictional losses is performed on this recreated vessel (for the single vessel case) and on the virtual fleet (for the fleet-scaled measurements).

2.2 Workflow

In order to commence the calculation steps, the deadweight of the vessel (DWT) is given as input value, along with the number of propeller blades, trim angle and longitudinal center of floaticity (LCF). The deadweight is the main variable defining all other main dimensions. For the propeller, four or five blades are considered. Trim angle is considered zero (even keel vessel) and the LCF is located at 48% of the waterline length (L_{wl}), measured from the rudder shaft line. The practice of 48% is somewhat arbitrate; however, it is a usual value for a typical bulk carrier. Hydrostatic values are used solely for calculating draft at the mid ship area, for the purposes of estimation formulae used throughout the study.

2.2.1 SeaWeb database

Seaweb database for the bulk carrier fleet is used as the main source of data for the creation of the ship. A database use offers the advantage of providing basic information of each registered vessel and based on this information the vessel can be recreated virtually in order to apply the necessary calculations. From the Seaweb database, for each vessel, information on length, breadth, depth, draft, displacement, deadweight and main engine model is retrieved.

2.2.2 Geometrical parameters

The following geometrical parameters are calculated:

- Class of vessel depending on the given deadweight (DWT)
- Service speed and slow-steaming value (if applied)
- Length between perpendiculars (L)
- Waterline length (L_{wl})
- Depth (D)
- Breadth (B)
- Draft (T), at summer load
- Double bottom height, (d_b)
- $\frac{DWT}{\Delta}$ ratio, displacement (Δ) and lightship weight (LS)
- Block coefficient (C_b) at summer load draft
- Midship Area Coefficient (C_M)
- Waterplane Area Coefficient (C_{wp})

For every mode of study (single vessel or fleet scale), these parameters are calculated by any one of the following methods:

- Empirical relations found in literature.
- The mean value of the SeaWeb list for vessels within a specified DWT margin of 3%.
- The empirical relation of all used, that yields the closest value to the L obtained from SeaWeb database.
- For the calculation of L, B, D, the calculation can be performed with a sense of randomness. In this case, the dimension is calculated from one of the three above methods. Then, between

the value and the information from the database, the standard deviation is estimated. Finally, the actual value is calculated as the dimension of SeaWeb plus this deviation:

2.2.2.1 Length

The length of a ship is the most important dimension regarding construction, loading and operation. As much as the length increases [24,28]:

- Bending moments increase
- Total resistance decreases for low-speed vessels (F_n>0.15)
- Cargo zone can be expanded (more payload capacity for the vessel)
- Lightship weight increases
- Restrictions on certain routes
- Weight of propulsion installation decreases for a certain speed

Calculation of length can occur:

- through empirical relations or use of Seaweb database without randomness factor.
- through empirical relations or use of Seaweb database with randomness factor.

Empirical relations used:

- Papanikolaou [24]: $L = 7.60301DWT^{0.300155}$
- Misra [31]: $L = 6.667DWT^{0.308}$
- Average of the above two equations.
- Use of Seaweb database: calculation of mean length for vessels within a 3% deadweight margin. L is the closest value of the other empirical relations to that of the mean length of Seaweb database.
- Optimum equation against Seaweb database: The Seaweb database obtained length, is considered as the mean value and the rest relations are considered as its measures. Then, the selected length is that of the equation with the minimum standard deviation. $L = L_{SeaWeb} \pm yS_{dev}$, where y is a random integer between -1,1.

2.2.2.2 Depth

The depth of the vessel is the dimension affecting the volume of cargo and the freeboard height. Larger depth can also lead to larger engine room and larger load draft.

Equations used for the vessel are:

- Papanikolaou [24]: $D = 0.584268DWT^{0.310795}$
- Misra [31]: $D = 0.081L + 1.516$
- Average of the above two equations
- Use of Seaweb database: calculation of mean depth for vessels within a 3% deadweight margin. D is the closest value of the other empirical relations to that of the mean depth of Seaweb database.
- Optimum equation against Seaweb database: The Seaweb database obtained depth, is considered as the mean value and the rest relations are considered as its measures. Then, the selected depth is that of the equation with the minimum standard deviation, $D = D_{SeaWeb} \pm yS_{dev}$, where y is a random integer between -1,1.

2.2.2.3 Breadth

The calculation of breadth for a vessel can be achieved accurately if other dimensions have been calculated in advance. Breadth affects the stability of the vessel, the wave making resistance, the weight and strength of structure as well as seakeeping and maneuverability of the vessel.

Equations used for the vessel are:

- Papanikolaou [24]: $B = 1.0559DWT^{0.309724}$
- Misra [31]: $D = 0.164L + 0.09$
- Papanikolaou [24]: $B = \frac{(9295.65+1.77644DWT)}{LD}$
- Average of the above three equations
- Use of Seaweb database: calculation of mean breadth for vessels within a 3% deadweight margin. B is the closest value of the other empirical relations to that of the mean breadth of Seaweb database.
- Optimum equation against Seaweb database: The Seaweb database obtained breadth, is considered as the mean value and the rest relations are considered as its measures. Then, the selected breadth is that of the equation with the minimum standard deviation, $B = B_{SeaWeb} \pm yS_{dev}$, where y is a random integer between -1,1.

2.2.2.4 Draft

The load draft is a major dimension of the vessel since it affects:

- Frictional resistance and wave making resistance through the wetted surface
- Stability of the vessel
- Cargo space available
- Propeller diameter
- Seakeeping and maneuvering of vessel

Equations used for the calculation of draft:

- Papanikolaou [24]: $T = 0.480719DWT^{0.298295}$
- Misra [31]: $T = \frac{D}{1.385}$
- Average of the two above mentioned relations

Finally, after T is defined, draft at forward, aft and midship area is calculated as follows:

For negative trim angles:

- $T_A = T - LCF \tan\frac{\theta\pi}{180}$
- $T_F = T + (L_{wl} - LCF) \tan\frac{\theta\pi}{180}$

Otherwise:

- $T_A = T + LCF \tan\frac{\theta\pi}{180}$
- $T_F = T - (L_{wl} - LCF) \tan\frac{\theta\pi}{180}$

Distances are measured from A.P.

- $T_M = \frac{T_F+T_A}{2}$

2.2.2.5 Double bottom height d_b

An estimation of the minimum double bottom height is calculated with the use of class rules [24,25].

- ABS: $d_b = 32B + 190\sqrt{T}$
- LR: $d_b = 28B + 205\sqrt{T}$, not less than 650 mm
- DNV-GL: $250 + 20B + 50T$, not less than 650 mm

2.2.2.6 Deadweight to displacement ratio $\frac{DWT}{\Delta}$

The deadweight to displacement ratio for bulk carriers usually varies between 0.74-0.87%. For its calculation, an empirical model proposed by Papanikolaou [24] is used:

$$\frac{DWT}{\Delta} = \mathbf{0.46676}DWT^{\mathbf{0.0529501}}$$

2.2.2.7 Lightship weight

The lightship weight is also estimated from empirical models provided by Papanikolaou [24]:

- $\frac{LS}{\Delta} = 0.656409 - 0.0449219\ln(DWT)$
- $LS = 10^{-4} \cdot 6.5134DWT^{0.678895}$

2.2.2.8 Displacement

The methods of calculating the displacement of the vessel, provided by the above-mentioned author [24], are listed below:

- $\Delta = 2.21442DWT^{0.943855}$
- $\Delta = LS + DWT$
- $\Delta = \frac{DWT}{\frac{DWT}{\Delta}}$

2.2.2.9 Block Coefficient C_B

Block coefficient is an indication of how close to a box shape of dimensions L, B, T is the vessel's hull. By default, $C_B = \frac{\nabla}{LBT}$. Block coefficient is needed in order to calculate the total resistance of the vessel. The equations [24,28,30] used are:

- Ship study equation [24]: $C_B = \frac{\Delta}{\rho k LBT}$, k=1.005 is a correlation constant, Δ, is the displacement of the vessel and ρ is sea water density at 15°C.
- Papanikolaou [24] empirical: $C_B = 0.515788DWT^{0.042626}$
- Mean value of the above two relations
- Estimations [24] of the form: $C_B = k_1 - k_2\frac{V}{\sqrt{g_i L}} + k_3\frac{V}{\sqrt{g_i L}}^2$, as shown in the following table

Table 2.1 C_B equation parameters

Equation		k_1	k_2	k_3	V	L	g_i
Horn		1.06	1.68	0	m/s	m	9.81
Ayre		1.08	1.68	0	m/s	m	9.81
Heckser		1	1.44	0	m/s	m	9.81
Van Lammeren		1.06	1.68	0.224	m/s	m	9.81
Troost		1.156	0.625	0	knots	ft	1
Chirilia		1.225	0.378	0	knots	ft	1
Silverleaf-Dawson		1.214	0.394	0	knots	ft	1
Alexander-Watson	$\frac{V}{\sqrt{L}} < 0.65$	1.12	0.5	0	knots	ft	1
	$0.65 < \frac{V}{\sqrt{L}} < 0.8$	1.03	0.5	0	knots	ft	1
	$\frac{V}{\sqrt{L}} > 0.8$	1.06	0.5	0	knots	ft	1

2.2.2.10 Midship area coefficient C_M

The midship area coefficient is an indication of how close to a rectangle shape of B, T is the midship area of the vessel's hull. By definition, $C_M = \frac{A_M}{BT}$.

The empirical relations used for C_M calculations are[24]:

- HSVA: $C_M = \frac{1}{1+(1-C_B)^{3.5}}$
- Van Lammeren: $C_M = 0.9 + 0.1C_B$
- Kerlen: $C_M = 1.006 - 0.0056{C_B}^{-3.56}$
- Papanikolaou (randomness included): $C_M = 0.93 + (0.997 - 0.93)k_4$, k_4 is a random variable in the unity interval [0,1].
- Average of the above four relations

2.2.2.11 Prismatic coefficient C_P

After defining C_B, C_M the prismatic area coefficient can be calculated as: $C_P = \frac{C_B}{C_M}$

2.2.2.12 Waterplane area coefficient C_{WP}

The waterplane area coefficient expresses the area at the waterline of a specific draft T as a portion of a rectangle of the dimensions L, T. By definition, $C_{WP} = \frac{A_{WL}}{LT}$

The empirical relations used for C_{WP} calculations are[24,28,30,32]:

- $C_{WP} = \frac{1+2C_B}{3}$
- $C_{WP} = 0.95C_P + 0.17(1 - C_P)^{\frac{1}{3}}$
- $C_{WP} = 0.778C_B + 0.248$
- Papanikolaou: $C_{WP} = 0.7C_P + 0.3$
- $C_{WP} = \frac{C_B}{0.471+0.551C_B}$
- Schneekluth: $C_{WP} = {C_P}^{\frac{2}{3}}$
- $C_{WP} = C_B + 0.1$
- Average of the above seven relations

2.2.2.13 LCB

The LCB parameter is affecting the resistance of the vessel. For typical cargo vessels such as bulk carriers and tankers it usually lies between -2.5%÷2.5% of L, measured amidships. In the absence of hydrostatic values and specific loading condition parameters, LCB cannot be estimated. So, two methods are used in order to achieve an accurate estimate of LCB [32].

- $LCB = 20(C_B - 0.675)$
- $LCB = \frac{L}{2}(1 + r_{lcb})$, where r_{LCB} is a random number in the interval [0, 0.3].

2.2.2.14 Wetted surface S

The wetted surface is affecting the resistance of the vessel. If the wetted surface increases, the contact with the surrounding water increases, leading to larger frictional resistance for a certain speed. For the purpose of the calculations, the wetted surface is calculated with the help of empirical formulae. Then an increase for bilge keels and rudder is applied, since the appendages of the vessel increase friction between hull and water.

The empirical relations used for wetted surface calculations are [24,28,30,32]:

- Lap-Keller: $S_{hull} = \nabla^{\frac{1}{3}}(3.4\nabla^{\frac{1}{3}} + \frac{L_{WL}}{2})$
- Holtrop-Mennen:

  $$S_{hull} = L(2T_M + B){C_B}^{0.5}(0.453 + 0.4425C_B - 0.2862C_M) - 0.003467\frac{B}{T_M} + 0.3696C_{WP}$$
- Danckwardt: $S_{hull} = \frac{\nabla}{B}(\frac{1.7}{C_B - 0.2(C_B - 0.65)} + \frac{B}{T_M}$
- Mumford: $S_{hull} = 1.7LT_M + \frac{T_M}{\nabla}$
- Froude: $S_{hull} = 3.4\nabla^{\frac{2}{3}}$
- BSRA: $S_{hull} = 3.371\nabla^{\frac{2}{3}} + 0.296\frac{L}{B} + 0.437\frac{B}{T_M} + 0.595C_B$
- SERIES 60: $S_{hull} = 3.432\nabla^{\frac{2}{3}} + 0.205\frac{L}{B} + 0.443\frac{B}{T_M} + 0.643C_B$
- The average of the seven above mentioned relations

The rudder projected area can be estimated from the relation:

- $A_{rud} = \frac{LT_A}{100}((\frac{B}{L})^2 50{C_B}^2 + 1)$
- $A_{bk} = \frac{(2l_{bk}\, b_{bk} + l_{bk}w_{bk})}{\cos\theta_{bk}}$

The surface of the appendages can be calculated as:

- $S_{app} = 2(A_{rud} + A_{bk})$

The total wetted surface is the sum of the naked hull value and the appendages increase:

- $S = S_{app} + S_{hull}$

2.2.2.15 Propeller Diameter

In general, larger propeller diameter can lead to increased propulsion efficiency; however, the larger the propeller, the lesser the speed that can be achieved for a certain P/D ratio.

Propeller diameter [25,33] can be estimated either as a function of T_A, or as a random proportion of 65-70% of T_A.

- $D_P = 0.395T_A + 1.3$
- $D_P = r_{prop}T_A$, where r_{prop} lies in the interval [0.65, 0.7]

2.2.3 Estimation of total resistance

Resistance calculation is performed for the service speed of the vessel, in order to estimate the power needed for propulsion and select a proper engine installation. Resistance is estimated with the use of empirical formulae in the absence of actual vessel data. Accurate resistance prediction cannot be achieved without experimental procedures. However, absolute accuracy is not needed, as the aim of the software is to perform an accurate resistance estimation for a reasonable selection of a two-stroke Diesel engine.

The total resistance of vessel is calculated as follows. [28,29,30,32,34]

$$R_t = R_{fr} + R_{vp} + R_a + R_{air} + R_w$$

In the above relation, the components of the total resistance are:

- R_{fr} is the frictional resistance of the vessel.
- R_{vp} is the viscous pressure resistance
- R_w is the wave-making resistance
- R_a is the correlation resistance
- R_{air} is the air resistance

2.2.3.1 Reynolds and Froude Numbers

For the calculation of certain parameters Reynolds number and Froude number are needed.

Reynolds number is calculated from the relation: $R_n = L_{wl}\frac{V}{u}$, whereas, the Froude number is calculated from the relation: $F_n = \frac{V}{\sqrt{gL_{wl}}}$

2.2.3.2 Frictional Resistance

Frictional resistance is the component of a vessel's total resistance, at which energy is consumed due to the tangential **shear forces** acting on each element of the hull. Frictional resistance can be regarded as the sum of naked hull skin friction resistance, the appendage skin friction and a component of surface roughness effect. Rudders, bilge keels, sea chest openings, thruster orifices and duct arrangements introduce an increase on the skin friction resistance [29]**.** To incorporate the effect of appendages on the friction resistance, for the purpose of this study, the appendages surface was calculated, as it was illustrated on paragraph wetted surface. Due to the complexity of the problem, methods and models of estimation of the friction coefficient C_f, are actually referring to a rectangular plate instead of the actual shape of the vessel. Friction force is then corrected for the specific geometry of interest. Frictional resistance coefficient C_f is calculated using the **ITTC** proposed model.

$$C_f = \frac{0.075}{(\log(R_n) - 2)^2}$$

Frictional resistance is the dominating component at low-speed vessels (bulk carriers, tankers). It is highly dependable on speed, wetted surface, roughness and the lines form of the vessel (as a blurred body with a U shape hull would lead to increased pressure drop due to friction) [34].

The friction resistance is then calculated by the formula: $\boldsymbol{R_f = \frac{1}{2}\rho C_f S V^2}$

2.2.3.3 Roughness correction on skin friction

When the ship travels at sea, the flow of surrounding water is **turbulent**, due to water viscosity and hull roughness. This turbulent flow creates vortexes vertical to ship movement. The produced boundary layers have a thin laminar sublayer which in general can flow around small roughness without separating. However, if the **local roughness** is large enough to project through this laminar sublayer, it is then capable of increasing **drag force**. Roughness effect is higher where the boundary layer is thinner (bilge keel area mostly than bow and stern areas) and at points where the local flow velocity is high. The key element to study the effect of roughness is the ratio of grain size to length of wetted surface. For galvanized steel the average grain size usually is 150 μm.

It is not always possible to obtain actual vessel data, regarding the localized condition of the hull surface. So, for the purpose of this study, in order to incorporate the effects of hull roughness on the friction resistance, a correction coefficient is used. [34]

In the absence of actual ship data, which is also the case of this study, the **Bowden Equation** is used**:** $\Delta C_f = 0.105(\frac{AHS}{Lwl})^{\frac{1}{3}} - 0.00064$, where $AHS = 150\mu m$, is the average hull roughness for galvanized steel.

In the presence of actual ship data, the **Towsin equation** can be used:

$$\Delta C_F = 0.00044((\frac{AHS}{L})^{\frac{1}{3}} - 10R_n{}^{-\frac{1}{3}}) + 0.000125.$$

The correction is an average estimation and cannot take into consideration roughness from hull deformations or other life cycle factors that affect the structure of the vessel. Roughness effects will be calculated in the correlation resistance component (2.2.3.6). [32,34]

2.2.3.4 Viscous Pressure Resistance

The viscous pressure resistance is the integral of all normal **forces acting vertically** on the hull, projected on the direction of the flow. If the fluid is ideal, then the sum of these pressures equals zero. However, when the fluid is real, a thick, turbulent boundary layer is created over the surface of the body, which at certain points in the afterbody, it separates. The existence of the layer and its growth, lead to a modified pressure distribution over the hull, different than that of the inviscid fluid case. As a consequence, the sum of the forces can no longer be zero and energy losses occur. Viscous pressure resistance is therefore dependent on wetted surface, geometry of the hull and hull roughness of the vessel. [34]

The majority of methods of calculation of viscous pressure resistance, treat it as a fraction k of the frictional resistance, $\boldsymbol{R_{vp} = kR_f}$.

The equations used are the following [30,32]:

- Granville: $k = 18.7(\frac{C_B B}{L})^2$
- Alte and Baur: $k = 14\frac{B(\frac{\nabla}{L})^3}{T_M}$
- Watanabe: $k = -0.095 + 25.6\frac{C_B}{\sqrt{\frac{B}{T_M}(\frac{L}{B})^2}}$
- Grigson: $k = 0.028 + 3.3\frac{S}{L^2}\sqrt{\frac{C_B B}{L}}$
- Wright: $k = 2.48{C_B}^{0.1526}(\frac{B}{T_M})^{0.0533}\left(\frac{B}{L}\right)^{0.3856} - 1$
- Holtrop:

$$k = 0.93 + 0.487118(1 + 0.011C_{stern})(\frac{B}{L})^{1.06806}(\frac{T_M}{L})^{0.46106}(\frac{L_{wl}}{L_R})^{0.121563}(\frac{{L_{wl}}^3}{\nabla})^{0.36486}(1 - C_P)^{-0.604247} - 1$$

where $L_R = L_{wl}\frac{1-C_P+0.06C_P\frac{LCB}{L}}{4C_P-1}$

- Schneekluth: $C_{VP} = 0.16 + 26C_V + \frac{B}{T_M} - \frac{13-0.001C_V}{6}(C_P + 58C_V - 0.408)\frac{(0.535-35C_V)}{1000}$

  where $C_V = \frac{\nabla}{{L_{wl}}^3}$.

For the viscous pressure resistance, a deep-water correction is applied, since reduced port depth results in an increase in the eddy field of the vessel[34].

$$k = k + 0.644(\frac{T_M}{h_p})^{1.72}$$

According to the used equation, the viscous pressure resistance is calculated by either the formula: $\boldsymbol{R_{vp} = kR_f}$, or: $\boldsymbol{R_{vp} = \frac{1}{2}C_{vp}\rho SV^2}$.

2.2.3.5 Wave making resistance

Wave making resistance exists, when a vessel is sailing **on the waterline surface**, as in the case of the ship [(34)]. This resistance component would not be present in the case of a submarine or an aircraft. The hull points at the waterline area are moving pressure points. As a result of their movement, waterline surface is forced to change its level. In order to counter against this change, the sea water consumes energy, in the form of pressure in order to return to its original position. So, wave making resistance is a proportion of **energy** that the ship needs to consume in order **to maintain** this generated **wave formation**. There is no simple method to predict the wave making resistance. Wave making resistance cannot be eliminated in the case of a ship and it is highly dependent on geometry of the hull and speed. Wave making resistance is dominant for high-speed vessels (**F_n>0.16**). However, since the study is focused on bulk carriers, the associated Froude number to the usual service speed of this vessels does not exceed the value of 0.16, so it is fair to imply that wave making resistance is 5% of the total resistance. Therefore, $\boldsymbol{R_w = 0.05R_t}$.

2.2.3.6 Correlation Resistance

The correlation coefficient was originally used in order to incorporate the effects of hull roughness on skin friction. Now, this coefficient expresses the correlation of resistance between model and ship. Research on this coefficient aims at incorporating in the calculations the practice obtained throughout different towing labs. The common value for C_A used in literature is **0.4%** of the total resistance. Another value commonly used is the Bowden Equation as the correction of C_A. Another empirical relation that can be used, proposed in the work of Volker [(30)] is: $\boldsymbol{C_A = 0.00035 - 2L10^{-6}}$. **ITTC 57** method can also be used [(34)], where C_A is calculated according to the following table:

Table 2.2 Correlation resistance correction

L [m]	C_A correction
<150	0.00035-0.0004
<210	0.0002
<260	0.0001
<300	0
<350	-0.0001
>350	-0.00025

In this study the Bowden equation is used, which was mentioned at (2.2.3.3). After C_A is established, correlation resistance is calculated as: $\boldsymbol{R_A = \frac{1}{2}\rho C_A SV^2}$

2.2.3.7 Air Resistance

Air velocity is measured at least 10 meters above sea level in order to take into consideration its influence on the operation of a certain structure. Air resistance has a lesser effect on the total resistance and it is highly dependent on the surface existing above the load waterline. Hence, it can be fairly assumed that air resistance depends on the vessel type [32].

For example, air resistance for a cruise vessel or a containership, which both carry solid structures and increased payload above the main watertight deck, has a significantly intense effect on the total resistance than another conventional cargo vessel travelling on full load. According to MAN technical papers [22], air resistance for a bulk carrier or a tanker can be found up to **4%** of the total resistance, whereas it can exceed **10%** in the case of a container vessel.

For the purposes of this study the following method is used [30,32]:

- ITTC '78: In this case the coefficient of air resistance is calculated as: $C_{aa} = 0.001\frac{(A_{ts}+A_{ls})}{S}$, where A_{ts} and A_{ls} are the transverse and longitudinal surfaces of superstructures, exposed to air motion respectively. It should be noted that, in the resistance calculation the vessel is assumed travelling head-to-head against the air direction, which in this case of air resistance maximized.

The air resistance is calculated as: $\boldsymbol{R_{air} = \frac{1}{2}C_{air}\rho_{air}(A_{ts+}A_{ls} + 2L(D-T))(V-V_{air})^2}$

The surface that is in contact with the flowing air is the A_{ts} and A_{ls} for the superstructures. The freeboard area is considered as a rectangle of dimensions (D-T) x L in order to approximate the contact surface. Also, the speed used for the calculation is the relative V_{ship}-V_{air}.

2.2.3.8 Fouling

With the progressing vessel life and continuous operation, hull painting gradually breaks down, resulting in erosion and attachment of marine plants, barnacles and weeds on the hull surface. This phenomenon is called fouling and it affects the **roughness** of the existing hull surface. Specifically, this attached slime has the ability to increase the wetted surface, resulting in **larger frictional resistance** and consequently, larger total resistance. In this manner, **additional propulsion power** is needed in order to maintain the propeller revolutions, or, the propeller revolutions will decrease for constant engine load [22].

The fouling growth rate is larger initially but slows down as the mechanism advances. Growth rates depend on the ports of operation, the season of the year, the duration at anchorage at the port, trade patterns and turnaround times. [32] Additional fouling can be found on propeller blades, reducing further the revolutions for constant engine load [29]. Hull fouling and propeller fouling are studied as two separate problems. During operation of the vessel, temporarily, fouling is controlled with hull treatment methods (underwater cleaning).

Throughout the lifetime of the vessel, supposing that no hull treatment is conducted, this increase can reach values up to 50% of the total resistance.

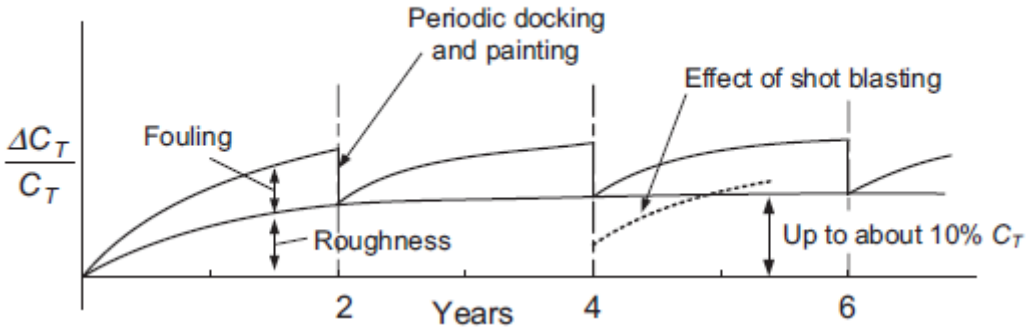

Figure 2.1 Fouling progression with time [32]

According to Molland, it can easily be seen that both fouling and roughness influences can never be completely eliminated. With the passage of time, hull roughness resistance effect will reach a permanent minimum level due to:

- aging of vessel
- hull deformations originating from cargo distribution
- sea state
- effects from shot blasting
- forces applied when on dry dock, since each time a ship is docked, since the support points differ from one drydocking to the next.

Fouling is dealt with proper antifouling coatings and paintings. Currently, self-polishing antifouling systems are being used, silicone-based which discourage marine growth from occurring. However, technology has not yet reached the complete prevention of the phenomenon and fouling must be treated in regular periods, in order to improving propulsion efficiency of the vessel and to reduce fuel oil consumption. Cleaning periods are arranged by class requirements of the vessel and occur at least every five years when the vessel is subject to drydocking class special survey. Each time the vessel leaves the drydock, it can be assumed that the fouling effect is zero.

The main engine must be capable of at least maintaining the necessary power in order for the vessel to sail at the constant, predefined service speed. However, this speed must be achieved even in the case of a fouled surface. In this study, a fouling margin of **15%** will be considered and applied on the total resistance in order to choose a Diesel engine for propulsion.

2.2.3.9 Wind and waves

On a scheduled voyage, the vessel must be able to reach and maintain the required speed. So, the main engine must be able to provide additional power according to the service weather. Rough weather increases heavily the power requirements that the propulsion system must achieve. Two parameters are affecting power demand; wind speed and waves generated from the upcoming wind. Usually, facing heavy weather, speed is reduced in order to avoid excessive slamming damage and accelerations, or the course is altered; nevertheless, fuel consumption is increased [29].

Weather influences can be obtained from theoretical or experimental methods [34]. Either wind tunnel and towing tank tests are applied or actual vessel voyage data are analyzed. Normally, the weather effect depends on wind speed, wave height, period and direction of vessel. Speed reduction curves for a specific vessel are obtained during sea trial period and the loss depends on the Beaufort Scale [30].

For the purpose of this study, weather conditions are not analyzed in detail. Instead, an additional margin of **10%** is applied on the total resistance, which considers a possible adverse weather condition.

2.2.3.10 Total Resistance

The total resistance is the sum of each resistance component:

$$\boldsymbol{R_{t,fw} = 1.05(R_f + R_{vp} + R_a + R_{air})(1 + m_{fl}m_{ww})}$$

Where $\mathbf{m_{fl}}$ is the fouling margin (15%) and $\mathbf{m_{ww}}$ is the wind and wave margin (10%).

This resistance is then used to predict the necessary propulsion power and, eventually, to select a two-stroke Diesel engine from an updated industry product catalogue [37].

2.2.3.11 Total resistance in full ballast condition

The same procedure is followed in order to calculate the resistance of a bulk carrier under full ballast loading condition. With the draft changed, geometrical and propulsion parameters are changed, which, in turn, affect the total resistance and the respective brake power of the engine. Calculation of ballast condition resistance aims at estimating the propulsion power needed at the case of full ballast condition. At first the new draft must be calculated, T_{wb}, then C_B and C_{WP}.

For the **draft** in water ballast condition, due to lack of other data, these equations are used for the calculation of draft:

$$T_{Awb} = D_{pr} + 0.6$$

$$T_{Fwb} = 0.027L$$

$$T_{wb} = T_{M,wb} = \frac{T_A + T_F}{2}$$

With the change in draft, **block** and **waterplane** area **coefficients** must be reestablished [26]:

$$C_{B,wb} = C_B\left(\frac{T_{M,wb}}{T_M}\right)^{\left(\frac{C_{WP}}{C_B}-1\right)}$$

$$C_{WP,wb} = C_{WP}\left(\frac{T_{M,wb}}{T_M}\right)^{\left(\frac{C_{WP}}{C_B}-1\right)}$$

The rest parameters listed on the following table are re-calculated with the use of the same formulae of paragraph 2.2.3.

Table 2.3 Parameters changed

Parameter changed-Full Ballast	
$C_{M,\,fb}$	Midship coefficient
$C_{P,\,fb}$	Prismatic coefficient
$L_{CB,\,fb}$	Center of Buoyancy
$S_{hull,\,fb}$	Wetted surface
$A_{rud,\,fb}$	Rudder wetted surface
Δf_b	Ballast displacement
$R_{n,\,fb}$	Reynolds number
$R_{f,\,fb}$	Frictional resistance
$R_{vp,\,fb}$	Viscous pressure resistance
$R_{air,\,fb}$	Air resistance
$R_{a,\,fb}$	Correlation resistance
$R_{t,\,fb}$	Total resistance

2.2.3.12 Total resistance in partially laden condition

Resistance is also estimated for the partially laden condition. Due to lack of hydrostatic diagram and tables for a vessel, the partially laden condition is considered as an intermediate condition between full loaded and full ballast. For this reason, a random variable is defined, $r_{d,\,pl}$ which receives percentage values in the interval of [0.1, 0.9]. This variable is used to calculate a draft larger than that of the full ballast condition. The drafts at forward perpendicular, aft perpendicular, and the midship draft for the intermediate loading condition are then calculated as:

$$T_{F,pl} = T_{F,wb}(1 + r_{d,pl})$$

$$T_{A,pl} = T_{A,wb}(1 + r_{d,pl})$$

$$T_{M,pl} = \frac{T_{A,pl} + T_{F,pl}}{2}$$

For the intermediate draft, C_B and C_{WP} are calculated using the same relations of the ballast condition.

$$C_{Bplb} = C_B\left(\frac{T_{M,pl}}{T_M}\right)^{\left(\frac{C_{WP}}{C_B}-1\right)}$$

$$C_{WP,pl} = C_{WP}\left(\frac{T_{M,pl}}{T_M}\right)^{\left(\frac{C_{WP}}{C_B}-1\right)}$$

The rest parameters listed on the following table are re-calculated with the use of the same formulae of paragraph 2.2.3.

Table 2.4 Parameters changed

Parameter changed-Partially Laden	
$C_{M,pl}$	Midship coefficient
$C_{P,pl}$	Prismatic coefficient
$L_{CB,pl}$	Center of Buoyancy
$S_{hull,pl}$	Wetted surface
$A_{rud,pl}$	Rudder wetted surface
Δ_{pl}	Partially laden displacement
$R_{n,pl}$	Reynolds number
$R_{f,pl}$	Frictional resistance
$R_{vp,pl}$	Viscous pressure resistance
$R_{air,pl}$	Air resistance
$R_{a,pl}$	Correlation resistance
$R_{t,pl}$	Total resistance

2.2.4 Estimation of propulsion power

After estimating the resistance of the vessel, propulsion parameters calculation follows. For the propulsive power to be predicted, the knowledge of propulsion efficiency is needed. The propulsion efficiency is divided into four components; the hull efficiency n_h, the open water propeller efficiency n_o, the relative rotative efficiency n_R and the shafting efficiency n_s [34].

2.2.4.1 Wake deduction

Friction from vessel's hull, when the ship is moving in the water, creates a boundary layer, where the water velocity varies. Specifically, at the contact surface, water velocity is the same as the vessel's speed, where at the end of this layer water velocity is zero. This distribution depends on the thickness of this created layer, whereas this thickness increases away from the fore end of the hull. This results in an uneven distribution of the velocity of water, which eventually meets the propeller at a lower speed. This speed reduction, or, the wake field as referred, is highly dependent on hull type, allowing the interpretation that every ship has a unique wake field. According to MAN technical papers [22] the wake fraction can be found between **0.2 and 0.45** for single screw vessels.

The wake deduction factor is calculated by pre-estimation equations for single-screw ships [28]:

- Kruger: $w = 0.75C_B - 0.24$
- Heckscher: $w = 0.7C_P - 0.18$
- Troost: $w = 0.25 + 2.5(C_B - 0.6)^2$
- The average of the above formulae.

Wake field is calculated for every cargo loading condition for the relevant draft, w_{fl}, w_{fb}, w_{pl}.

2.2.4.2 Thrust deduction

With the rotation of the propeller behind the ship, water velocity is increased. This results in a reduction of water pressure, (Bernoulli effect), an increase in drag and thus an increase in the resistance of the vessel. Alternatively, it is a fraction of thrust loss, stating that the propeller must overcome the towing resistance plus the drag due to this pressure drop [22].

The equations for use regarding single-screw ships are [34]:

- Danckwardt: $t = 0.5C_B - 0.15$
- Heckscher: $t = 0.5C_B - 0.12$
- SSPA: $t = w(1.57 - 2.3\frac{C_B}{C_{WP}} + 1.5C_B)$

- The average of the above formulae.

Thrust deduction can be found between **0.12 and 0.3** for single screw vessels [22] and is calculated for every cargo loading condition for the relevant draft, t_{fl}, t_{fb}, t_{pl}.

2.2.4.3 Hull efficiency

Hull efficiency, through the wake and thrust deduction, expresses propeller and hull interaction [28], as it is the ratio of the effective power (towing power) against the thrust that the propeller delivers to the water. For a single screw ship[34], the values of this coefficient usually lie between **1.1 and 1.4**, whereas for twin screw vessels is approximately **0.95-0.98**. In order to estimate the hull efficiency coefficient, the wake and thrust deduction factors need to be calculated as shown in the below formula.

$\boldsymbol{\eta_H = \frac{1-t}{1-w}}$, where w is the wake deduction factor and t the thrust deduction factor.

Hull efficiency is calculated for every cargo loading condition for the relevant draft, n_{Hfl}, n_{Hfb}, n_{Hpl}.

2.2.4.4 Thrust Force

The thrust force is calculated from the obtained total resistance and the thrust deduction factor:

$$T_h = \frac{R_t}{1-t}$$

2.2.4.5 Expanded area ratio

Expanded area ratio [34], $\frac{A_E}{A_O}$ is necessary for the calculations of relative rotative efficiency. A_E represents the expanded area of the propeller, where A_O is the surface of the propeller disc

$A_o = \frac{\pi}{4} D^2$.

For the approximation of this ratio the Keller equation is used: $\frac{A_E}{A_O} = \frac{(1.3+0.3z)T_h}{(p_o - p_v){D_p}^2} + 0.2$ where p_o is the static pressure at the shaft center line and p_v is the water vapor pressure. For the purpose of this study all vessels have been considered to be equipped with Wageningen B-Screw propeller series. By this consideration, the expanded area ratio will be selected from table *2.5* according to number of propeller blades and the closest approximation the Keller equation provides [29].

TABLE 6.4 Extent of the Wageningen B-Screw Series (Taken From Reference 6)

Blade Number (Z)	Blade Area Ratio A_E/A_O										
2	0.30										
3		0.35		0.50		0.65		0.80			
4			0.40		0.55		0.70		0.85	1.00	
5				0.45		0.60		0.75			1.05
6					0.50		0.65		0.80		
7						0.55		0.70		0.85	

Table 2.5 Wageningen blade area ratio [29]

2.2.4.6 Relative rotative efficiency

Relative rotative efficiency is the ratio between the propeller efficiency when operating in the wake field behind the hull against the propeller efficiency which operates in open water. This occurs from the nature of the speed around the propeller; at the propeller-hull system the water meets the propeller in a rotative direction instead of being constant and under a specific angle. Values for single screw vessels are often unity and can reach up to **1.07**, which means that in this case, the rotation of the flow is beneficial for the propulsion of the vessel.

Formulae used for the calculation are [29]:

- Holtrop: $\eta_R = 0.9922 - 0.05908\frac{A_E}{A_o} + 0.07424(C_P - 0.0225\frac{LCB}{L})$
- BSRA: $\eta_R = 0.5524 + 0.8443C_B - 0.5054{C_B}^2 + 1.1511\frac{D_{pr}}{L} + 0.4718\frac{D_{pr}}{\nabla^{1/3}}$

Relative rotative efficiency is calculated for every cargo loading condition for the relevant draft, n_{Rfl}, n_{Rfb}, n_{Rpl}.

2.2.4.7 Open water propeller efficiency

When the propeller operates in open water, due to absence of hull, the wake field is homogenous [22,34], which is not true for the case of hull-propeller system. Open water efficiency is the efficiency of the propeller when operating in a homogenous wake field and defined as: $\boldsymbol{\eta_O = \frac{THP_0}{DHP_O}}$ where **THP₀** is the thrust power and **DHP₀** the dead horse power (power the propeller actually receives) in open water [34]. This coefficient is dependent on propeller **diameter**, the number of **blades**, the **pitch** and the **speed** of advance $V_a = V(1-w)$. The larger the open water efficiency, the less power losses at the propeller. For the purpose of the study and in the absence of ship data, η_o is calculated through the quasi-propulsive coefficient, η_D.

Open water propeller efficiency is calculated for every cargo loading condition for the relevant draft, n_{Ofl}, n_{Ofb}, n_{Opl}.

2.2.4.8 Quasi propulsive coefficient

The quasi-propulsive coefficient, η_D reflects the power losses due to each hydrodynamic parameter calculated [28]. The power transmitted from the propeller to the water in order to produce the necessary thrust is not the same, since the torque varies due to hull efficiency, relative rotative efficiency and open water propeller efficiency. The total impact of these three efficiencies that influences the selection of installed machinery is expressed via the quasi-propulsive coefficient, η_D:

$$\boldsymbol{\eta_D = \frac{Towing\ power}{Power\ delivered\ to\ propeller} = \eta_o\eta_H\eta_R}$$

This coefficient can be found between **60-70%** for a cargo ship [28]. In early stages of design, it can be estimated from empirical formulae with the knowledge of propeller revolutions and displacement volume. The values of these formulae become more accurate if at least one of the respective efficiencies is known.

The equations/methods used for the calculation of n_D are:

- Danckwardt: $\eta_D = 0.836 - 0.000165\mathrm{n}\nabla^{\frac{1}{6}}$
- Keller: $\eta_D = 0.885 - 0.00012n\sqrt{L}$

Open water efficiency is the calculated as $n_O = \frac{n_D}{n_H n_R}$.

Quasi propulsive efficiency is calculated for every cargo loading condition for the relevant draft, n_{Dfl}, n_{Dfb}, n_{Dpl}.

2.2.4.9 Propulsive coefficient

Propulsive coefficient, η_p, is defined as the complete efficiency of the propulsion system (or the total of power losses during transmission of torque from the engine to the propeller and thrust generation), expressing both hydrodynamic and frictional losses. Propulsive coefficient usually lies between **70-75%.**

$$\eta_p = \eta_H \eta_R \eta_o \eta_s = n_D n_S$$

The propulsive coefficient is calculated by:

- Use of n_D and n_S
- Running Grid.exe (a method of calculating rotational speed and the propulsion coefficient based on a resistance estimation provided by Politis [34])

Propeller revolutions and quasi propulsive coefficient are obtained by the use of grid program.

Propulsion efficiency and revolutions of the propeller are calculated for every cargo loading condition for the relevant draft, n_{Pfl}, n_{Pfb}, n_{Ppl}, N_{fl}, N_{fb}, N_{pl}.

2.2.4.10 Effective Power P_e

The effective power is the minimum required energy for towing the vessel. P_e is simply calculated by: $\boldsymbol{P_e = R_{t,fw} V}$

2.2.4.11 Dead Horse Power P_D

Dead horse power P_D, i.e., the power delivered to the propeller is found by correcting P_e with the relevant hydrodynamic coefficients. $\boldsymbol{P_D = \frac{P_e}{\eta_H \eta_R \eta_O} = \frac{P_e}{n_D}}$.

2.2.4.12 Shaft Horse Power, shafting losses and propulsive coefficient

After establishing the hydrodynamic coefficients and calculating the dead horse power of the vessel, the shaft horse power can be estimated. During the transmission of power from the engine to the propeller, certain power losses occur at the shafting system bearings due to friction from the rotation of the shaft. According to abundant literature [16÷18,29÷32], the losses are often of the magnitude **1-2%** of the brake power of the engine. Vlachos [16], stated that for a specific VLCC, the shafting losses are a fraction of **0.5%** of the brake power of installed engine, indicating that the 1% measure sometimes might be conservative. Shafting losses depend on the condition of the shafting system, whether or not a misalignment exists and on the viscosity of the lubricating oil, excluding other operating parameters. Thus, there is no yet a direct analytical method of calculating the losses.

For the purpose of the study, in order to be able to select a valid engine, shaft losses η_s will be considered as **2%**. This estimation will be validated later on, when the friction study is conducted.

$$\boldsymbol{P_s = \frac{P_D}{n_s} = \frac{P_E}{\eta_p}}$$

Ps, is the power required for propulsion of the vessel, including all the losses met in the shafting system and hull-water interaction, in case of a fully fouled hull and under heavy weather service conditions. In other words, it is the maximum power output that the propulsion installation generates.

2.2.5 Maximum continuous rating and engine selection

The propeller revolutions, n, are obtained from running the grid.exe [34] by using as input the number of blades, expanded area ratio, wake and thrust deduction, shaft efficiency and the total resistance under the maximum influence of fouling and heavy service weather.

At this point, every parameter needed in order to define the brake power of the installed propulsion unit has been estimated. The point of interest (the maximum service point that the engine is expected to operate at) must at least generate power equal to P_s at n revolutions **(P_s, n)**. The created vessel will be "fitted" a two-stroke Diesel engine. There are a few considerations to be taken into account regarding selection of the proper engine model. A two-stroke Diesel engine, which today remains the most efficient propulsion solution, is defined by a very large stroke, which is the key parameter for increased efficiency. Thus, one limitation for the engine selection is the **engine room height**, which is limited by the depth of the vessel. In order to overcome this problem, for this study, vessels with depth less than **10.5** m (for ensuring that a large engine can be fitted) are being excluded in the calculation steps.

A two-stroke engine can be set to operate in various points, which are included in the engine's layout diagram. A typical layout engine diagram is shown in Figure 2.2.

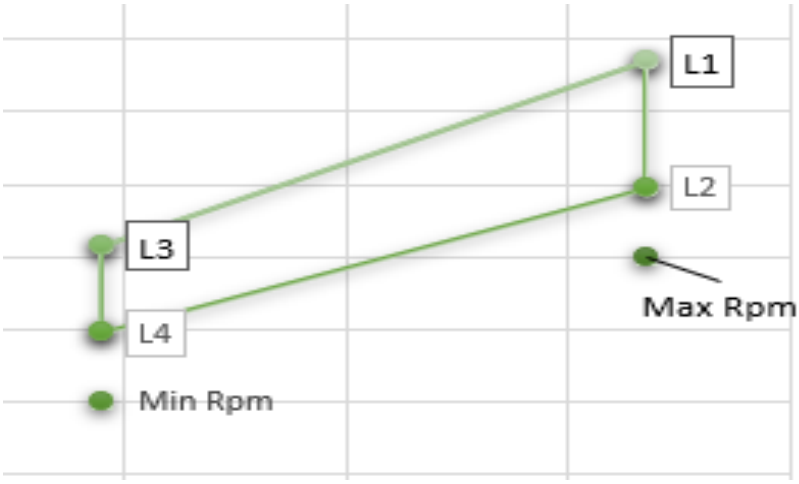

Figure 2.2 Engine layout diagram

The ***L1-L2-L3-L4*** map, is the set of all possible service points under which the engine model can operate. So, another aspect to be considered before selecting an engine for the vessel, is that the calculated service point M is as close to the L_1 value as possible (regarding both power and rpm). The reason for this is clearly economic, as it would be more profitable to install an engine close to its maximum capabilities, with respect to the installation weight.

With the calculated shaft horse power P_s and the relevant revolutions for that certain amount of power, a two-stroke Diesel engine is selected from an updated MAN product catalogue [37].

2.2.5.1 Propeller law and service conditions

The brake power of the vessel in terms of resistance is expressed as $P_B = \frac{R_t V}{n_p}$. Also, for a Diesel engine, the brake power is proportional to the rate of revolution and the mean effective pressure: $P_B = cn\bar{p}_e$. When operating at constant mean effective pressure p_e, the relation between power and revolutions is linear, $\boldsymbol{P_B = cn}$ (1). Moreover, resistance is a function of the square of the speed of the vessel:

$R_t = \frac{1}{2}\rho C_T S V^2 \rightarrow \boldsymbol{R_t = CV^2}$ (2).

If the vessel is equipped with a **fixed pitch propeller,** then the speed of the vessel is proportional to the rate of revolution of the propeller, through the coefficient of advance number of the propeller, J. The advance number is a dimensionless coefficient that correlates the linear and tangential velocity of water flow around the propeller. The coefficient is expressed as $J = \frac{V_A}{nD_p}$, where V_A is the speed of advance, $V_A = (1-w)V$. If the revolutions of the propeller do not change (which implies that the mean effective pressure of the engine does not change), J is a constant and V is proportional to the revolutions, n by the relation: $V = \frac{nJD_p}{1-w} \rightarrow \boldsymbol{V = Cn}$ (3).

From relations (1) and (2), it is derived that brake power is proportional to the third power of speed: $P_B = CV^3$. By exploiting relation (3), brake power is proportional to the third power of revolutions $\boldsymbol{P_B = Cn^3}$. This relation is known as the propeller law [22,34].

Measurements and experience have shown that the power slightly differs for various vessel types [22]. For large high-speed ships $P_B = Cn^4$, whereas for medium speed vessels, $P_B = Cn^{3.5}$. For low-speed ships like tankers and bulk carriers, the modified propeller law is: $\boldsymbol{P_B = Cn^{3.2}}$.

When the ship sails under clean hull and calm weather, the brake power of engine and propeller revolutions are described by the propeller law $\boldsymbol{P = cn^{3.2}}$, where $\boldsymbol{c = \frac{Ps}{n_{mcr}{}^{3.2}}}$.

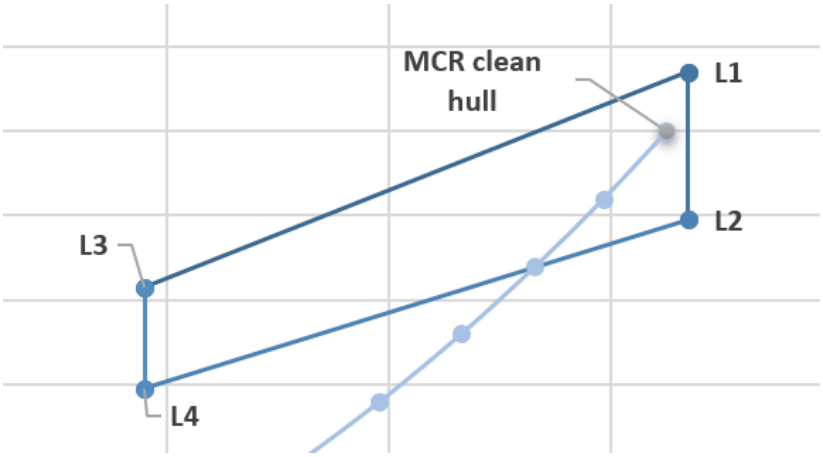

Figure 2.3 Engine load diagram-Clean hull

However, as time progresses and hull fouling is increased, due to this added resistance, the engine is forced to provide extra power in order to maintain the revolutions at a constant level and the service speed unchanged. This is clearly shown in the figure 2.4.

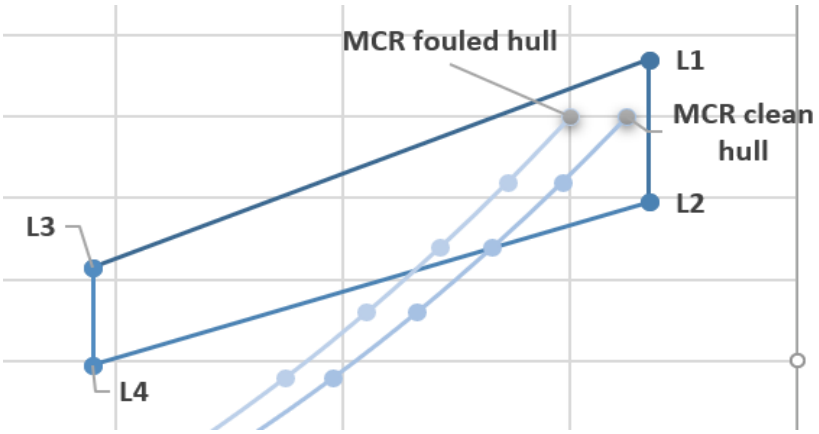

Figure 2.4 Engine load diagram-Fouled hull

It can easily be seen that the law abiding to P and n is no longer line C_1, but C_2 which is moved to the left of the original "clean hull" curve. The MCR point changes and the new coordinates are $(P_{s,fouled}, n_{mcr,fouled})$. The new propeller law, governing the power demand of the fouled hull is

$\boldsymbol{P = c' n^{3.2}}$, where now $\boldsymbol{c' = \frac{Ps_{fouled}}{n_{mcr,fouled}{}^{3.2}}}$.

This curve is further moved to the left if the vessel sails under both fouled hull and heavy weather. Another law relates the power needed to the necessary revolutions, as illustrated in figure 2.5. In general, each different service condition that affects the total resistance, influences propulsion efficiency in this manner.

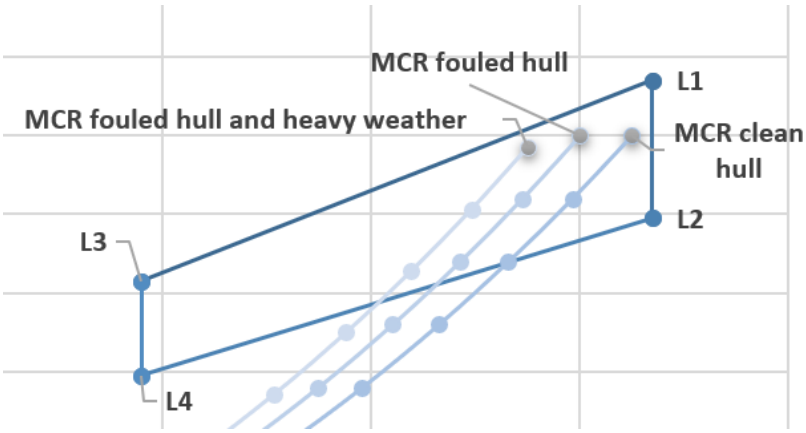

Figure 2. 5 Engine load diagram heavy fouled hull

2.2.5.2 Engine selection

After the resistance estimation, a two-stroke Diesel engine is selected from a valid industry catalogue. The model of the engine might not be the same existing in the SeaWeb database; however, since the vessel is recreated the selected engine would at least be a similar propulsor to the existing.

2.2.6 Setting the operational point of the vessel

Apart from the selection of a Diesel engine and the estimation of an installed brake power, the operational point of the vessel must be set. It is not a necessity for a low-speed bulk carrier to be operating under the maximum rating of their engine. There are numerous reasons for that. The most important is that the vessel is forced either by the charter party or the policy of management to run on reduced speed (also referred as slow steaming). Another important aspect is that the vessel may not be able to reach up to its maximum propulsion power. This could be a result of:

- Machinery aging
- Excessive hull fouling (period from previous drydock repair)
- Inadequate maintenance of machinery

In addition to these factors, the fact that the ship might not be sailing at maximum cargo load conditions must also be considered. The explanation is that when the draft changes, the resistance is changed, thus, the necessary power for propulsion is different than that of the maximum continuous rating.

Friction losses are different between the MCR power and an intermediate operational point. As the engine load decreases, the mean effective pressure is reduced more drastically than the mean friction pressure loss. As a result, the total friction losses might be higher for the operational point.

For the virtual vessel, of all these factors, fouling and slow-steaming are considered. Defective machinery and improper maintenance are excluded since these factors cannot be controlled by simple assumptions.

2.2.6.1 Cargo loading condition

As stated, at an instant timeframe a bulk carrier might be loaded at a different condition than the full load. So, in order to perform accurate calculations, a probabilistic model which decides at what cargo condition the vessel is loaded, is considered. A decision-random variable r_{cargo} is defined, which receives percent values that refer to a specific cargo loading condition. The study is narrowed down in three cases; full load condition, full ballast and partially laden. The probability of travelling on full load condition is assumed 70%, 20% for full ballast and 10% for a partially laden vessel. The random variable receives either one of the following values: $\boldsymbol{r_{cargo}} = \begin{cases} \mathbf{0.1} \\ \mathbf{0.2} \\ \mathbf{0.7} \end{cases}$. Values are assigned to r_{cargo} randomly. Depending on the value of r_{cargo}, the total resistance is calculated accordingly.

2.2.6.2 Hull fouling (period from previous drydock repair)

As mentioned in paragraph *2.2.3.8*, the total resistance of a vessel is increased due to fouling of the hull. When the vessel is newly constructed or recently dry-docked, hull roughness and fouling effects are almost eliminated, thus barely affecting the total resistance. When the vessel leaves dock, it is considered as newly treated and the total resistance is with a small deviation the predicted resistance for towing. However, after a short duration of operation, even less than six months, marine growth starts, increasing the resistance. As time progresses, the growth will continue, in smaller rates, but will not cease. So, it can be assumed that, right before entering a drydock for survey and repairs, the effect on the total resistance is considered to be maximum.

At this point, a random variable is defined, $\mathbf{r_{period}}$, which is defined as: $0 \leq r_{period} \leq 1$.

This variable is zero for a recently docked vessel, when there is no fouling effect on resistance. The value of unity represents the case of heavy fouled hull, prior entering a drydock. In any other case, the variable represents an intermediate period between drydock repairs, at which the effect of

fouling is intense, but not maximum. The total resistance of the operational point, at any cargo loading condition, including this random variable is: $\boldsymbol{R = R_t(1 + r_{period} m_{fl} m_{ww})}$,

m_{fl} and m_w is the 15% maximum fouling margin and wind-wave 10% maximum margin respectively that were considered paragraph 2.2.3.10.

2.2.6.3 Actual voyage service speed

Slow steaming is the operation of a vessel at reduced service speed of the order 10-20%. Slow steaming is an economic practice in order to cut down fuel costs, reduce operational expenses of the vessel and, as a consequence, increase its competitiveness. After all, the more competitive a vessel is, the more easily can be hired for a voyage. Another important benefit of this practice, is the reduction of exhaust gases and the improved control of nitrogen and Sulphur oxides that are emitted. Whether or not a vessel operates under slow-steaming condition depends on the company policy and the agreement on the charter party. However, there are two limitations for a vessel on how much the speed can be cut down. The first limitation is the turbocharger. If the vessel is not equipped with by-pass method of turbocharger for low engine loads, then the engine must always operate at a load where the turbocharger operates efficiently; the exhaust gas pressure must be enough to conserve the rotation of turbine. The second limitation is the restricted frequency of the shafting system. By lowering the revolutions, the frequency is reduced, with the danger of entering the area of resonance frequencies, which can lead the shafting system to failure.

As done in the two previous cases, a probabilistic model is considered, which decides whether the vessel is operated under slow steaming or travels at full speed and, in the case of slow steaming, defines the reduction order. First of all, a 50% the global bulk carrier fleet is considered to be travelling under reduced engine load of 10 or 20%, whereas the rest of the fleet is assumed to be travelling under maximum service conditions. As a consequence, a binomial random variable, r_{sr}, of a probability $p = \frac{1}{2}$, is introduced, which decides whether or not the vessel runs under slow steaming.

$$\boldsymbol{V_s} = \begin{cases} \boldsymbol{(1 - r_{rd})V}, & \boldsymbol{0 \le r_{sl} \le 0.5} \\ \boldsymbol{V}, & \boldsymbol{0.5 < r_{sl}} \end{cases}$$

2.2.6.4 Resistance of operational service point

For the calculation of total resistance at the operational point, the variable r_{cargo} is used at first. Depending on its value, for the operational resistance one of the three total calculated is used (R_{tfl}, R_{twb}, R_{tpl}).

$$\boldsymbol{R} = \begin{cases} \boldsymbol{R_{t,fl}(1 + r_{period} r_{fl} r_w)(\frac{V_s}{V})^2} \\ \boldsymbol{R_{t,fb}(1 + r_{period} r_{fl} r_w)(\frac{V_s}{V})^2} \\ \boldsymbol{R_{t,pl}(1 + r_{period} r_{fl} r_w)(\frac{V_s}{V})^2} \end{cases}$$

2.2.6.5 Power of operational service point

The propulsion efficiency is calculated for the operational point. Hull efficiency is dependent on the draft, so according to r_{cargo}, the relevant hull efficiency is used in the calculations. The same applies for relative rotative efficiency. Next, the grid.exe is exploited again, with resistance R as input, in order to provide propulsion efficiency, n_p and revolutions, N, for the operational point.

The brake power is: $\boldsymbol{P = \frac{RV}{n_p}}$ and the propeller law is defined by P, N is: $\boldsymbol{P = CN^{3.2}}$.

2.2.7 Shafting system weight

The shafting system weight is needed in order to estimate the friction losses at the bearings due to rotation of the shaft and to validate the η_s coefficient. In the absence of actual vessel data, some necessary considerations and assumptions are made:

The shafting system of the virtual fleet consists of:

- A two-stroke Diesel engine.
- A thrust shaft and bearing included in the engine components.
- An intermediate shaft with one intermediate bearings.
- The propeller shaft with one aft and one forward stern tube bearings.

Additionally:

- All bearings are oil lubricated.
- In the friction calculations, permanent deformations are not taken into consideration.
- Shaft system is properly aligned.
- Bearings are usual cylindrical journals of diameter D_b and length L_b

For the definition of lengths, diameters and weights, the 2008 DNV method is used. However, for more accuracy, data from [27] regarding shaft lengths are used, in order to provide more accurate results.

The shafting system is constructed by steel. Steel density is assumed $\rho_{st} = 7{,}8\ \frac{t}{m^3}$ while the yield stress is assumed $\sigma_{Y,st} = 500\ Mpa$. In addition, propeller shaft liners are assumed to be constructed by stainless steel, or steel alloy adequately resistant to marine corrosion. Stainless steel density is assumed to be $\rho_{s,st} = 7{,}9\ \frac{t}{m^3}$.

2.2.7.1 Shaft diameters

Each shaft diameter is calculated by the formula: $\boldsymbol{d = F.k.\sqrt[3]{\frac{P_B}{n(1-\frac{d_i}{d_a})}}.C_w}$

In the above formula:

- d_i, is the shaft diameter
- d_a is the outer shaft diameter
- $\left(1-\frac{d_i}{d_a}\right)$=1 considering d<0.4$d_a$
- F=100 for Diesel engines
- C_w is a material constant, $C_w = \frac{560}{\sigma_u+160}$, where σ_u is the tensile strength of the material.
- P_B, is the brake power before the thrust bearing
- N are the relevant rpm
- k, is a constant that is:
  - 1 for the intermediate shaft,
  - 1.1 for the thrust shaft, provided that it is separate from the engine components

- 1.22 for propeller shafts and keyless propellers or 1,26 in the case of key.

2.2.7.2 Shaft lengths

According to GL 2008 method [38], each shaft length is calculated as the maximum distance between bearings by the formula: $\boldsymbol{l_{max} = k_1\sqrt{d}}$. In this formula:

- d, is the relevant shaft diameter in mm
- k1,
  - is 450 oil lubricated white metal
  - is 280 for grease lubricated grey metal
  - lies between 280-350 for water lubrication

However, this formula provides extreme measurements for a typical shaft length. So, regression formulae from actual ship data [27] are used. Specifically, for the propeller shaft length and intermediate shaft length, the relevant equations are:

- $\boldsymbol{l_{pr} = 4 \cdot 10^{-8} DWT^2 + 0.0126 DWT + 4938}$
- $\boldsymbol{l_{int} = 599.48 DWT^{0.2173}}$

2.2.7.3 Flanges

Flange diameters of each shaft are calculated as: $\boldsymbol{d_f = 2d}$, whereas the thickness is:

- 0.2d for the thrust and intermediate shaft
- 0.25d for the propeller shaft

2.2.7.4 Propeller shaft liners

Propeller shaft liners provide protection of the metal shaft from contact and corrosion from sea water. Thickness of propeller shaft liners is given in mm by the formula: $\boldsymbol{s = 0.03 d_{pr} + 7.5}$

2.2.7.5 Propeller

According to Schneekluth [25], the propeller weight on air is calculated as $\boldsymbol{W_{p,air} = K_p {D_{pr}}^3}$ for manganese bronze propellers, where K_p is a coefficient that can be estimated by the formula:

$$\boldsymbol{K_p = \frac{d_{pr}}{D_{pr}}\left(1.85\frac{A_E}{A_O} - \frac{z-2}{100}\right)}$$

2.2.7.6 Weights

Thrust shaft weight is calculated as: $w_{th} = \pi \frac{d_{th}^2}{4} l_{th} \rho_{st}$

Intermediate shaft weight is calculated as: $w_{int} = \pi \frac{d_{int}^2}{4} l_{th} \rho_{st}$

Propeller shaft weight is calculated as: $w_{pr} = \pi \frac{d_{pr}^2}{4} l_{th} \rho_{st}$

Thrust shaft flange weight is calculated as: $w_{f,th} = \pi \frac{d_{fth}^2}{4} t_{th} \rho_{st}$

Intermediate shaft flanges weight is calculated as: $w_{f,int} = 2\pi \frac{d_{fint}^2}{4} t_{int} \rho_{st}$

Propeller shaft flanges weight is calculated as: $w_{f,pr} = \pi \frac{d_{fpr}^2}{4} t_{pr} \rho_{st}$

Propeller shaft liners weight is calculated as: $w_{p,ln} = 2\pi \frac{s^2 - d_{pr}^2}{4} l_{pr} \rho_{sst}$

Propeller weight in water is calculated as: $W_{pr} = K_p {D_{pr}}^3 (1 - \frac{\rho_w}{\rho_{mb}})$

The total shafting weight is: $\boldsymbol{W_{sh} = W_{pr} + w_{pr} + w_{pr,f} + w_{p,ln} + w_{int} + w_{f,int} + w_{th} + w_{f,th}}$

2.2.8 Friction Calculation

Friction calculation is separated in two stages. At first the calculation of friction for shafting system components, then friction calculation for the Diesel engine.

2.2.8.1 Friction at the shafting system

Friction at the shafting system is lost in the transmission of power from the engine to the propeller. Energy is lost as heat transfer at the bearings and every contact part along the shafting line. Mainly, losses occur at the thrust bearing, the intermediate bearing(s) and the aft and forward propeller bearings.

Friction of shafting system is estimated for both MCR service condition and partial engine load. A quick method in order to estimate accurately the friction losses is the use of Sommerfeld number for a shafting system operating under steady state. To determine load-carrying capacity or any other bearing characteristic, the eccentricity ratio must first be determined. The Sommerfeld number is a dimensionless parameter related to the eccentricity ratio, given by: $\boldsymbol{S = \frac{\mu N D L}{W} (\frac{R}{C})^2}$

In the above relation:

- μ is the dynamic viscosity of the lubrication oil
- N are the revolutions of the shaft
- W is the load carried to the bearing
- D is the inner diameter of the bearing
- L is the length of the bearing
- R is the radius of the bearing
- C is a radial clearance

The radial clearance is calculated as: $C = 0.002d$, where d is the diameter of each shaft. Consequently, diameter of bearing is: $\boldsymbol{D = d + 2C}$. An $\frac{L}{D}$ ratio is considered for bearings of each shaft. Specifically, $\frac{L}{D}$ is taken as:

- 1 for intermediate and thrust shaft bearings
- 2 for the aft propeller shaft bearing
- 0.8 for the forward propeller shaft bearing

In order to calculate the friction losses, the load is assumed to be distributed at the bearings depending on their size. In other words, the pressure, p_{sh}, applied to each bearing, resulting from the total weight, is constant. If w_{ap}, w_{fp}, w_{int}, w_{th} are the respective weights that each bearing is able to carry, then the shafting weight is: $\boldsymbol{W_{th} = w_{ap} + w_{fp} + \frac{w_{int}}{z_{int}} + w_{th}}$ where z_{int} is the number of intermediate bearings. For each of the respective bearings, the weight and the pressure are dependent on the contact surface, $\boldsymbol{w_i = pA_i}$. These two relations, yield that: $\boldsymbol{p_{sh} = \frac{W_{sh}}{\sum A_i}}$ where ΣA_i is the total area of all bearings on which the weight is applied. Since the journal is cylindrical, $A_i = LD$. After establishing these parameters, the Sommerfeld number is calculated. For each bearing, for the

calculated Sommerfeld number, according to Booser [18], a dimensionless $f\frac{R}{C}$ coefficient is given, where f is the friction coefficient. Friction force is calculated as: $F_{f,i} = fw_i$ and power lost to each bearing is given by the relation: $P_{f,i} = 2\pi RNF_{f,i}$. By performing this method for every bearing, the total shafting friction power loss is: $\boldsymbol{P_f = P_{f,ap} + P_{f,fp} + P_{f,int} + P_{f,th}}$

2.2.8.2 Engine Friction

The mechanical losses of a Diesel engine are difficult to estimate without direct measurement of the installation in operation, or actual data. For the purpose of this study, the mean pressure of mechanical losses is estimated through the following three empirical models, which provide friction loss estimation with the use of common engine parameters as input.

2.2.8.2.1 Mrzljak model

According to this model, the mean friction pressure loss is given by the empirical formula:

$\boldsymbol{p_{f,mr} = k_1\left(1 + \frac{1}{Z_{cyl}}\right) + \frac{3}{D_{cl}} + k_2 mep + k_3 c_s}$ where:

- k_1=0.0384, k_2=0.018, k_3=0.04
- D_{cl} is the engine bore in mm
- mep is the engine mean effective pressure in MPA
- c_s is the mean piston speed in m/s

Mechanical losses power is then given by the formula: $\boldsymbol{P_{fr,mr} = \frac{\pi Z_{cyl} S_{en} D_{cl}{}^2 p_{f,mr} N}{60}}$

2.2.8.2.2 Millington model

According to this model, the mean friction pressure loss is given by the empirical formula:

$\boldsymbol{p_{f,ml} = 6895(R_{en} - 4) + 48.2N + 401 c_s{}^2}$, where R_{en} is the compression ratio of the engine.

Mechanical losses power is then given by the formula: $\boldsymbol{P_{fr,ml} = \frac{\pi Z_{cyl} S_{en} D_{cl}{}^2 p_{f,ml} N}{60}}$

2.2.8.2.3 Petrovsky model

According to Petrovsky, the mechanical losses power of a two-stroke marine Diesel engine can be expressed with an experimental model of the form:

$\boldsymbol{P_{fr,pt} = AN^b}$, where A is a constant and $1.0 < b < 1.2$ for low-speed engines.

Mrzljak and Millington models are used in order to calculate constant A for the MCR point of the vessel. So, $A = \frac{\frac{P_{fr,mr} + P_{fr,ml}}{2}}{N_{mcr}{}^b}$, while b is calculated with linear interpolation according to engine model (engine size).

Friction power loss is calculated as the average of the three above models:

$$\boldsymbol{P_{fr} = \frac{P_{fr,mr} + P_{fr,ml} + P_{fr,pt}}{3}}$$

Friction calculation is done for both MCR point and the arbitrate operational point.

2.3 Single vessel example

Before proceeding to fleet scale calculations, a vessel example is illustrated. The calculation procedure is done twice; one for the MCR service point and one for an operational service point. As a

reference, a Panamax vessel of a 75000-t deadweight will be used, from the data of the study done by Georgakis [27]. Data of the reference vessel are stated in the following table:

Table 2.6 Principal particulars

REFERENCE VESSEL DATA	
L_{OA}	225 m
L	217.51 m
B	31.96 m
D	19.44 m
T scantling	14.04 m
T design	12.5 m
Service speed	14.5 kn
C_B	0.86
DWT	75314 t
Δ	87003 t
Engine model	MAN 5-S60MC-C
Brake power	8990 kW
Revolutions at MCR	101 RPM
Propeller diameter	6.75 m

2.3.1 Calculation of vessel parameters

2.3.1.1 Length

The equations used for the length calculation provided the following results.

Table 2. 7 Length values

EQUATION	VALUE
Papanikolaou	220.94 m
Misra	211.57 m
Average of Papanikolaou and Misra	216.25 m
SeaWeb	**217.51 m**
Optimum equation	216.25 m

Since the length of the reference vessel is 217 m, the SeaWeb equation provided the most accurate results.

LCF=0.48L=104.44 m

Lwl=224.31 m

2.3.1.2 Depth

The equations used for the depth calculation provided the following results.

Table 2.8 Depth values

EQUATION	VALUE
Papanikolaou	19.13 m
Misra	19.14m
Average of Papanikolaou and Misra	19.14 m
SeaWeb	**19.44 m**
Optimum equation	19.14 m

Since the depth of the reference vessel is 19.6 m, the SeaWeb equation provided the most accurate results.

2.3.1.3 Breadth

The equations used for the breadth calculation provided the following results.

Table 2.9 Breadth values

EQUATION	VALUE
Papanikolaou	34.16 m
Papanikolaou	33.73 m
Misra	35.77 m
Average of Papanikolaou and Misra	34.55 m
SeaWeb	**31.96 m**
Optimum equation	33.73 m

Since the breadth of the reference vessel is 32.26 m, the SeaWeb equation provided the most accurate results.

2.3.1.4 Draft

The draft of the example vessel is calculated with the relation: $T = \frac{D}{1.385}$. The result provided was **14.04** m. Since the vessel is even keel, $T=T_A=T_F$.

2.3.1.5 Deadweight to displacement ratio

$$\frac{DWT}{\Delta} = 0.46676 DWT^{0.0529501} = \mathbf{0.846}$$

2.3.1.6 Lightship weight

$$LS = 6.5134 DWT^{0.678895} = \mathbf{13288.1}\ t$$

2.3.1.7 Displacement

$$\Delta = LS + DWT = \mathbf{88288.1}\ t$$

2.3.1.8 Block coefficient

For the block coefficient estimation, the average of the two empirical methods provided by Papanikolaou are used.

$$C_{B1} = 0.515788 DWT^{0.042626} = 0.832$$

$$C_{B2} = \frac{1000\Delta}{\rho k_{dwt} LBT} = 0.885$$

$$C_B = \frac{C_{B1} + C_{B2}}{2} = \mathbf{0.858}$$

2.3.1.9 Midship coefficient

Midship coefficient is calculated by using the Kerlen equation:

$$C_M = 1.006 - 0.0056{C_B}^{-3.56} = \mathbf{0.996}.$$

2.3.1.10 Prismatic coefficient

$$C_P = \frac{C_B}{C_M} = \mathbf{0.858}$$

2.3.1.11 Waterplane area coefficient

Waterplane area coefficient is calculated by using the equation for average hull:

$$C_{WP} = \frac{1 + 2C_B}{3} = \mathbf{0.903}$$

2.3.1.12 LCB

LCB is calculated from the equation of BSRA:

$$LCB = 20(C_B - 0.675) = \mathbf{116.735}\ m$$

2.3.1.13 Wetted surface

The naked hull wetted surface is calculated using the LAP-KELLER relation:

$$S_{hull} = \nabla^{\frac{1}{3}}(3.4\nabla^{\frac{1}{3}} + \frac{L_{WL}}{2}) = \mathbf{11527.38}\ \boldsymbol{m^2}$$

The rudder projected area is:

$$A_{rud} = 2\frac{LT_A}{100}((\frac{B}{L})^2 50{C_B}^2 + 1) = \mathbf{109.28}\ \boldsymbol{m^2}$$

The bilge keel configuration considered for the vessel is the BK15 [see appendix]. This yield:

$$A_{bk} = 2\frac{(2l_{bk}\ b_{bk} + l_{bk} w_{bk})}{\cos\theta_{bk}} = \mathbf{101.54}\ \boldsymbol{m^2}$$

The total wetted surface is then: $\boldsymbol{S = 11738.2\ m^2}$

2.3.1.14 Propeller Diameter

The propeller diameter is calculated as: $D_{pr} = 0.395T_A + 1.3 = \mathbf{6.84\ m}$

2.3.1.15 Reynolds and Froude Numbers

$$R_n = L_{wl}\frac{V}{u} = \mathbf{1.407 \cdot 10^9}$$

$$F_n = \frac{V}{\sqrt{gL_{wl}}} = \mathbf{0.159}$$

2.3.1.16 Frictional resistance

According to ITTC the frictional resistance coefficient is:

$$C_f = \frac{0.075}{(\log(R_n) - 2)^2}$$

The frictional resistance is then calculated as:

$$R_f = \frac{1}{2}\rho C_f S V^2 = \mathbf{491.687\ kN}$$

2.3.1.17 Viscous pressure resistance

The Holtrop calculation method is used to estimate the viscous pressure resistance of the vessel:

$$1 + k = 0.93 + 0.487118(1 + 0.011C_{stern}) \cdot$$

$$\cdot \left(\frac{B}{L}\right)^{1.06806}\left(\frac{T_M}{L}\right)^{0.46106}\left(\frac{L_{wl}}{L_R}\right)^{0.121563} \cdot$$

$$\cdot \left(\frac{{L_{wl}}^3}{\nabla}\right)^{0.36486}(1 - C_P)^{-0.604247}$$

$$C_{stern} = 0$$

$$L_R = L_{wl}\frac{1 - C_P + 0.06C_P\frac{LCB}{L}}{4C_P - 1}$$

So, the viscous resistance is a k fraction of the frictional: $R_{vp} = kR_f = \mathbf{128.854}\ kN$

2.3.1.18 Wave-making resistance

The wave-making resistance is considered as **5**% of the total resistance.

2.3.1.19 Air resistance

For the calculation of the air resistance, the ITTC '78 method is used.

$$C_{air} = 0.001\frac{(A_{ts} + A_{ls})}{S}$$

$$R_{air} = \frac{1}{2}C_{air}\rho_{air}\left(A_{ts+}A_{ls} + 2L(D-T)\right)(V - V_{air})^2 = \mathbf{2.165\ kN}$$

A_{ts} and A_{ls} are the transverse and longitudinal surfaces of superstructures exposed to air motion respectively, for a head-to-head vessel-air direction.

2.3.1.20 Correlation resistance

For the correlation resistance, the Bowden formula is used.

$$C_a = 0.105(\frac{AHS}{Lwl})^{\frac{1}{3}} - 0.00064$$

The correlation resistance is then calculated as:

$$R_a = \frac{1}{2}\rho C_a S V^2 = \mathbf{34.092\ kN}$$

2.3.1.21 Total resistance

The total resistance, for a 15% fouling increase and 10% weather conditions increase, is:

$$R_{t,fw} = 1.05(R_f + R_{vp} + R_a + R_{air})(1 + m_{fl}m_{ww}) = \mathbf{681.839\ kN}$$

Total resistance in ballast condition for a 15% fouling increase and 10% weather conditions increase, is:

$$R_{t,fw} = \mathbf{852.3\ kN}$$

2.3.1.22 Main engine and maximum service point M

According to the total resistance for the maximum load draft condition, the engine installed is the following:

Table 2.10 Engine details of vessel

ENGINE MAIN DATA	
Maker	MAN
Model	7G50ME-C9.6
Bore	0.5
Stroke	2.5
Cylinder Number	7
Compression Ratio	15.05

The propeller law for this service point is: $\boldsymbol{P = 0.00262N^{3.2}}$

2.3.1.23 Wake field

The average wake field as shown in [paragraph] is: $w = 0.288$

2.3.1.24 Thrust deduction factor

The thrust deduction factor as shown in [paragraph] is: $t = 0.412$

2.3.1.25 Hull efficiency

The hull efficiency as shown in [paragraph] is: $n_h = 1.21$

2.3.1.26 Relative rotative efficiency

The Relative rotative efficiency as shown in [paragraph] is: $n_R = 1.022$

2.3.1.27 Open water efficiency

The open water efficiency as shown in [paragraph] is: $n_o = 0.463$

2.3.1.28 Shafting efficiency

Shafting efficiency is $n_S = 0.98$

2.3.1.29 Propulsion efficiency

Propulsion efficiency is $n_P = 0.56$

Power at MCR service point is: $P_s = 8480\ kW$

Propeller revolutions at MCR point are: $N_{MCR} = 91.2\ RPM$

2.3.1.30 Shafting system dimensions and weights:

Table 2.11 Shafting system weights

PARAMETER	VALUE
Total weight [kg]	28907.7
Propeller weight [kg]	14.68
Propeller Shaft Diameter [m]	0.436
Propeller Shaft Length [m]	6.11
Propeller Shaft Weight [kg]	7174.36
Propeller Shaft Flange Diameter [m]	0.873
Propeller Shaft Flange Length [m]	0.109
Propeller Shaft Flange Weight [kg]	512.68
Aft Bearing Diameter [m]	0.437
Aft Bearing Length [m]	0.873
Forward bearing Diameter [m]	0.436
Forward bearing Length [m]	0.327
Propeller Shaft Liners Width [m]	0.021
Propeller Shaft Liners Weight [kg]	783.7
Intermediate Shaft Diameter [m]	0.358
Intermediate Shaft Length [m]	6.873
Intermediate Shaft Weight [kg]	5423.6
Intermediate Shaft Flange Diameter [m]	0.716
Intermediate Shaft Flange Width [m]	0.054
Intermediate Shaft Flange Weight [kg]	338.8

Intermediate Bearing Diameter [m]	0.358
Intermediate Bearing Length [m]	0.358

Table 2.12 Materials

MATERIALS	VALUES
Viscosity of shaft lubricating oil [Pa.s]	0.3
Steel density [t/m^3]	7850
Stainless steel density [t/m^3]	8000
Manganese Bronze density [t/m^3]	8359

2.3.2 Calculation procedure results

2.3.2.1 Power and revolutions at different voyage conditions

Table 2.13 Power and propeller revolutions at each voyage

Loading Condition Draft	Hull Condition	Power		Revolutions	
		MCR	Operational	MCR	Operational
Summer Load	Clean Hull	8480	4152	91.2	73
	Partially Fouled Hull	11197	99	5482.7	79.4
	Fully Fouled Hull	11320	99	5543	79
Partially Laden	Clean Hull	9404	94.2	4605	75.4
	Partially Fouled Hull	12445	102.5	6094	82
	Fully Fouled Hull	12582	102	6161	82
Full Ballast	Clean Hull	11428	5596	100	80
	Partially Fouled Hull	15154	119	7421	95
	Fully Fouled Hull	15319	119	7501	94.8

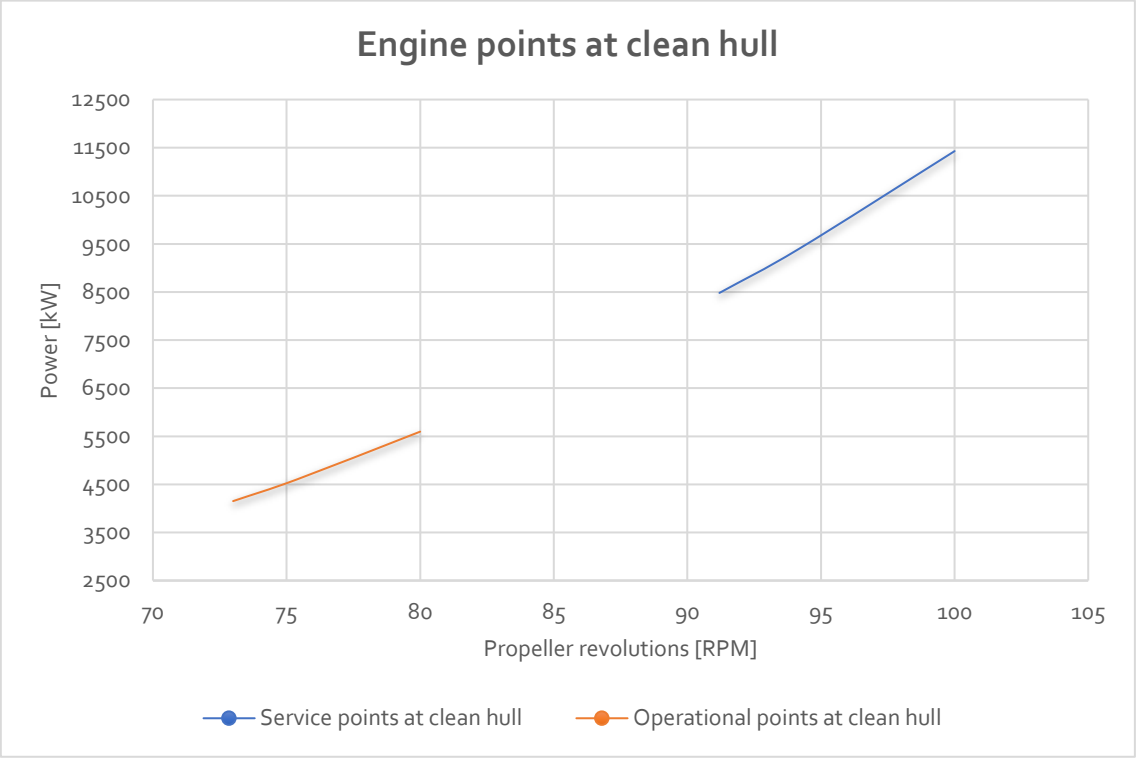

Figure 2.6 Engine operating points-Clean hull

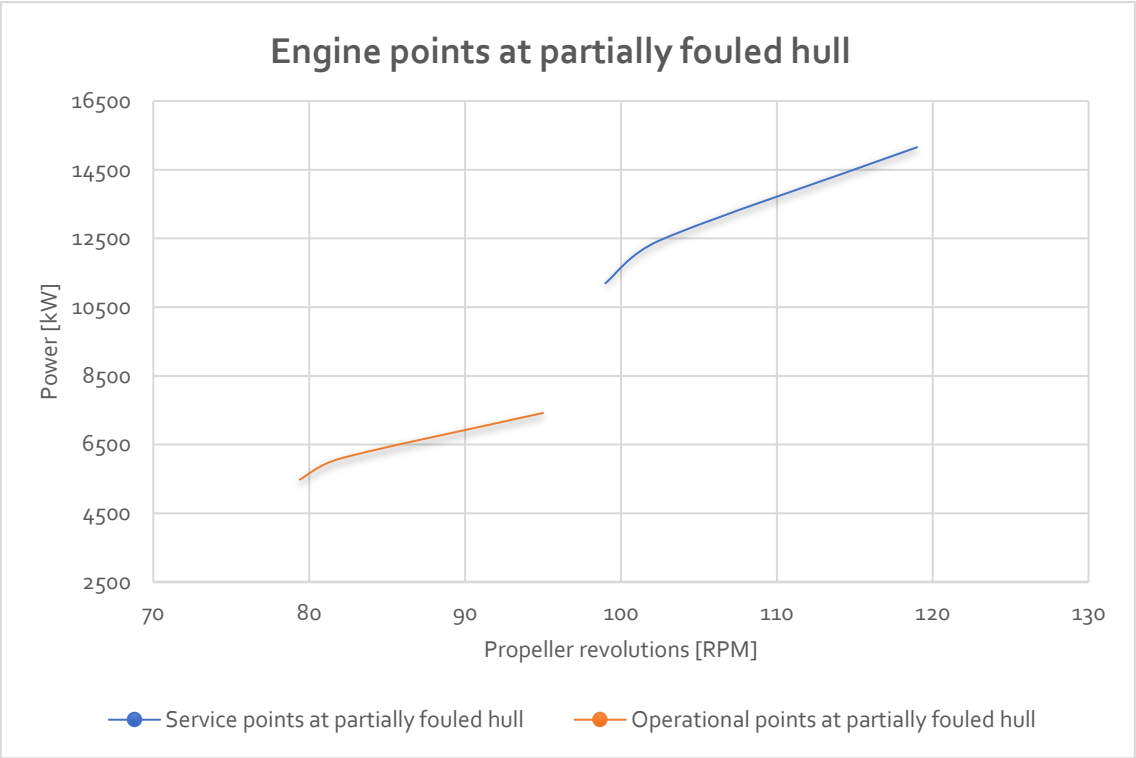

Figure 2.7 Engine operating points at partially fouled hull

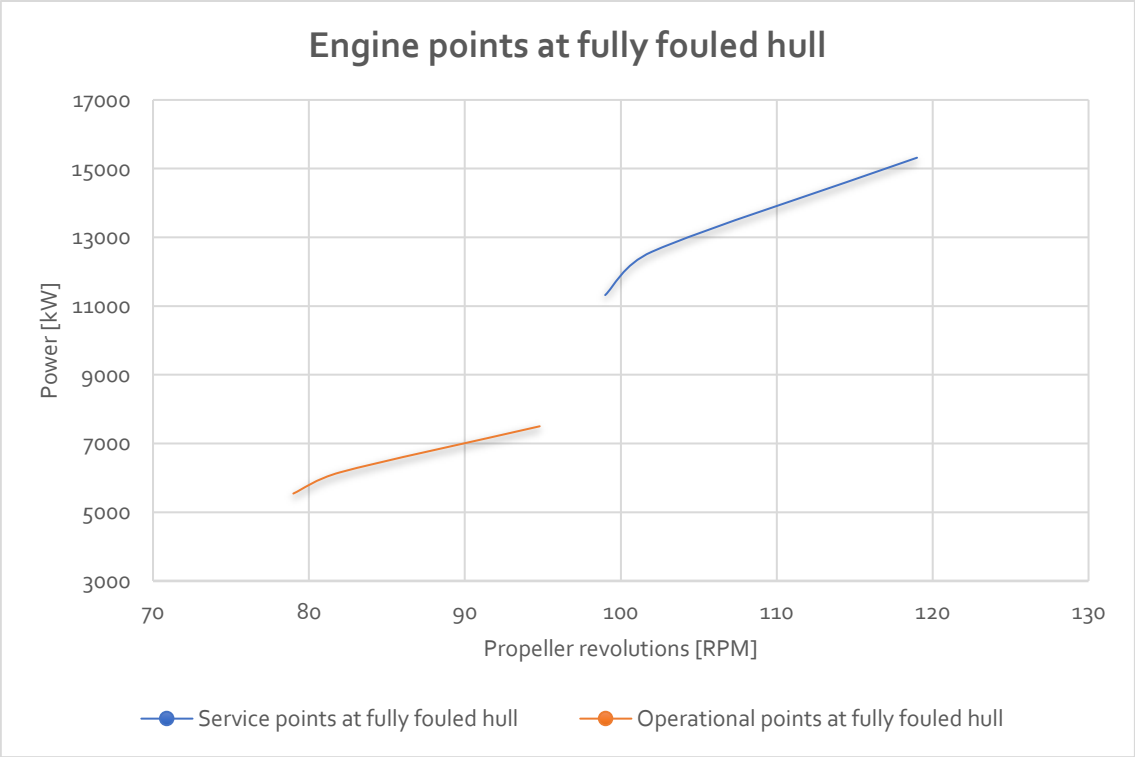

Figure 2.8 Engine operating points at fully fouled hull

2.3.2.2 Shafting friction

Table 2.14 Shafting frictional losses

Loading Condition Draft	Hull condition	Shafting friction in kW		Shafting friction in % of brake power	
		MCR	Operational	MCR	Operational
Summer Load	Clean Hull	11.948	7.685	0.141	0.185
	Partially Fouled Hull	14.123	9.066	0.126	0.165
	Fully Fouled Hull	14.038	9.011	0.124	0.163
Partially Laden	Clean Hull	12.599	8.064	0.134	0.175
	Partially Fouled Hull	15.070	9.673	0.121	0.159
	Fully Fouled Hull	14.980	9.617	0.119	0.156
Full Ballast	Clean Hull	14.169	9.070	0.124	0.162
	Partially Fouled Hull	20.203	12.970	0.133	0.175
	Fully Fouled Hull	20.102	12.910	0.131	0.172

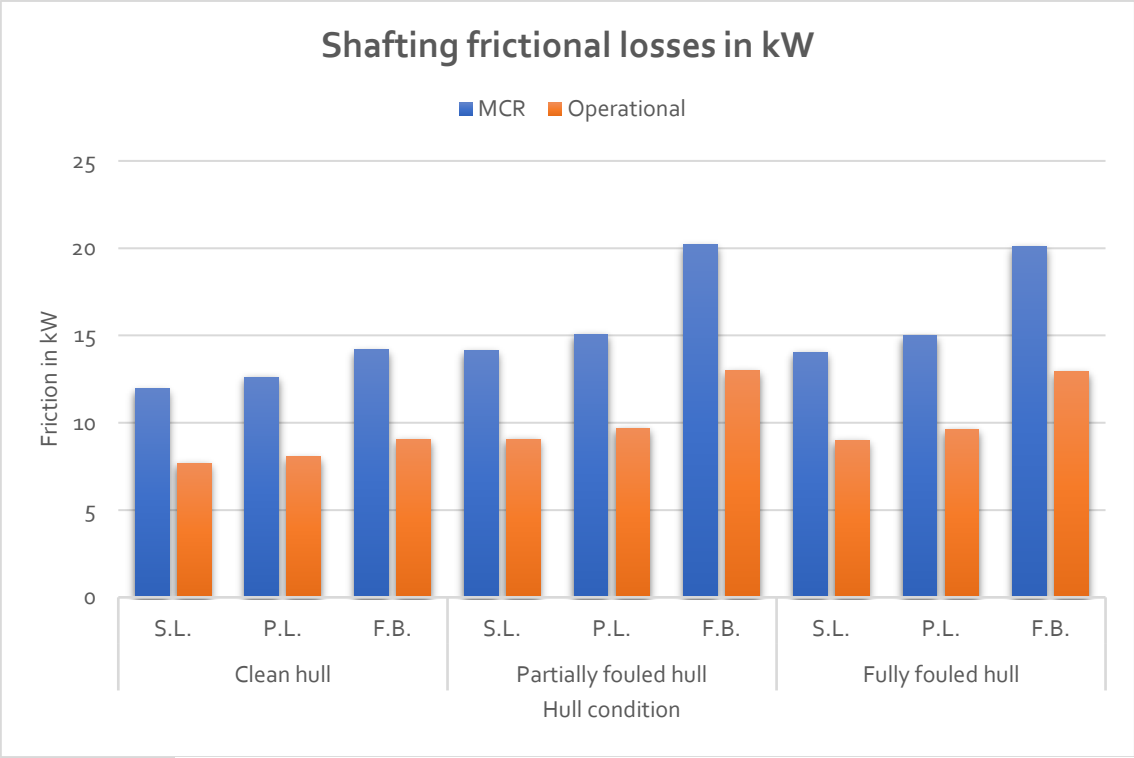

Figure 2.9 Shafting frictional losses in kW

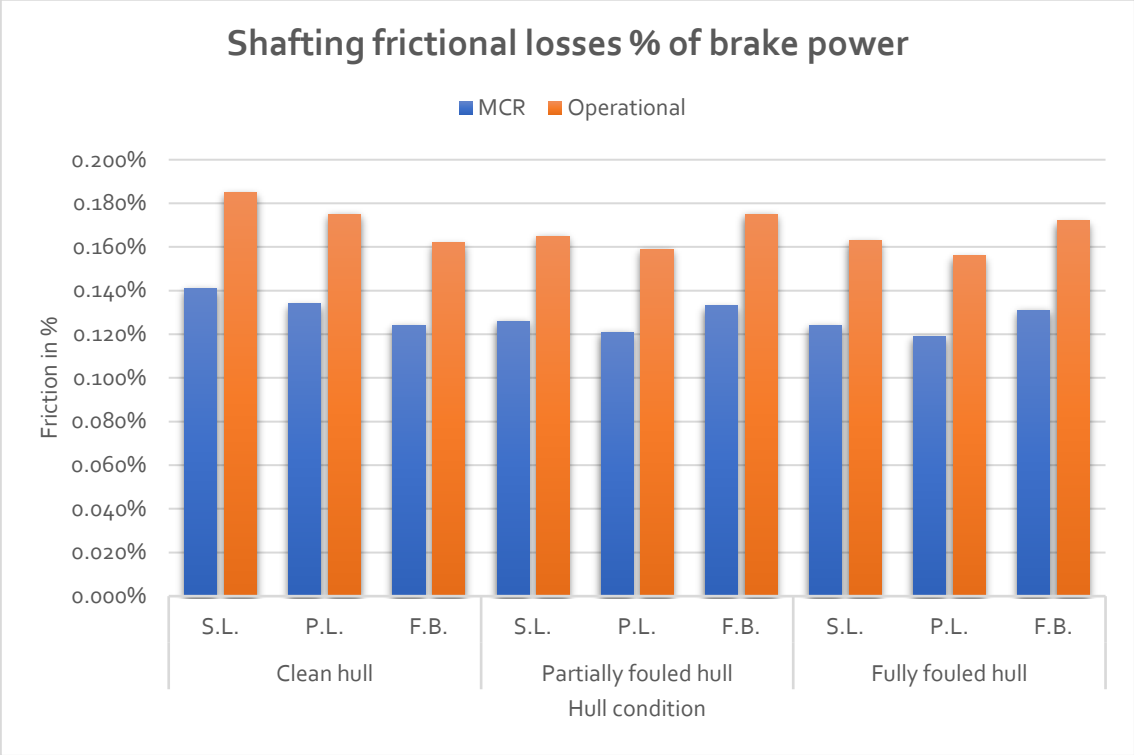

Figure 2.10 Shafting frictional losses in %

2.3.2.2.1 Aft bearing friction

Table 2.15 Aft bearing losses

Loading Condition Draft	Hull condition	Total friction in kW		Total friction in % of brake power	
		MCR	Operational	MCR	Operational
Summer Load	Clean Hull	7195.68	4616.23	0.085	0.1112
	Partially Fouled Hull	8512.57	5448.61	0.076	0.0994
	Fully Fouled Hull	8461.34	5415.7	0.0747	0.0977
Partially Laden	Clean Hull	7627.71	4882.5	0.0811	0.106
	Partially Fouled Hull	9086.32	5817.15	0.07301	0.0955
	Fully Fouled Hull	9033.39	5783.14	0.0718	0.0981
Full Ballast	Clean Hull	8578.43	5491.01	0.07506	0.0981
	Partially Fouled Hull	12194.8	7814.39	0.0805	0.1053
	Fully Fouled Hull	12133.7	7774.97	0.0792	0.1036

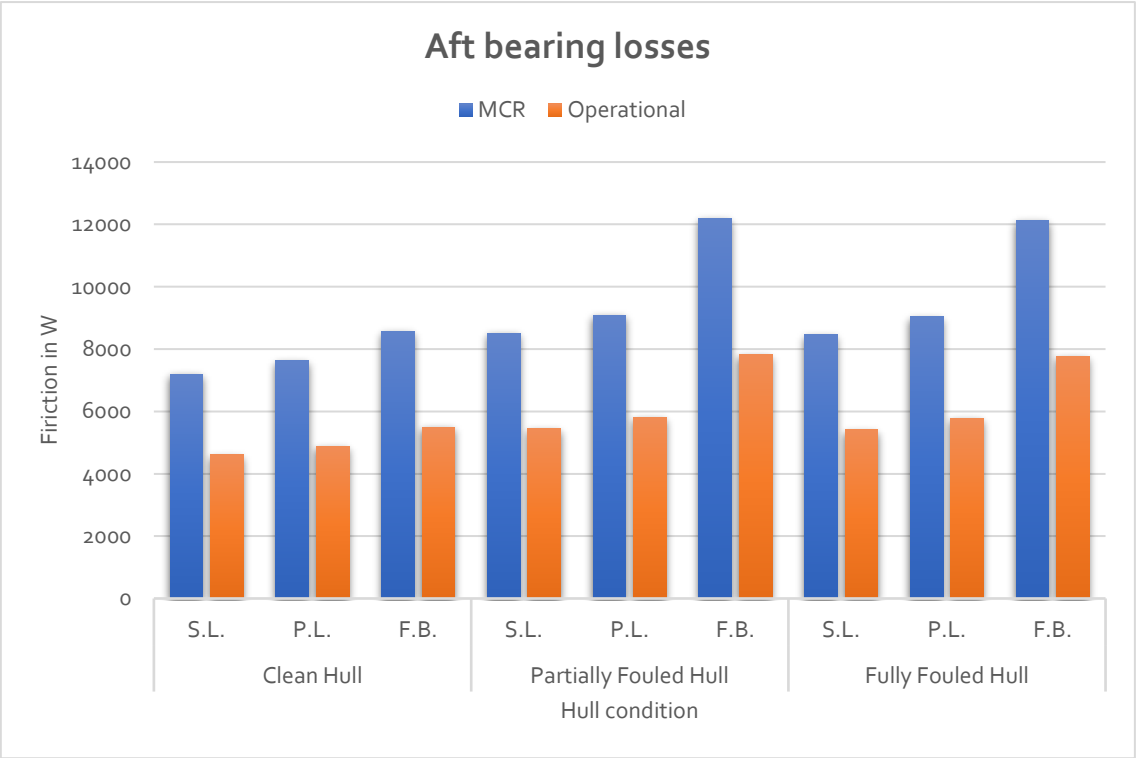

Figure 2.11 Aft bearing losses in kW

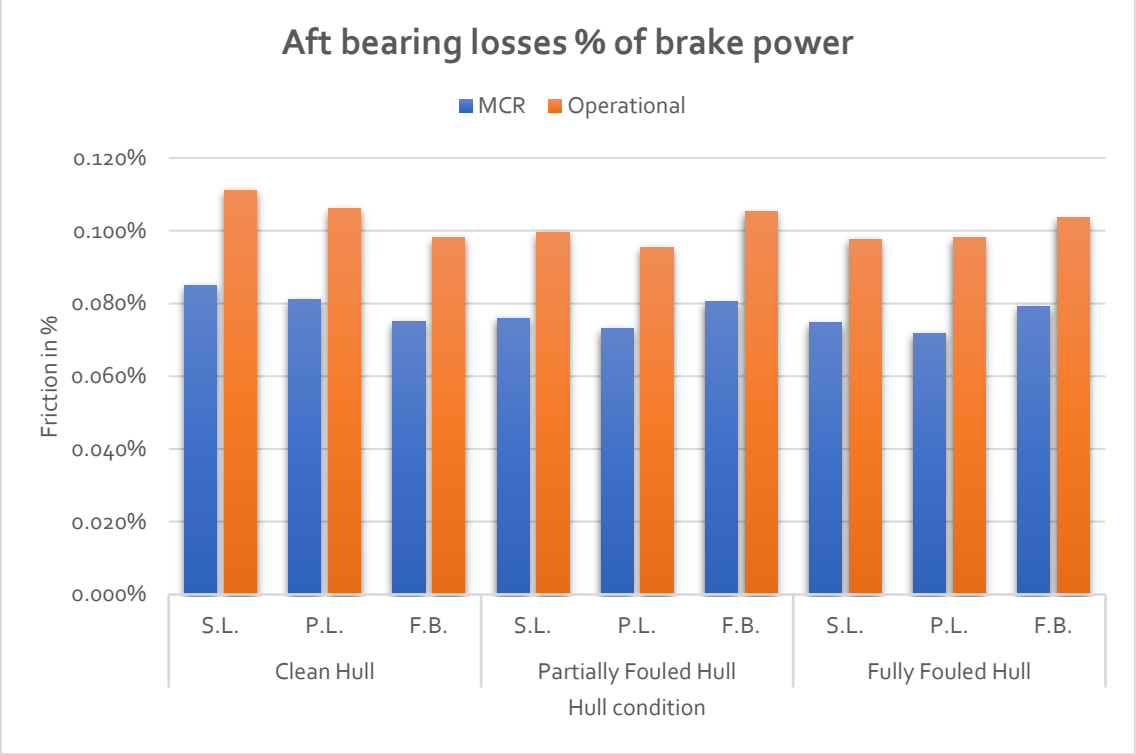

Figure 2.12 Aft bearing losses %

2.3.2.2.2 Fore Bearing losses

Table 2.16 Forward bearing losses

Loading Condition Draft	Hull condition	Total friction in kW		Total friction in % of brake power	
		MCR	Operational	MCR	Operational
Summer Load	Clean Hull	2753.57	1782.71	0.0325	0.0429
	Partially Fouled Hull	3249.13	2099.44	0.029	0.0383
	Fully Fouled Hull	3229.86	2087.1	0.02853	0.03765
Partially Laden	Clean Hull	2867.23	1835.74	0.0305	0.0399
	Partially Fouled Hull	3646.94	2237.62	0.0278	0.0367
	Fully Fouled Hull	3445.03	2224.88	0.0274	0.0361
Full Ballast	Clean Hull	3224.43	2064.39	0.0282	0.0369
	Partially Fouled Hull	4632.62	2986.97	0.0306	0.0403
	Fully Fouled Hull	4609.6	2972.18	0.0301	0.0396

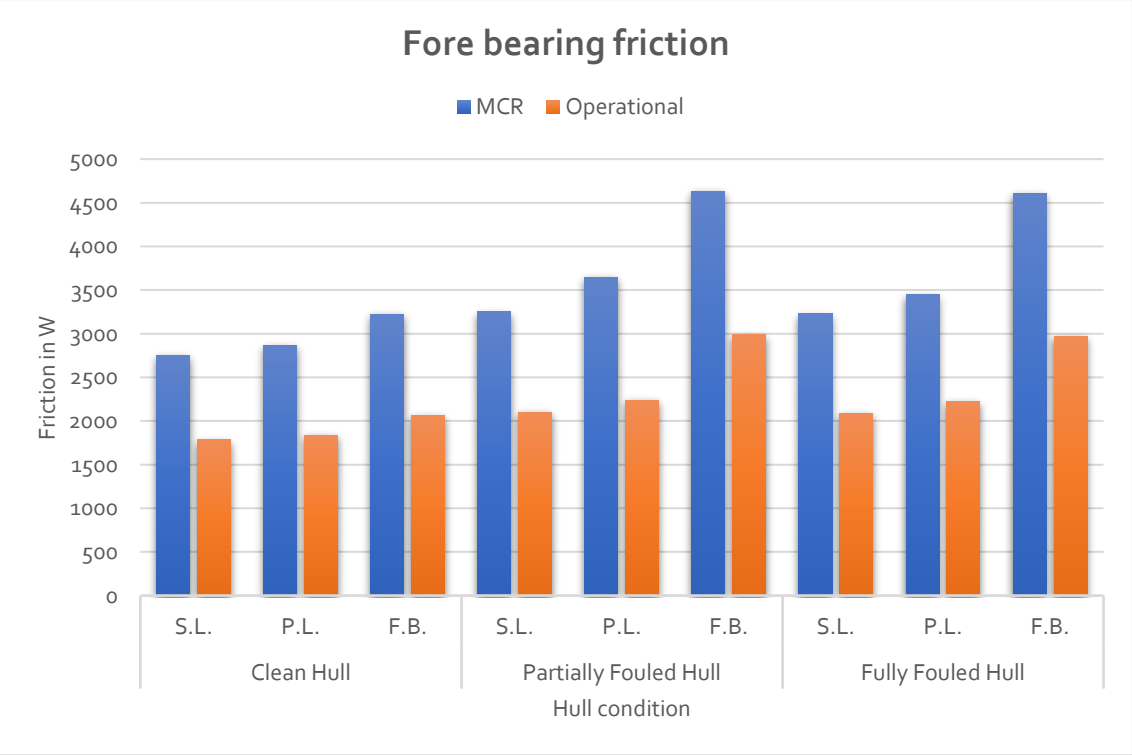

Figure 2.13 Forward bearing losses in kW

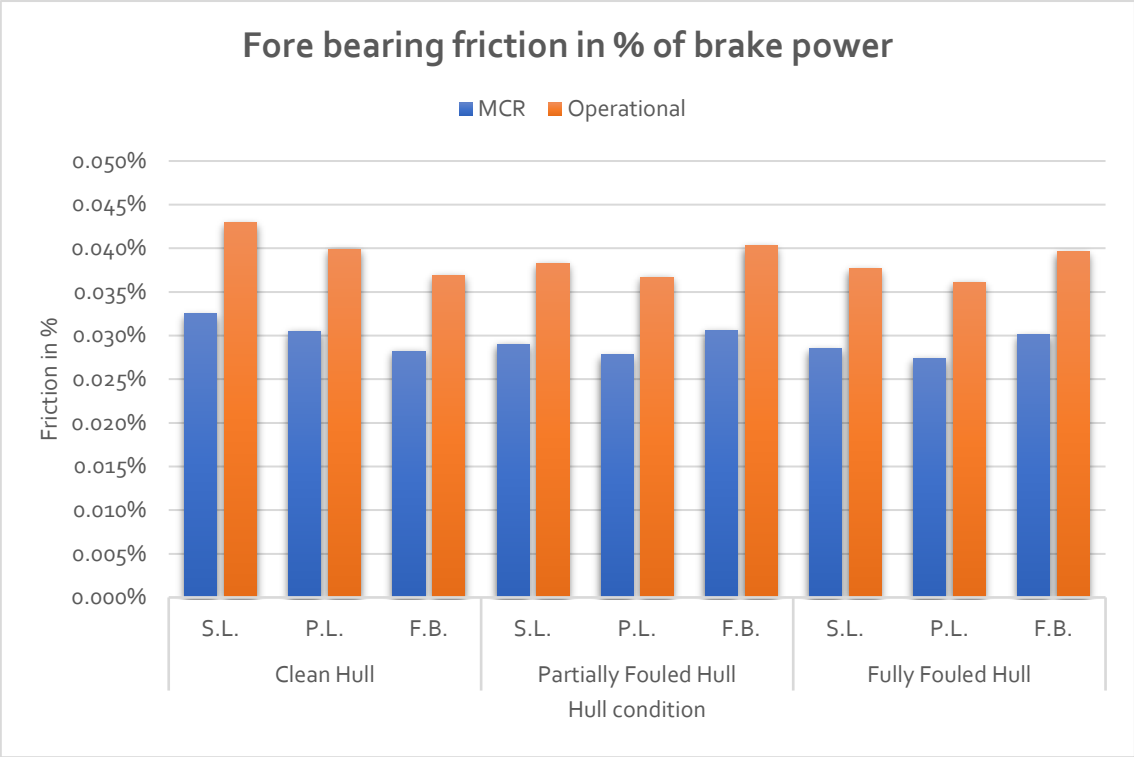

Figure 2.14 Forward bearing losses %

2.3.2.2.3 Intermediate bearing losses

Table 2.17 Intermediate bearing losses

Loading Condition Draft	Hull condition	Total friction in kW		Total friction in % of brake power	
		MCR	Operational	MCR	Operational
Summer Load	Clean Hull	1998.85	1286.21	0.02357	0.03098
	Partially Fouled Hull	2360.96	1517.54	0.02109	0.02767
	Fully Fouled Hull	2346.84	1508.52	0.02073	0.02721
Partially Laden	Clean Hull	2103.64	1346.7	0.02237	0.02924
	Partially Fouled Hull	2519.11	1618.53	0.02024	0.02656
	Fully Fouled Hull	2504.52	1609.21	0.0199	0.02612
Full Ballast	Clean Hull	2365.78	1514.49	0.02070	0.02706
	Partially Fouled Hull	3375.45	2168.91	0.02227	0.02923
	Fully Fouled Hull	3358.56	2158.08	0.02192	0.02877

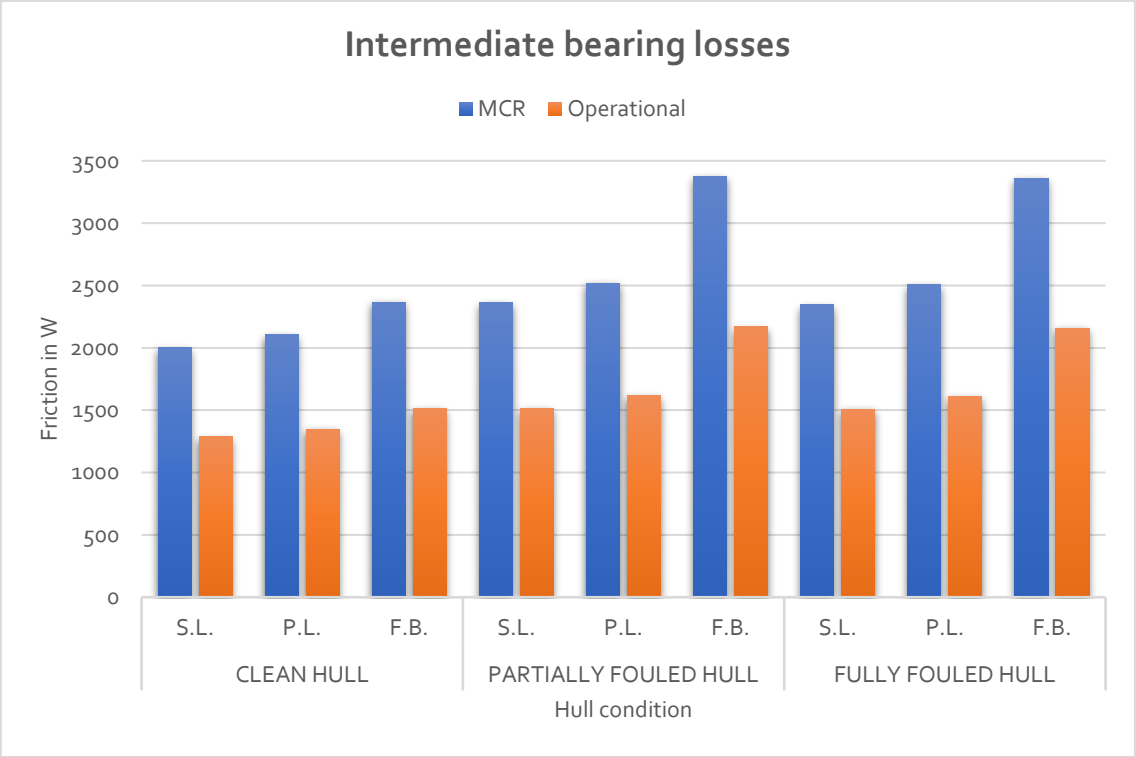

Figure 2.15 Intermediate bearing losses

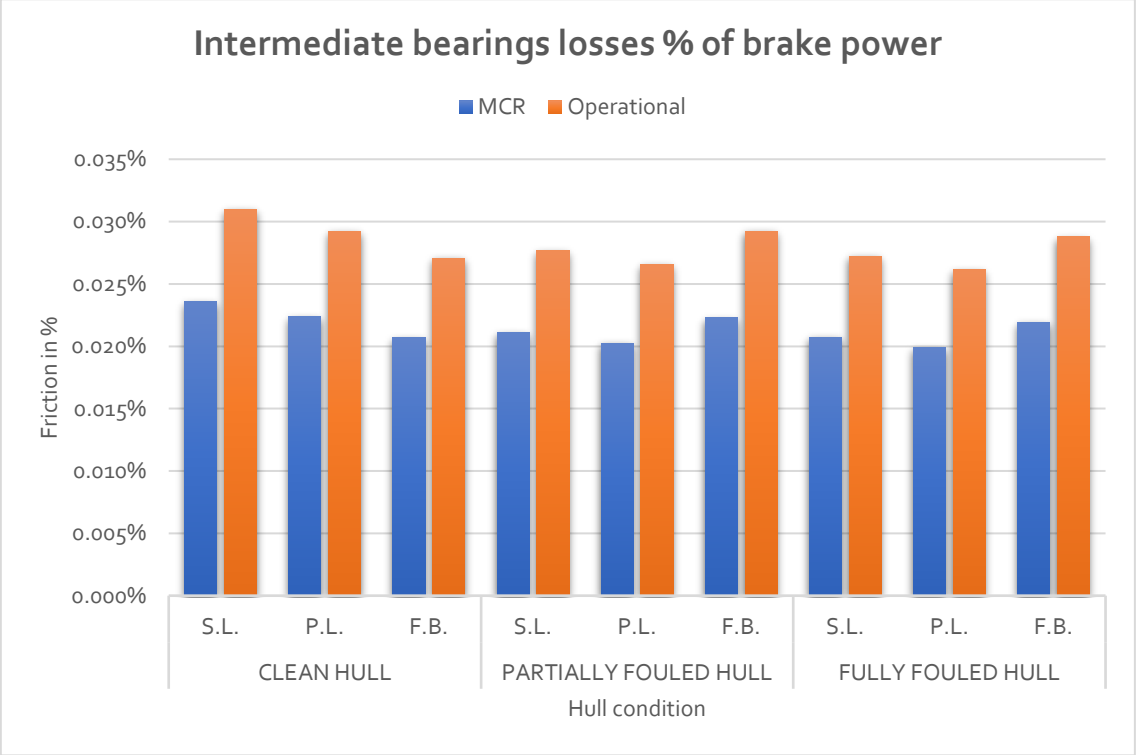

Figure 2.16 Intermediate bearing losses %

2.3.2.3 Engine friction

Table 2.18 Engine frictional losses

Loading Condition Draft	Hull condition	Engine friction in kW		Engine friction in % of brake power	
		MCR	Operational	MCR	Operational
Summer Load	Clean Hull	328.900	240	3.879	5.779
	Partially Fouled Hull	373.870	269.290	3.340	4.912
	Fully Fouled Hull	372.465	268.326	3.290	4.841
Partially Laden	Clean Hull	345.270	250.681	3.671	5.444
	Partially Fouled Hull	393.526	3.162	281.977	4.627
	Fully Fouled Hull	392.091	280.995	3.116	4.561
Full Ballast	Clean Hull	377.900	271.900	3.307	4.860
	Partially Fouled Hull	494.045	346.56	3.260	4.670
	Fully Fouled Hull	492.381	345.459	3.214	4.605

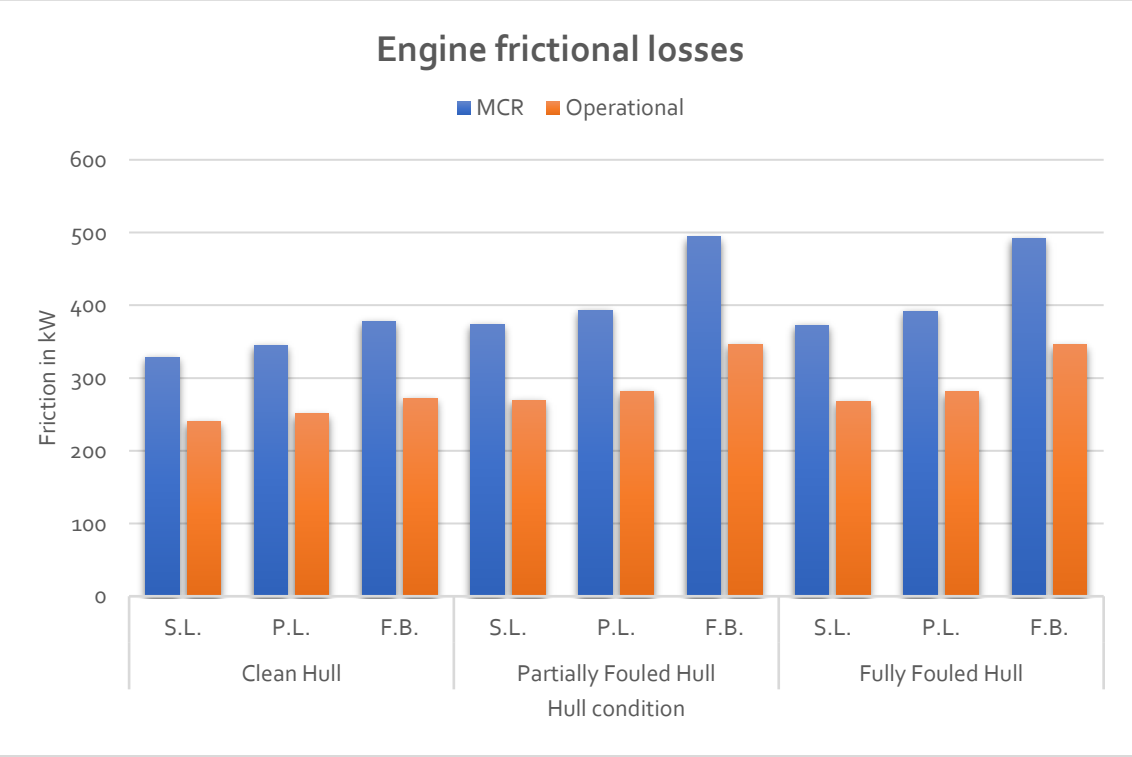

Figure 2.17 Engine frictional losses in kW

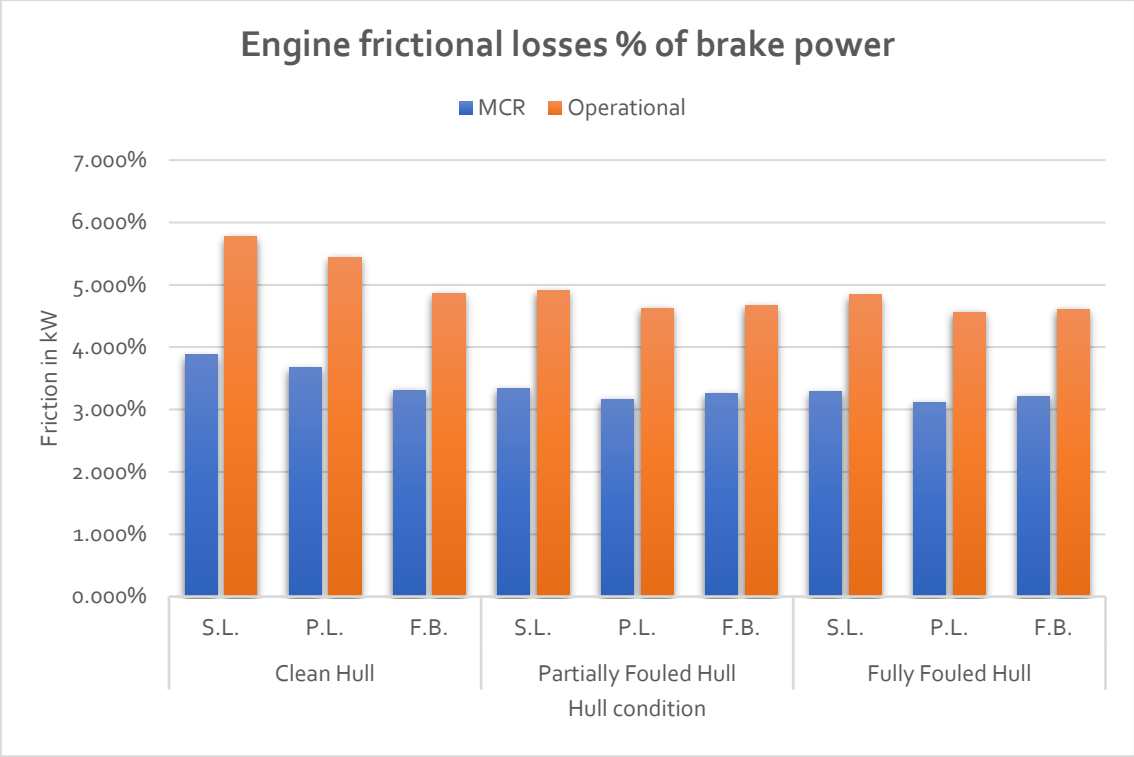

Figure 2.18 Engine frictional losses %

2.3.2.4 Total friction

Figure 2.19 Total frictional losses

Loading Condition Draft	Hull condition	Total friction in kW		Total friction in % of brake power	
		MCR	Operational	MCR	Operational
Summer Load	Clean Hull	340.86	247.611	4.02	5.964
	Partially Fouled Hull	387.991	278.357	3.465	5.077
	Fully Fouled Hull	386.503	277.338	3.414	5.003
Partially Laden	Clean Hull	357.867	258.746	3.805	5.619
	Partially Fouled Hull	408.597	291.65	3.283	4.786
	Fully Fouled Hull	407.074	290.613	3.235	4.717
Full Ballast	Clean Hull	392.111	281.004	3.307	5.021
	Partially Fouled Hull	514.248	359.531	3.393	4.845
	Fully Fouled Hull	512.482	358.364	3.345	4.777

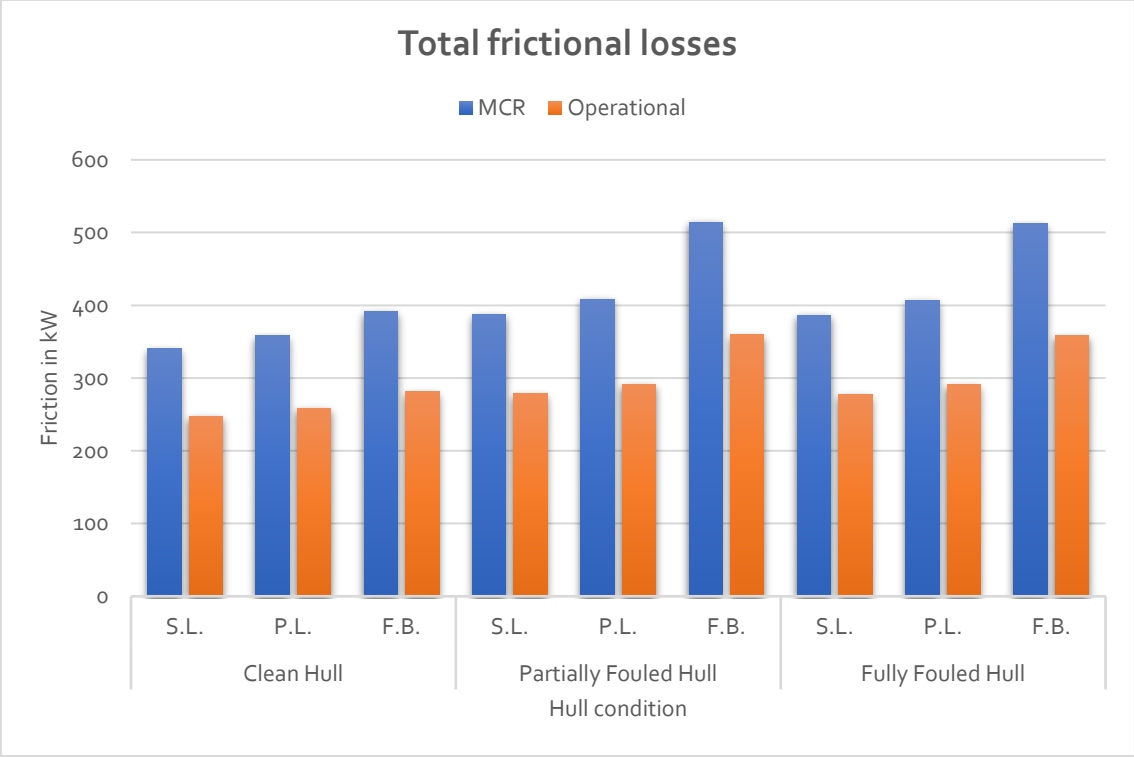

Figure 2.20 Total frictional losses in kW

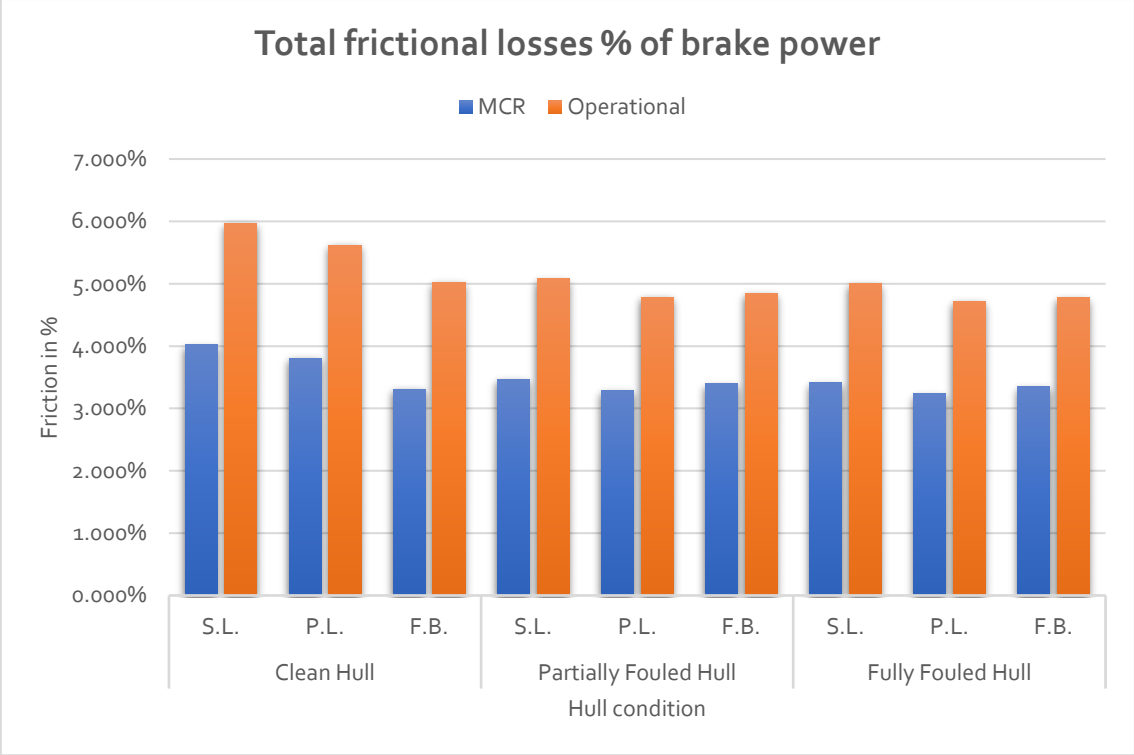

Figure 2.21 Total frictional losses in kW

3.Parametric study

3.1 Introduction

In this chapter a parametric study is performed on the attribute of friction losses according to the changing bulk carrier vessel class. The simulation is done for 100 vessels, 20 per vessel class, Handysize, Handymax, Panamax, Capesize, VLBC. Shafting friction losses, engine friction losses and total friction losses are illustrated in the following diagrams both in quantitative and percentage forms. Finally, based on these measurements, a regression model for friction power loss estimation is suggested, based on these values with the changing parameters of vessel size, installed power, hull condition (added resistance due to fouling and weather conditions) and service speed levels.

For each vessel, eighteen scenarios are considered, regarding service speed, hull fouling condition and draft at a specific loading. The three hull conditions are: clean hull, 50% margin and 100% margin of extra resistance. For each resistance, three loading conditions are created, fully loaded vessel, partially laden vessel and full ballast condition. All these cases divide into two subcategories; travelling at full-service speed or sailing under slow steaming conditions with a 20% reduction. All are summarized in the following diagram.

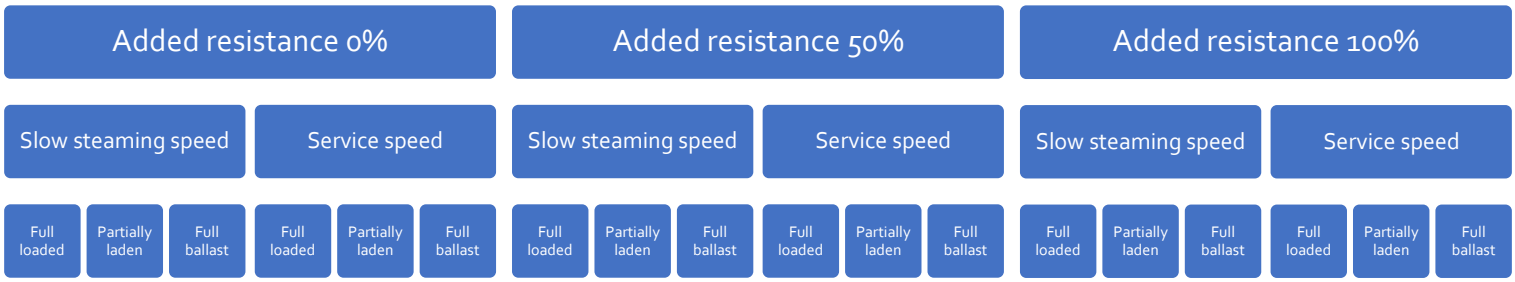

Figure 3.1 Scenarios under study

For each of the twenty vessels, the average value was obtained, for power, revolutions, vessel dimensions and friction measurements. By performing the same procedure as mentioned in chapter 2.3, the following results were received for each vessel class.

Table 3.1 Principal dimensions

VESSEL CLASS	DWT	Δ	LS	L	B	D
Handysize	27125	33768.3	6643.3	161.4	25.9	13.7
Handymax	44750	54091.5	9341.5	180.8	30.6	16.3
Panamax	67350	79686.5	12336.5	205.4	32.1	18.8
Capesize	139475	159564.4	20089.5	258.2	42.6	22.6
VLBC	312687.5	347605.0	34917.5	324.3	58.9	28.8

Table 3.2 Principal dimensions

VESSEL CLASS	T_{fl}	T_{fb}	T_{pl}	V	V_{sl}	P_B	N
Handysize	9.9	5.1	7.5	13.7	12.1	5574.7	124.3
Handymax	11.8	5.7	8.7	14.2	12.4	8231.9	113.5
Panamax	13.6	6.4	10.0	14.5	12.8	10709.5	101.6
Capesize	16.3	7.7	12.0	14.5	12.8	17145.9	93.1
VLBC	20.8	9.4	15.1	14.5	12.6	29166.8	82.7

The brake power and the relevant revolutions are the operational point at maximum service speed; the power that the engine needs to generate in order to move the vessel at full speed under the maximum estimated resistance.

For each MCR point for the different drafts and the different hull conditions, the necessary power and rotational speed were calculated with the estimation of the total resistance and the use of the grid.exe program. Each operational point was calculated by use of the propeller law, since the same curve applies for reduced speed at a constant draft at a certain period of operation of the vessel.

As explained in *2.2.5.1*, the revolutions of the propeller and the service speed are proportional. By using the grid.exe the combination of power and revolutions for each operational point for the different cases are calculated. By cutting down to the slow steaming speed, the revolutions will be reduced in a proportional way. So, after estimating the service points, by using the propeller curve law, the operational points can be estimated, as: $\boldsymbol{N_s = \frac{V_s}{V} N}$. From N_s, the relevant operational power is obtained from the propeller law curve, $\boldsymbol{P = cN_s^{3.2}}$.

The service points of each case for every hull fouling condition are illustrated in the following tables:

Table 3.3 Power and revolutions at clean hull

CLEAN HULL					
VESSEL CLASS	Handysize	Handymax	Panamax	Capesize	VLBC
Power MCR Full load	4196.7	6186.9	8025.2	12806.8	21737.2
Revolutions MCR Full load	115.1	105.0	93.8	84.3	73.1
Operational power Full load	2054.9	3029.4	3929.5	6270.9	10643.7
Revolutions Operational Full load	92.1	84.0	75.0	67.4	58.5
Power MCR Full ballast	5328.3	8051.1	10698.3	17890.1	31442.0
Revolutions MCR Full ballast	123.9	113.9	102.4	93.6	84.8
Operational Power Full ballast	2609.0	3942.2	5238.5	8759.9	15395.6
Revolutions Operational Full ballast	99.1	91.1	81.9	74.9	67.8
Power MCR Partially laden	4580.5	6783.4	8861.1	14382.8	24649.1
Revolutions MCR Partially laden	118.3	108.1	96.7	87.3	77.4
Operational Power Partially laden	2242.9	3321.5	4338.9	7042.5	12069.5
Revolutions Operational Partially laden	94.7	86.5	77.4	69.9	61.9

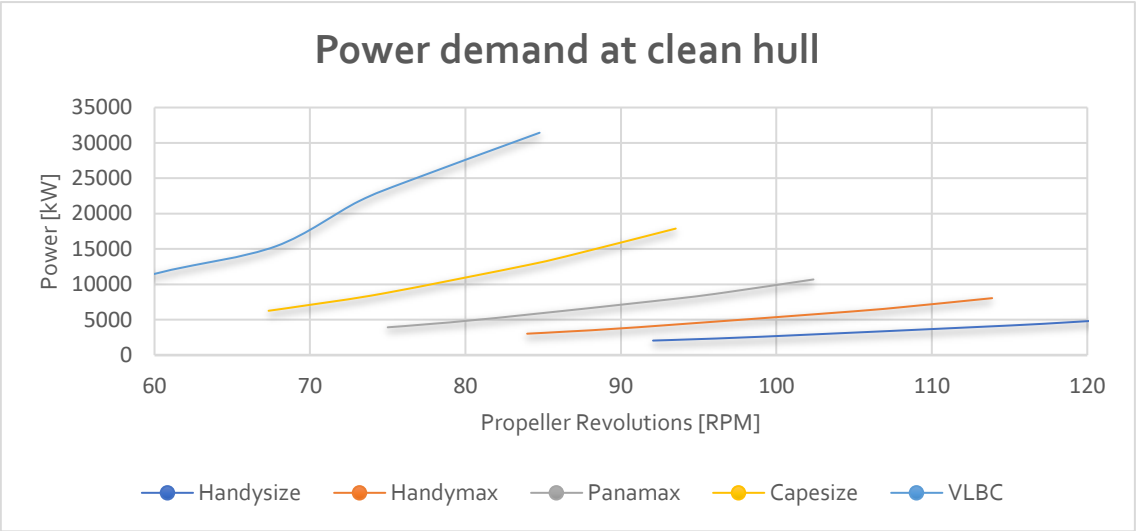

Figure 3.2 Power demand at clean hull

Table 3.4 Power and revolutions at partially fouled hull

PARTIALLY FOULED HULL					
VESSEL CLASS	**Handysize**	**Handymax**	**Panamax**	**Capesize**	**VLBC**
Power MCR Full load	5515.6	8146.0	10597.1	16965.6	28866.5
Revolutions MCR Full load	124.7	113.9	101.9	93.4	83.0
Operational power Full load	2700.7	3988.7	5188.9	8307.3	14134.6
Revolutions Operational Full load	99.7	91.1	81.5	74.7	66.4
Power MCR Full ballast	7016.0	10624.6	14160.9	23765.2	41875.3
Revolutions MCR Full ballast	134.4	123.7	114.5	106.8	93.4
Operational Power Full ballast	3435.4	5202.3	6933.9	11636.7	20504.4
Revolutions Operational Full ballast	107.5	99.0	91.6	85.4	74.7
Power MCR Partially laden	6021.8	8936.5	11707.9	19073.2	32762.6
Revolutions MCR Partially laden	128.2	117.3	105.1	99.1	86.6
Operational Power Partially laden	2948.6	4375.8	5732.8	9339.2	16042.3
Revolutions Operational Partially laden	102.6	93.8	84.1	79.3	69.3

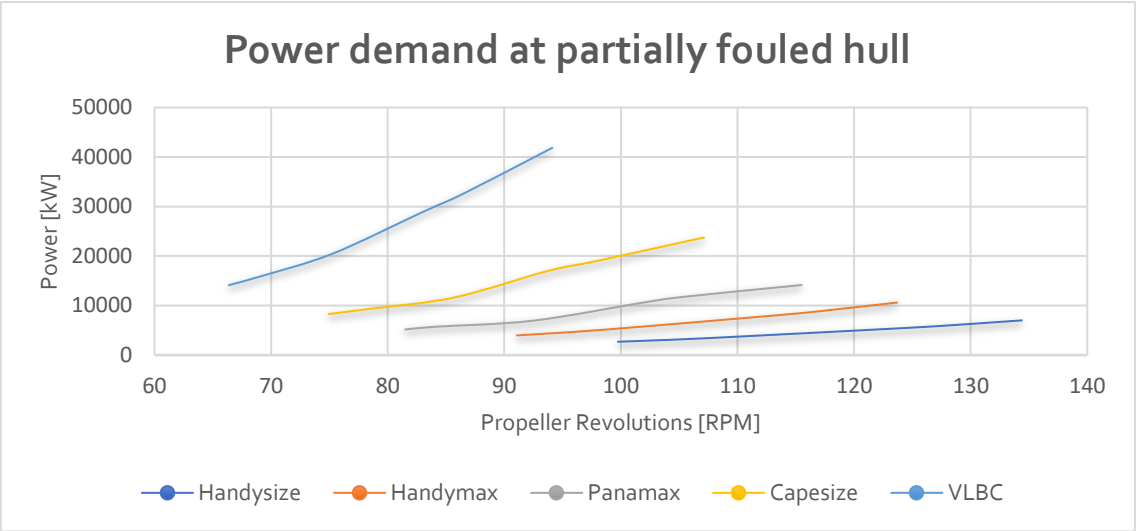

Figure 3. 3 Power demand at partially fouled hull

Table 3. 5 Power and revolutions at fully fouled hull

FULLY FOULED HULL					
VESSEL CLASS	**Handysize**	**Handymax**	**Panamax**	**Capesize**	**VLBC**
Power MCR Full load	5574.7	8231.9	10709.5	17145.9	29166.8
Revolutions MCR Full load	124.3	113.5	101.6	93.1	82.7
Operational power Full load	2729.7	4030.8	5243.9	8395.5	14281.6
Revolutions Operational Full load	99.5	90.8	81.3	74.5	66.2
Power MCR Full ballast	7092.1	10735.4	14312.6	24014.8	42318.9
Revolutions MCR Full ballast	134.0	123.4	115.2	107.5	93.8
Operational Power Full ballast	3472.7	5256.6	7008.2	11758.9	20721.5
Revolutions Operational Full ballast	107.2	98.7	92.2	86.0	75.1
Power MCR Partially laden	6086.2	9030.8	11833.6	19272.1	33092.9
Revolutions MCR Partially laden	127.9	117.0	104.9	98.3	86.1
Operational Power Partially laden	2980.1	4422.0	5794.4	9436.6	16204.0
Revolutions Operational Partially laden	102.3	93.6	83.9	78.6	68.8

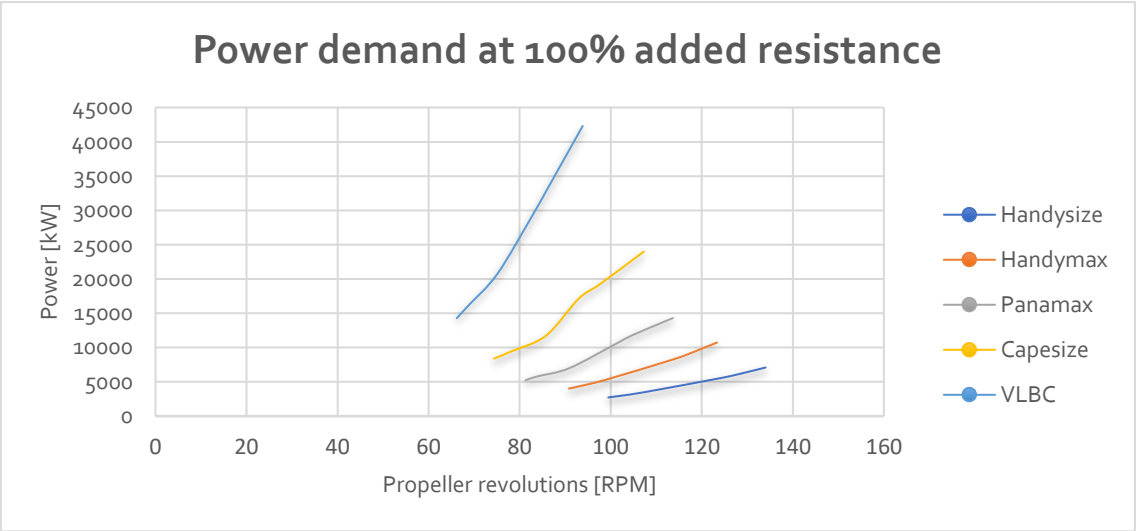

Figure 3. 4 Fully fouled hull

3.2 Study results

In the next paragraphs the results of the simulation are illustrated. Charts, based on the friction calculations show the attribute of frictional losses against the changing size of added resistance, draft and speed.

3.2.1 Shafting friction losses

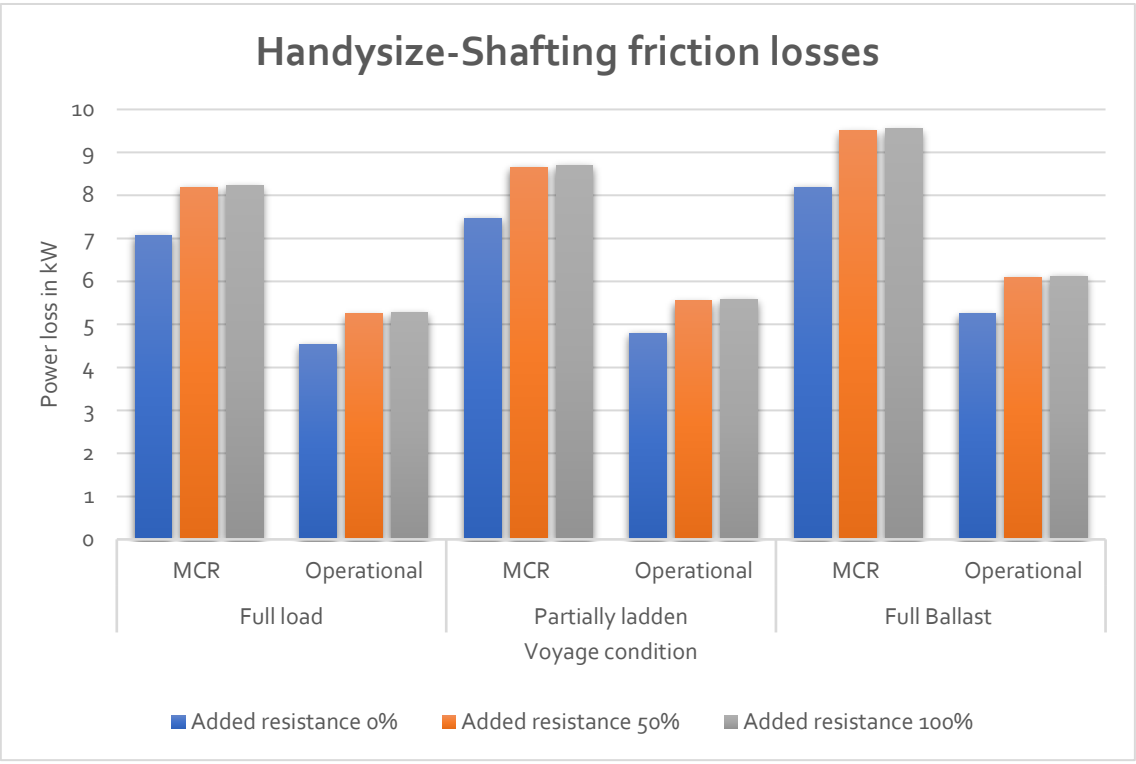

Figure 3.5 Handysize frictional losses in kW

From the above column charts, quantitative shafting friction losses increase with:

- Reduction in draft.

- Sailing at full speed (engine operating under maximum service point).
- Increase of the additional resistance caused by fouling.
- Increase in vessel size.

The main parameter affecting shafting friction losses is the **rotational speed** of the crankshaft and hence; the propeller. Higher revolutions lead to increased Sommerfeld Number, which causes the friction coefficient to be larger resulting at increased power losses.

A reduction of draft implies that the resistance of the vessel is lower. Thus, at a constant engine load, the revolutions will increase with the reduced resistance.

If the hull of the vessel is clean (absence of fouling) and additionally if the vessel sails in calm weather, then resistance is also less and higher rpm can be achieved with constant engine load. Obviously, if the engine is operated under maximum service conditions whether resistance decreases or not, then the revolutions again are higher and the amount of energy lost. The friction losses per shaft bearing are illustrated. As mentioned in paragraph **2.2.7** the bearings considered are the aft and the fore bearings of the propeller shaft and the intermediate bearing of the intermediate shaft, while the thrust is assumed to be built in the engine.

3.2.1.1 Aft bearing frictional losses

Aft bearing, forward and intermediate bearing losses per bulk carrier class:

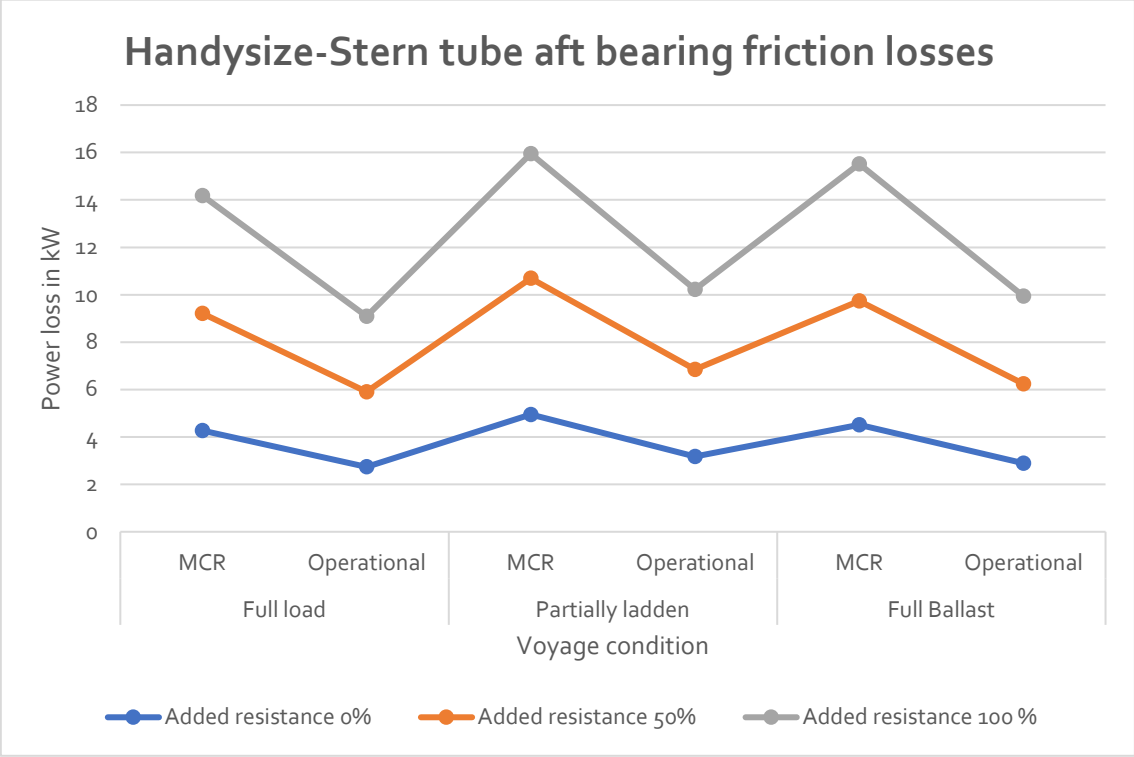

Figure 3.6 Handysize aft bearing losses

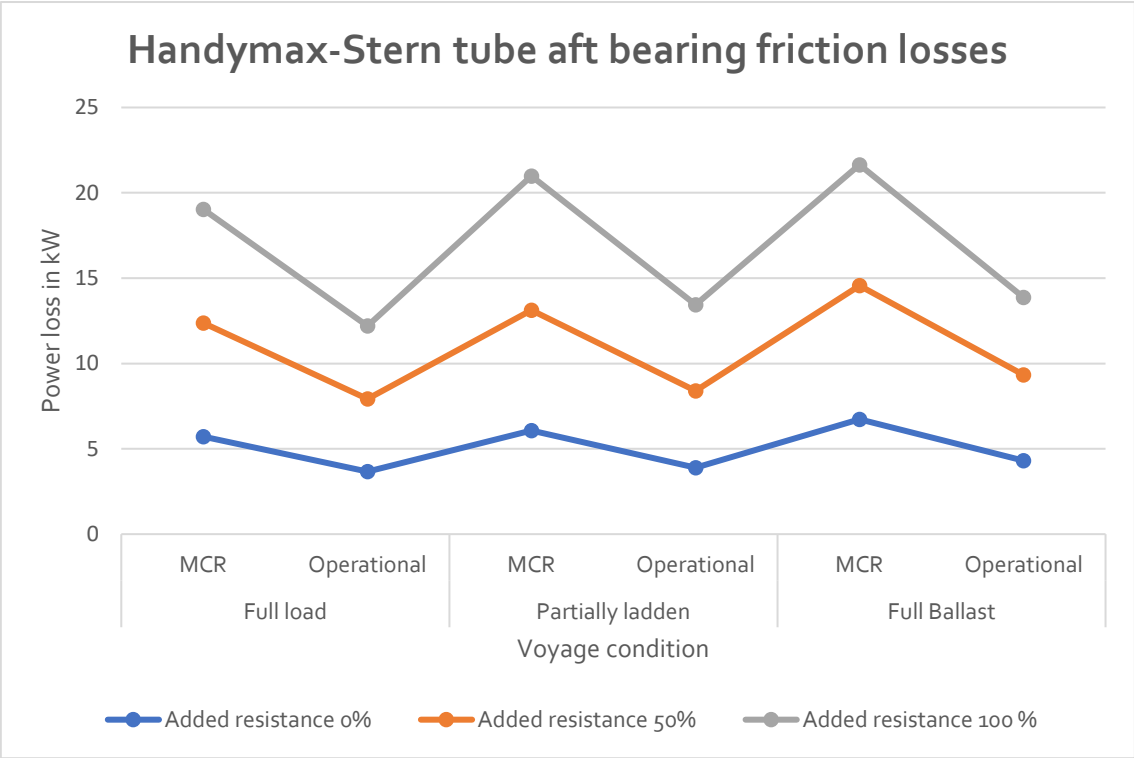

Figure 3.7 Handymax aft bearing losses

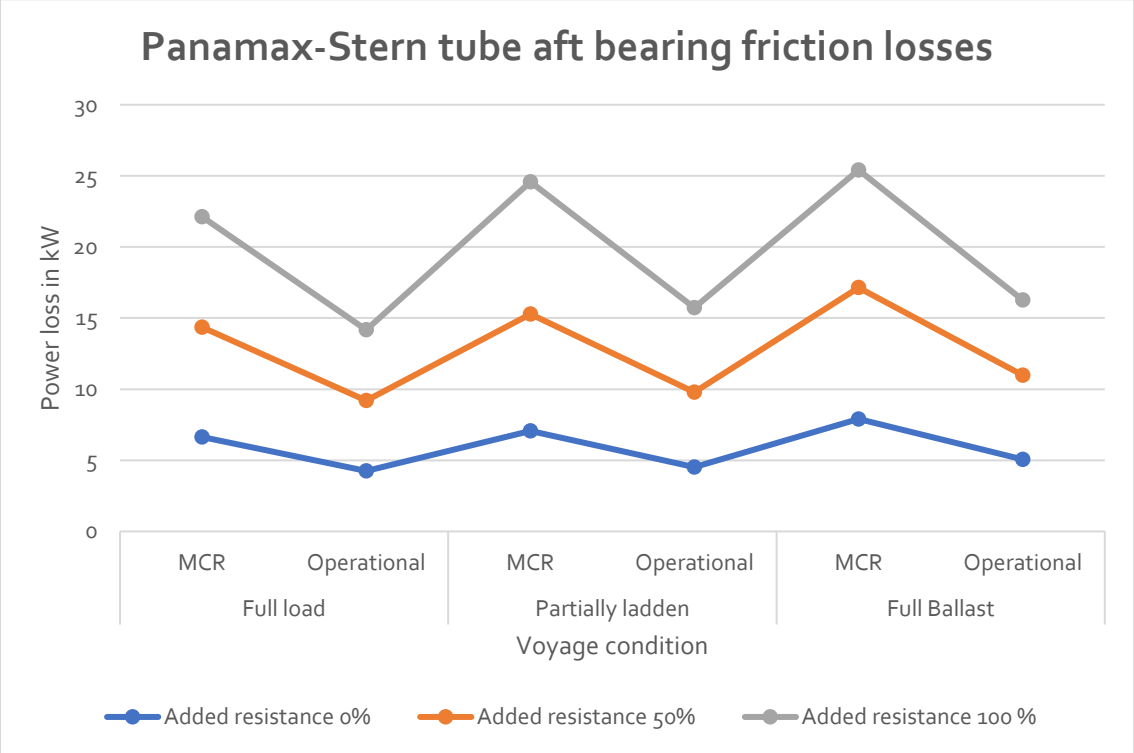

Figure 3.8 Panamax aft bearing losses

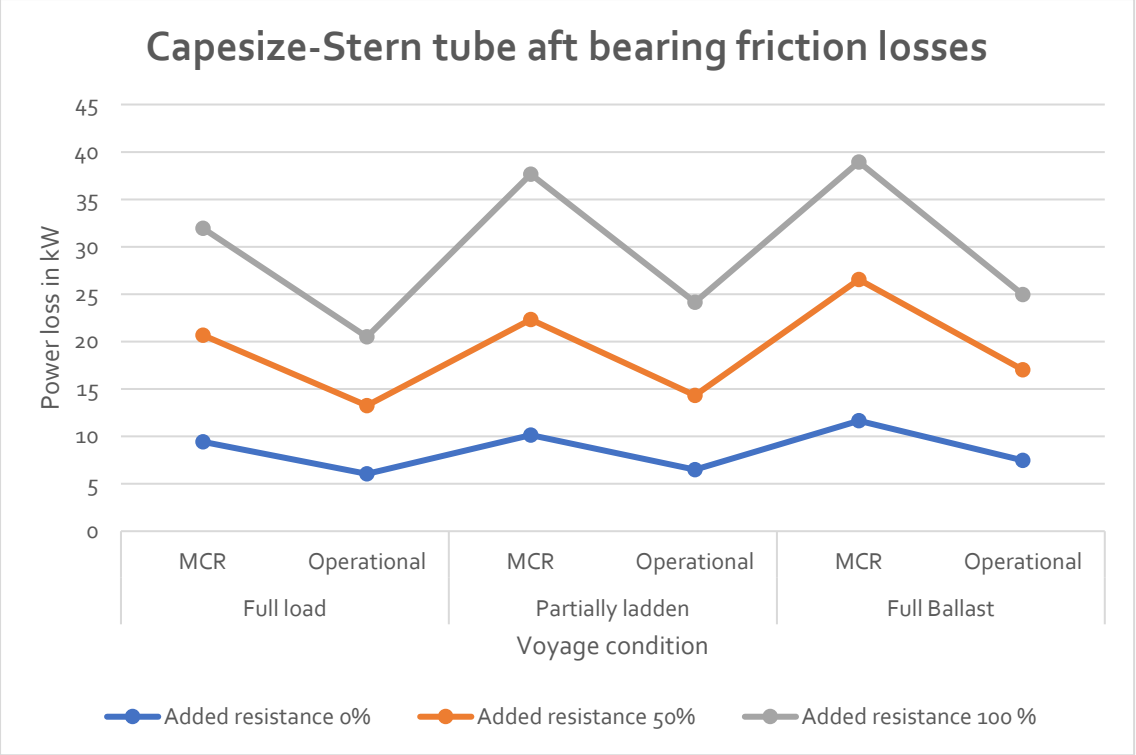

Figure 3.9 Capesize aft bearing losses

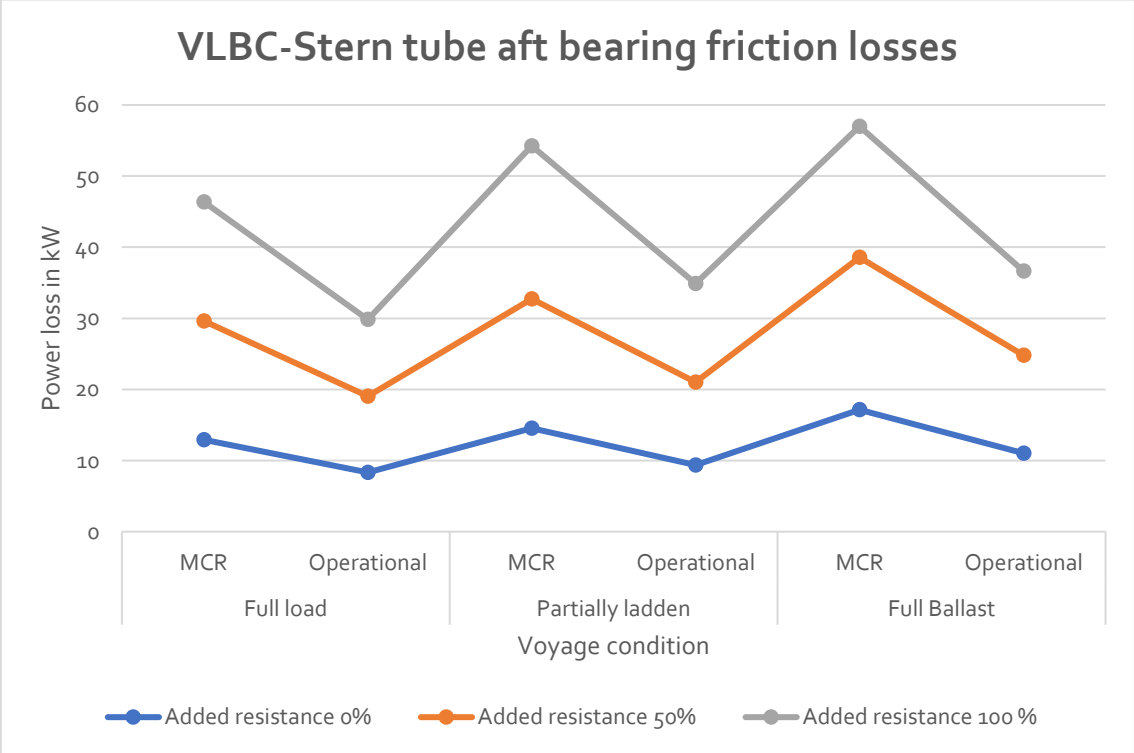

Figure 3.10 VLBC aft bearing losses

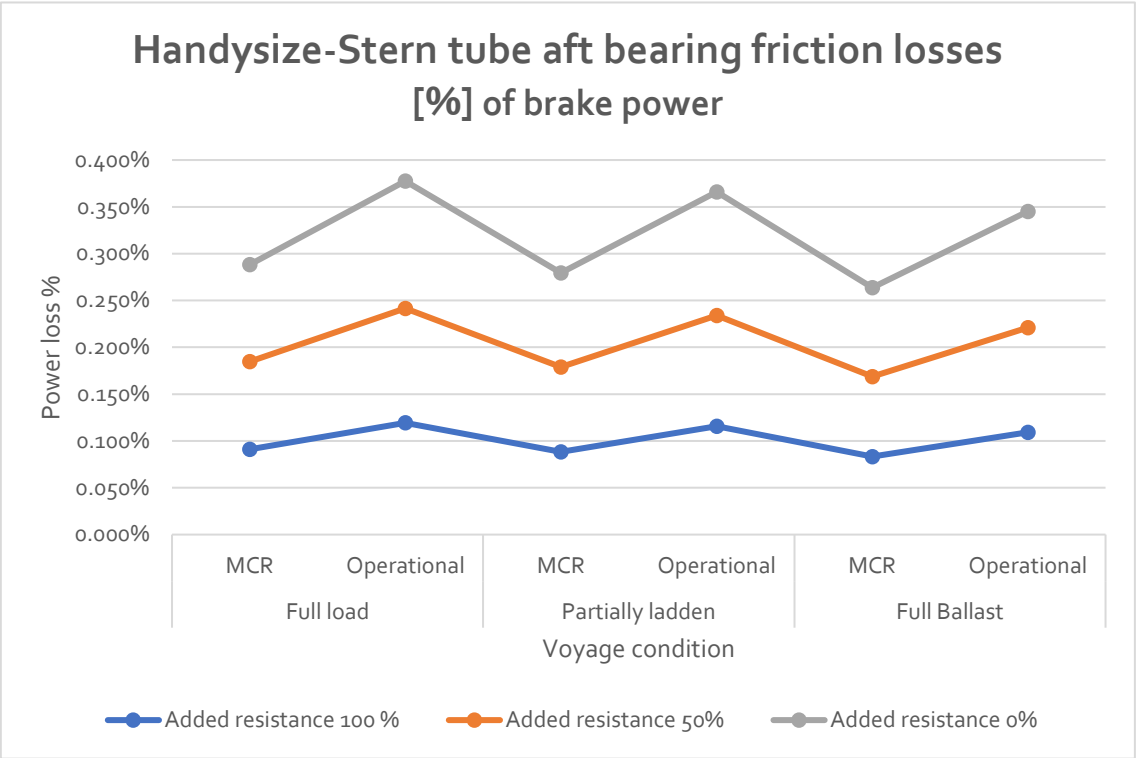

Figure 3.11 Handysize aft bearing losses %

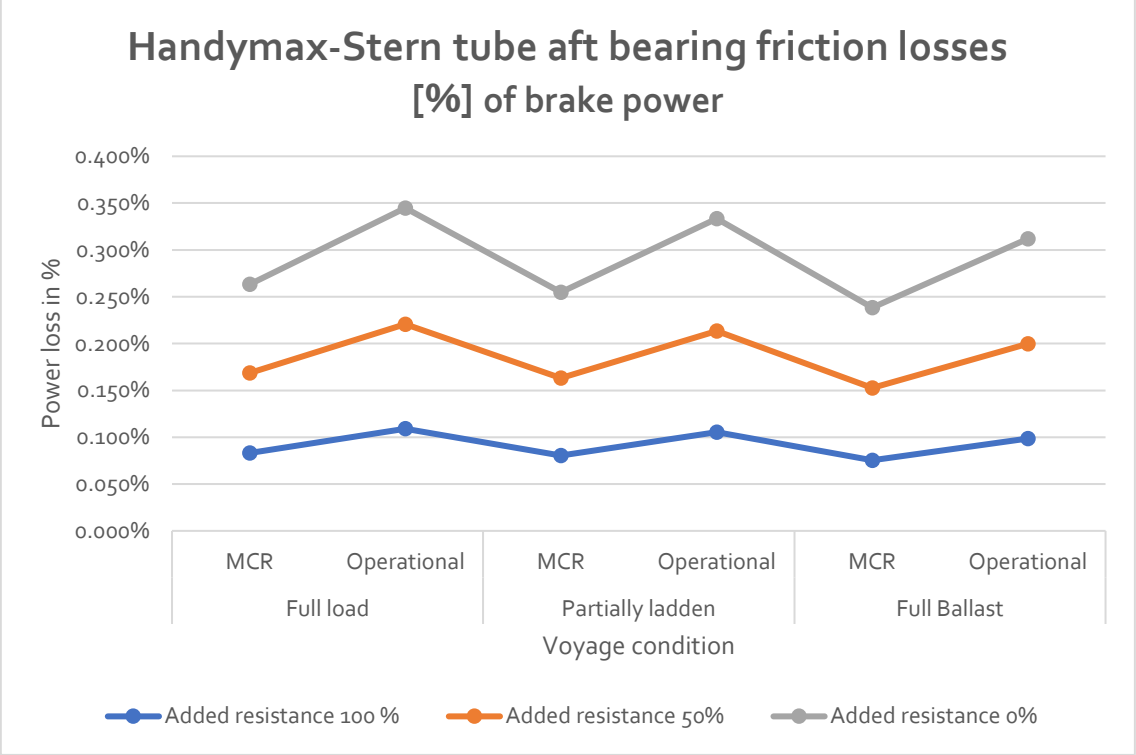

Figure 3.12 Handymax aft bearing losses %

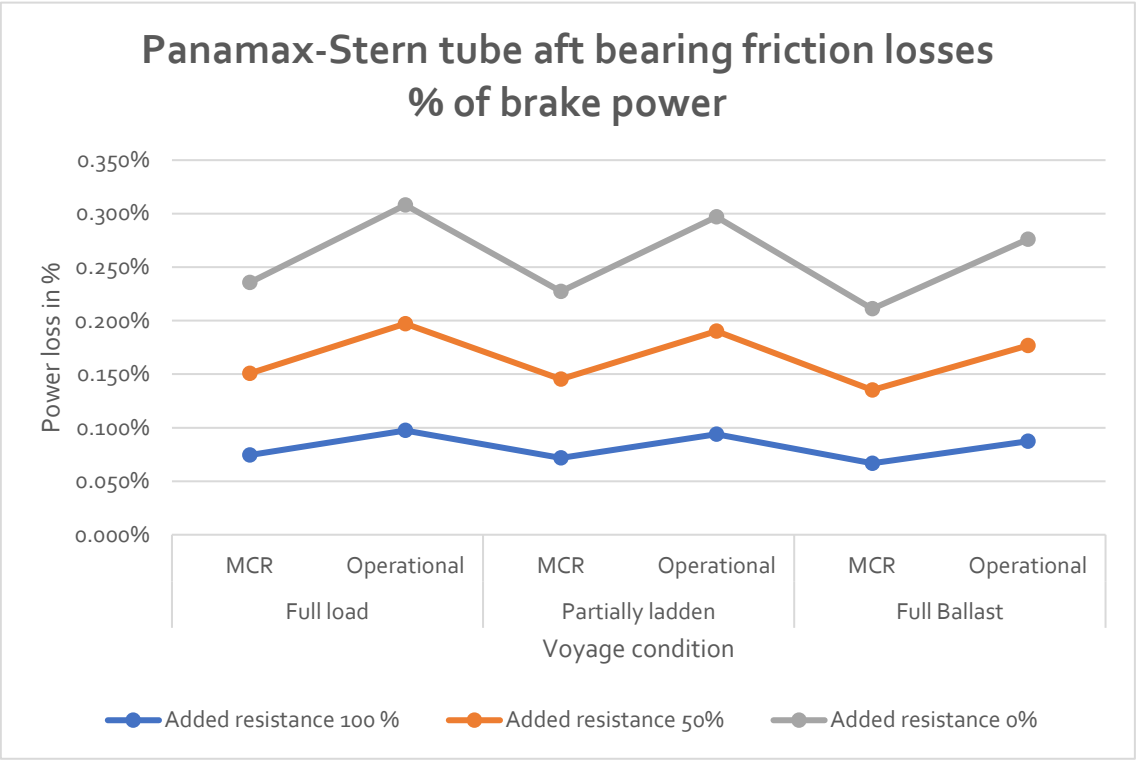

Figure 3.13 Panamax aft bearing losses %

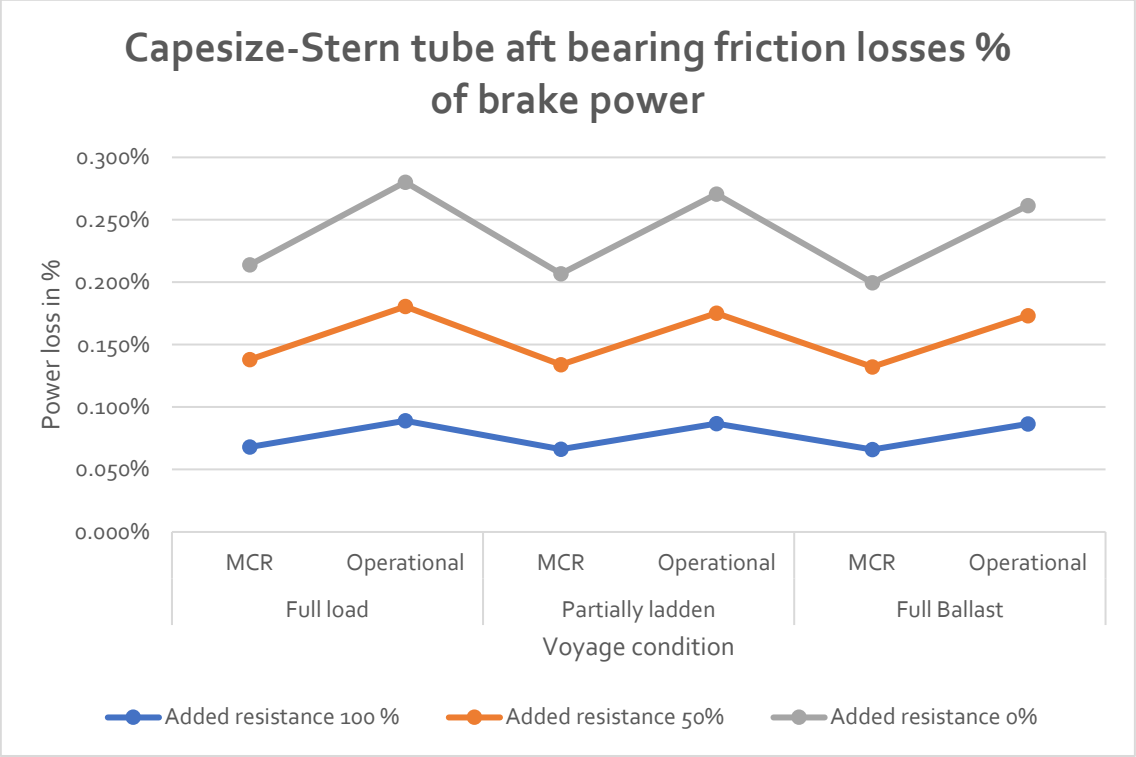

Figure 3.14 Capesize aft bearing losses %

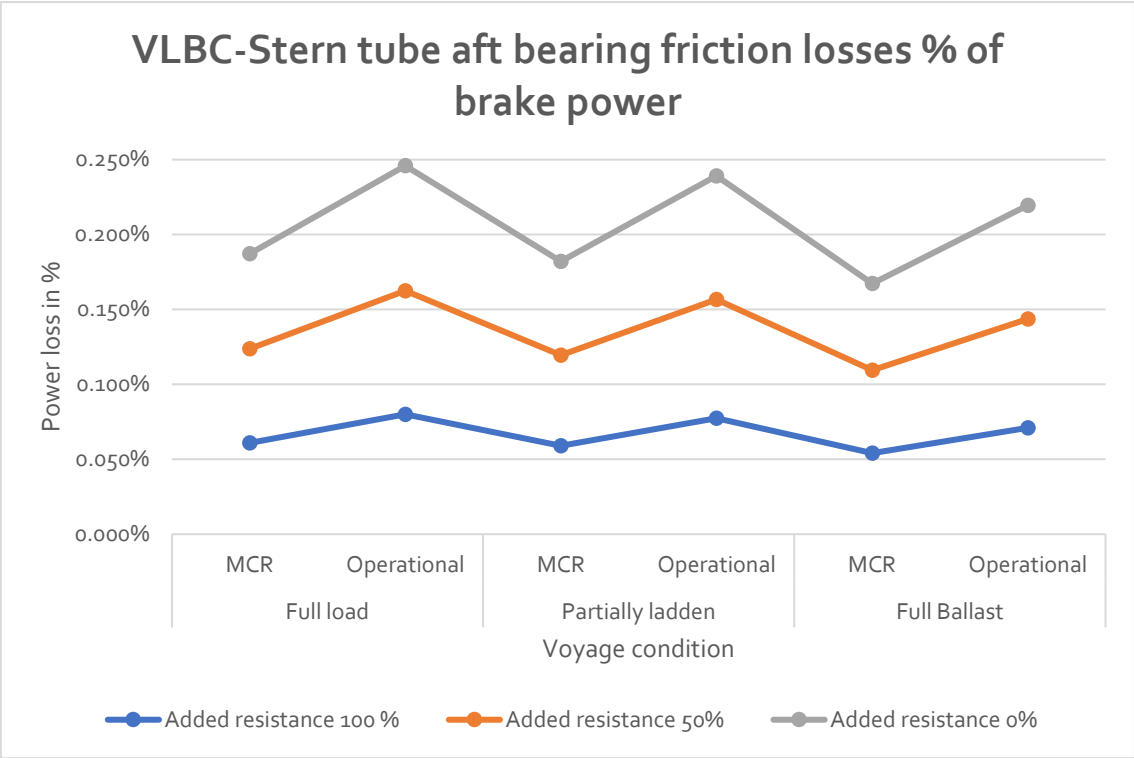

Figure 3.15 VLBC aft bearing losses %

3.2.1.2 Forward bearing frictional losses

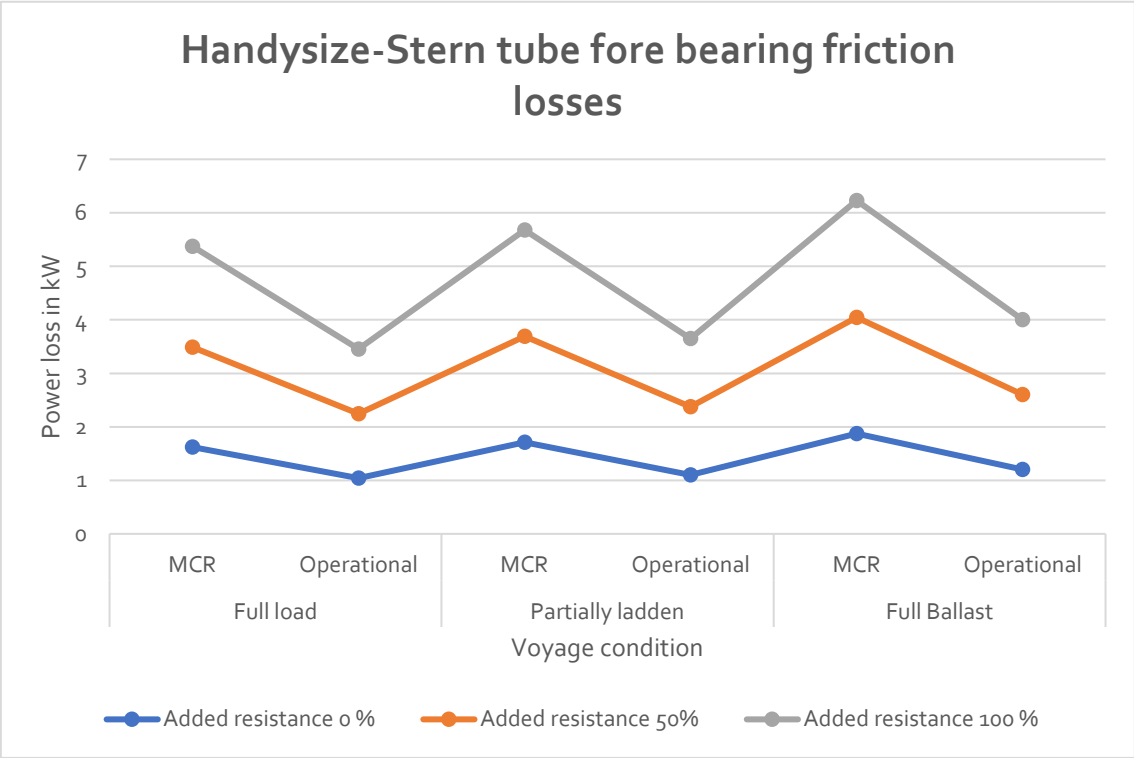

Figure 3.16 Handysize forward bearing losses

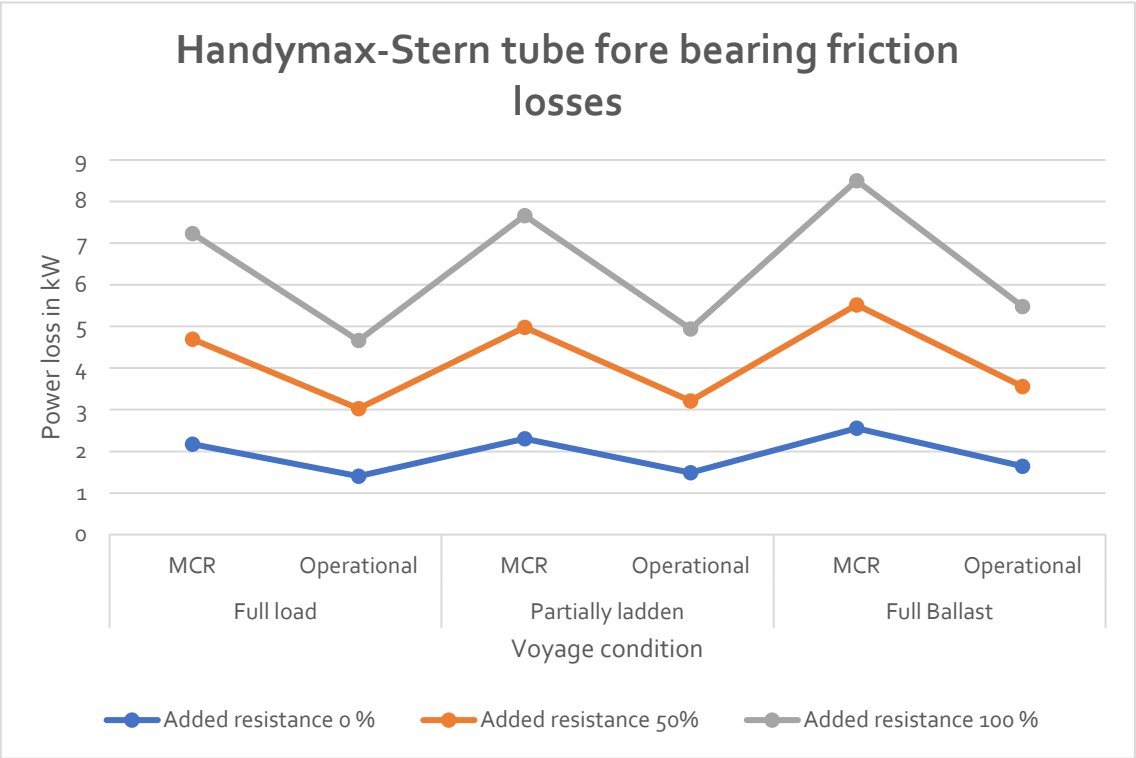

Figure 3.17 Handymax forward bearing losses

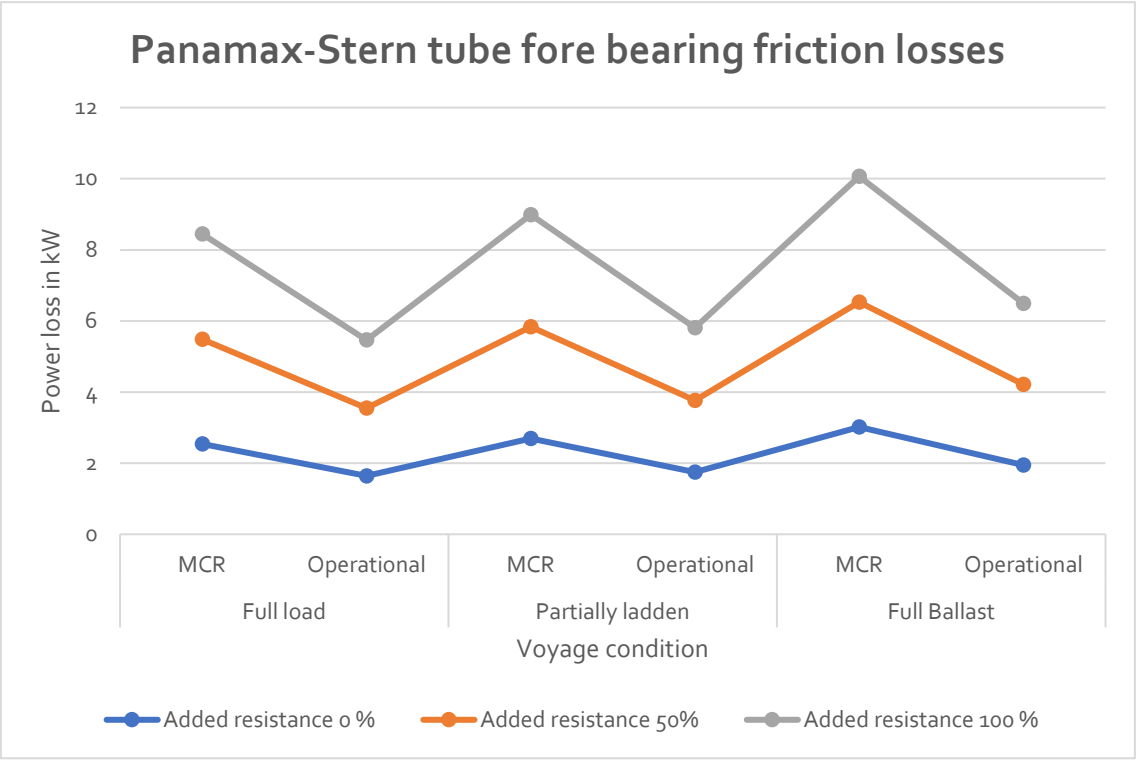

Figure 3.18 Panamax forward bearing losses

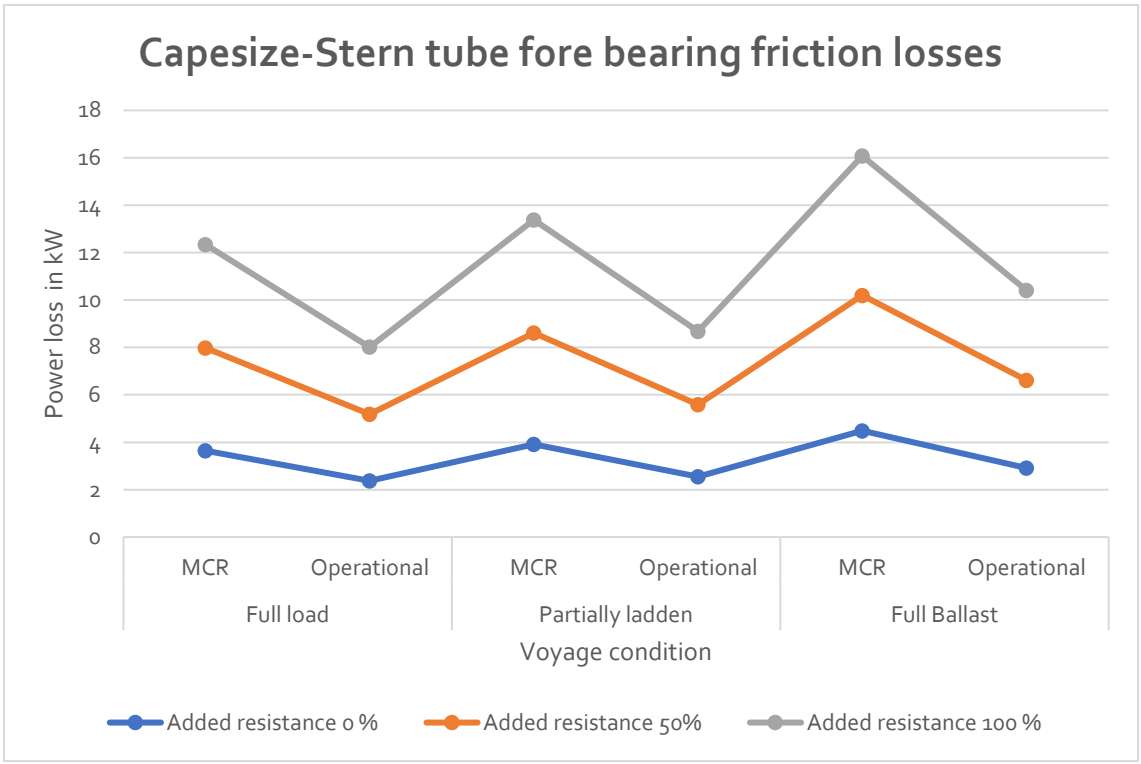

Figure 3.19 Capesize forward bearing losses

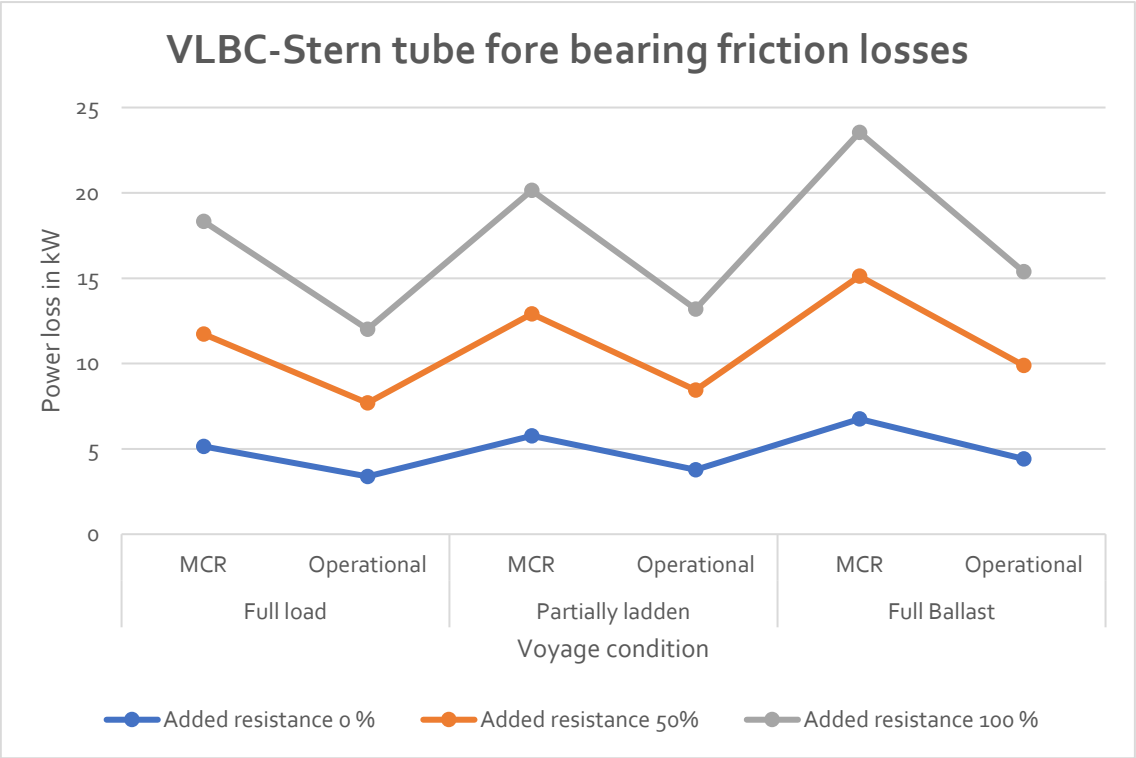

Figure 3.20 VLBC forward bearing losses

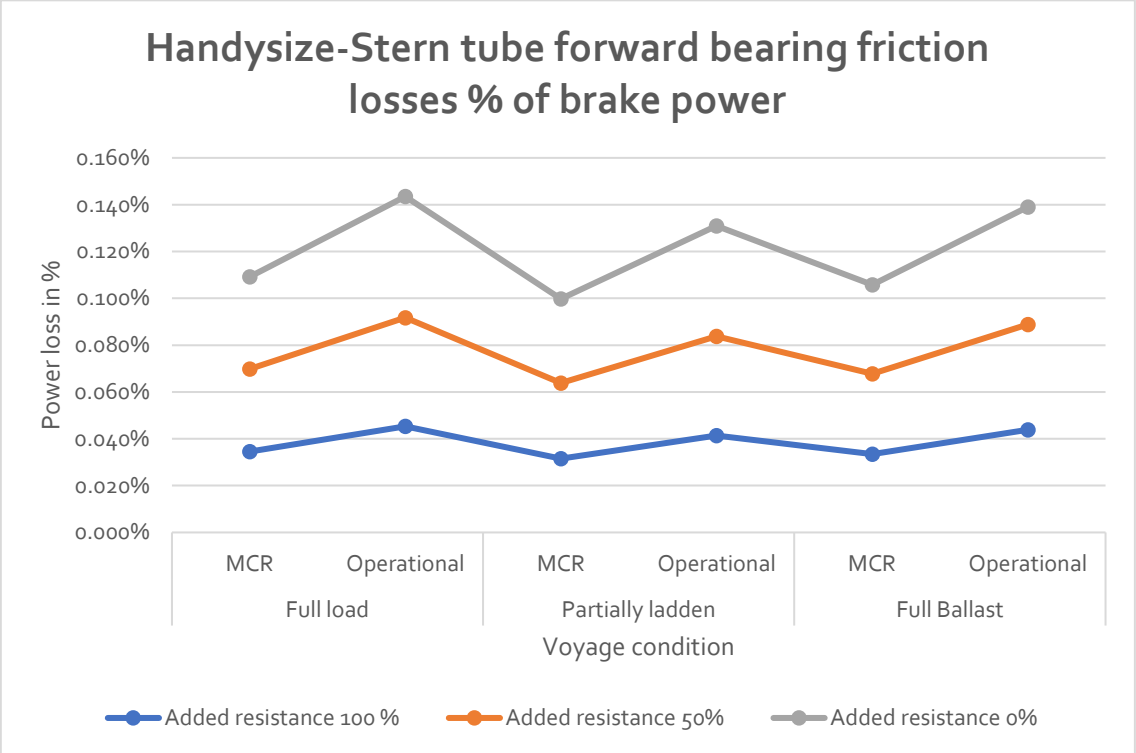

Figure 3.21 Handysize forward bearing losses %

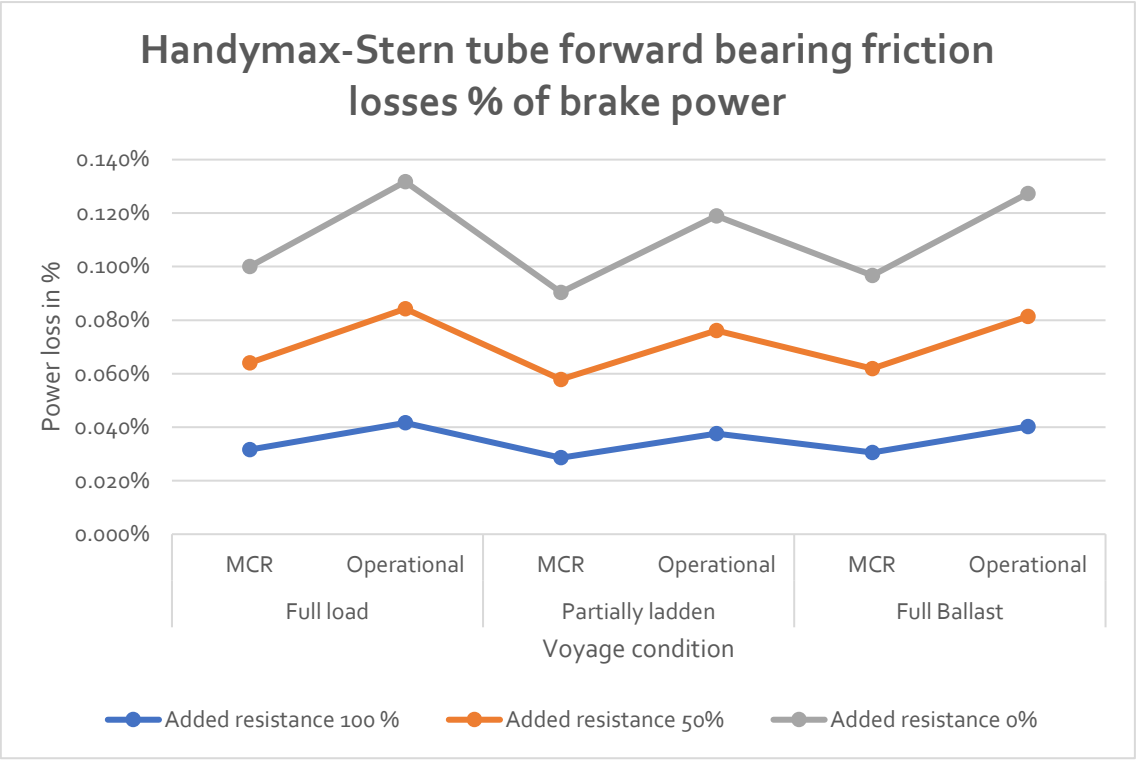

Figure 3.22 Handymax forward bearing losses %

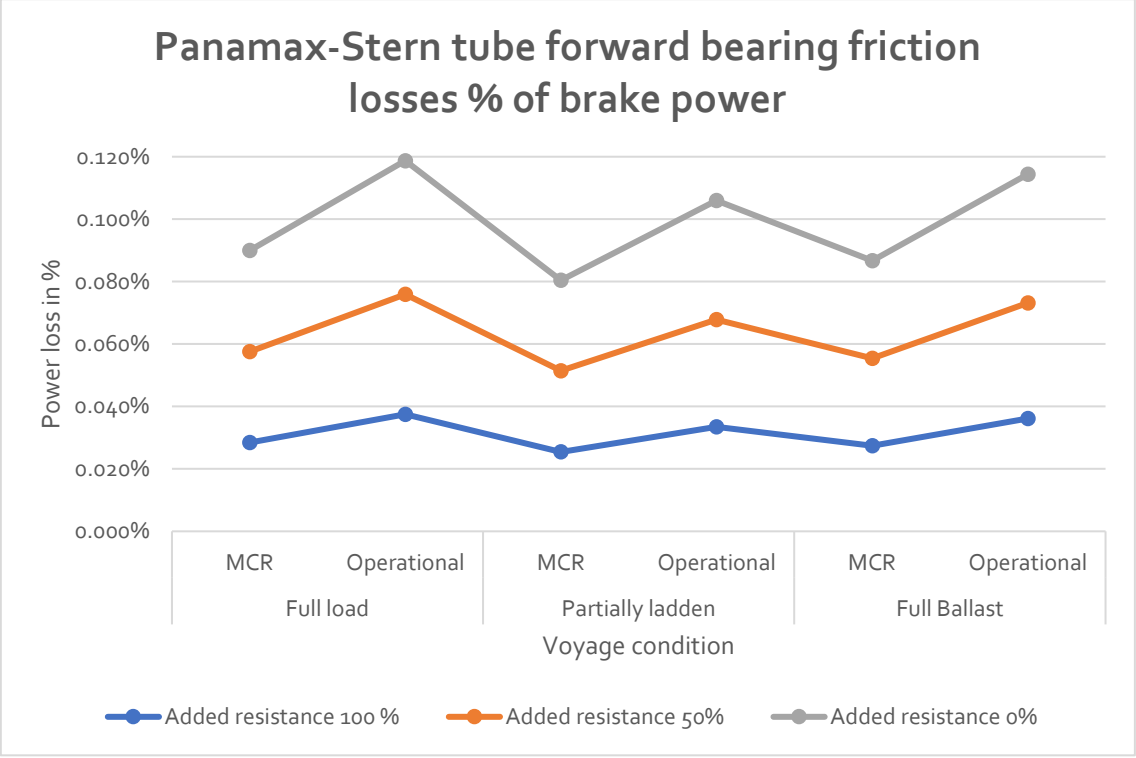

Figure 3.23 Panamax forward bearing losses %

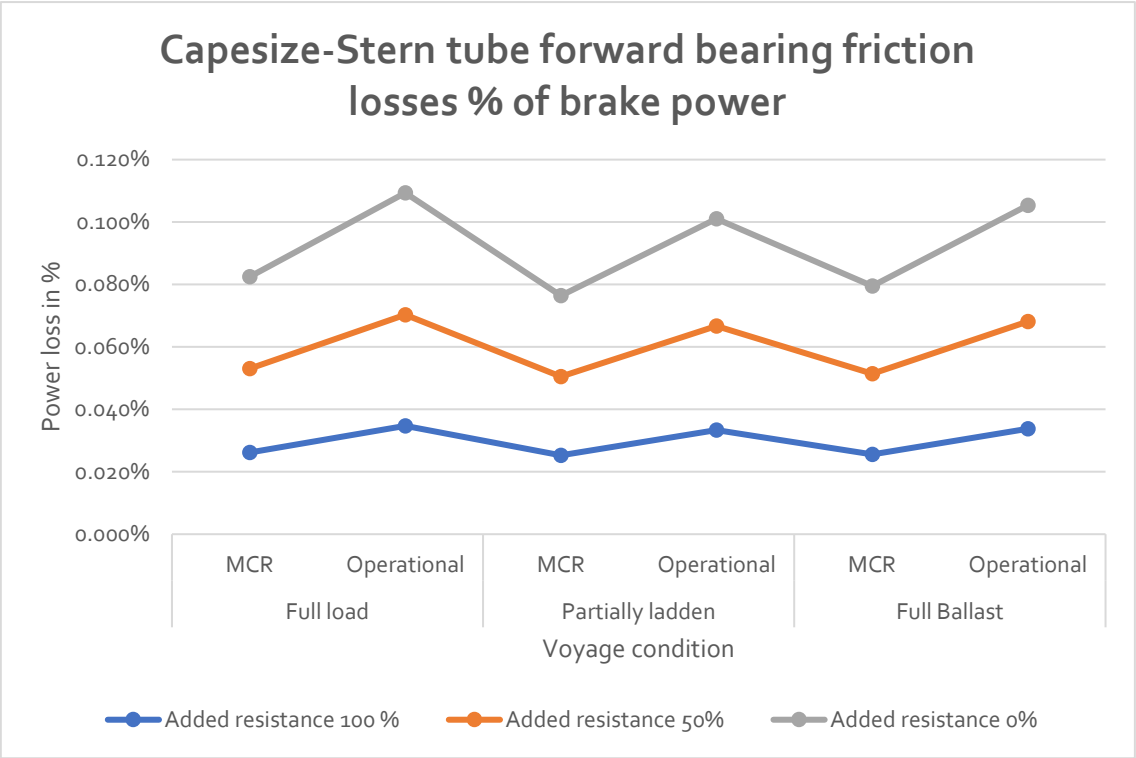

Figure 3.24 Capesize forward bearing losses %

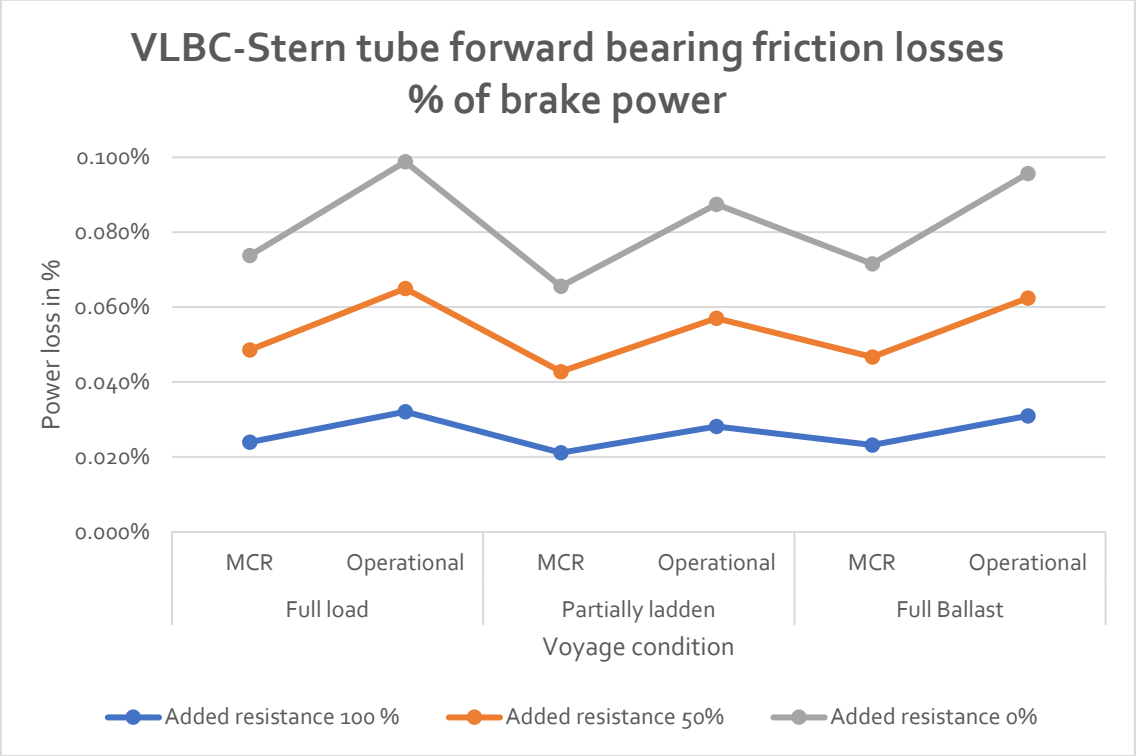

Figure 3.25 VLBC forward bearing losses %

3.2.1.3 *Intermediate* bearing *frictional losses*

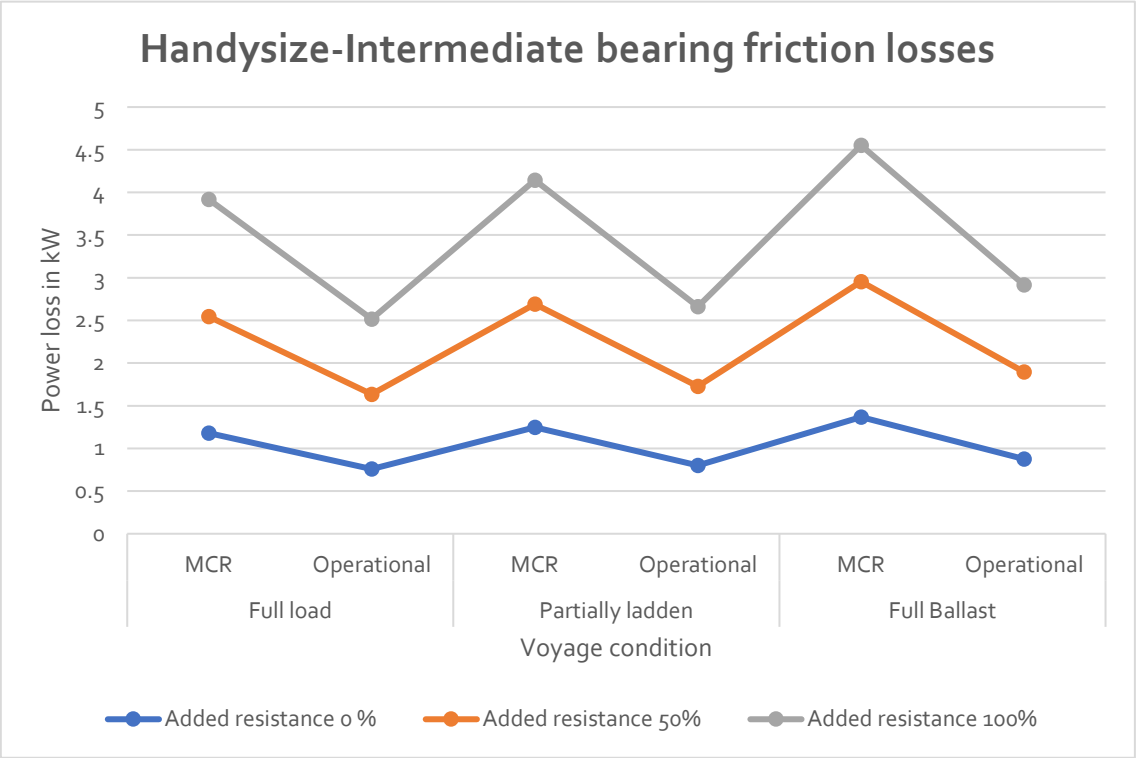

Figure 3.26 Handysize intermediate bearing losses

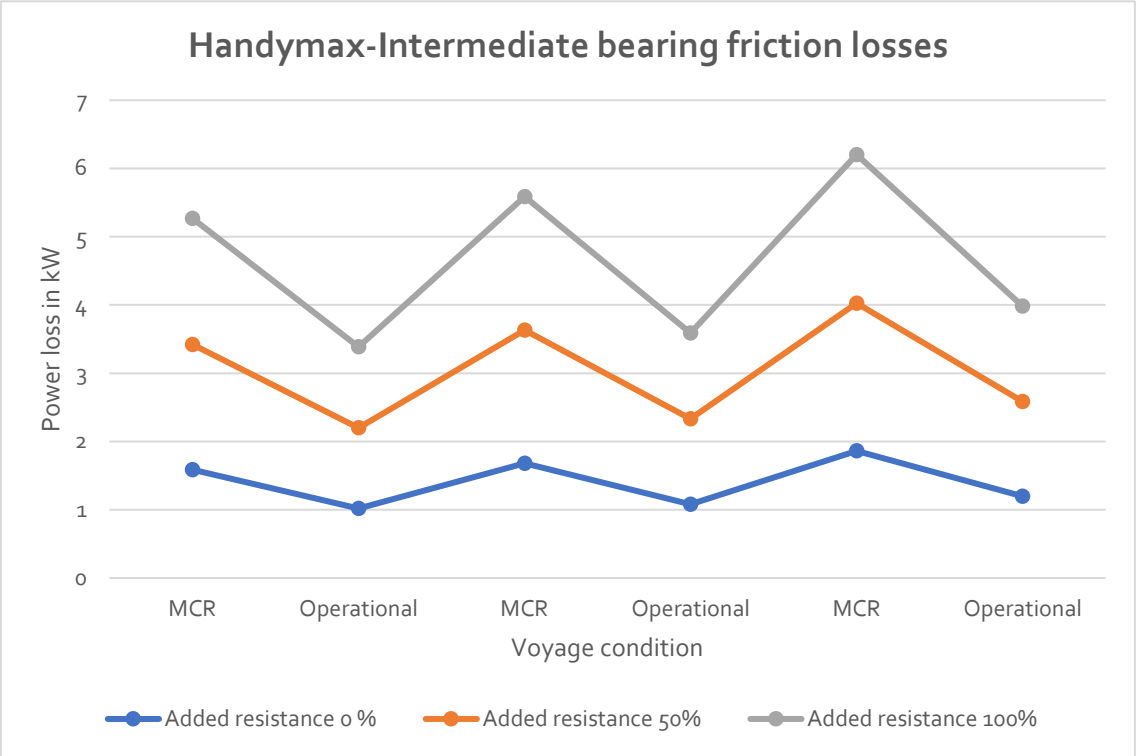

Figure 3.27 Handymax intermediate bearing losses

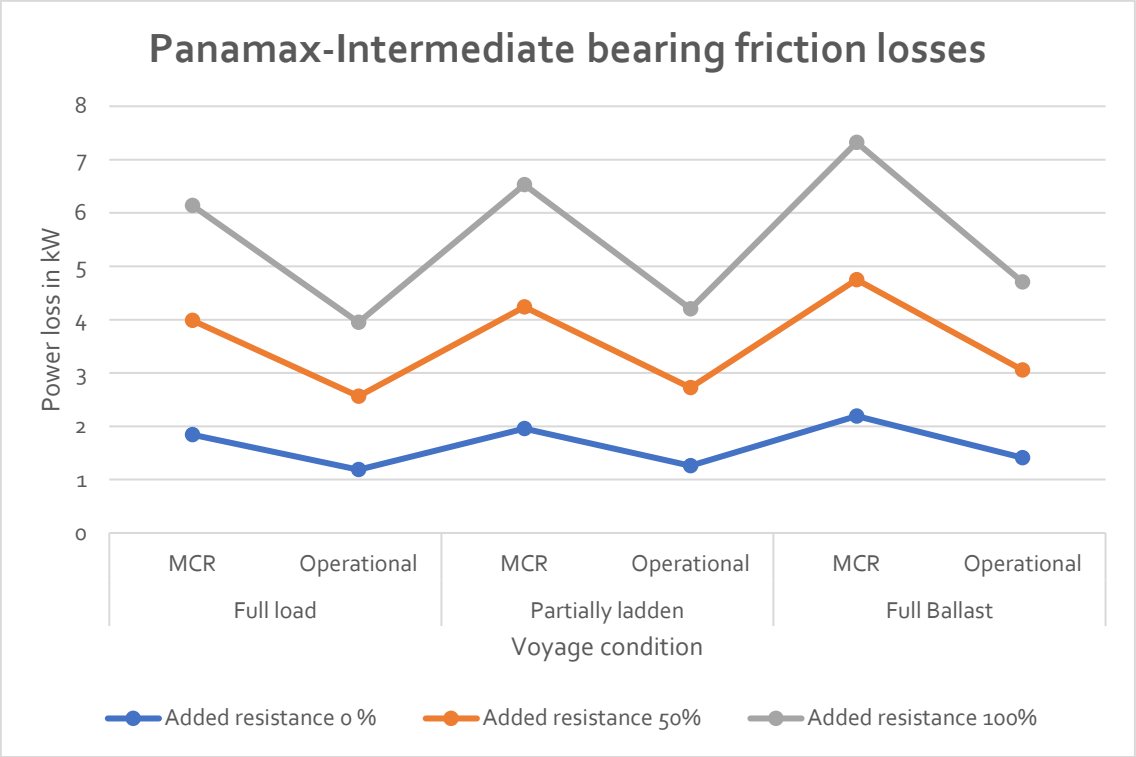

Figure 3.28 Panamax intermediate bearing losses

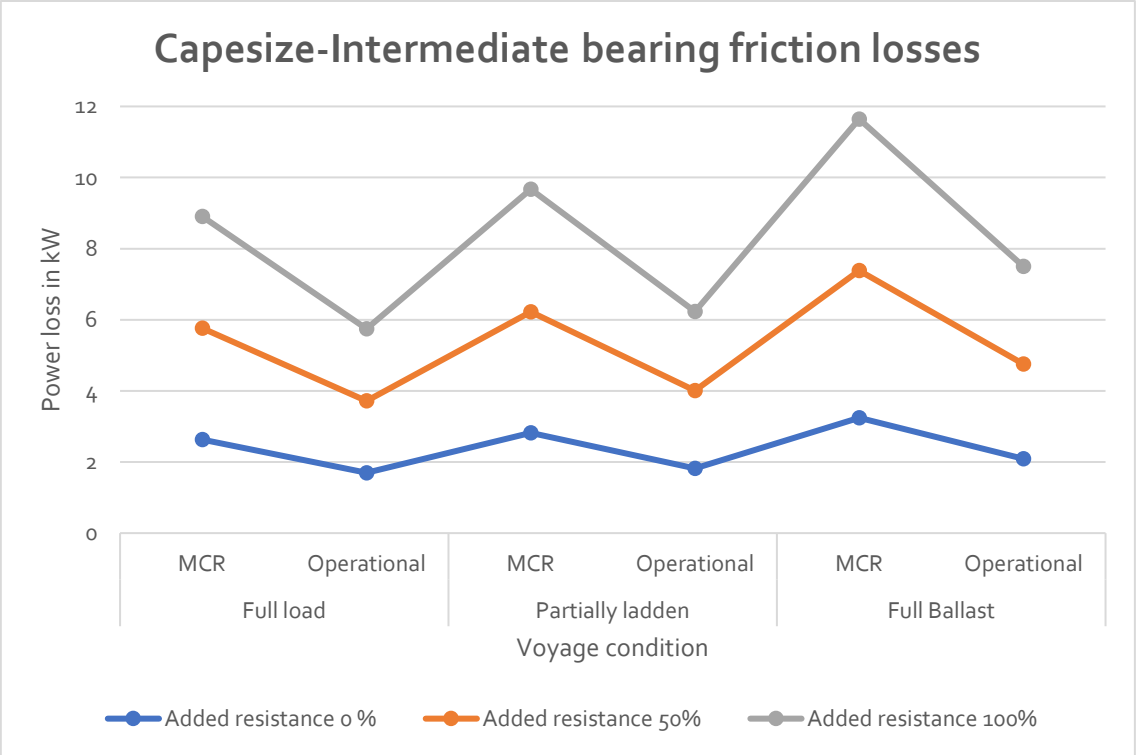

Figure 3.29 Capesize intermediate bearing losses

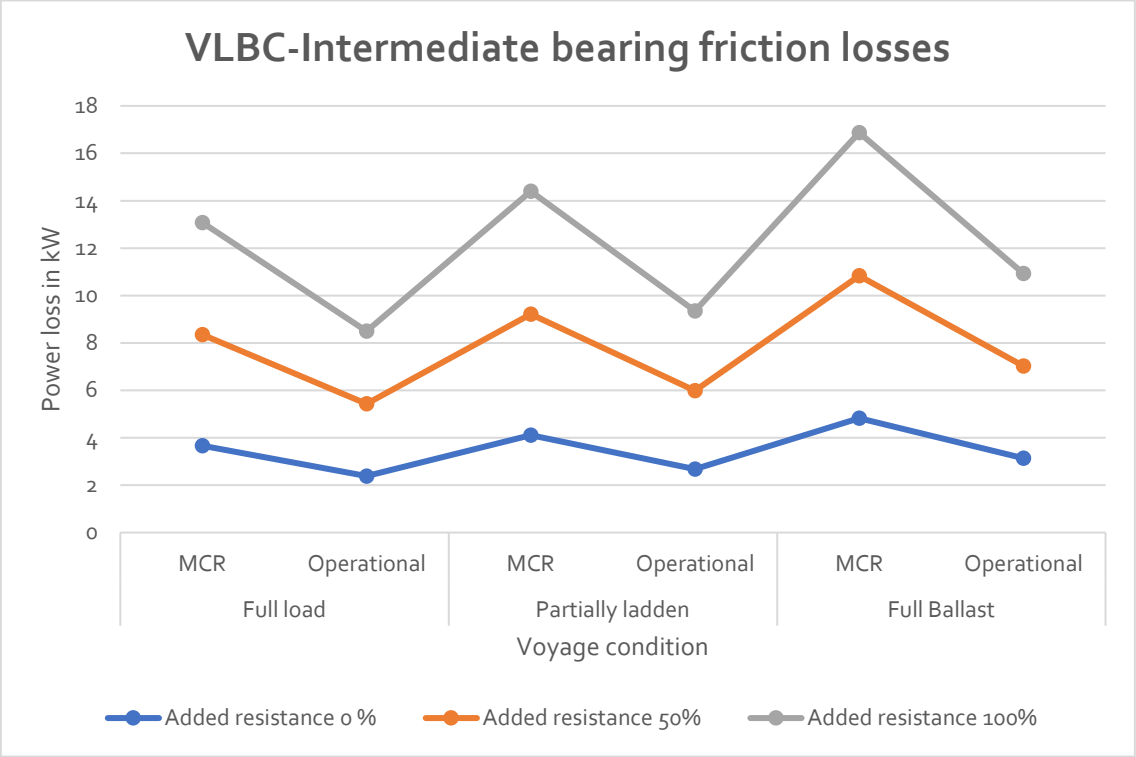

Figure 3.30 VLBC intermediate bearing losses

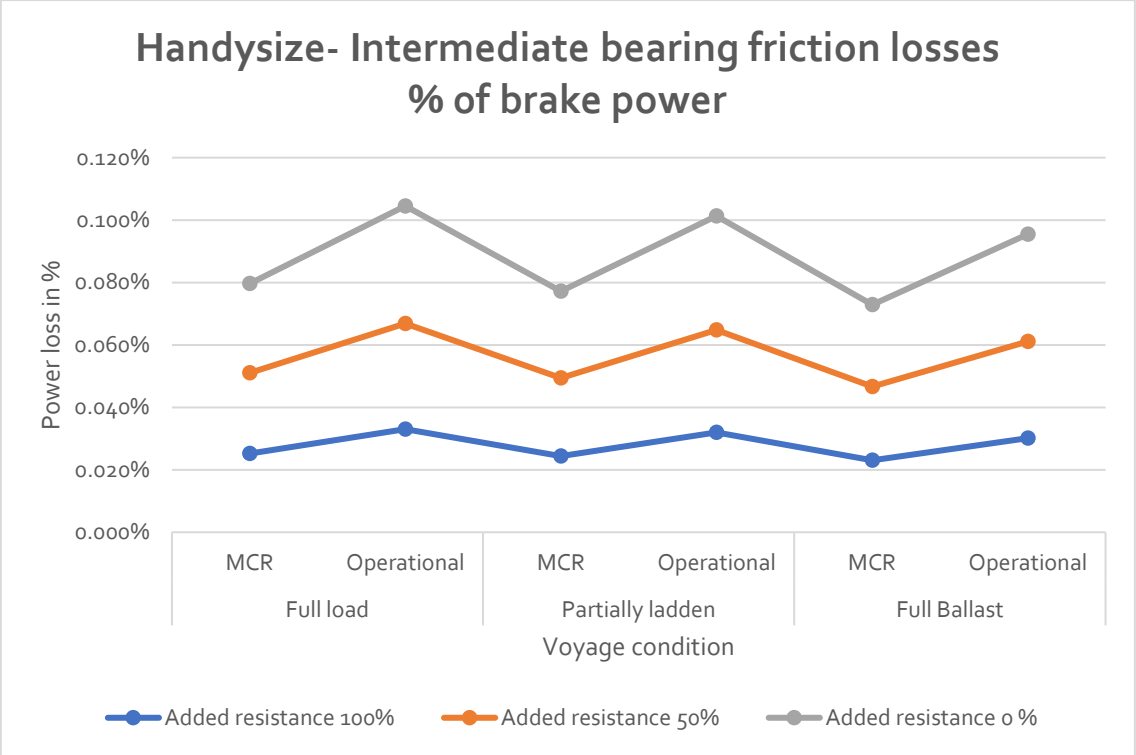

Figure 3.31 Handysize intermediate bearing losses %

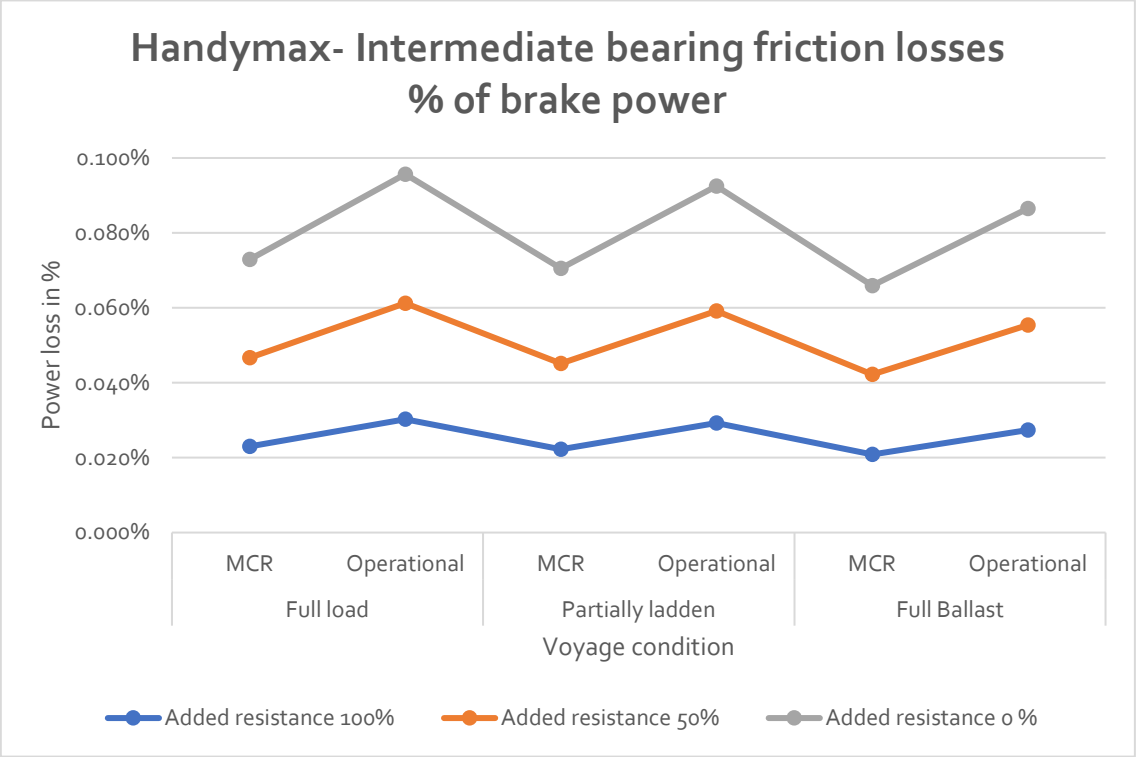

Figure 3.32 Handymax intermediate bearing losses %

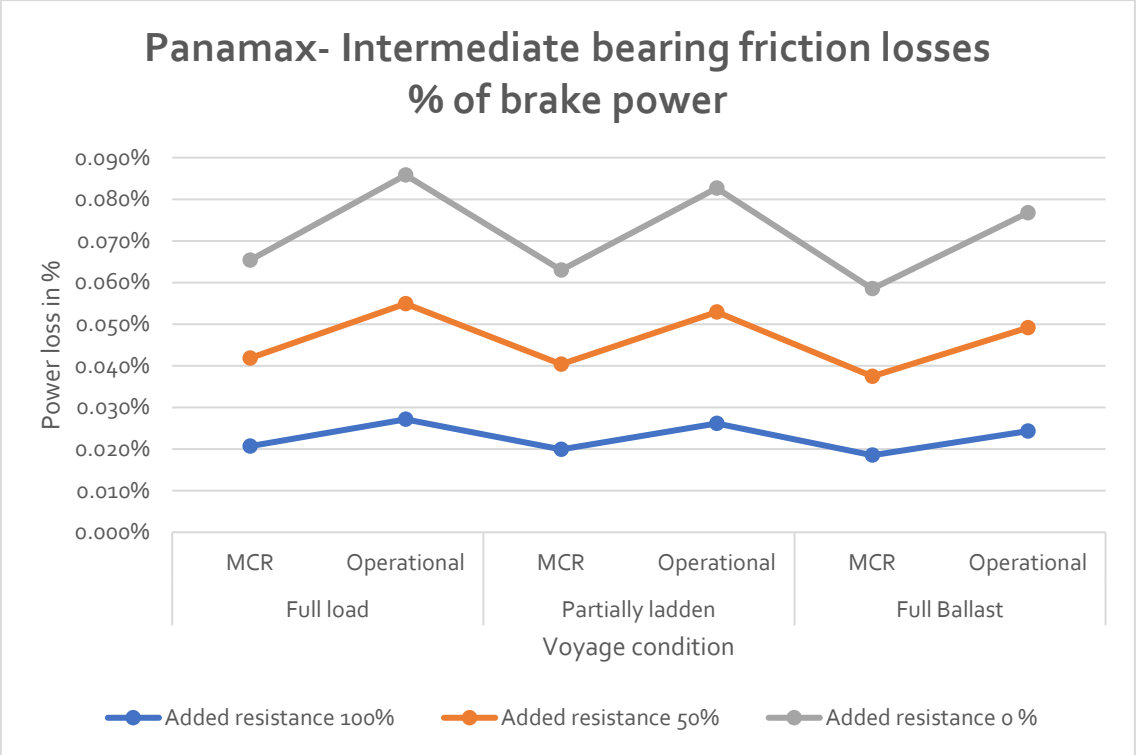

Figure 3.33 Panamax intermediate bearing losses %

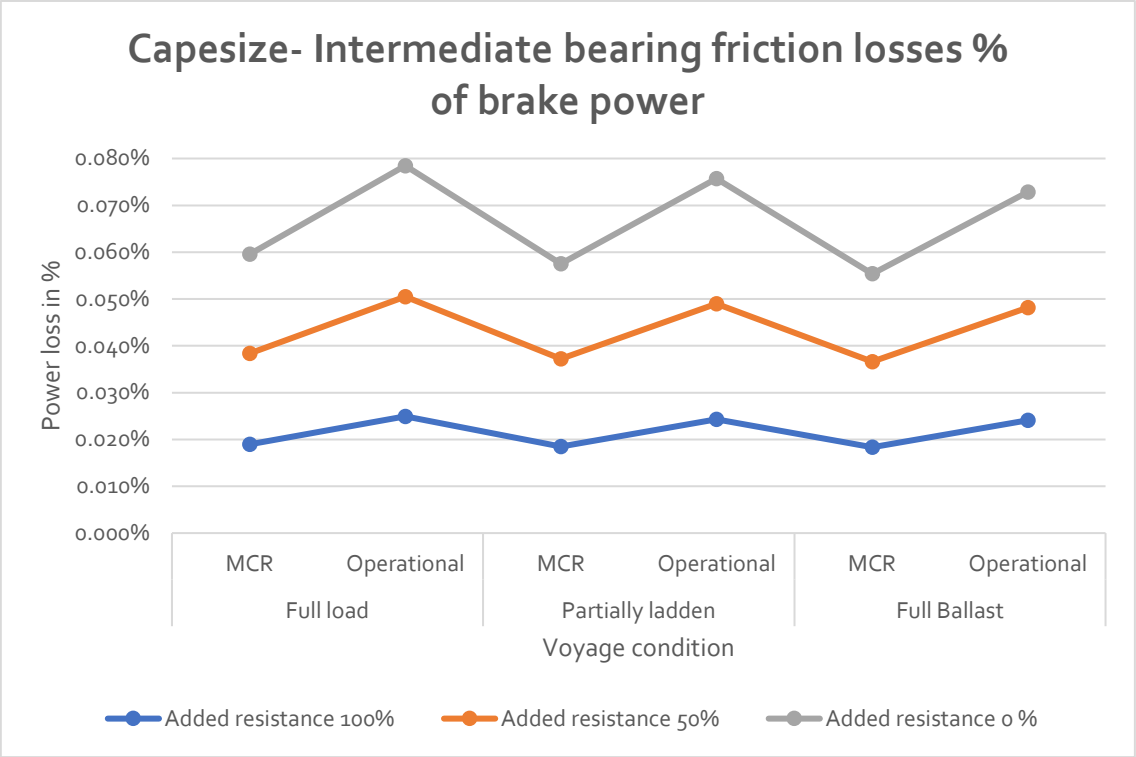

Figure 3.34 Capesize intermediate bearing losses %

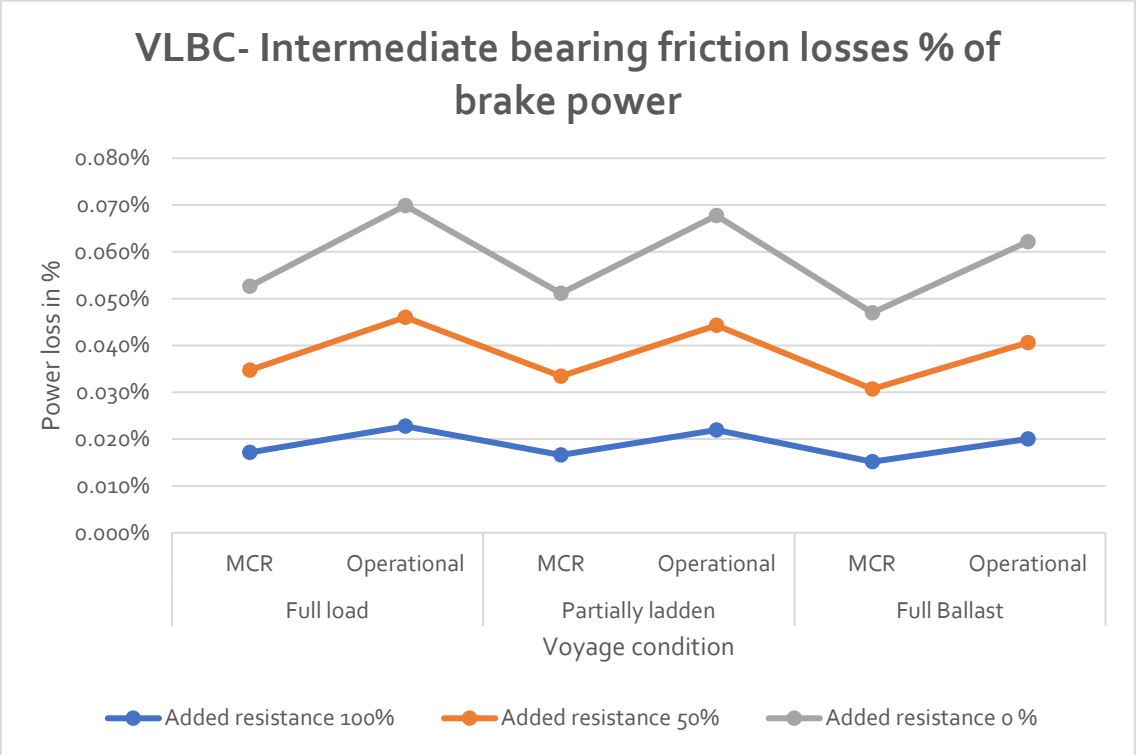

Figure 3.35 VLBC intermediate bearing losses %

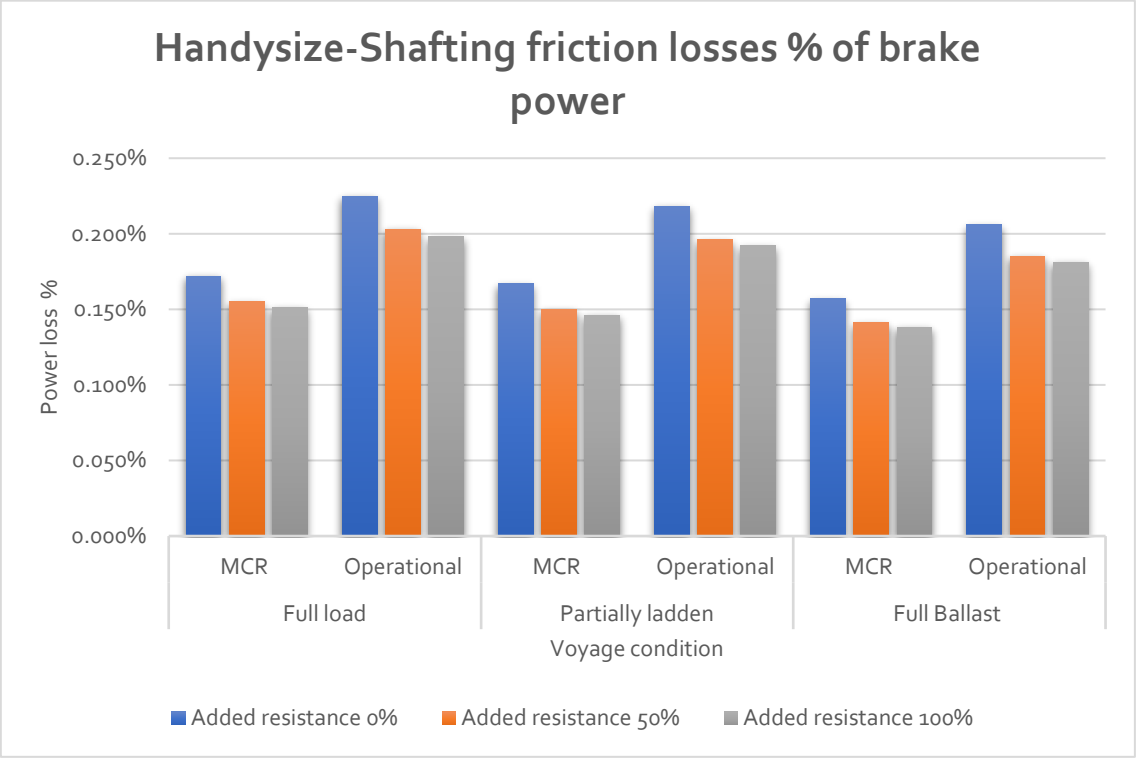

Figure 3.36 Handysize shafting frictional losses %

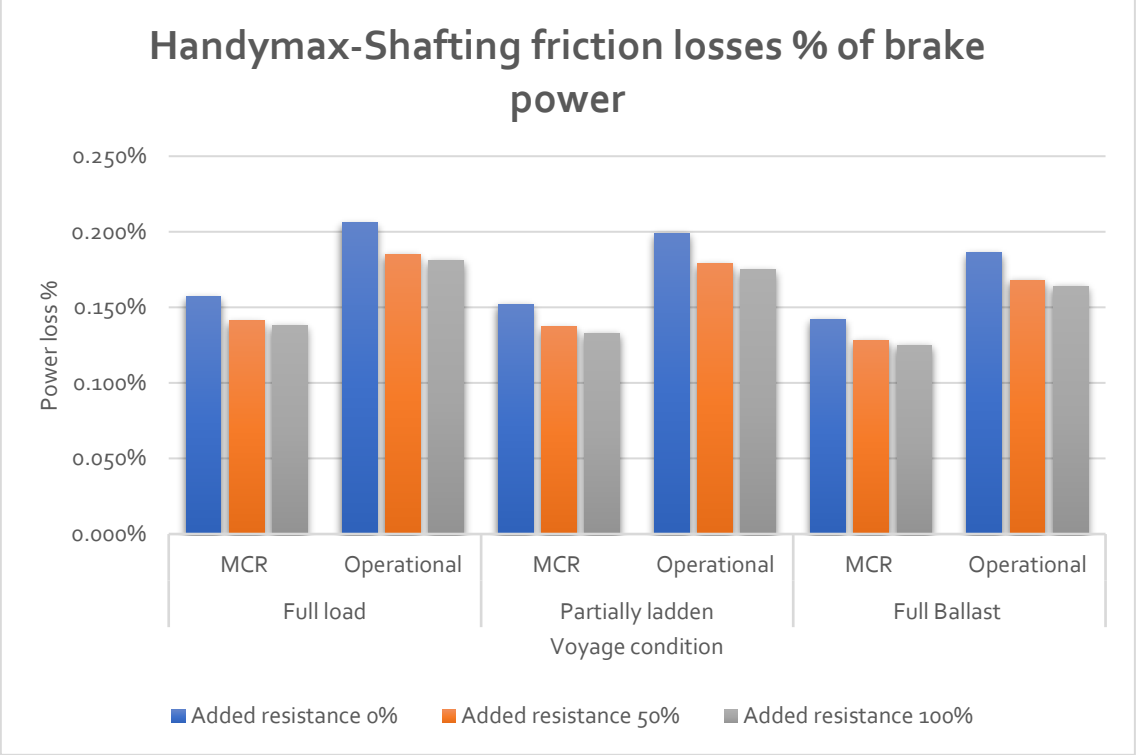

Figure 3.37 Handymax shafting frictional losses %

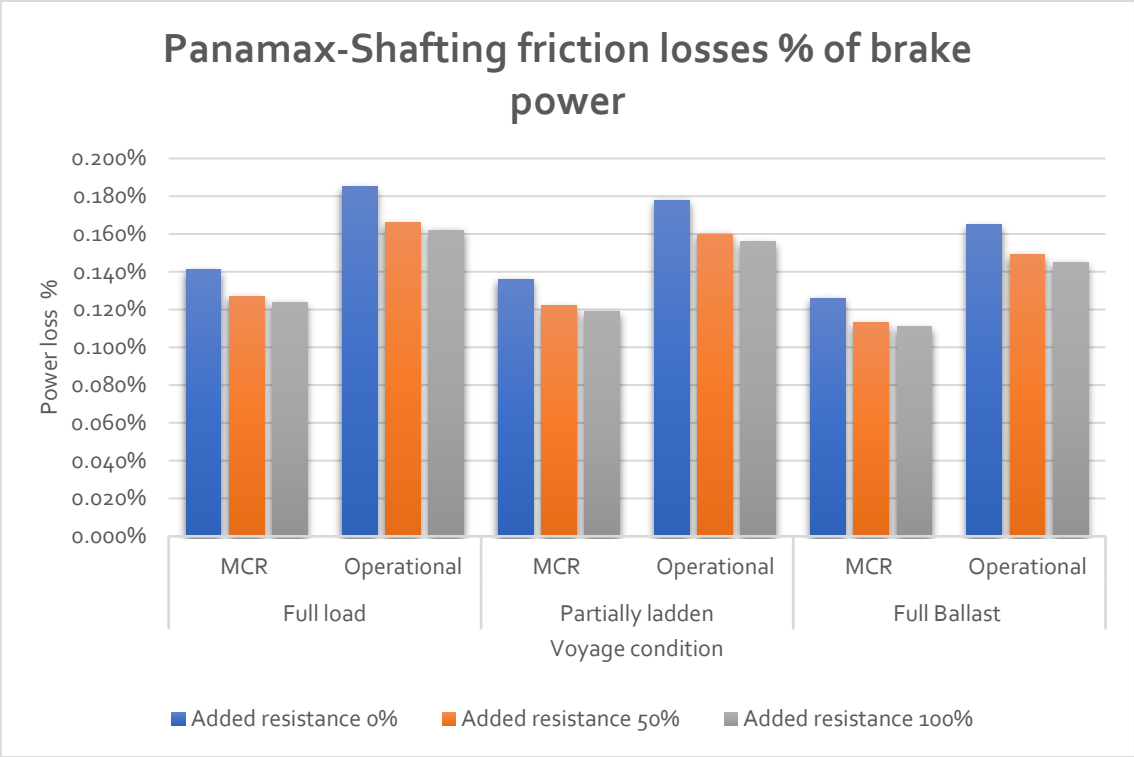

Figure 3.38 Panamax shafting frictional losses %

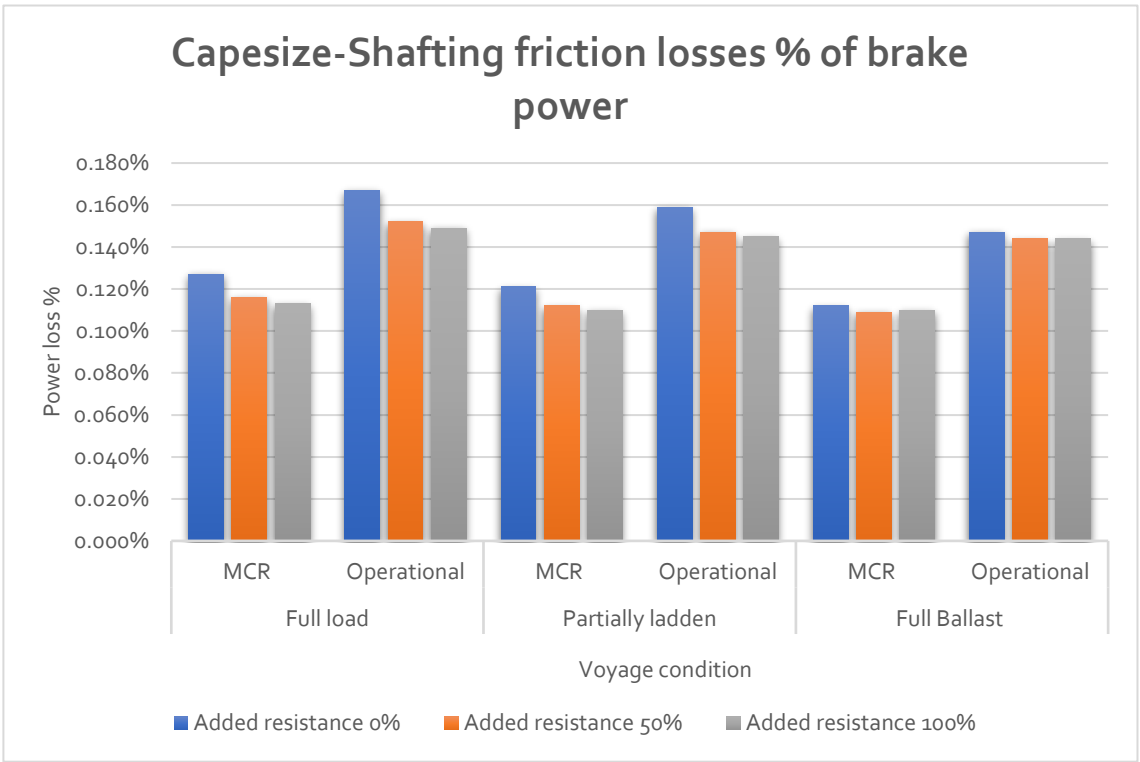

Figure 3.39 Capesize shafting frictional losses %

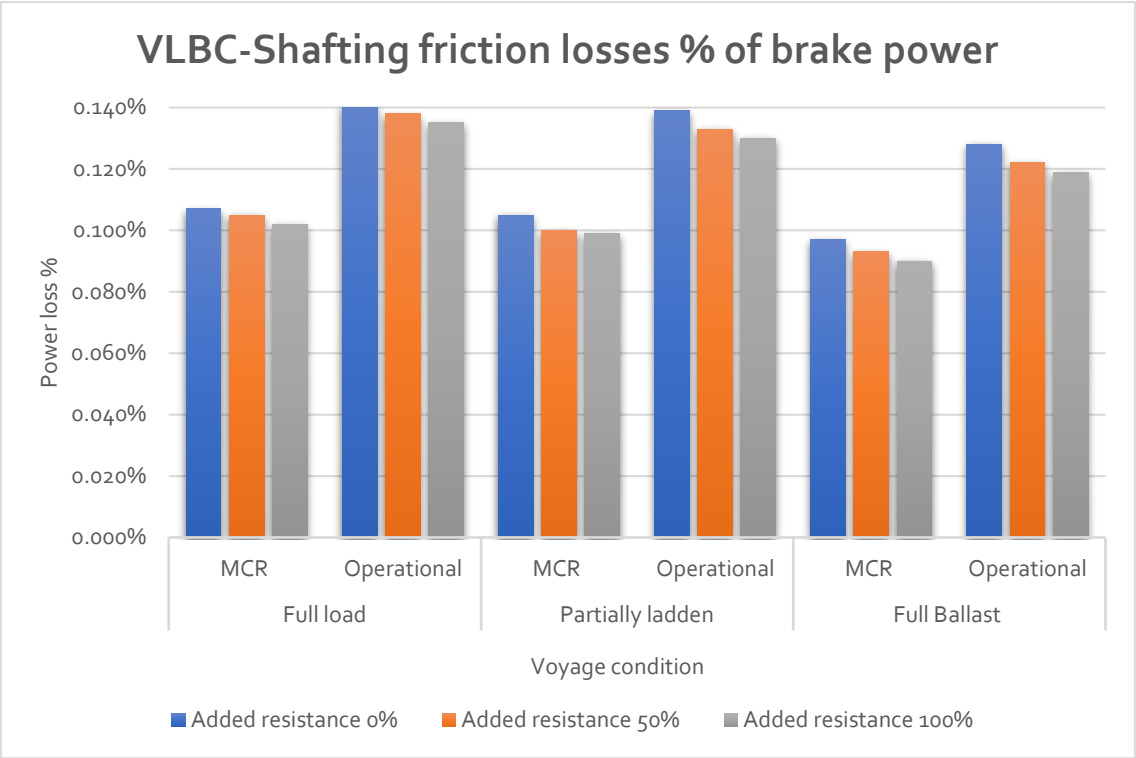

Figure 3.40 VLBC shafting frictional losses %

The aft bearing is the shaft component carrying the heaviest loads during the operation of the propulsion installation. The fore bearing is the bearing with the next larger amount of friction losses, while the intermediate bears the lowest. In every case, the friction losses in quantitative form, are larger for a decreasing draft, an increased added resistance and the speed at its maximum service values. Moreover, friction losses increase with vessel size, with the VLBC class being the most energy consuming.

Another important parameter affecting friction losses is the weight of the shafting system. Heavier installations generate larger loads that the bearings are bound to withstand. Of course, a large vessel in means of deadweight needs to consume more power for propulsion, so larger engines are installed. The increased installed propulsion power leads to heavier shafting systems, affecting thus friction losses.

In contrast with the quantitative case, the shafting friction losses as a percentage are less with the decreasing draft, vessel size and higher with increased speed and hull fouling. This is attributed to the fact that the operational power is higher for a large vessel, fully fouled, operating at its maximum engine output, while the relevant revolutions at that service point are low (the larger the two-stroke engine, the less revolutions per minute are needed). So, even though a VLBC would generate the highest shafting friction losses among other vessel types, due to its size and installed propulsion unit, these losses are the smallest percentage among other vessel classes.

As a percent of operating brake power, friction losses attribute from the quantitative case in the opposite manner; they are maximum for Handysize vessels and keep reducing as the vessel size increases. As small-sized the vessel is, the equipped engine would run on higher revolutions; thus, affecting friction losses. Moreover, the installed brake power increases with vessel size. So, the percentage losses are higher for small classed vessels, in contrast with the quantitative case.

3.2.2 Engine friction losses

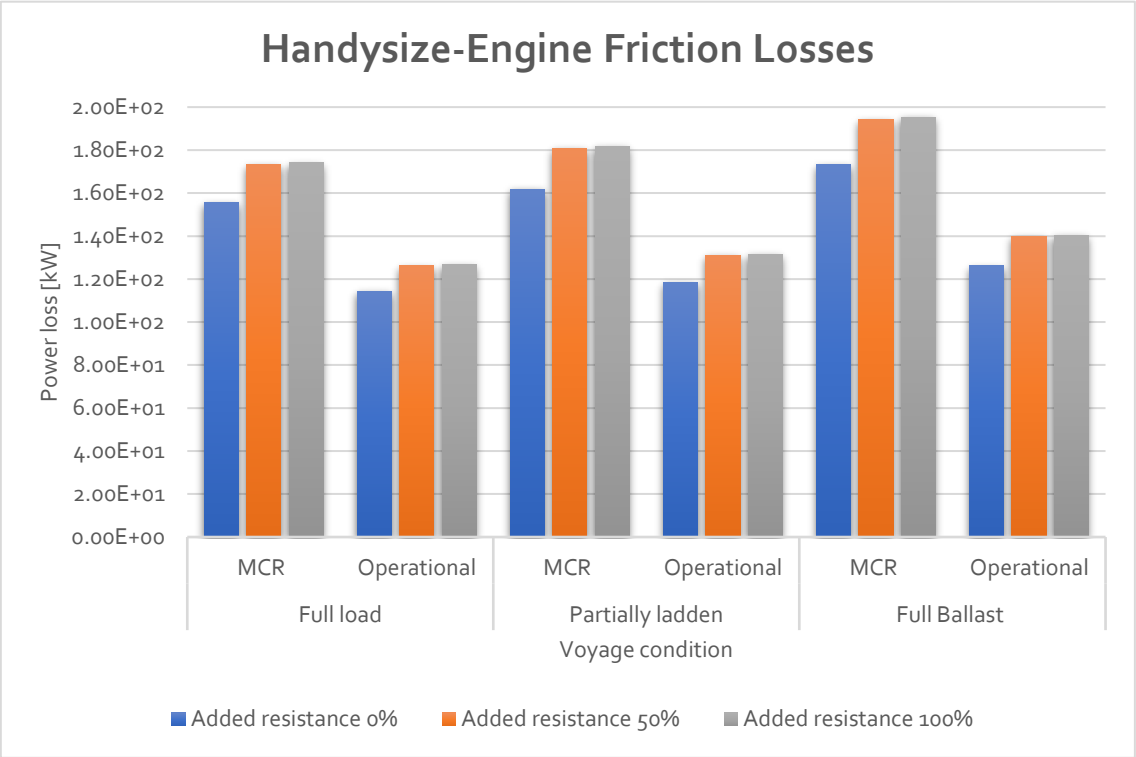

Figure 3.41 Handysize engine frictional losses kW

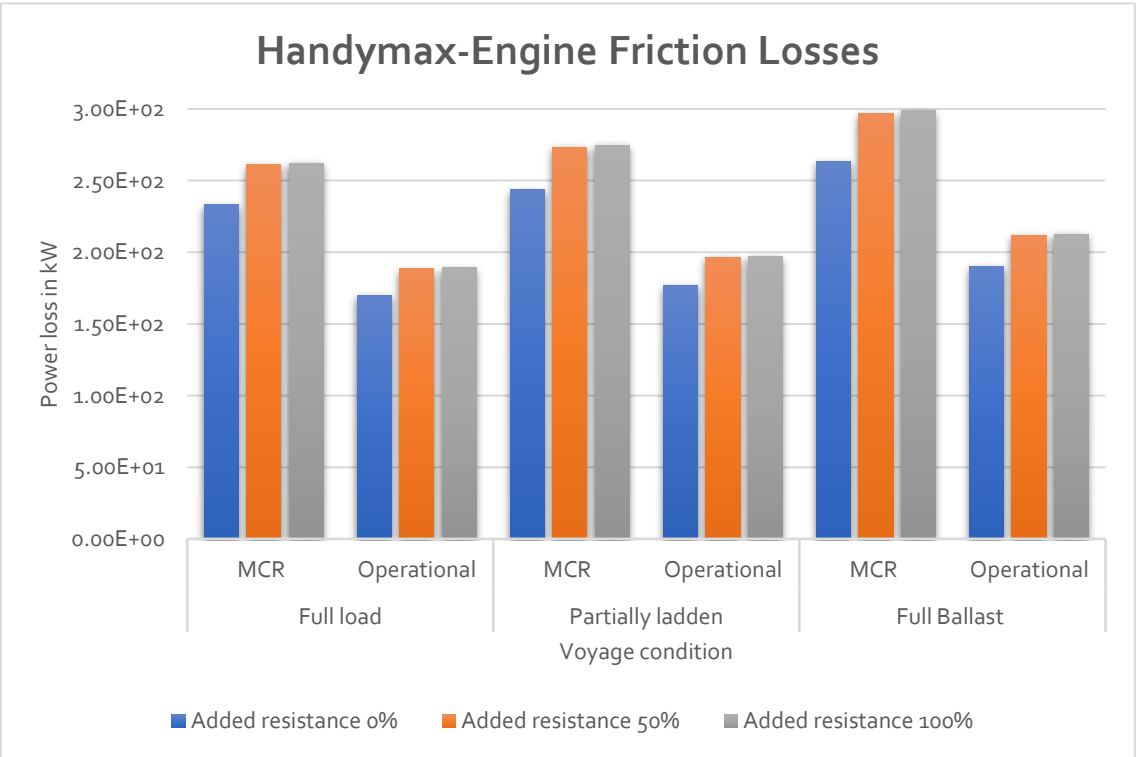

Figure 3.42 Handymax engine frictional losses kW

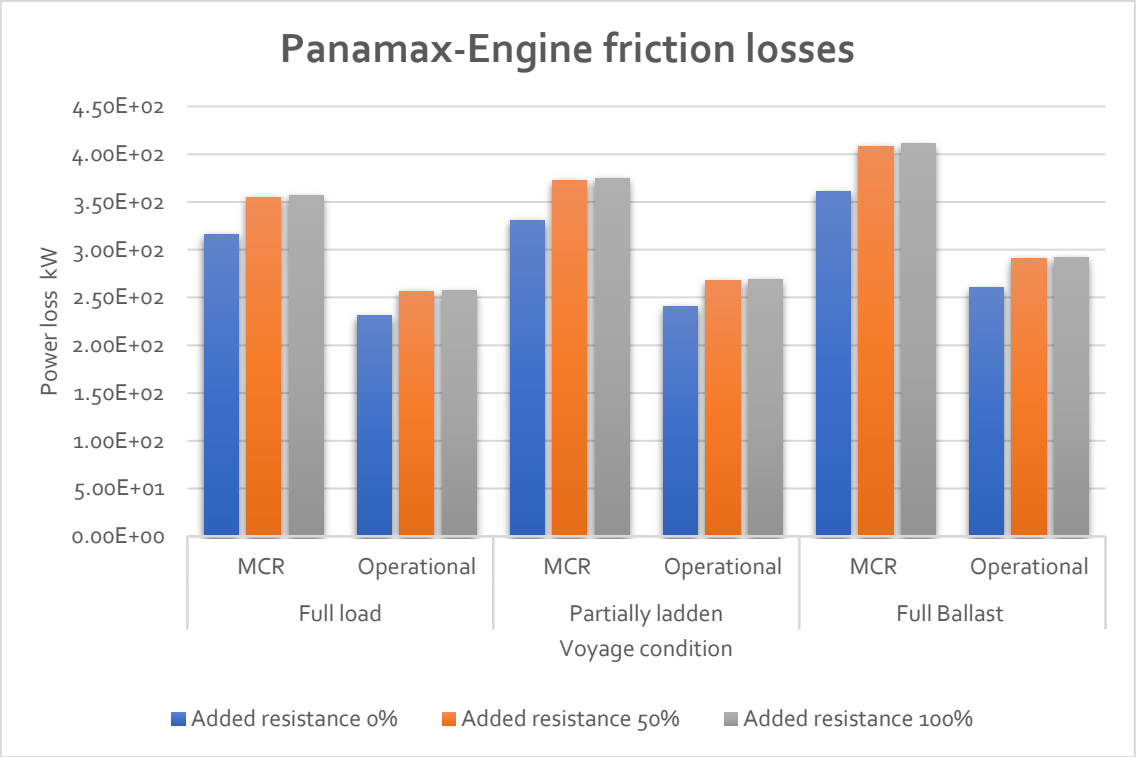

Figure 3.43 Panamax engine frictional losses kW

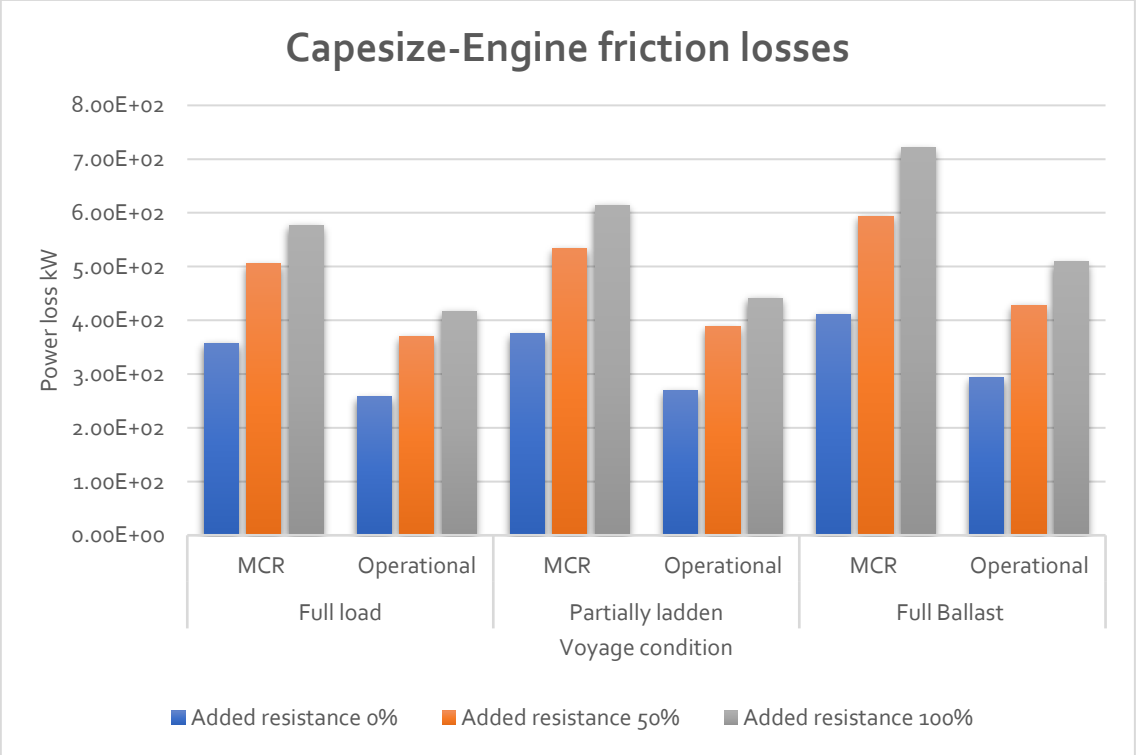

Figure 3.44 Capesize engine frictional losses kW

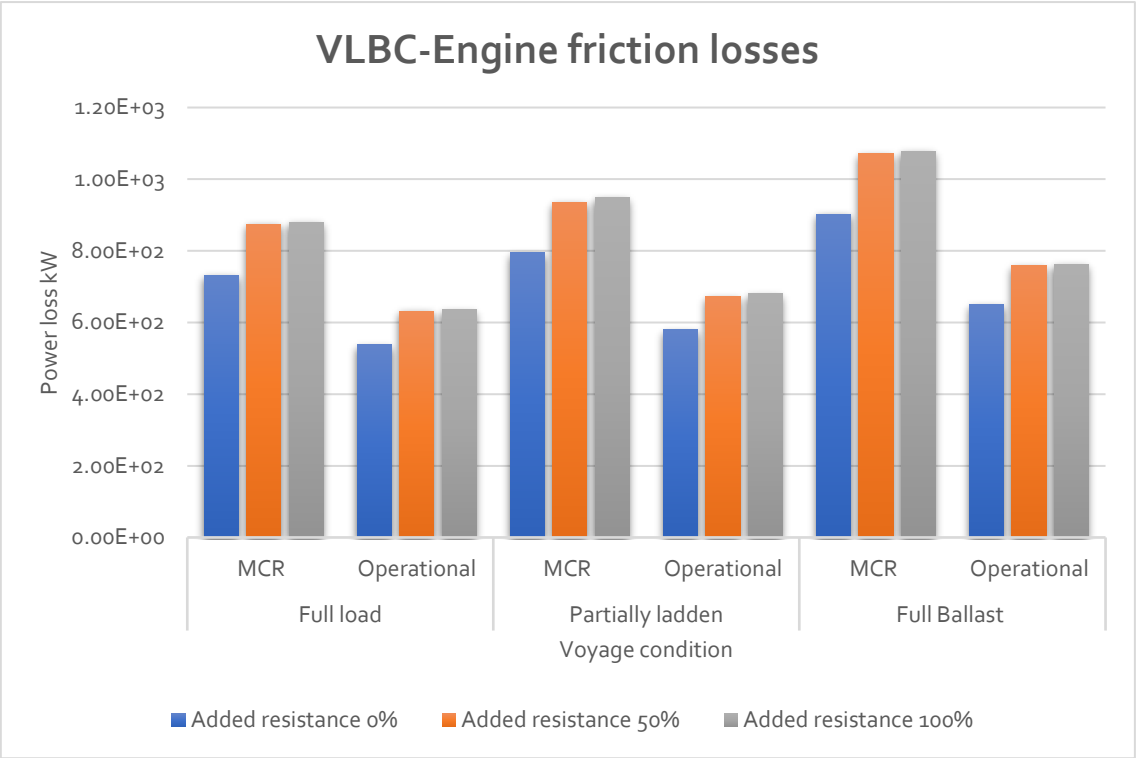

Figure 3.45 VLBC engine frictional losses kW

Engine friction losses were calculated by the use of empirical relations. These relations take into account the following parameters:

- Engine cylinder number
- Engine stroke
- Engine bore
- Engine mean effective pressure
- Engine mean piston speed
- Engine compression ratio
- Engine crankshaft revolutions

So, the attribute of the engine friction losses is dependent on these parameters. From these parameters, pressure and speed are variable; the rest are constant for a certain engine model.

As an amount of energy, friction losses increase by:

- Vessel size
- Increased service speed
- Reducing draft of vessel (as in the case of shafting losses)

Engine friction varies also by the increase of added resistance. For the case of shafting losses, reduced resistance leads to increased propeller revolutions for the constant system weight. However, this is not valid for the engine friction losses. Reduced resistance means operation of engine at a reduced load; a reduced mean effective pressure and crankshaft speed. As the engine load drops, the mean effective pressure reduction is more significant than the friction pressure reduction. So, the friction losses depend on the combination of revolutions and pressure values on a specific load for a specific engine model.

Based on this observation, a dependency between losses and draft is distinguished. A decrease in draft leads to an increase in engine losses. The wetted surface is reduced at lower draft, lowering the power demand for propulsion.

The effect of service speed is the same for the engine friction case as for the shafting; reduced speed leads also to reduced power losses due to friction.

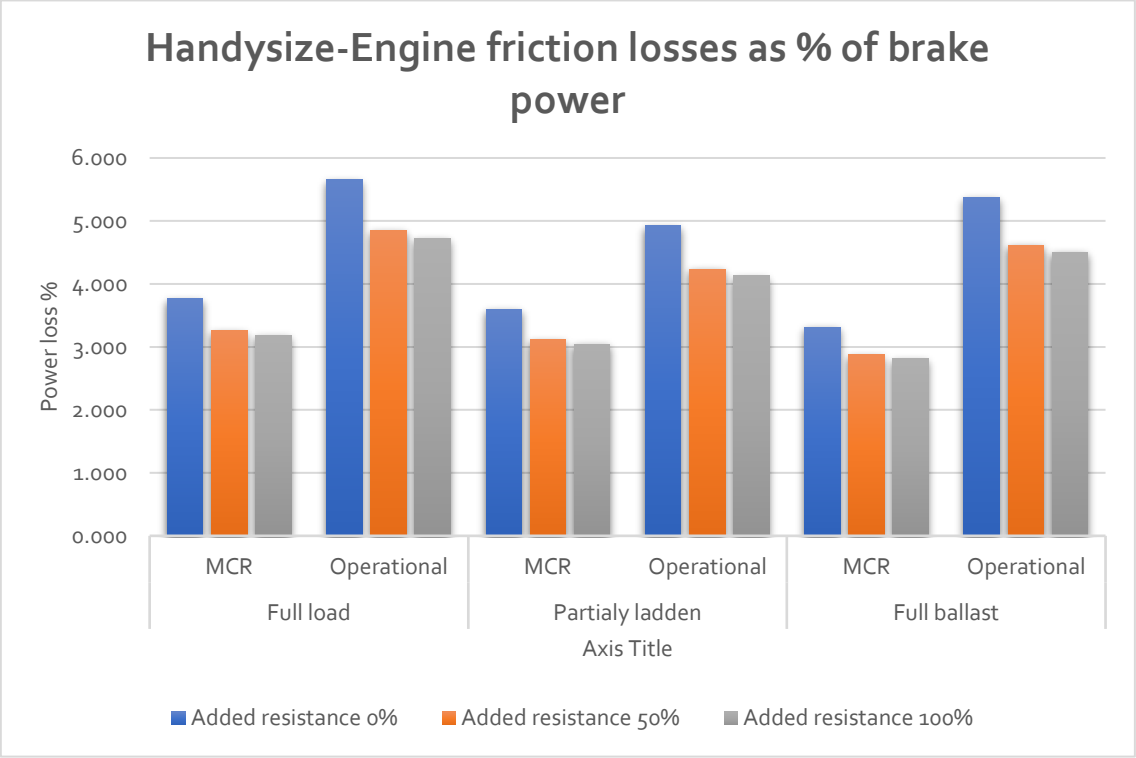

Figure 3.46 Handysize engine frictional losses %

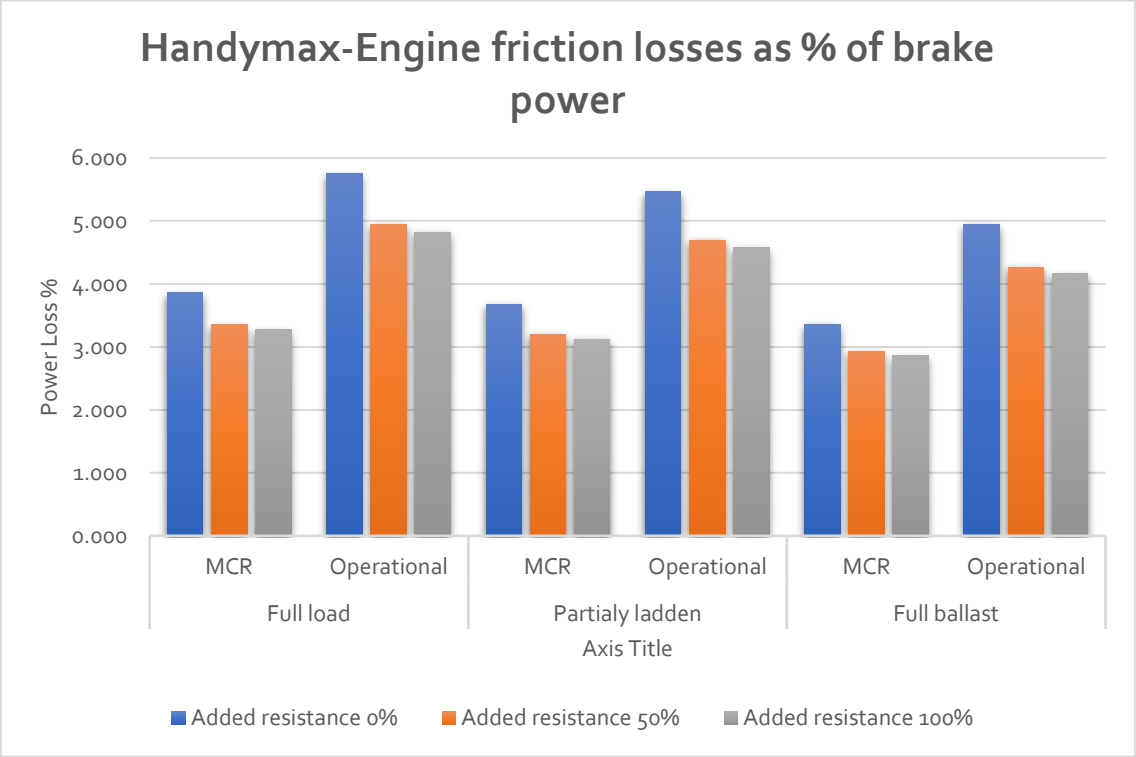

Figure 3.47 Handymax engine frictional losses %

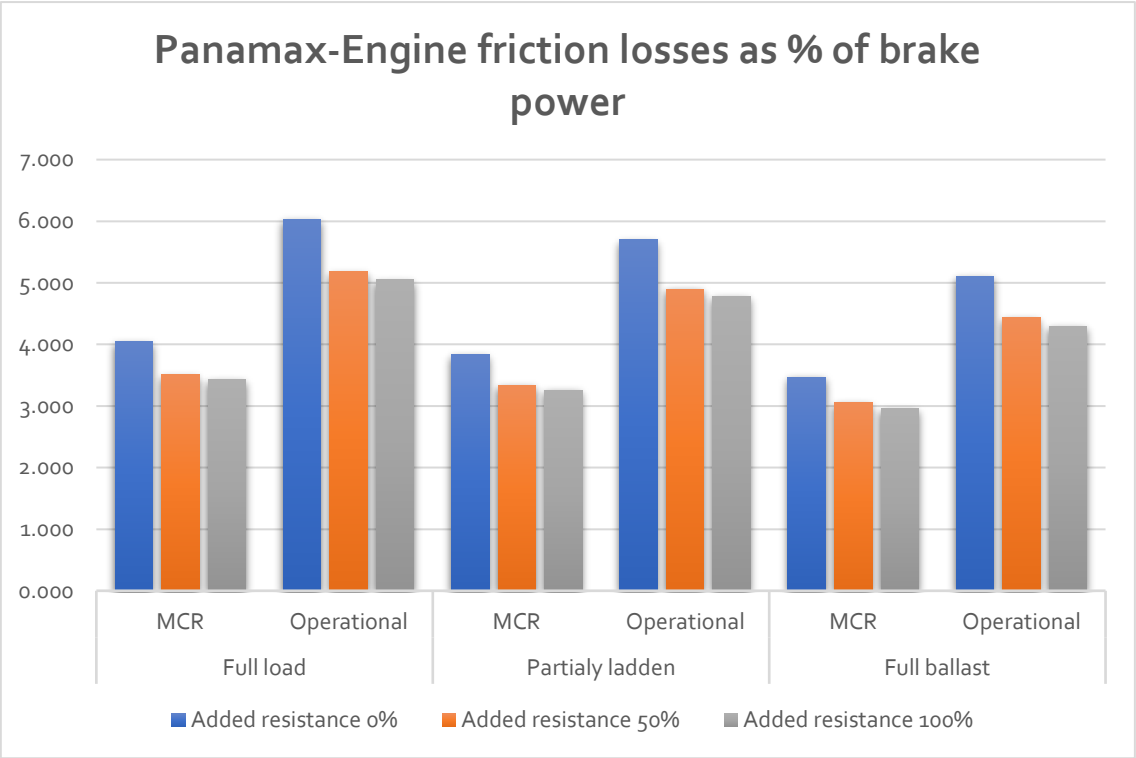

Figure 3.48 Panamax engine frictional losses %

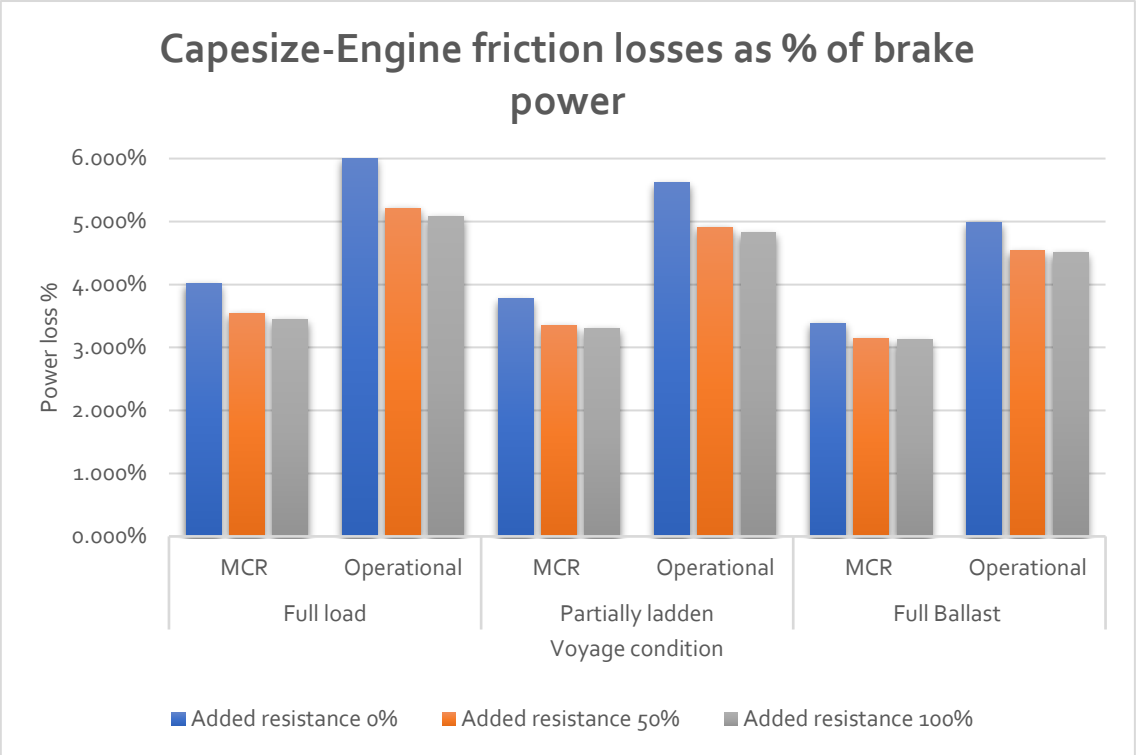

Figure 3.49 Capesize engine frictional losses %

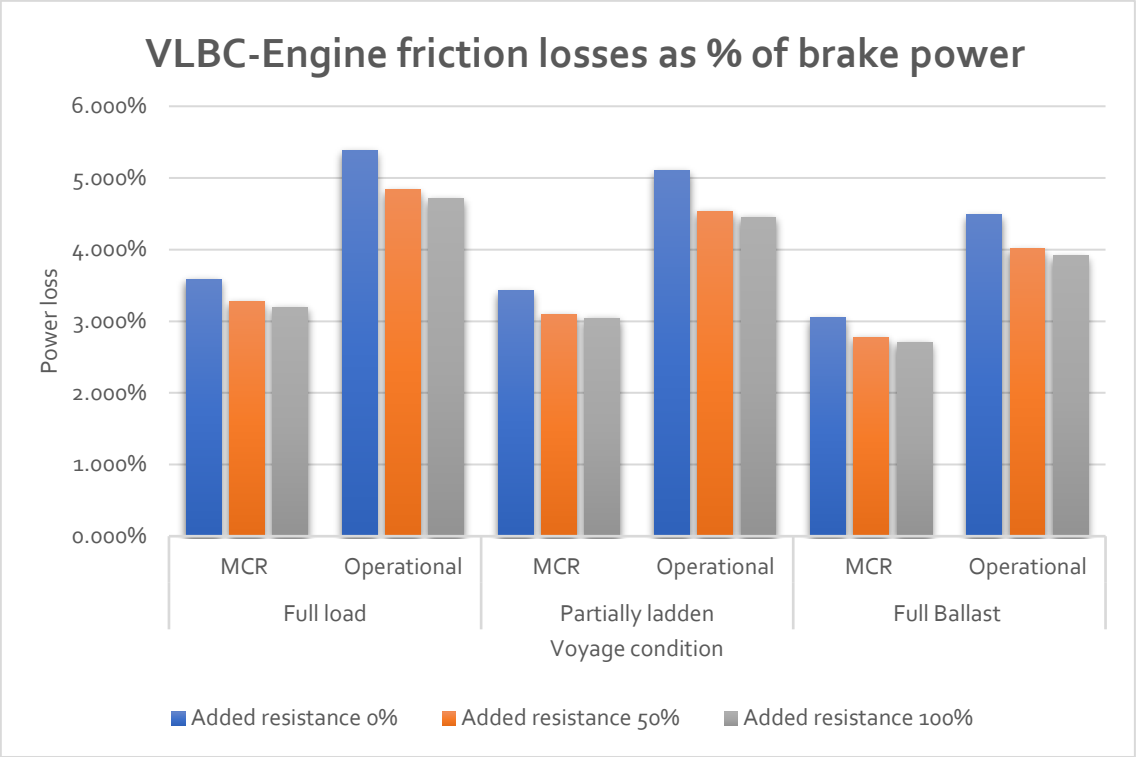

Figure 3.50 VLBC engine frictional losses %

As a percentage of brake power, engine friction losses behave in an inverse manner. They increase as draft and vessel size decrease and as resistance and speed increase. As explained in the quantitative case, engine load drops, (which means that less fuel is injected in the combustion chamber) the drop in mean effective pressure and mean friction pressure loss is uneven. As tested by Ulman [6], friction pressure loss is not affected by crankshaft speed and engine size but merely depends on mean piston speed; thus, friction is not reduced proportionally to the engine load. However, mean piston speed is constant among different engine models. In this manner, engine friction loss can be considered constant. Brake power is calculated as:

$$\boldsymbol{P = \frac{\pi}{4} Z_{cyl} s p b^2 \frac{N}{60}}$$

The mean effective pressure is the same for each engine model. So, for two different engine models, brake power is a function of:

- Bore
- Stroke
- Cylinder number
- Crankshaft revolutions

If both engines have the same cylinder number, then brake power depends only on bore and stroke, while the revolutions will be higher for the smaller engine.

$$\boldsymbol{P = csNb^2}$$

Consequently, friction losses in quantitative form are higher for a large engine, whereas, for the same engine, in percentage form, friction losses are low.

3.2.2.1 Frictional losses main engine components

For the engine loss distribution, values proposed by Clausen [12] are used in order to calculate the losses per engine part. The next figures, illustrates the power lost at engine components for the changing speed, draft and resistance.

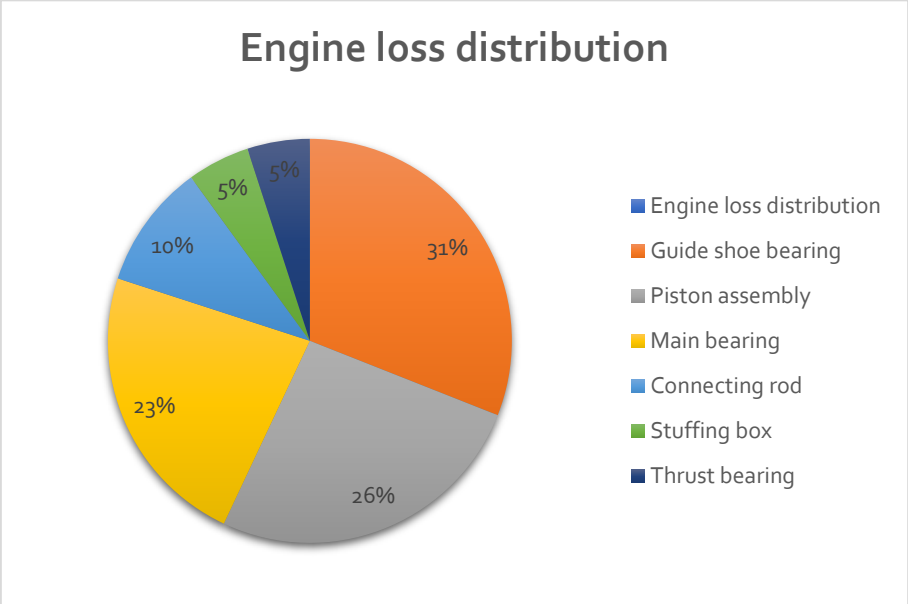

Figure 3.51 Engine loss distribution [12]

3.2.2.1.1 Guide shoe frictional losses

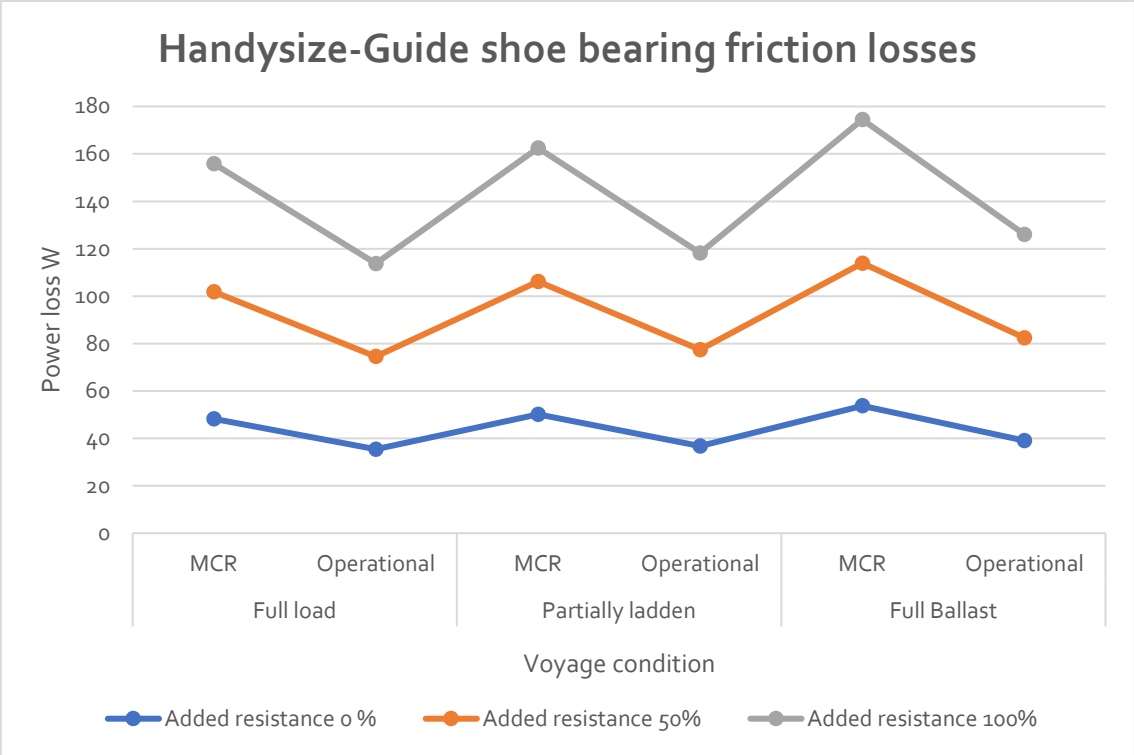

Figure 3.52 Handysize guide shoe frictional losses W

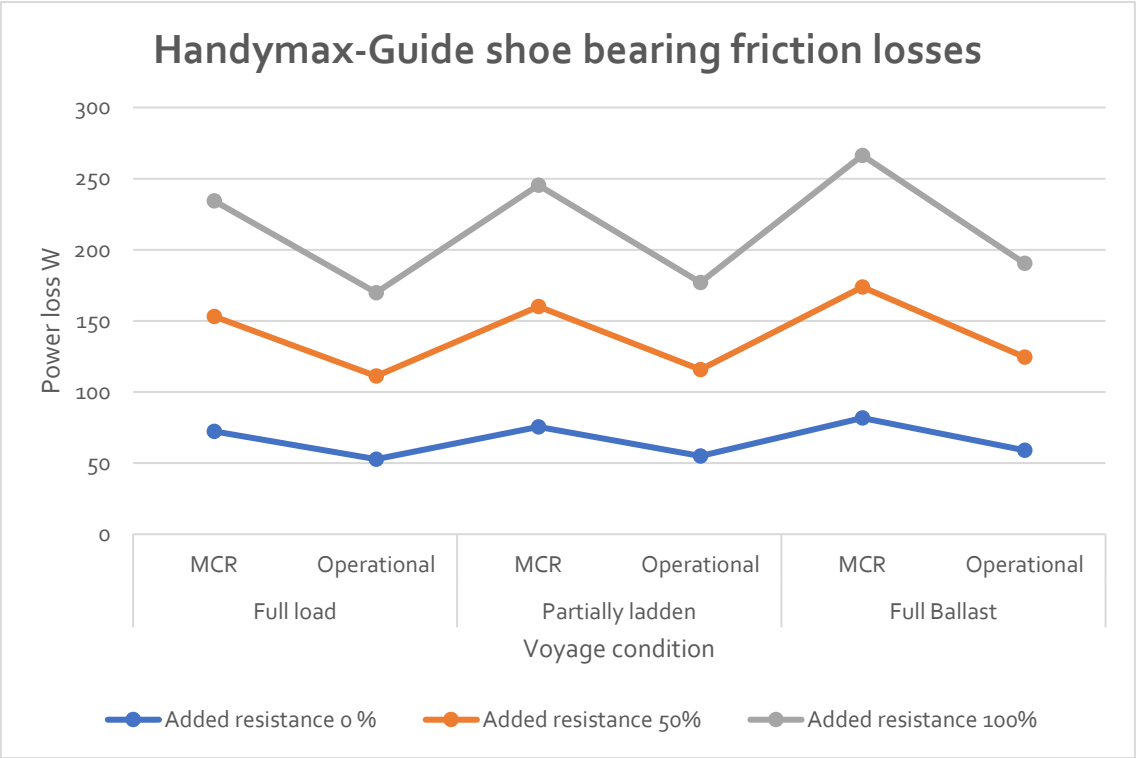

Figure 3.53 Handymax guide shoe frictional losses W

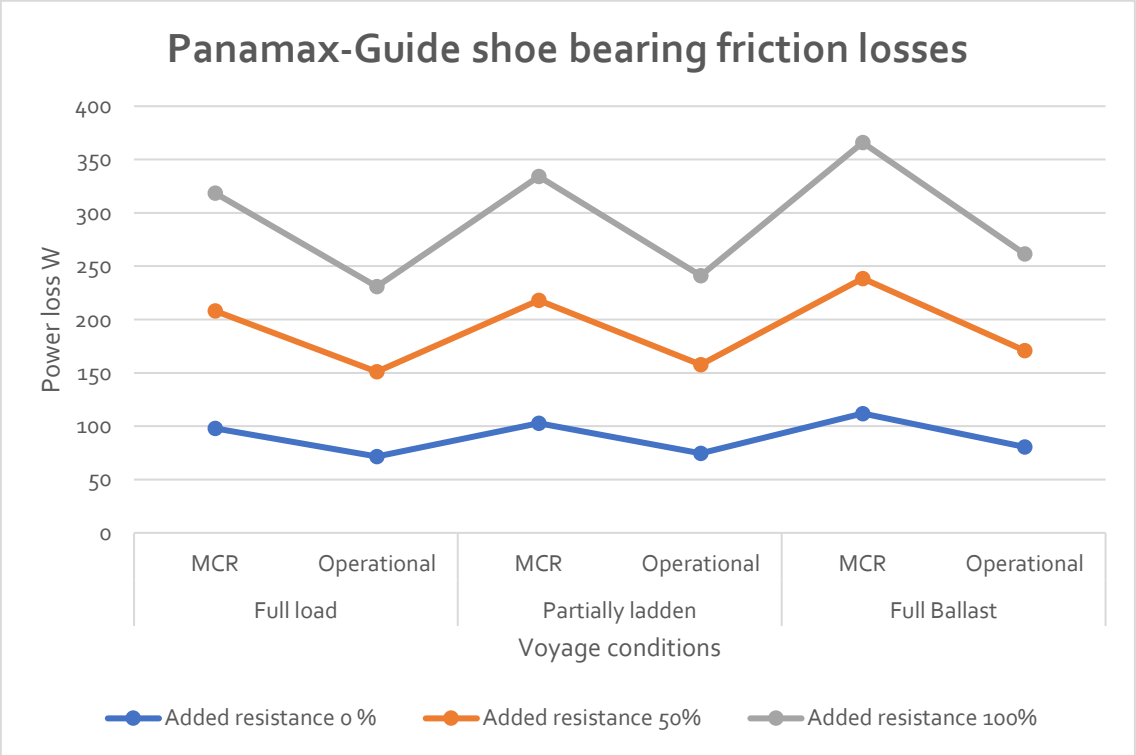

Figure 3.54 Panamax guide shoe frictional losses W

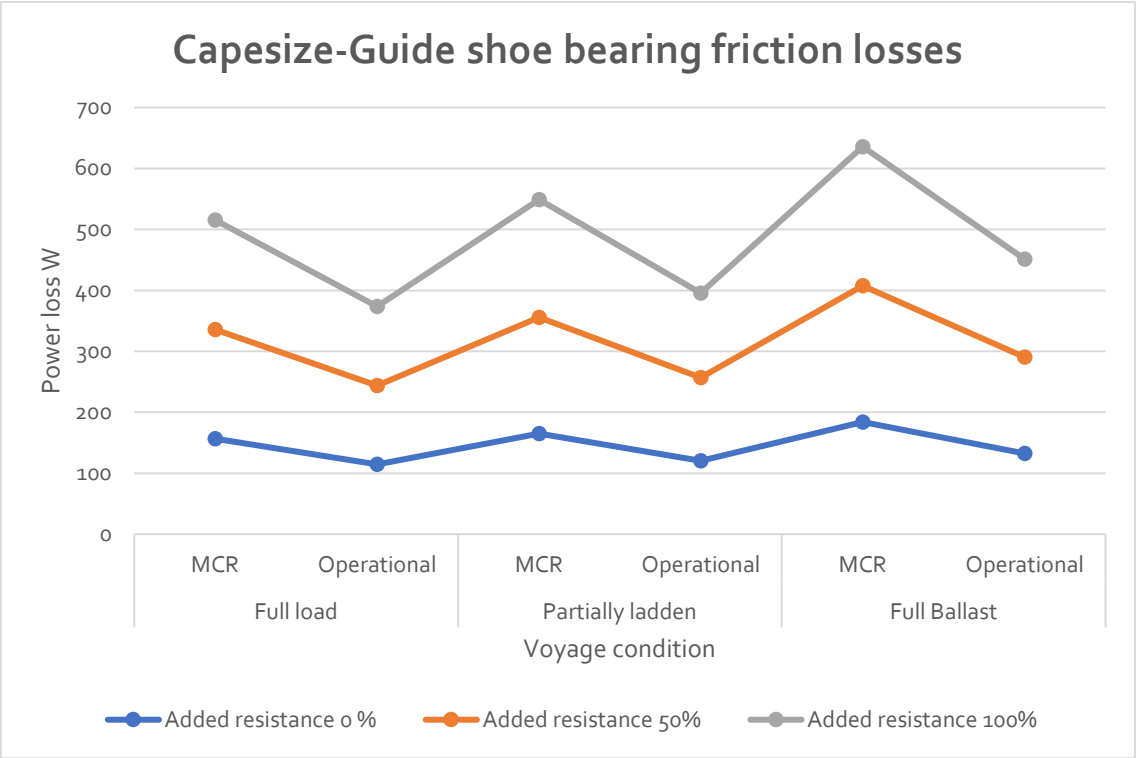

Figure 3.55 Capesize guide shoe frictional losses W

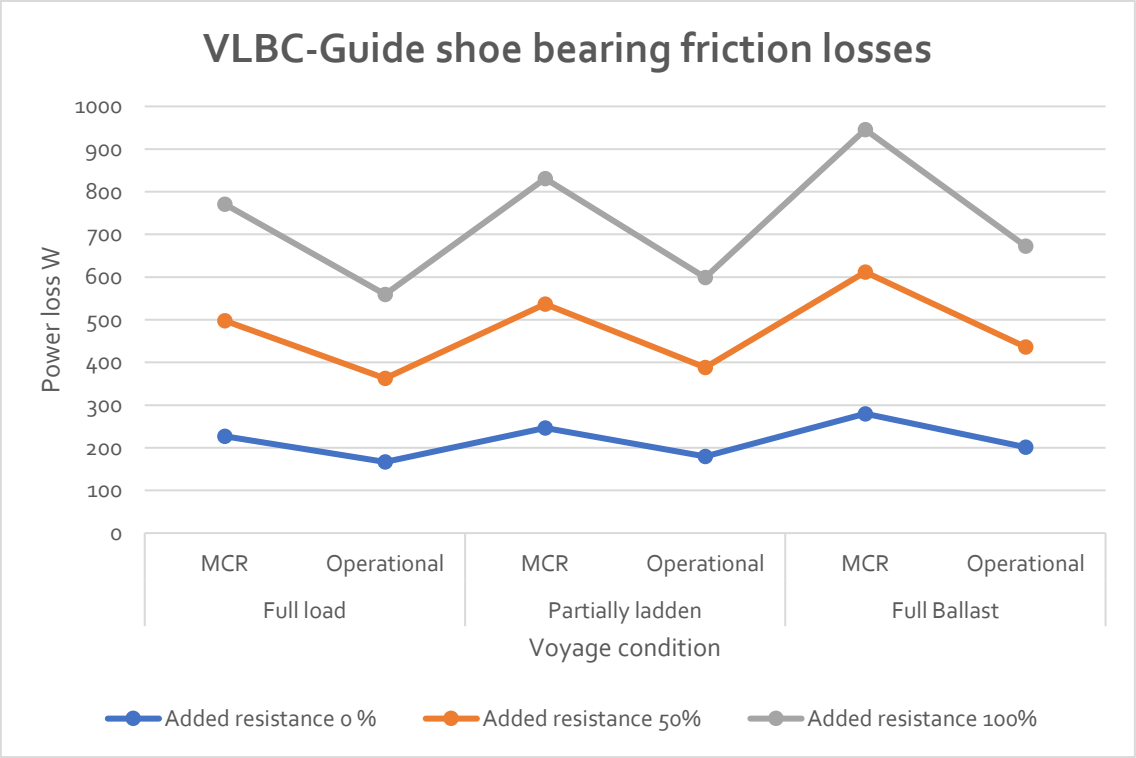

Figure 3.56 VLBC guide shoe frictional losses W

3.2.2.1.2 Piston frictional losses

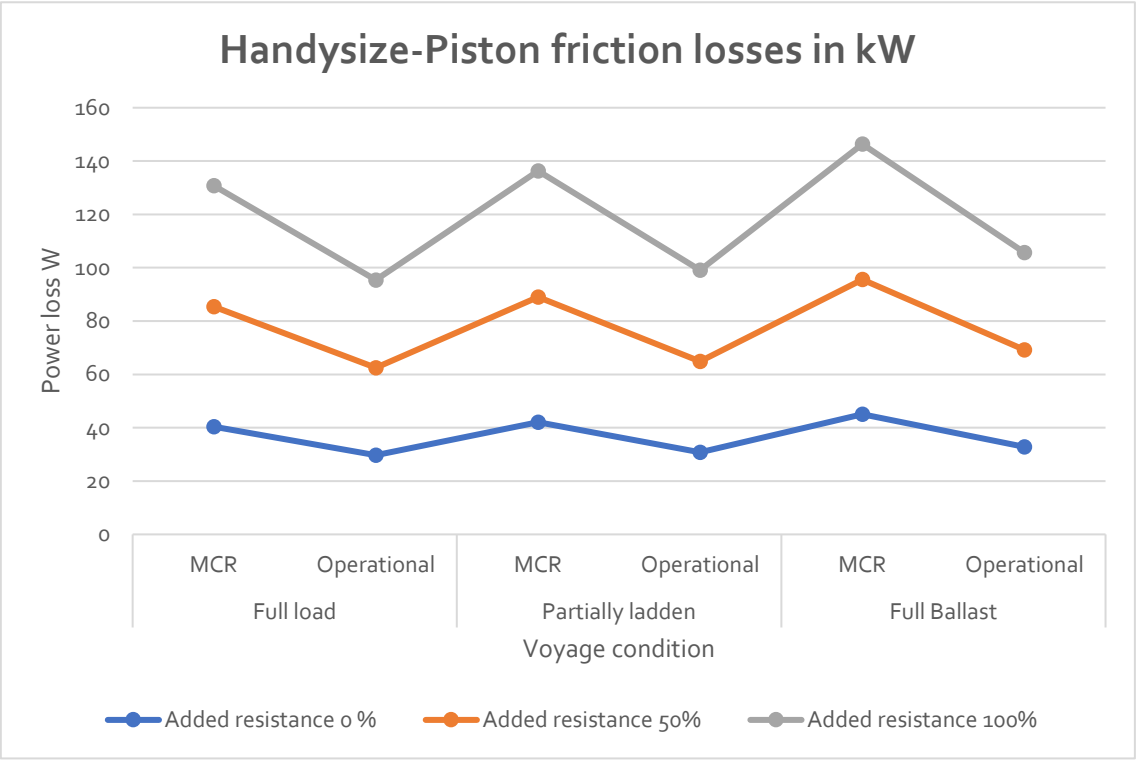

Figure 3.57 Handysize piston frictional losses W

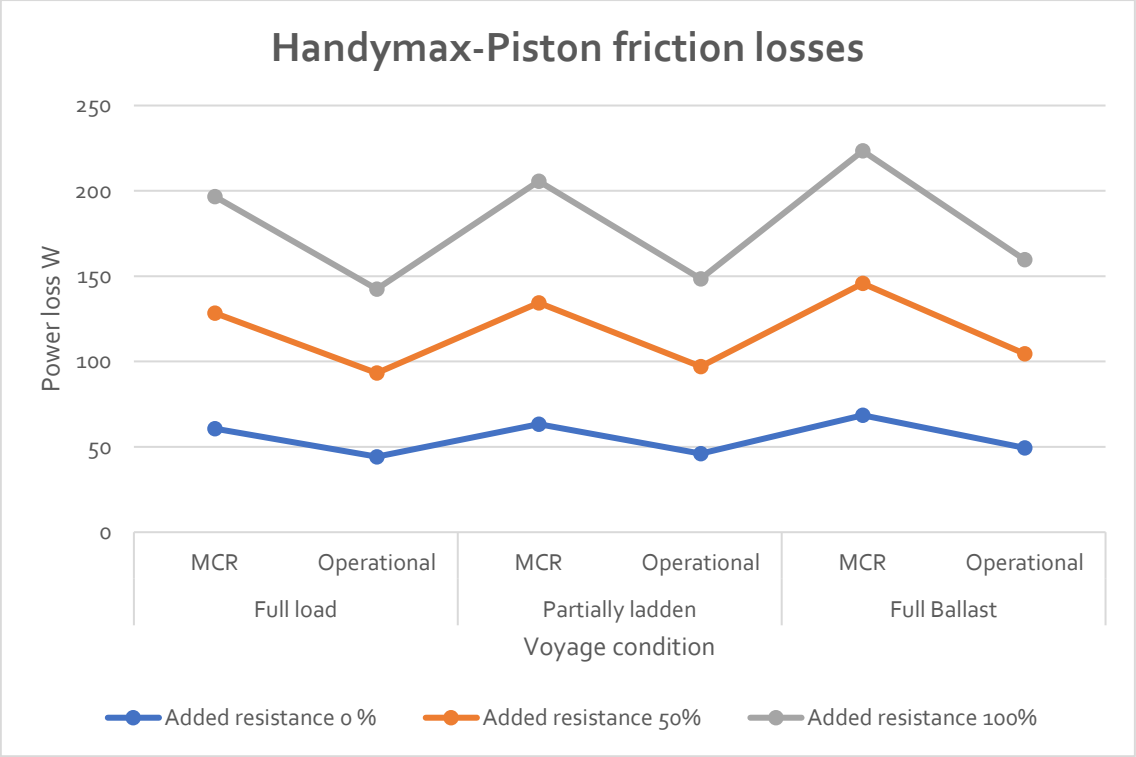

Figure 3.58 Handymax piston frictional losses W

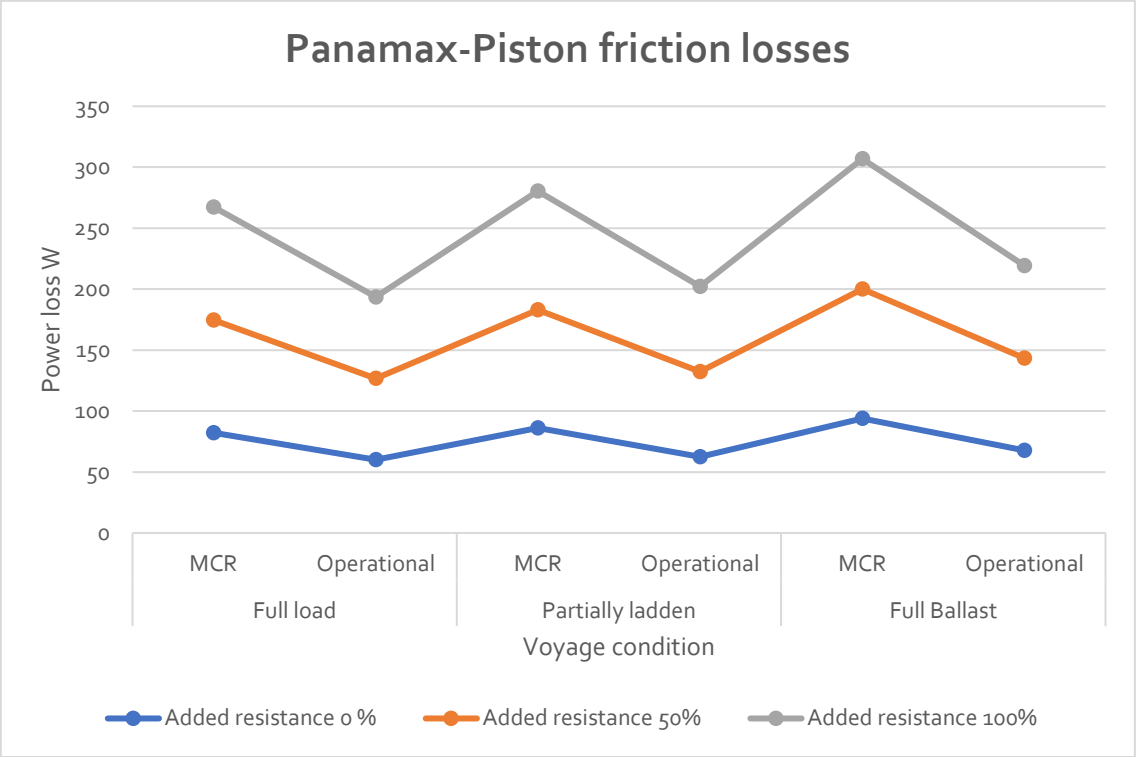

Figure 3.59 Panamax piston frictional losses W

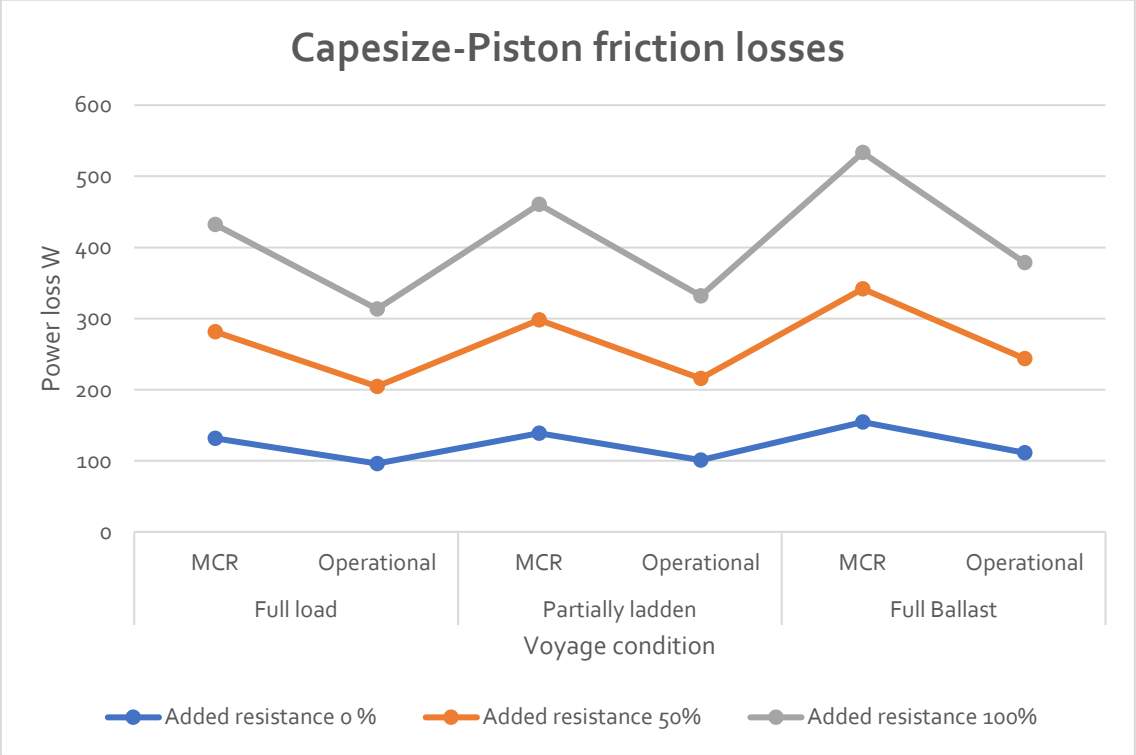

Figure 3.60 Capesize piston frictional losses W

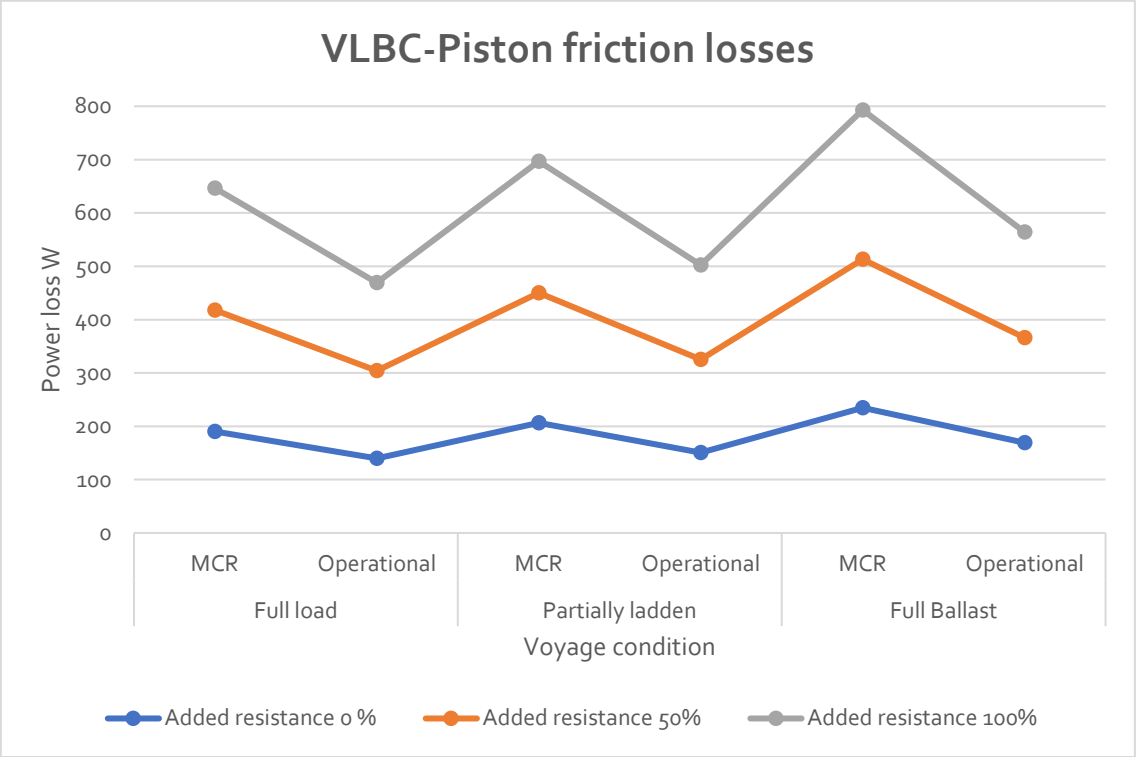

Figure 3.61 VLBC piston frictional losses W

3.2.2.1.3 Main bearing frictional losses

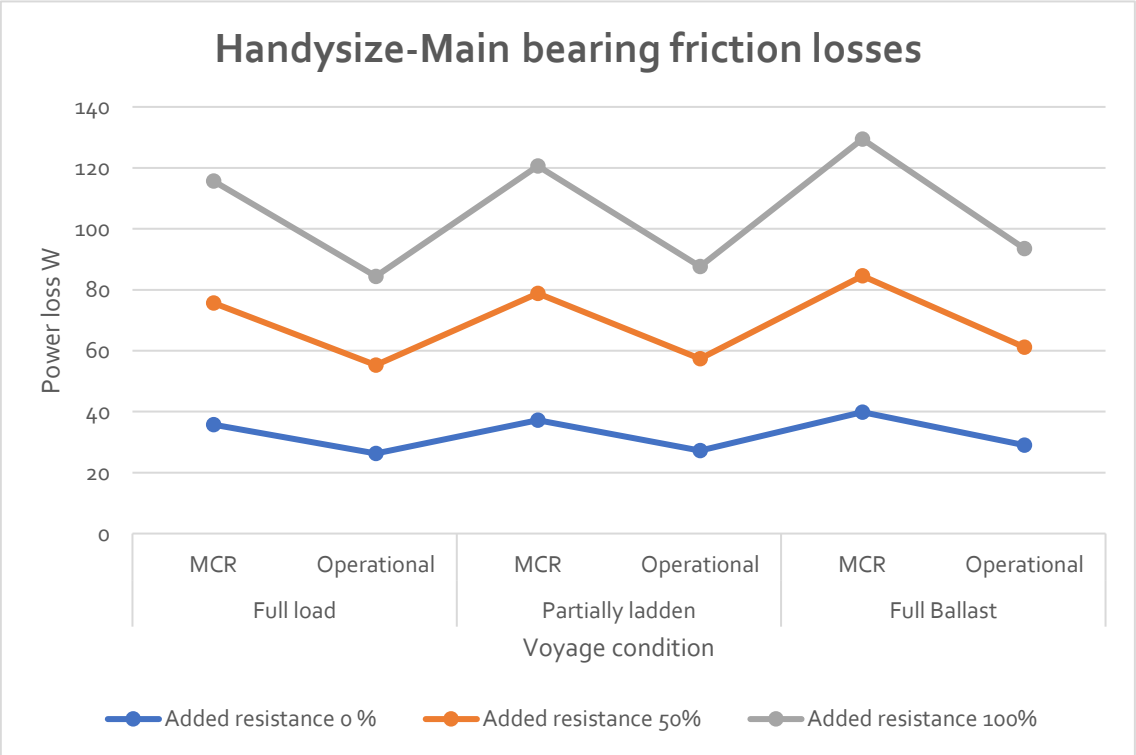

Figure 3.62 Handysize main bearing frictional losses W

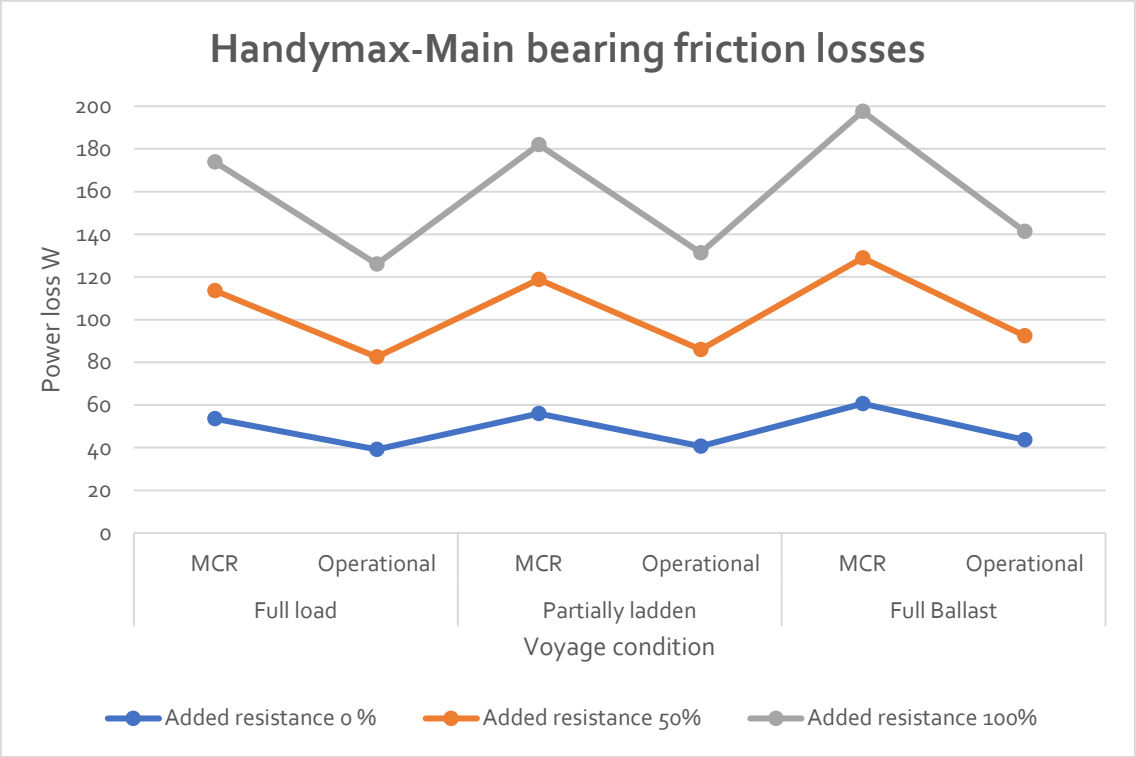

Figure 3.63 Handymax main bearing frictional losses W

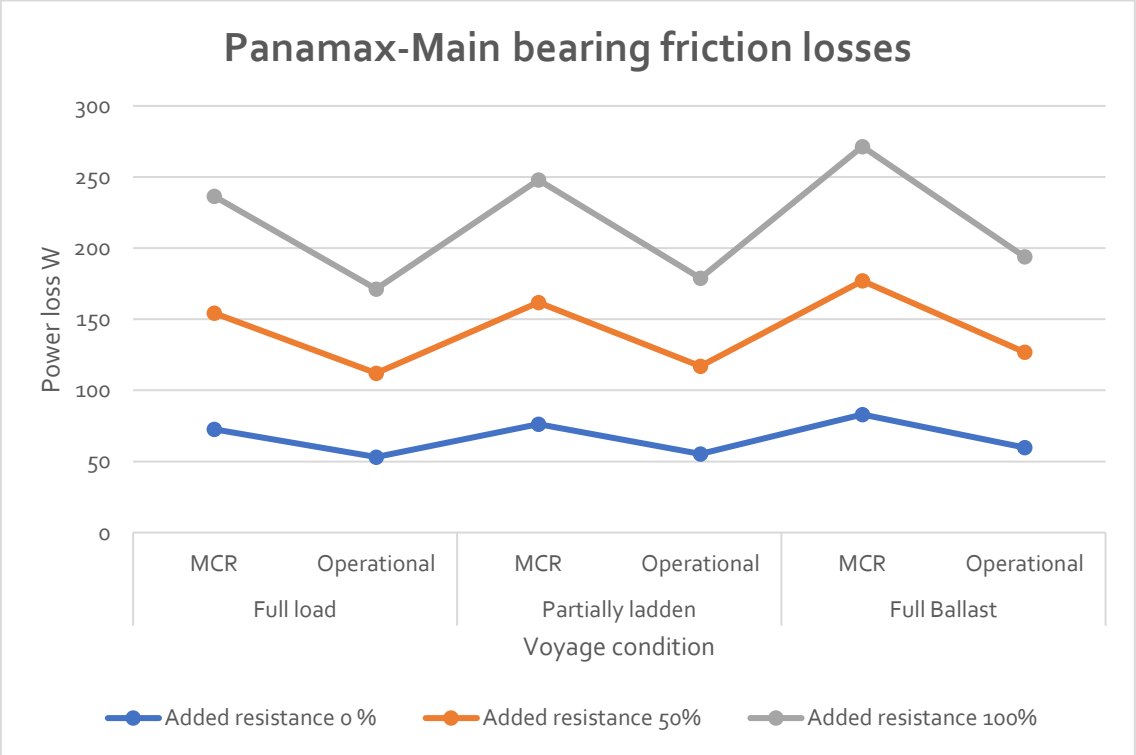

Figure 3.64 Panamax main bearing frictional losses W

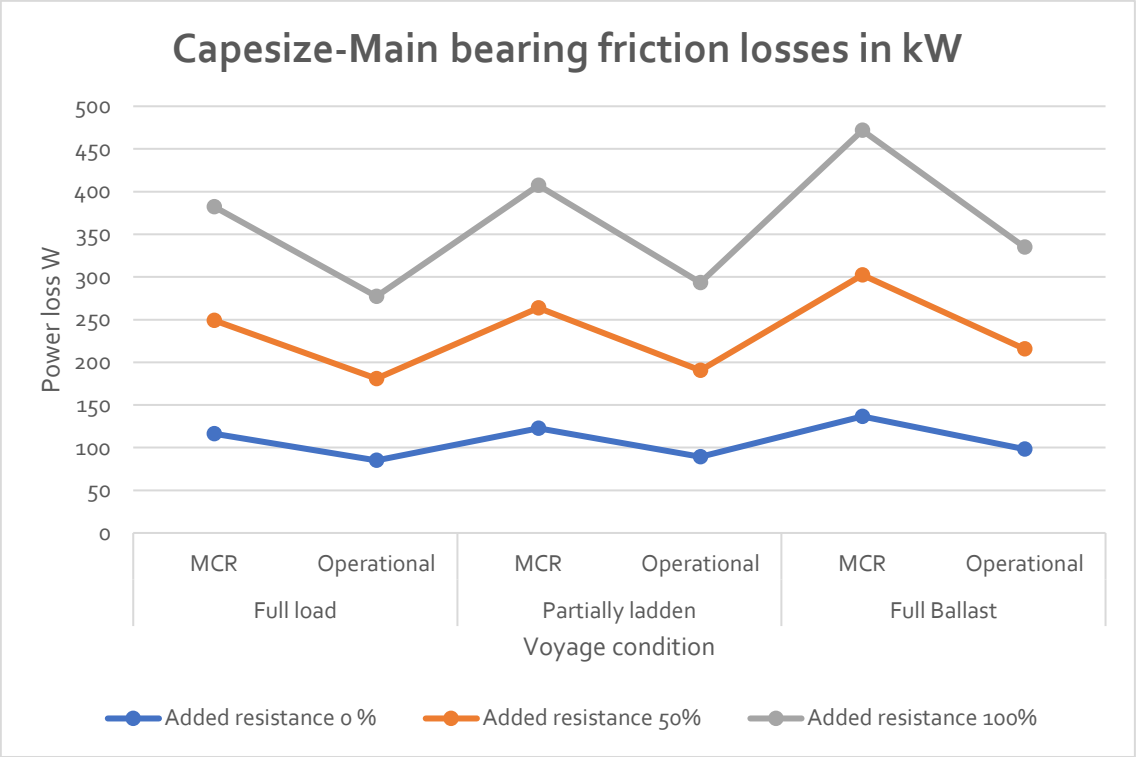

Figure 3.65 Capesize main bearing frictional losses W

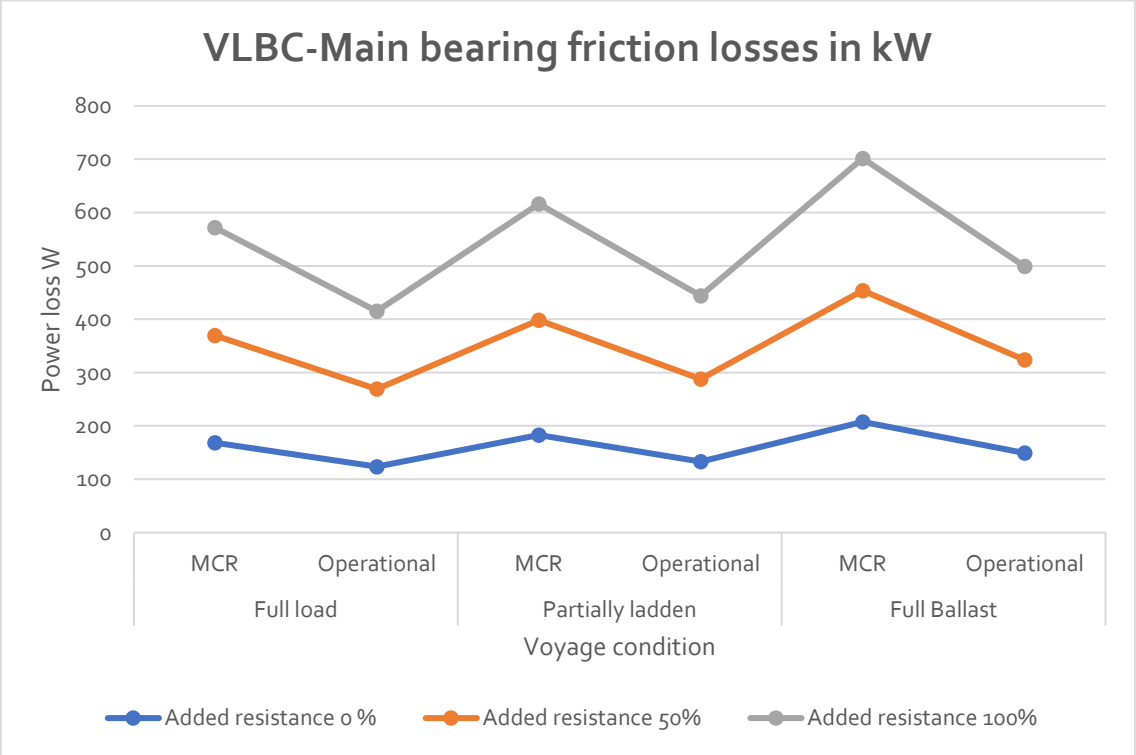

Figure 3.66 VLBC main bearing frictional losses W

3.2.2.1.4 Connecting rod frictional losses

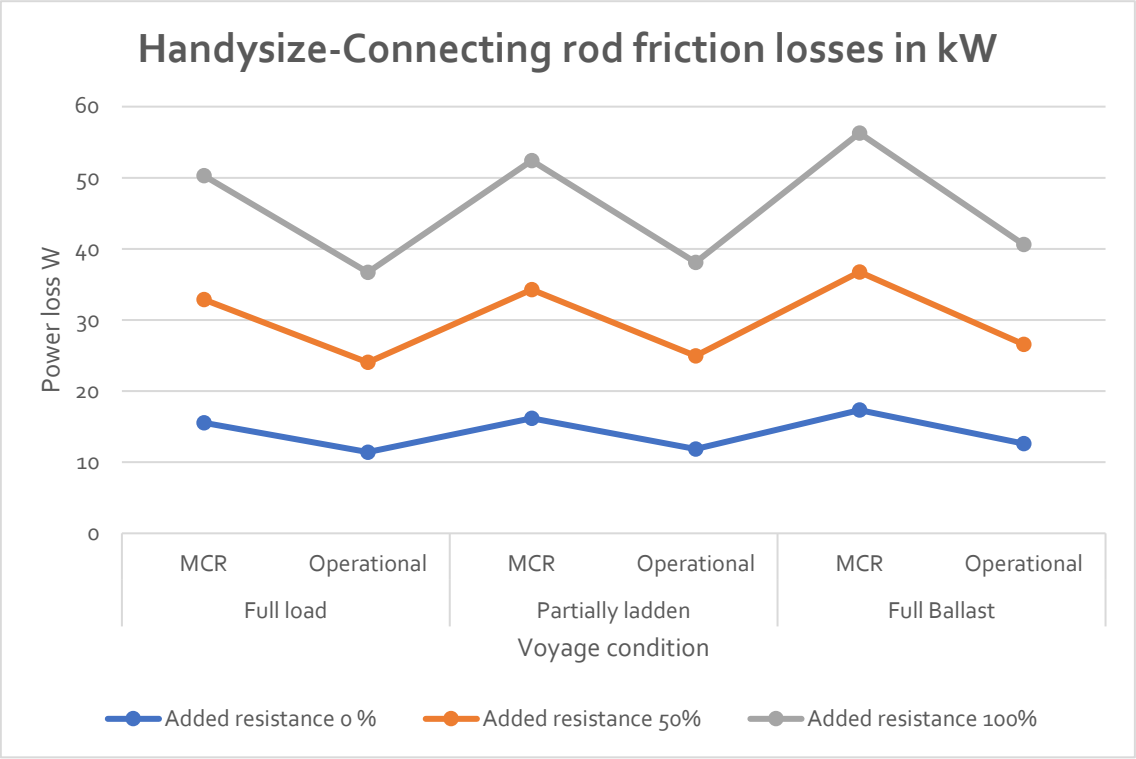

Figure 3.67 Connecting rod frictional losses W

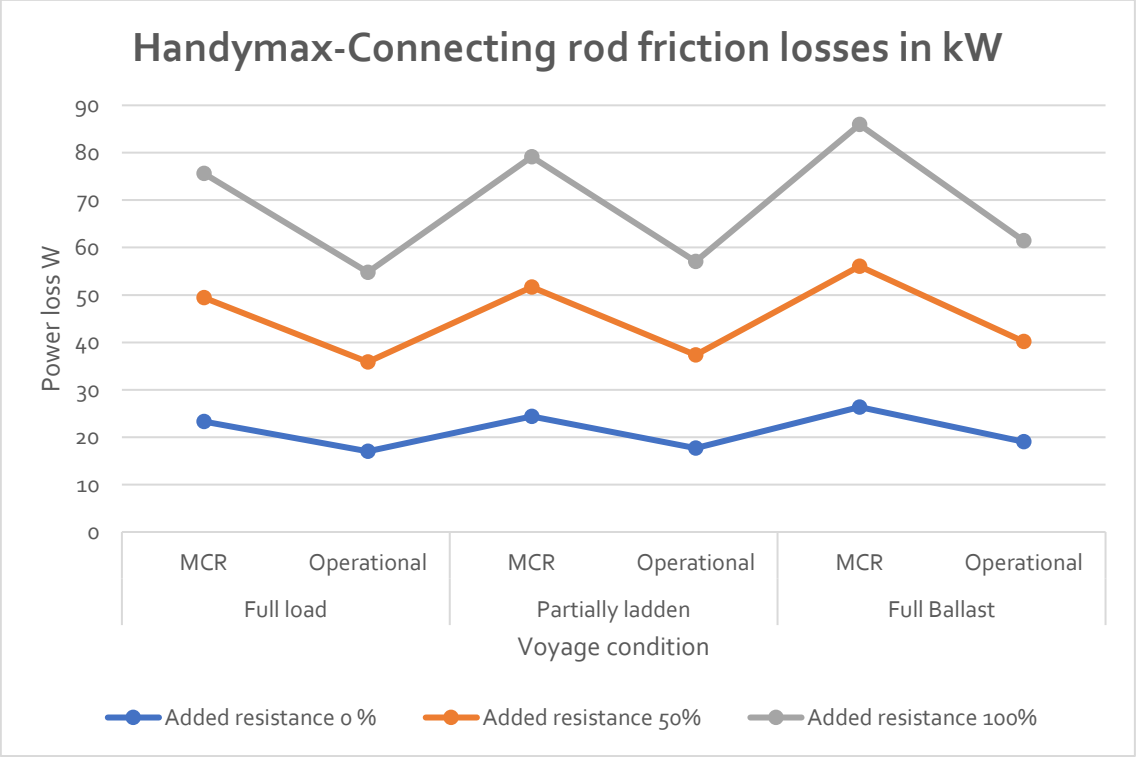

Figure 3.68 Handymax connecting rod frictional losses W

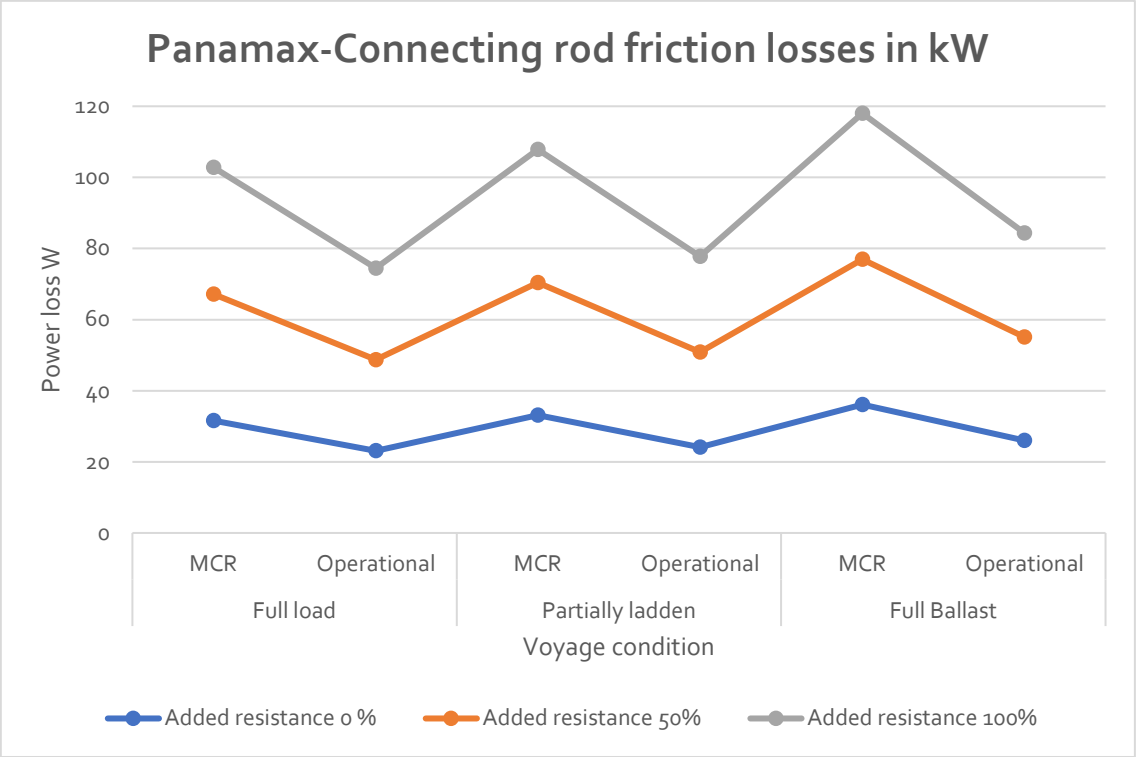

Figure 3.69 Panamax connecting rod frictional losses W

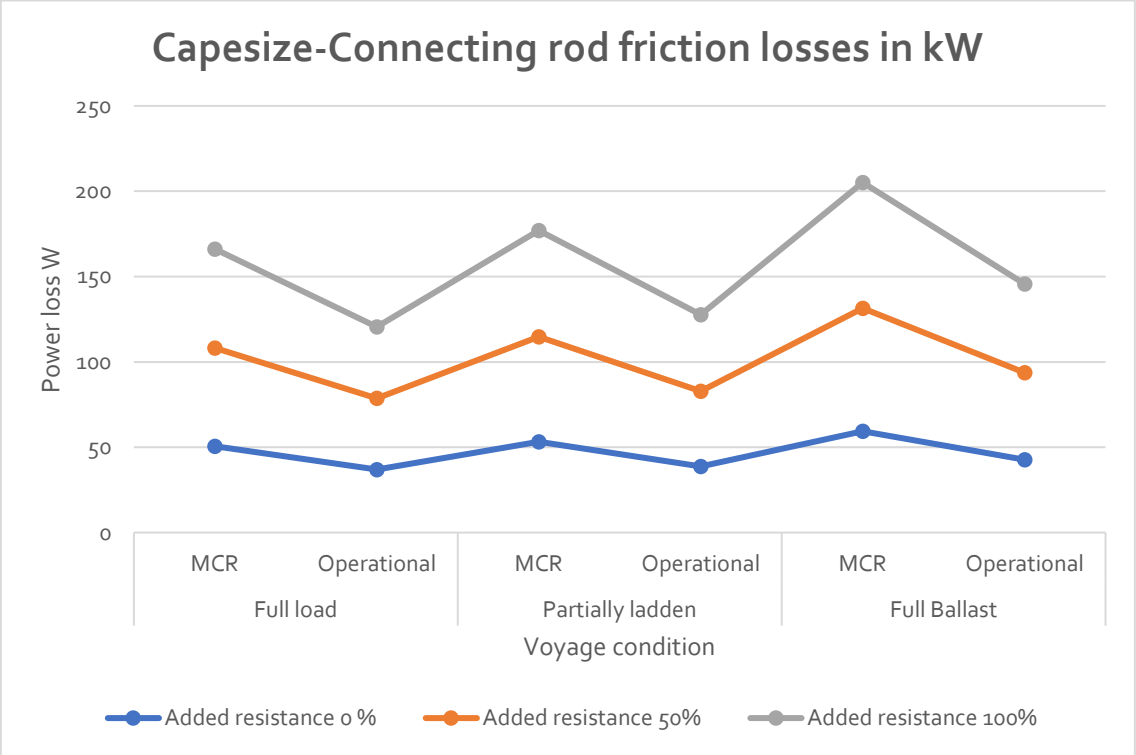

Figure 3.70 Capesize connecting rod frictional losses W

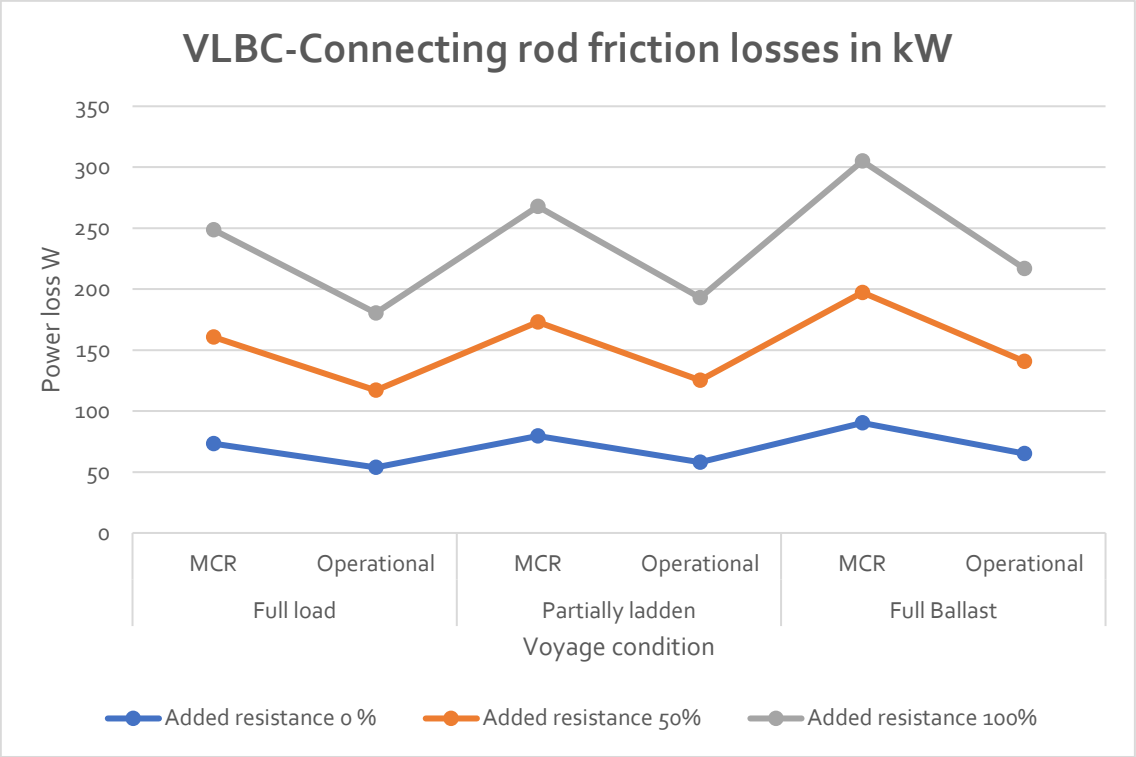

Figure 3.71 VLBC connecting rod frictional losses W

3.2.2.1.5 Thrust bearing frictional losses

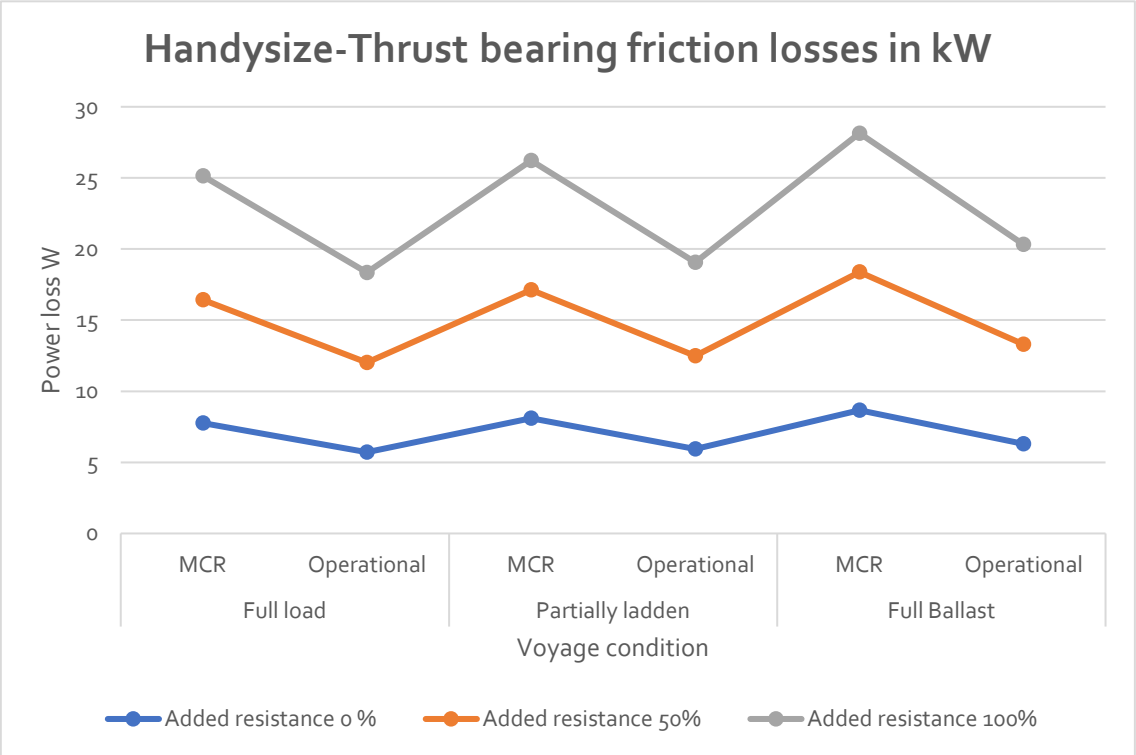

Figure 3.72 Handysize thrust bearing frictional losses W

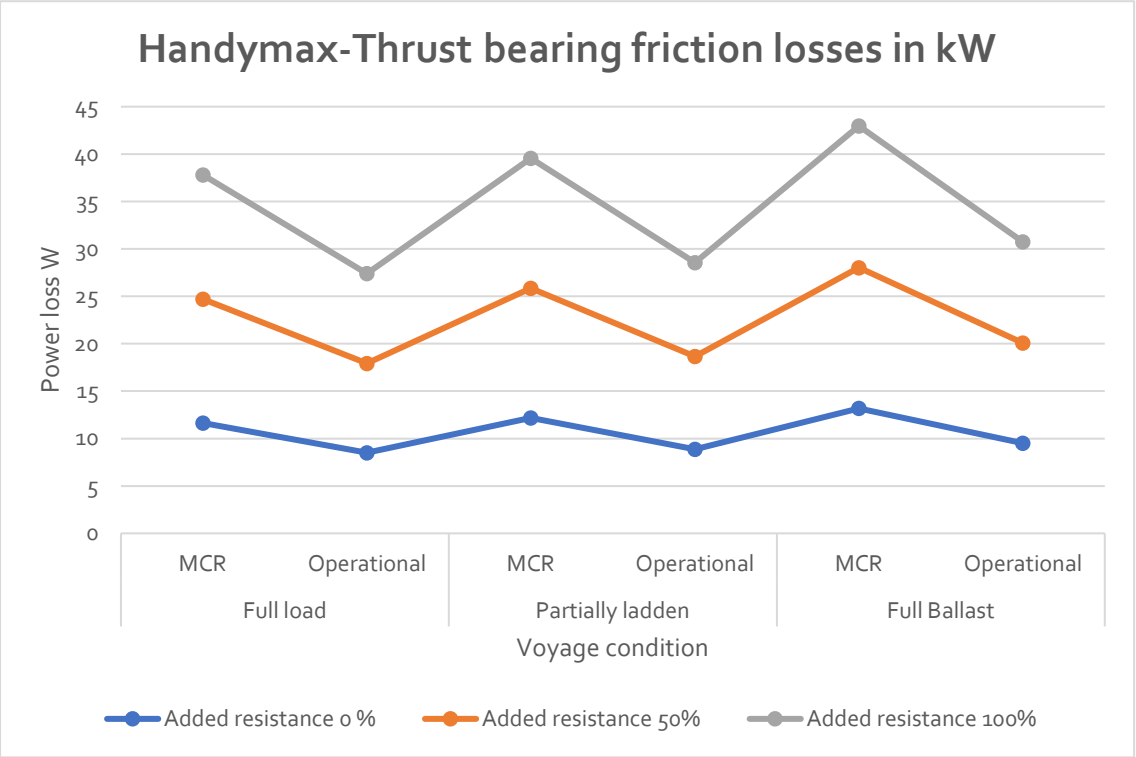

Figure 3.73 Handymax thrust bearing frictional losses W

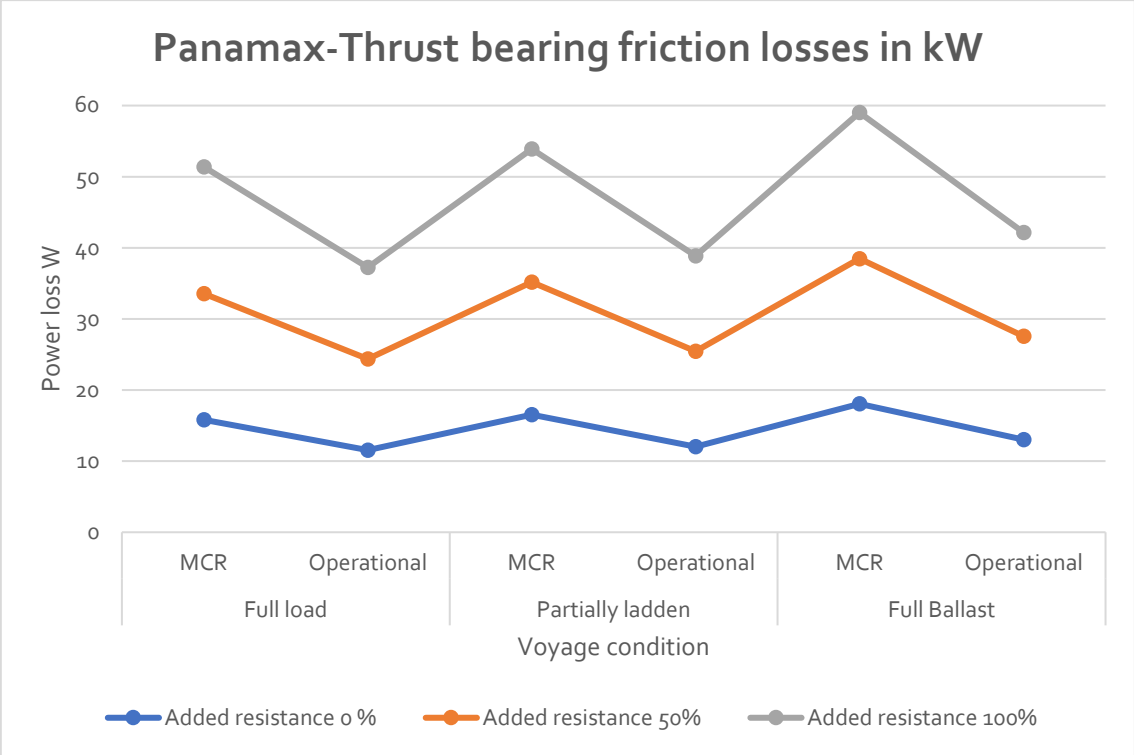

Figure 3.74 Panamax thrust bearing frictional losses W

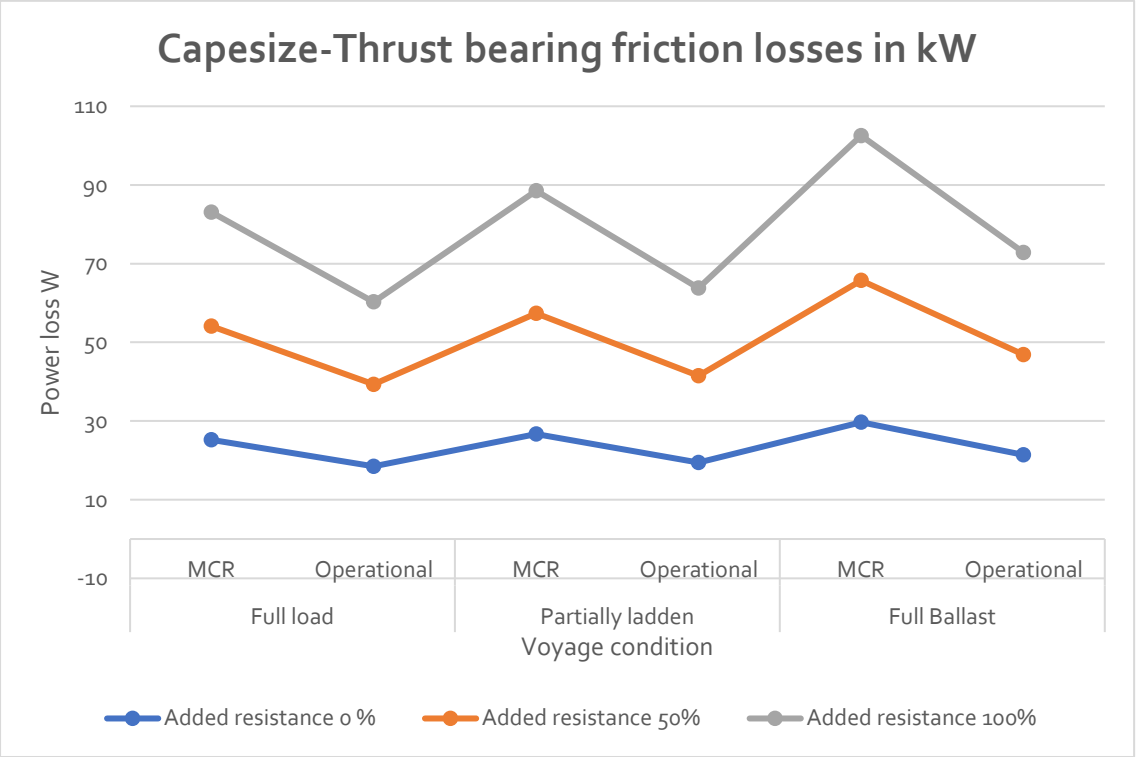

Figure 3.75 Capesize thrust bearing frictional losses W

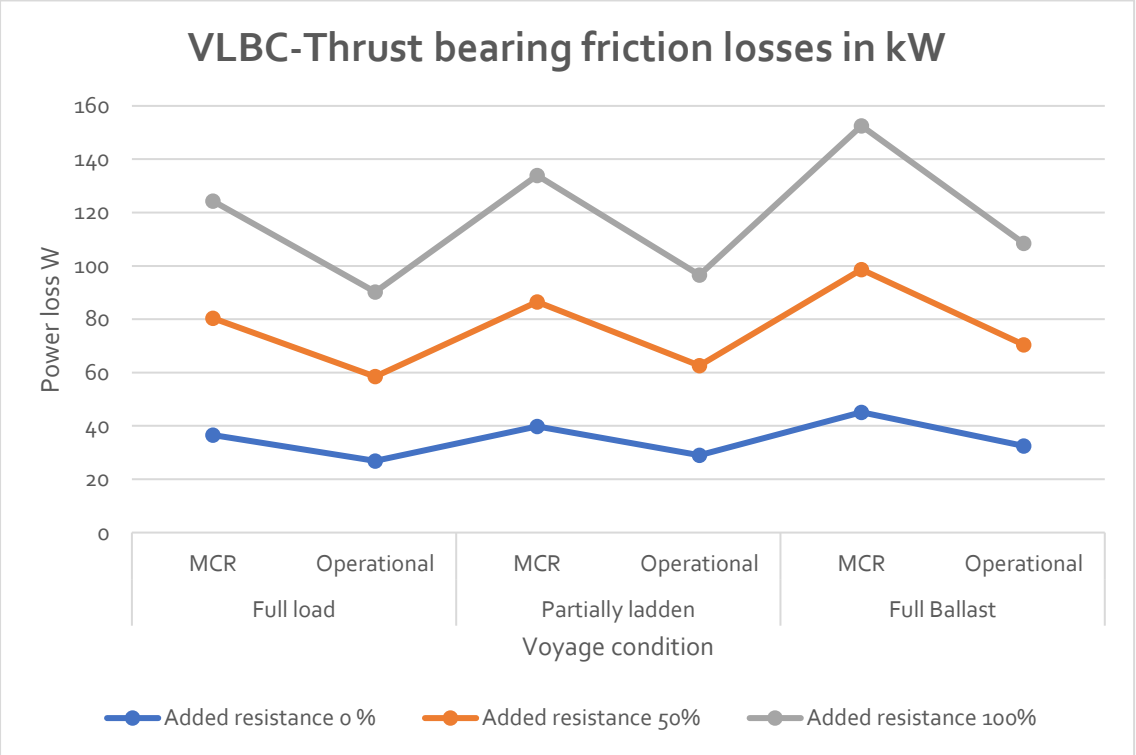

Figure 3.76 VLBC thrust bearing frictional losses W

3.2.2.1.6 Stuffing box frictional losses

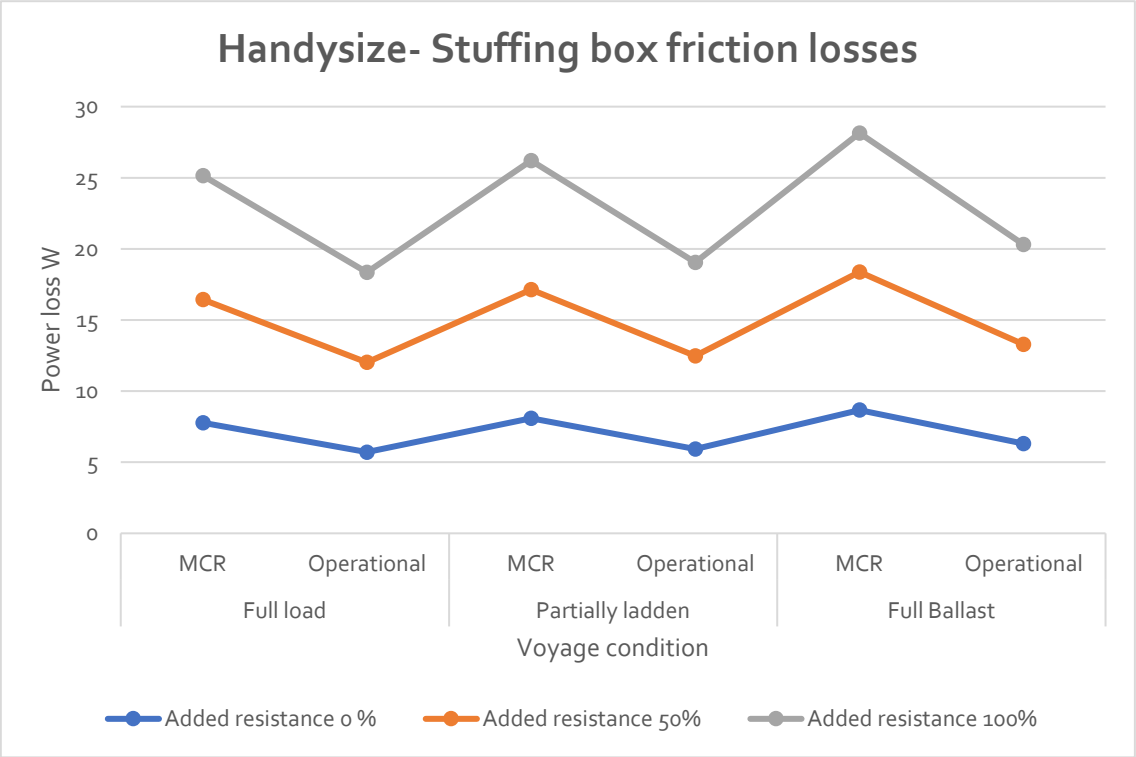

Figure 3.77 Handysize stuffing box frictional losses W

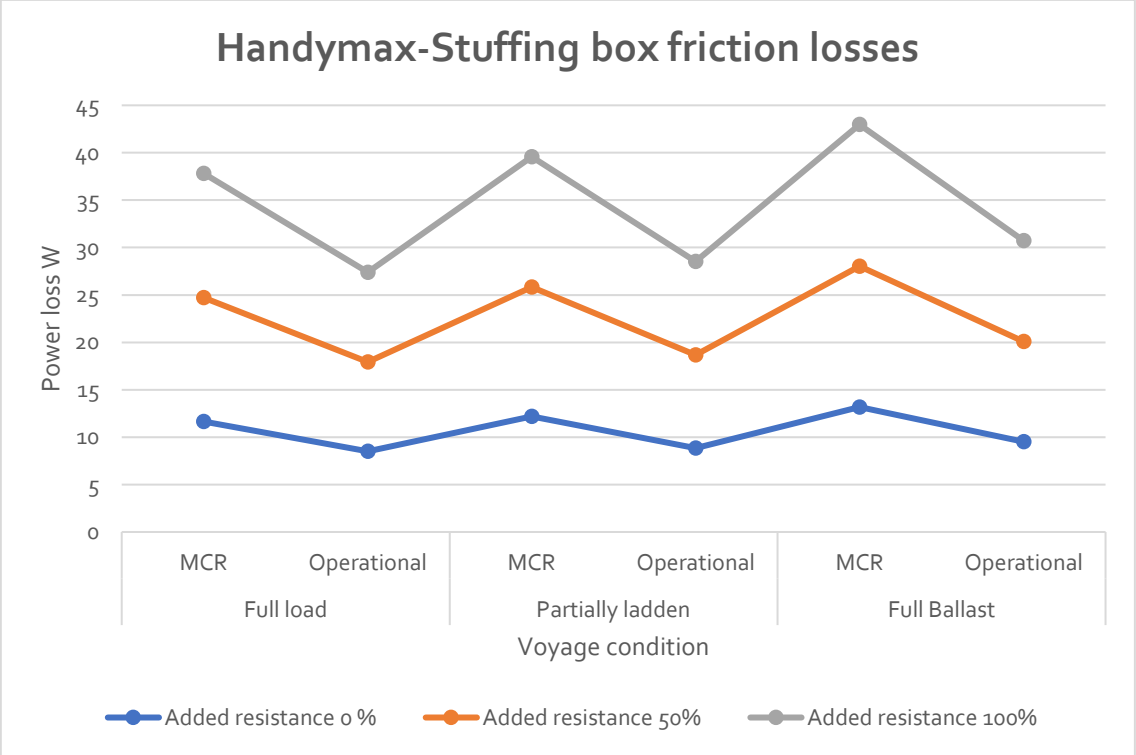

Figure 3.78 Handymax stuffing box frictional losses W

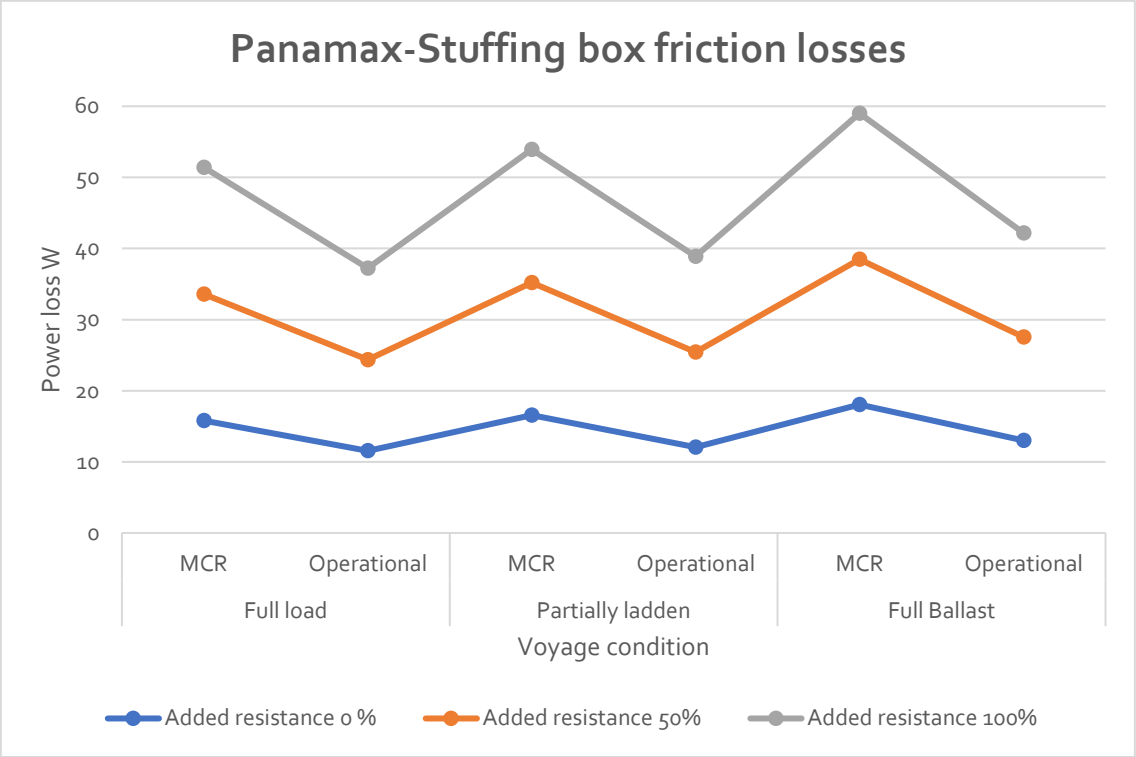

Figure 3.79 Panamax stuffing box frictional losses W

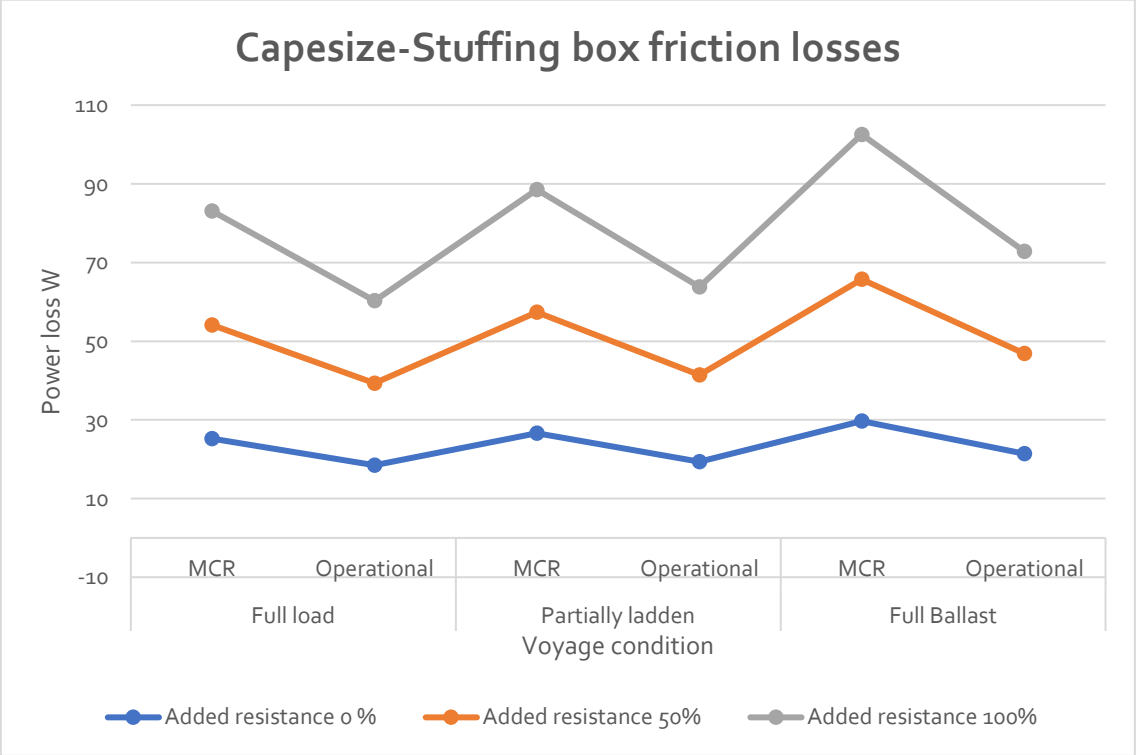

Figure 3.80 Capesize stuffing box frictional losses W

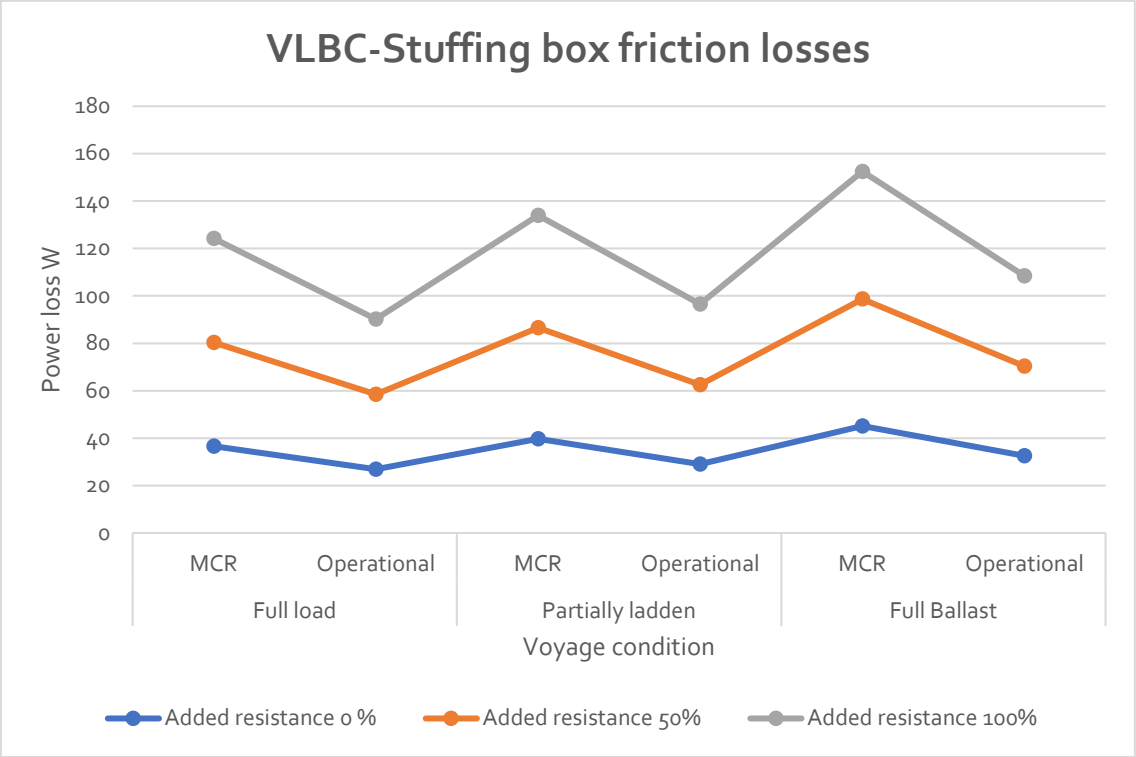

Figure 3.81 VLBC stuffing frictional losses W

3.2.3 Total friction losses

Total losses are the sum of shafting friction losses and engine friction losses. So, they highly dependent on engine friction losses nature. As a quantity of energy lost, the total losses increase with the service speed and with the reduction of draft.

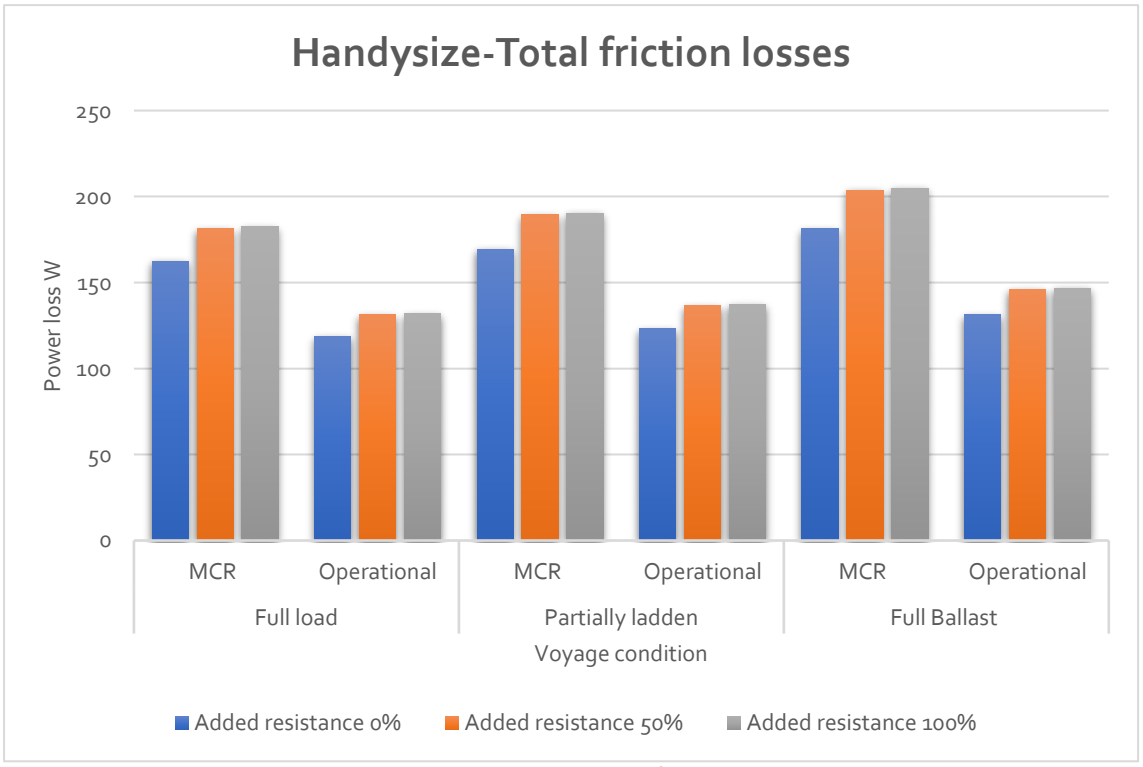

Figure 3.82 Handysize total frictional losses W

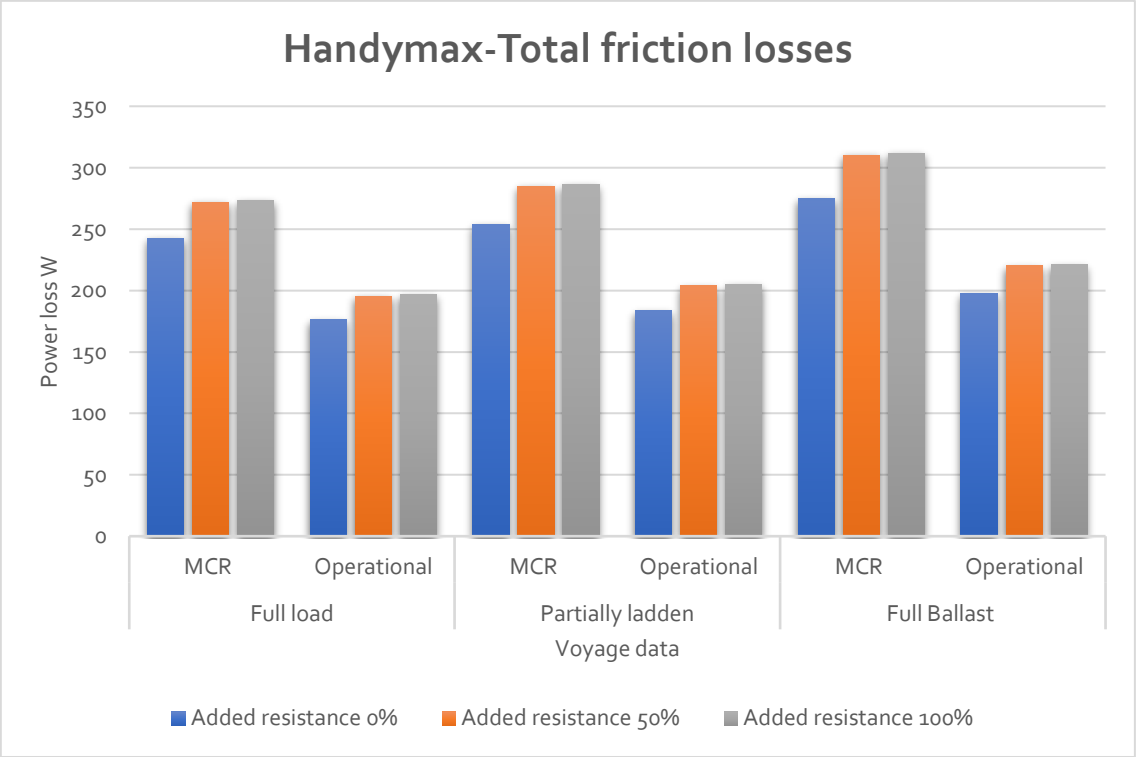

Figure 3.83 Handymax total frictional losses W

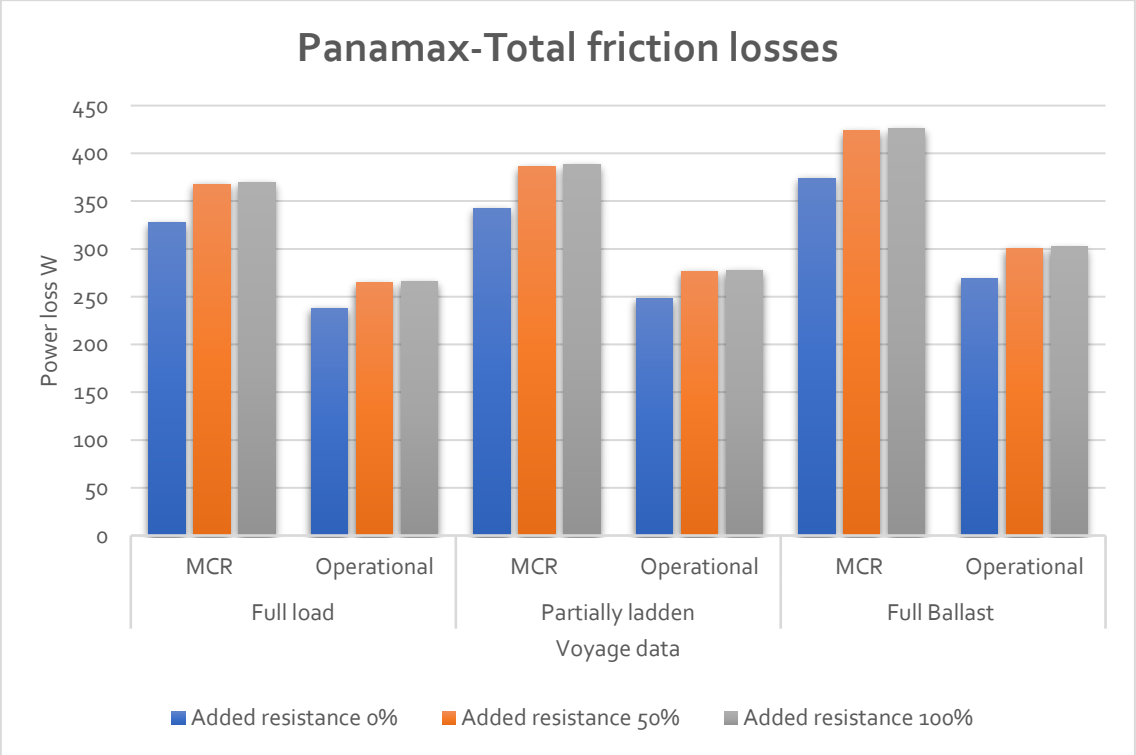

Figure 3.84 Panamax total friction losses in W

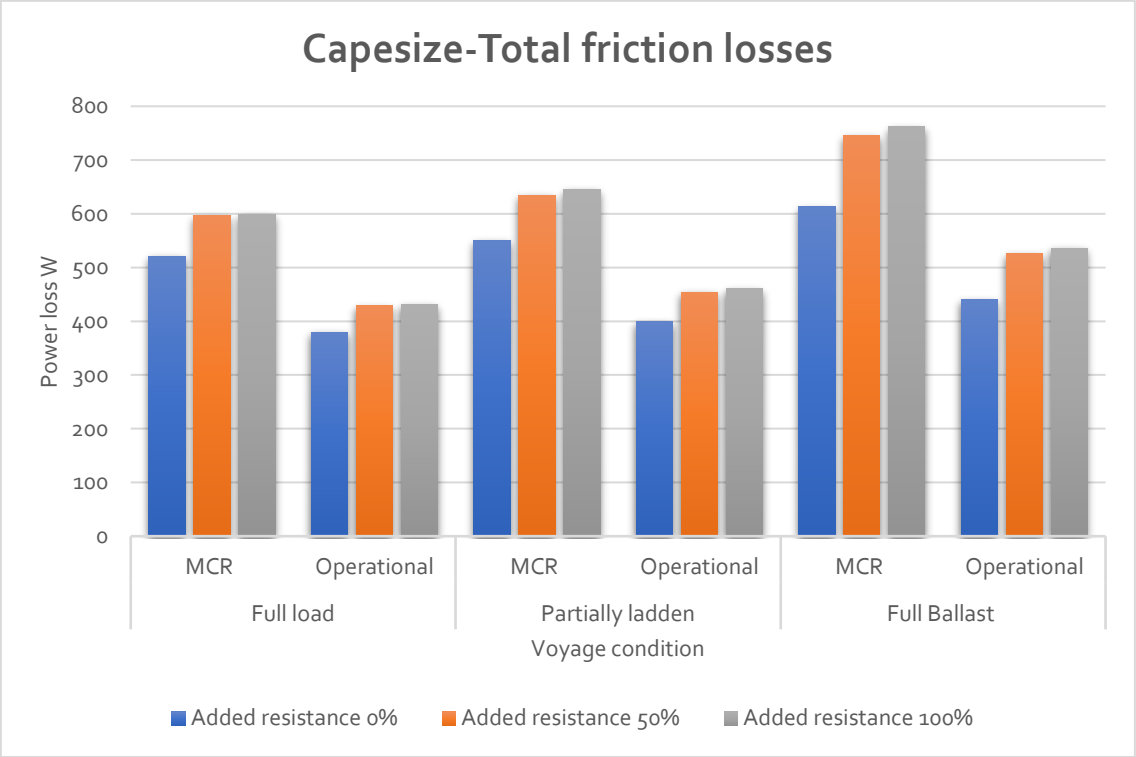

Figure 3.85 Capesize total friction losses in W

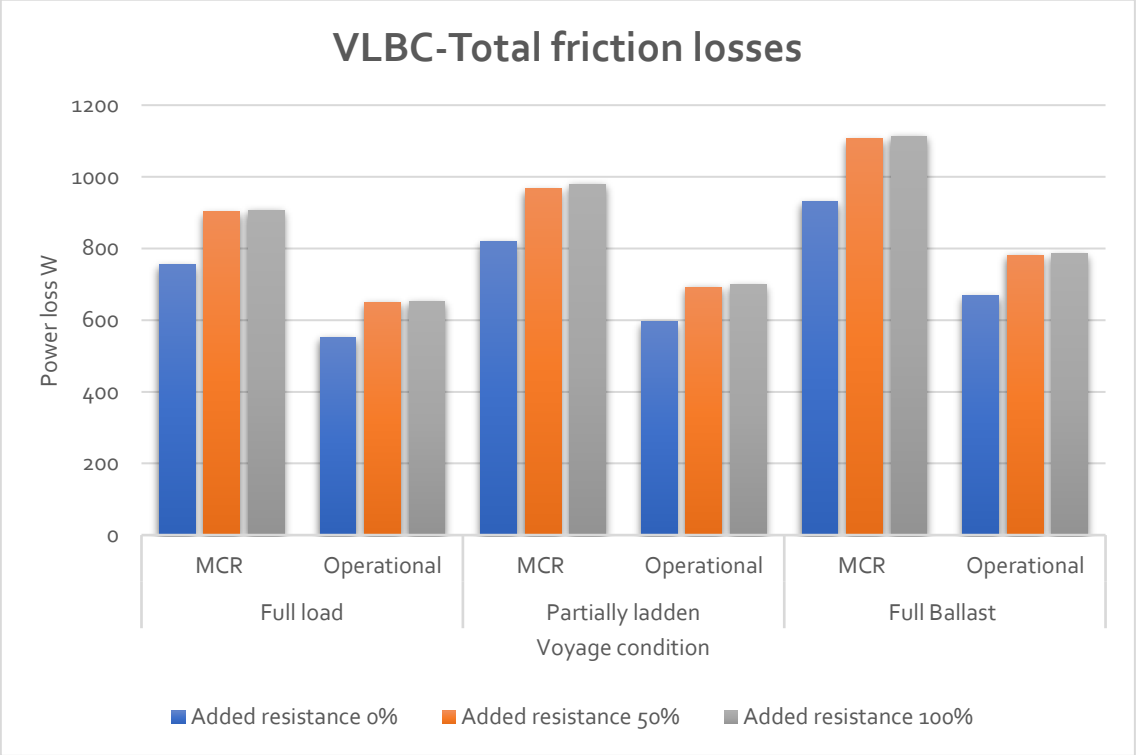

Figure 3.86 VLBC total friction losses in W

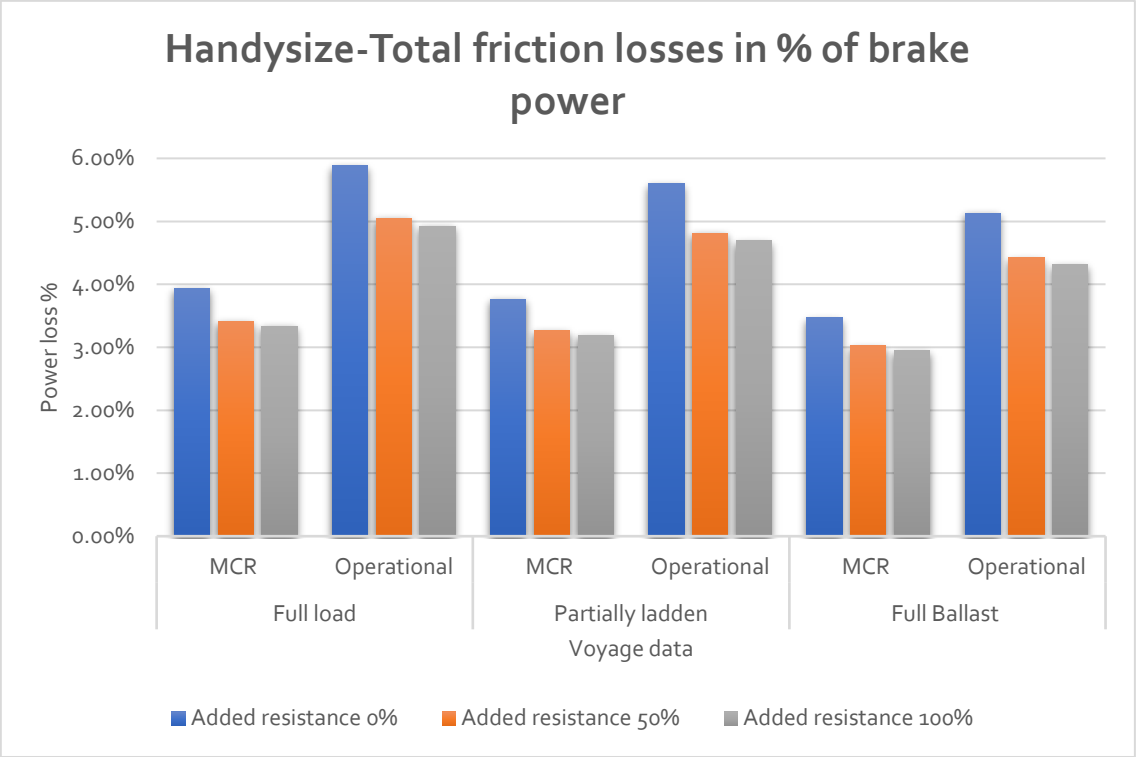

Figure 3.87 Handysize total friction losses %

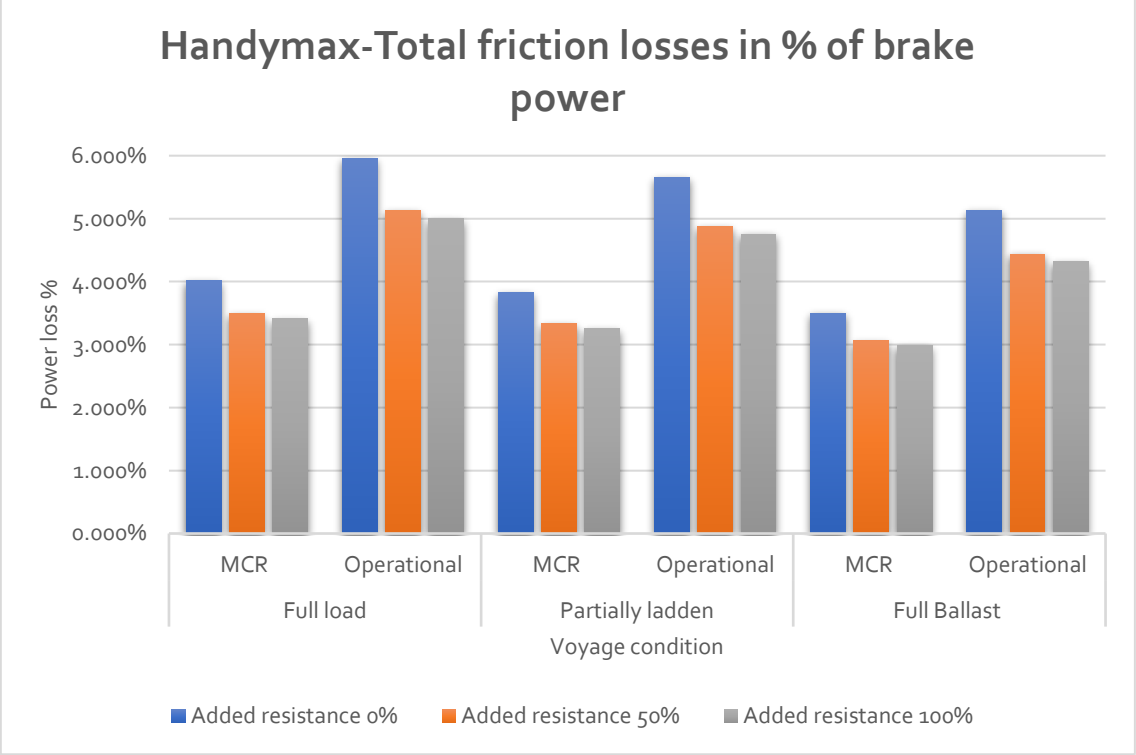

Figure 3.88 Handymax total friction losses %

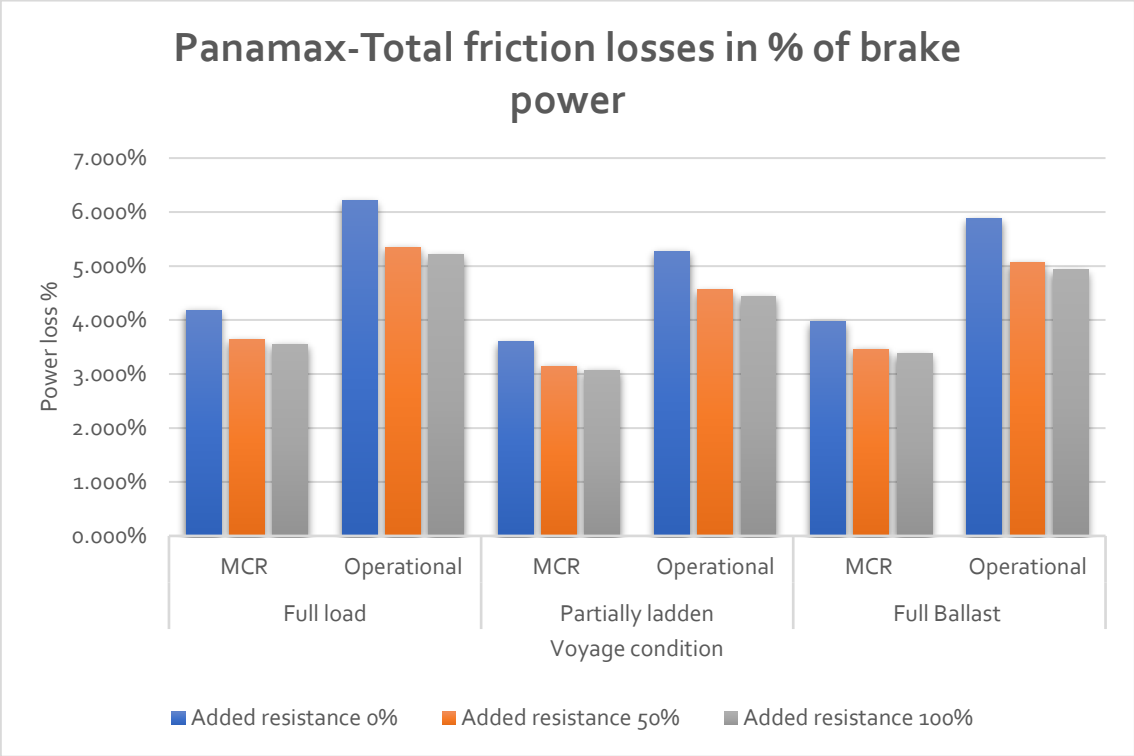

Figure 3.89 Panamax total friction losses %

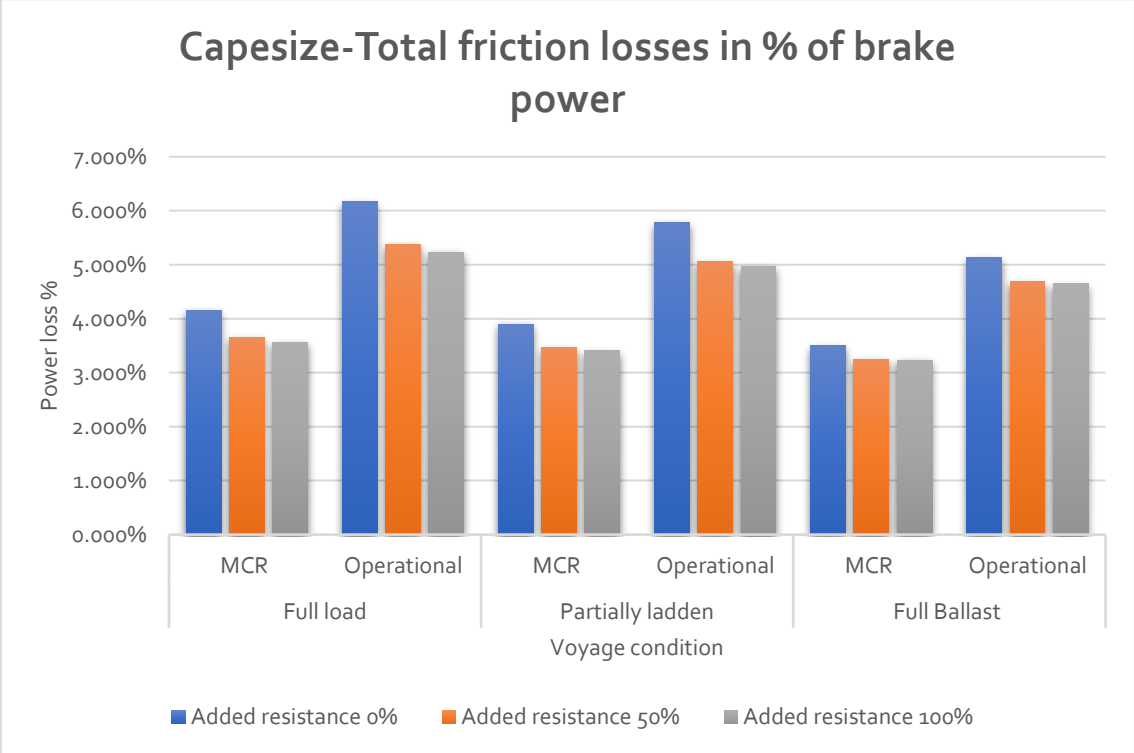

Figure 3.90 Capesize total friction losses %

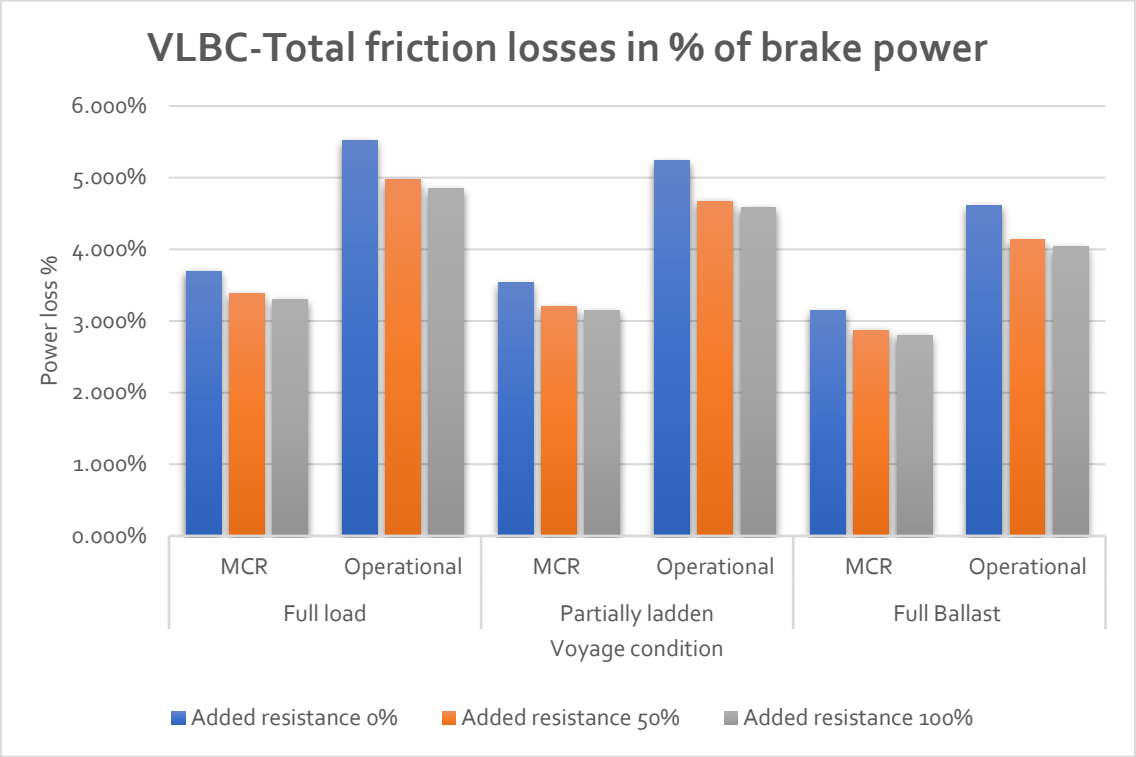

Figure 3.91 VLBC total friction losses %

The total losses in percentage form, as in the case of its components, attribute inversely to the case of quantitative losses. So, in terms of mechanical efficiency, a large sized vessel operating at the MCR engine point at a certain draft and at a certain added resistance condition, is the most efficient vessel. This proves that the growing vessel size is more beneficial in terms of fuel, emissions and efficiency.

3.2.3 Regression model for friction power loss estimation

In this chapter, by exploiting the data computed for the above-mentioned vessels, a non-linear regression model is generated for the estimation of the friction power loss. As already discussed, friction is affected by various parameters, both geometrical (such as the draft of vessel) and mechanical (such as the weight of shafting system). The proposed model relates the **total friction power loss** met in the propulsion installation (engine and shafting losses), the dependent random variable, with a set of independent random variables as:

$$P_f = -103.976 + 0.399 W_{sh}^{0.362} P^{0.376} N^{0.065} (LBDT)^{-0.025} 0.982^{(1-r_{rd}+r_{period})}$$

The independent random variables are explained in the following table:

Table 3.6 Model variables and units

Independent variable		Units
Weight of shafting system	W_{sh}	kg
Power at an engine load	P	kW
Revolutions at the same engine load	N	RPM
Length between perpendiculars	L	m
Maximum breadth	B	m
Depth of vessel	D	m
Draft of the vessel	T	m
Fraction of added resistance	r_{rd}	-
Fraction of maximum service speed	r_{period}	-

Power loss, P_f, is estimated in terms of **kW**. This model can be used at **preliminary design** of a bulk carrier, which provides an estimation of friction at a specified voyage condition described by these variables. The accuracy of the model was found **0.23%.**

3.2.4 Energy lost due to friction from each class in an annual calendar period

According to Georgakis [27] the total days of operation during a year of a bulk carrier are divided as:

Table 3.7 Annual distribution of operational vessel days

Annual distribution of days of operation	
Total days	365
In port operation	95
Travelling at full load	180
Travelling at full ballast	90
Voyage days	270

However, in the above table only the case of a full loaded and a full ballast vessel are considered. In order to include the case of a partially laden vessel, the operation calendar is modified as:

Table 3.8 Annual distribution of operational vessel days-modified

Annual distribution of days of operation	
Total days	365
In port operation	95
Travelling at full load	189
Travelling at full ballast	54
Travelling partially laden	27
Voyage days	270

For the purpose of the study, in order to estimate the annual friction losses caused by the bulk carrier fleet, a distribution for draft, added resistance and speed must be made.

Table 3.9 Probabilities for different loading conditions

Probabilities at different loading conditions	
Percentage at full load r_{fl}	0.7
Percentage at partial load r_{pl}	0.1
Percentage at full ballast r_{fb}	0.2

The probabilities considered for each hull condition are shown in the following table.

Table 3.10 Probabilities for different added resistance conditions

Probabilities at different added resistance conditions	
Clean hull r_{ch}	0.1
Partially fouled hull (50%) r_{ph}	0.7
Fully fouled hull (100%) r_{fh}	0.2

The probability of the speed level of a bulk carrier is considered binomial.

Table 3.11 Probabilities for different speed conditions

Probabilities at different speed conditions	
Service speed r_{MCR}	0.5
Slow steaming speed r_{OP}	0.5

Since not all vessels sail at the same speed, draft or hull condition, the effect of these parameters must be included in the calculations. So, power loss during one-year period is calculated as the

weighted average of all eighteen cases (draft, resistance, speed). It is expressed by introducing the variables P_{ijk}, which are obtained for a different loading condition, hull fouling condition and speed level, eighteen in total for each vessel class. Index i, represents the draft of the loading condition, index j the added resistance condition and index k the speed level.

$$i = 1 \div 3$$
$$j = 1 \div 3$$
$$k = 1 \div 2$$

Since friction loss by main engine use is under investigation in this study, only the voyage days are considered in the calculations.

$$\begin{aligned} Power = r_{MCR}\Big(& r_{ch}\Big(r_{fl}P^{fl}_{ft,ch,mcr} + r_{pl}P^{pl}_{ft,ch,mcr} + r_{fb}P^{fb}_{ft,ch,mcr}\Big) \\ & + r_{ph}\Big(r_{fl}P^{fl}_{ft,ph,mcr} + r_{pl}P^{pl}_{ft,ph,mcr} + r_{fb}P^{fb}_{ft,ph,mcr}\Big) \\ & + r_{fh}\Big(r_{fl}P^{fl}_{ft,fh,mcr} + r_{pl}P^{pl}_{ft,fh,mcr} + r_{fb}P^{fb}_{ft,fh,mcr}\Big)\Big) \\ & + r_{OP}\Big(r_{ch}\Big(r_{fl}P^{fl}_{ft,ch,Op} + r_{pl}P^{pl}_{ft,ch,Op} + r_{fb}P^{fb}_{ft,ch,Op}\Big) \\ & + r_{ph}\Big(r_{fl}P^{fl}_{ft,ph,Op} + r_{pl}P^{pl}_{ft,ph,Op} + r_{fb}P^{fb}_{ft,ph,Op}\Big) \\ & + r_{fh}\Big(r_{fl}P^{fl}_{ft,fh,Op} + r_{pl}P^{pl}_{ft,fh,Op} + r_{fb}P^{fb}_{ft,fh,Op}\Big)\Big) \end{aligned}$$

$$Power = \sum_{k=1}^{2} r_k \sum_{j=1}^{3} r_j \sum_{i=1}^{3} r_i P_{ijk}$$

According to the above probabilistic formula and tables [3.8÷3.11] the amount of energy lost due to each class of the bulk carrier fleet are illustrated in the following table:

Table 3.12 Daily and annual power loss per bulk carrier class

Class	Number of vessels	Daily power loss per class		Annual power loss per class	
		GWh	TJ	GWh	TJ
Handysize	2272	8.684	31.263	2344.757	8441.126
Handymax	2195	12.578	45.280	3396.019	12225.670
Panamax	3696	28.713	103.366	7752.419	27908.710
Capesize	2971	38.079	137.083	10281.194	37012.300
VLBC	660	12.722	45.801	3435.042	12366.150
Total	**11794**	**100.776**	**362.794**	**27209.430**	**97953.950**

Table 3.13 Daily and annual propulsion power production

Class	Number of vessels	Daily power production per class		Annual power production per class	
		GWh	TJ	GWh	TJ
Handysize	2272	224.897	809.631	60722.296	218600.265
Handymax	2195	322.623	1161.441	87108.100	313589.159
Panamax	3696	708.875	2551.952	191396.364	689026.909
Capesize	2971	926.750	3336.299	250222.404	900800.655
VLBC	660	340.968	1227.485	92061.376	331420.954
Total	**11794**	**524.113**	**9086.807**	**681510.539**	**2453437.941**

The vessel class with the largest energy losses is the Capesize class, followed by the Panamax class. These two classes compose the majority of the bulk carrier fleet. VLBCs, although they are the largest sized class, they do not account for the majority of energy losses. Therefore, from the above table, VLBC's and Handysize vessels are the most competitive vessels in terms of engine and shafting friction loss.

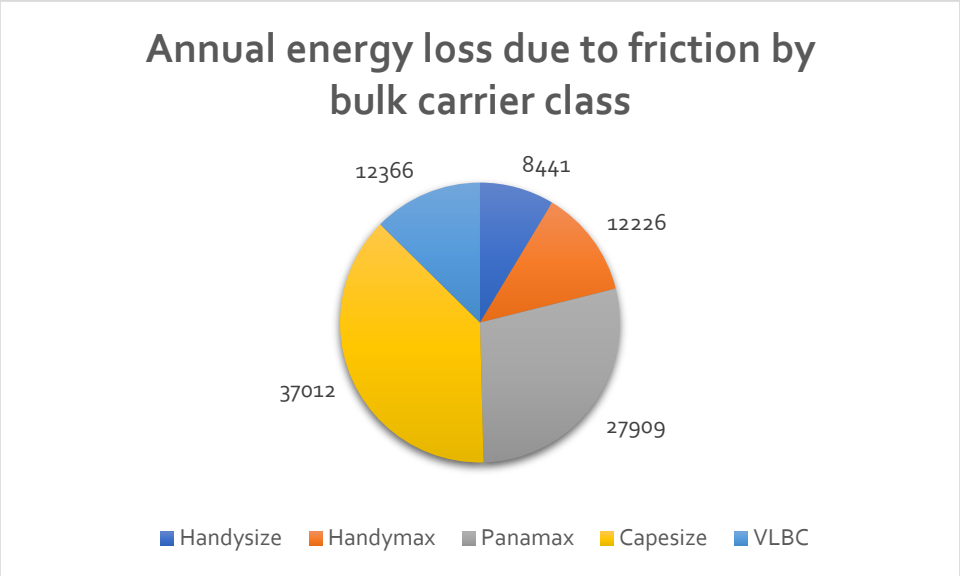

Figure 3.92 Annual energy loss due to friction per bulk carrier class

4 Global scale bulk carrier fleet study

4.1 Introduction

In this chapter, annual friction calculation is performed on global fleet scale. Through a representation of the Seaweb bulk carrier fleet database, by creating vessels bearing similarities to the vessels registered in Seaweb, friction losses in an annual period are estimated for different cases, by changing parameters regarding service speed and slow steaming values. Energy consumption is estimated for power loss due to friction and due to main engine operation. Finally, the friction model proposed in paragraph *3.2.3* and the results of the parametric study were tested against the global scaled results.

4.2 Friction loss calculation and fuel consumption due to friction

The Seaweb database, being comprised by 10347 bulk carriers, was used as a reference for the simulations. Specifically, by using the methods described in chapter 2, a virtual representation of the database was performed, followed by test simulations. Every dimension and geometrical parameter of each vessel was calculated, with each measure lying within a 3% margin of the actual database. For each vessel, the maximum total resistance was calculated, with a 25% margin of extra added resistance. Then, the necessary shaft power and a Diesel engine for propulsion were defined.

Next, by randomly selecting added resistance margin (time period of vessel passed between drydock repairs), draft, and service speed level, the operation point of the engine was calculated. Finally, friction losses and main engine fuel oil consumption were calculated for that operational point.

In order for the simulations to apply for tier II regulation, the vessels of the database used for the calculations, met, the following criteria.

- Construction date from 2005 and afterwards. In this sense, the life span of the used vessels is 15 years (3 drydock repairs at maximum).
- In order to eliminate the case of a vessel equipped with a four-stroke Diesel engine for propulsion, vessels with depth less than 10.5 meters were excluded.
- Each vessel burns heavy fuel oil with the below specifications:
    - LCV=39550 $\frac{kJ}{kg}$
    - Sulphur content 0.05%

For each simulation, in order to set the operational point of the engine for each voyage:

- A resistance factor was randomly selected, in order to simulate the time period of each vessel since its last drydock repair. In this way, the added resistance due to fouling and weather conditions is estimated.
- A draft value was randomly selected, since not all vessels travel at the same draft every moment of every operational day.

Nine simulations were performed and for each:

- A different fraction of the bulk carrier fleet was considered to operate under slow steaming values.
- A 10% or 20% maximum service speed reduction was applied for the fraction of fleet applying slow steaming.

Each simulation represents one day of an assumed voyage for each bulk carrier at a certain timeframe of the year. At that timeframe, a group of vessels travel at full load, another at full ballast and the rest at intermediate draft values, all under different resistance conditions. Each daily measure was multiplied by the number of days of main engine operation (270 according to Georgakis [27]), in order to estimate the effect at an annual period. The following measures were calculated for the bulk carriers following the necessary criteria:

- Daily and annual shafting friction losses
- Daily and annual engine friction losses
- Daily and annual total friction losses (shafting and engine)
- Daily and annual friction losses at stern tube bearings, intermediate bearing
- Daily and annual friction losses at main engine components (guide shoe, main bearing, piston, connecting rod, stuffing box and thrust bearing)
- Daily and annual fuel consumed due to friction losses
- Daily and annual fuel consumed due to operation of main engine

4.2.1 Simulation run 1

Table 4.1 Simulation 1 input parameters

Simulation input parameters	
Fleet fraction under slow steaming conditions	0%
Service speed reduction	0%
Fleet fraction at full load	70%
Fleet fraction at full ballast	20%
Fleet fraction at partial load	10%
Position of LCF amidships by stern	2%
Trim angle of vessel	0
Number of intermediate bearings	1
Shafting oil dynamic viscosity Pa	0.3

Table 4.2 Simulation 1 frictional losses

Fleet energy loss	Daily		Annual	
	GWh	TJ	GWh	TJ
Total friction	64.895	233.622	17521.642	63077.909
Engine friction	63.072	227.060	17029.513	61306.245
Shafting friction	1.823	6.562	492.129	1771.666

Table 4.3 Simulation 1 shafting system bearing frictional losses

Fleet energy loss	Daily		Annual	
	GWh	TJ	GWh	TJ
Aft stern tube bearing	1.095	3.941	295.557	1064.005
Forward stern tube bearing	0.305	1.099	82.425	296.729
Intermediate bearing	0.423	1.522	114.148	410.931

Table 4.4 Simulation 1 main engine components frictional losses

Fleet energy loss	Daily		Annual	
	GWh	TJ	GWh	TJ
Guide shoe	19.522	70.389	5279.149	19004.936
Piston	16.399	59.036	4427.673	15939.624
Main bearing	14.507	52.224	3916.788	14100.436
Connecting rod	6.307	22.706	1702.951	6130.624
Stuffing box	3.154	11.353	851.476	3065.312
Thrust bearing	3.154	11.353	851.476	3065.312

Table 4.5 Simulation 1 fuel consumption

Fuel amount	Daily	Annual
	$t.10^3$	$t.10^3$
Fuel consumed due to friction	11.191	3021.648
Fuel consumed due to main engine operation	290.128	78334.632

4.2.2 Simulation run 2

Table 4.6 Simulation 2 input parameters

Simulation input parameters	
Fleet fraction under slow steaming conditions	30%
Service speed reduction	10%
Fleet fraction at full load	70%
Fleet fraction at full ballast	20%
Fleet fraction at partial load	10%
Position of LCF amidships by stern	2%
Trim angle of vessel	0
Number of intermediate bearings	1
Shafting oil dynamic viscosity Pa	0.3

Table 4.7 Simulation 2 frictional losses

Fleet energy loss	Daily		Annual	
	GWh	TJ	GWh	TJ
Total friction	64.645	232.723	17454.196	62835.106
Engine friction	62.823	226.162	16962.124	61063.648
Shafting friction	1.822	6.561	492.072	1771.666

Table 4.8 Simulation 2 shafting system bearing frictional losses

Fleet energy loss	Daily		Annual	
	GWh	TJ	GWh	TJ
Aft stern tube bearing	1.095	3.941	295.522	1063.878
Forward stern tube bearing	0.305	1.099	82.415	296.695
Intermediate bearing	0.423	1.522	114.135	410.886

Table 4.9 Simulation 2 main engine components frictional losses

Fleet energy loss	Daily		Annual	
	GWh	TJ	GWh	TJ
Guide shoe	19.475	70.110	5258.218	18929.73
Piston	16.334	58.802	4410.152	15876.55
Main bearing	14.449	52.017	3901.289	14044.64
Connecting rod	6.282	22.616	1696.212	6106.365
Stuffing box	3.141	11.308	848.106	3053.182
Thrust bearing	3.141	11.308	848.106	3053.182

Table 4.10 Simulation 2 fuel consumption

Fuel amount	Daily	Annual
	$t.10^3$	$t.10^3$
Fuel consumed due to friction	11.159	3013
Fuel consumed due to main engine operation	268.081	72382

4.2.3 Simulation run 3

Table 4.11 Simulation 3 input parameters

Simulation input parameters	
Fleet fraction under slow steaming conditions	30%
Service speed reduction	20%
Fleet fraction at full load	70%
Fleet fraction at full ballast	20%
Fleet fraction at partial load	10%
Position of LCF amidships by stern	2%
Trim angle of vessel	0
Number of intermediate bearings	1
Shafting oil dynamic viscosity Pa	0.3

Table 4.12 Simulation 3 frictional losses

Fleet energy loss	Daily		Annual	
	GWh	TJ	GWh	TJ
Total friction	64.433	231.957	17396.808	62628.509
Engine friction	62.610	225.397	16904.739	60857.060
Shafting friction	1.822	6.561	492.067	1771.450

Table 4.13 Simulation 3 shafting system bearing frictional losses

Fleet energy loss	Daily		Annual	
	GWh	TJ	GWh	TJ
Aft stern tube bearing	1.095	3.940	295.521	1063.876
Forward stern tube bearing	0.305	1.099	82.415	296.693
Intermediate bearing	0.423	1.522	114.134	410.881

Table 4.14 Simulation 3 main engine components frictional losses

Fleet energy loss	Daily		Annual	
	GWh	TJ	GWh	TJ
Guide shoe	19.409	69.873	5.240	18865.68
Piston	16.279	58.603	4.395	15822.836
Main bearing	14.400	51.841	3.888	13997.123
Connecting rod	6.261	22.540	1690.474	6085.706
Stuffing box	3.131	11.270	845.237	3042.853
Thrust bearing	3.131	11.270	845.237	3042.853

Table 4.15 Simulation 3 fuel consumption

Fuel amount	Daily	Annual
	$t.10^3$	$t.10^3$
Fuel consumed due to friction	11.188	3020.865
Fuel consumed due to main engine operation	24.927	67302.450

4.2.4 Simulation run 4

Table 4.16 Simulation 4 input parameters

Simulation input parameters	
Fleet fraction under slow steaming conditions	50%
Service speed reduction	10%
Fleet fraction at full load	70%
Fleet fraction at full ballast	20%
Fleet fraction at partial load	10%
Position of LCF amidships by stern	2%
Trim angle of vessel	0
Number of intermediate bearings	1
Shafting oil dynamic viscosity Pa	0.3

Table 4.17 Simulation 4 frictional losses

Fleet energy loss	Daily		Annual	
	GWh	TJ	GWh	TJ
Total friction	64.527	232.298	17422.340	62720.440
Engine friction	62.705	225.737	16930.260	60948.940
Shafting friction	1.823	6.561	492.084	1771.502

Table 4.18 Simulation 4 shafting system bearing frictional losses

Fleet energy loss	Daily		Annual	
	GWh	TJ	GWh	TJ
Aft stern tube bearing	1.095	3.940	295.530	1063.906
Forward stern tube bearing	0.305	1.099	82.417	296.701
Intermediate bearing	0.423	1.522	114.137	410.894

Table 4.19 Simulation 4 main engine components frictional losses

Fleet energy loss	Daily		Annual	
	GWh	TJ	GWh	TJ
Guide shoe	19.439	69.978	5248.381	18894.170
Piston	16.303	58.692	4401.868	15846.72
Main bearing	14.422	51.919	3893.96	14018.250
Connecting rod	6.270	22.574	1693.026	6094.894
Stuffing box	3.135	11.287	846.513	3047.447
Thrust bearing	3.135	11.287	846.513	3047.447

Table 4.20 Simulation 4 fuel consumption

Fuel amount	Daily	Annual
	$t.10^3$	$t.10^3$
Fuel consumed due to friction	11.137	3007.021
Fuel consumed due to main engine operation	257.195	69442.7

4.2.5 Simulation run 5

Table 4.21 Simulation 5 input parameters

Simulation input parameters	
Fleet fraction under slow steaming conditions	50%
Service speed reduction	20%
Fleet fraction at full load	70%
Fleet fraction at full ballast	20%
Fleet fraction at partial load	10%
Position of LCF amidships by stern	2%
Trim angle of vessel	0
Number of intermediate bearings	1
Shafting oil dynamic viscosity Pa	0.3

Table 4.22 Simulation 5 frictional losses

Fleet energy loss	Daily		Annual	
	GWh	TJ	GWh	TJ
Total friction	64.243	231.274	17345.530	62443.9
Engine friction	62.421	224.715	16853.640	60673.11
Shafting friction	1.821	6.558	491.886	1770.790

Table 4.23 Simulation 5 shafting system bearing frictional losses

Fleet energy loss	Daily		Annual	
	GWh	TJ	GWh	TJ
Aft stern tube bearing	1.094	3.939	295.411	1063.478
Forward stern tube bearing	0.305	1.098	82.384	296.583
Intermediate bearing	0.423	1.521	114.091	410.729

Table 4.24 Simulation 5 main engine components frictional losses

Fleet energy loss	Daily		Annual	
	GWh	TJ	GWh	TJ
Guide shoe	19.350	69.662	5248.629	18808.660
Piston	16.229	58.426	4381.947	15775.010
Main bearing	14.357	51.685	3876.338	13954.820
Connecting rod	6.242	22.471	1685.364	6067.311
Stuffing box	3.121	11.236	842.682	3033.656
Thrust bearing	3.121	11.236	842.682	3033.656

Table 4.25 Simulation 5 fuel consumption

Fuel amount	Daily	Annual
	$t.10^3$	$t.10^3$
Fuel consumed due to friction	11.186	3020.327
Fuel consumed due to main engine operation	228.17	61753.55

4.2.6 Simulation run 6

Table 4.26 Simulation 6 input parameters

Simulation input parameters	
Fleet fraction under slow steaming conditions	80%
Service speed reduction	10%
Fleet fraction at full load	70%
Fleet fraction at full ballast	20%
Fleet fraction at partial load	10%
Position of LCF amidships by stern	2%
Trim angle of vessel	0
Number of intermediate bearings	1
Shafting oil dynamic viscosity Pa	0.3

Table 4.27 Simulation 6 frictional losses

Fleet energy loss	Daily		Annual	
	GWh	TJ	GWh	TJ
Total friction	64.354	231.675	17375.620	62552.230
Engine friction	62.532	225.117	16883.750	60781.510
Shafting friction	1.822	6.558	491.867	1770.720

Table 4.28 Simulation 6 shafting system bearing frictional losses

Fleet energy loss	Daily		Annual	
	GWh	TJ	GWh	TJ
Aft stern tube bearing	1.094	3.939	295.399	1063.436
Forward stern tube bearing	0.305	1.098	82.380	296.570
Intermediate bearing	0.423	1.521	114.087	410.714

Table 4.29 Simulation 6 main engine components frictional losses

Fleet energy loss	Daily		Annual	
	GWh	TJ	GWh	TJ
Guide shoe	19.385	69.786	5233.964	18842.270
Piston	16.258	58.530	4389.776	15803.190
Main bearing	14.382	51.777	3883.263	13979.750
Connecting rod	6.253	22.512	1688.375	6078.151
Stuffing box	3.127	11.256	844.188	3039.076
Thrust bearing	3.127	11.256	844.188	3039.076

Table 4.30 Simulation 6 fuel consumption

Fuel amount	Daily	Annual
	$t.10^3$	$t.10^3$
Fuel consumed due to friction	11.113	3000.578
Fuel consumed due to main engine operation	241.013	65073.460

4.2.7 Simulation run 7

Table 4.31 Simulation 7 input parameters

Simulation input parameters	
Fleet fraction under slow steaming conditions	80%
Service speed reduction	20%
Fleet fraction at full load	70%
Fleet fraction at full ballast	20%
Fleet fraction at partial load	10%
Position of LCF amidships by stern	2%
Trim angle of vessel	0
Number of intermediate bearings	1
Shafting oil dynamic viscosity Pa	0.3

Table 4.32 Simulation 7 frictional losses

Fleet energy loss	Daily		Annual	
	GWh	TJ	GWh	TJ
Total friction	64.037	230.975	17290.121	62244.43
Engine friction	62.215	223.975	16798.149	60473.330
Shafting friction	1.822	6.560	491.972	1771.101

Table 4.33 Simulation 7 shafting system bearing frictional losses

Fleet energy loss	Daily		Annual	
	GWh	TJ	GWh	TJ
Aft stern tube bearing	1.094	3.939	295.462	1063.663
Forward stern tube bearing	0.305	1.098	82.399	296.635
Intermediate bearing	0.423	1.521	114.111	410.802

Table 4.34 Simulation 7 main engine components frictional losses

Fleet energy loss	Daily		Annual	
	GWh	TJ	GWh	TJ
Guide shoe	19.287	69.432	5207.426	18746.730
Piston	16.176	58.234	4367.519	15723.07
Main bearing	14.310	51.514	3863.574	13908.870
Connecting rod	6.222	22.398	1679.815	6047.333
Stuffing box	3.111	11.199	839.907	3023.667
Thrust bearing	3.111	11.199	839.907	3023.667

Table 4. 35 Simulation 7 fuel consumption

Fuel amount	Daily	Annual
	$t.10^3$	$t.10^3$
Fuel consumed due to friction	11.198	3023.478
Fuel consumed due to main engine operation	195.829	53602.770

4.2.8 Simulation run 8

Table 4.36 Simulation 8 input parameters

Simulation input parameters	
Fleet fraction under slow steaming conditions	100%
Service speed reduction	10%
Fleet fraction at full load	70%
Fleet fraction at full ballast	20%
Fleet fraction at partial load	10%
Position of LCF amidships by stern	2%
Trim angle of vessel	0
Number of intermediate bearings	1
Shafting oil dynamic viscosity Pa	0.3

Table 4.37 Simulation 8 frictional losses

Fleet energy loss	Daily		Annual	
	GWh	TJ	GWh	TJ
Total friction	63.918	230.104	17257.760	62127.950
Engine friction	62.095	223.542	16765.640	60356.31
Shafting friction	1.823	6.562	492.122	1771.639

Table 4.38 Simulation 8 shafting system bearing frictional losses

Fleet energy loss	Daily		Annual	
	GWh	TJ	GWh	TJ
Aft stern tube bearing	1.094	3.941	295.553	1063.989
Forward stern tube bearing	0.305	1.099	82.423	296.724
Intermediate bearing	0.423	1.522	114.146	410.925

Table 4.39 Simulation 8 main engine components frictional losses

Fleet energy loss	Daily		Annual	
	GWh	TJ	GWh	TJ
Guide shoe	19.249	69.298	5197.349	18710.460
Piston	16.145	58.121	4359.067	15692.640
Main bearing	14.282	51.415	3856.098	13881.950
Connecting rod	6.222	22.354	1676.564	6035.631
Stuffing box	3.105	11.177	838.282	3017.815
Thrust bearing	3.105	11.177	838.282	3017.815

Table 4.40 Simulation 8 fuel consumption

Fuel amount	Daily	Annual
	$t.10^3$	$t.10^3$
Fuel consumed due to friction	11.185	3020.029
Fuel consumed due to main engine operation	188.407	50869.780

4.2.9 Simulation run 9

Table 4.41 Simulation 9 input parameters

Simulation input parameters	
Fleet fraction under slow steaming conditions	100%
Service speed reduction	20%
Fleet fraction at full load	70%
Fleet fraction at full ballast	20%
Fleet fraction at partial load	10%
Position of LCF amidships by stern	2%
Trim angle of vessel	0
Number of intermediate bearings	1
Shafting oil dynamic viscosity Pa	0.3

Table 4.42 Simulation 9 frictional losses

Fleet energy loss	Daily		Annual	
	GWh	TJ	GWh	TJ
Total friction	64.303	231.490	17361.74	62502.26
Engine friction	62.480	224.929	16869.640	60730.710
Shafting friction	1.823	6.561	472.097	1771.549

Table 4.43 Simulation 9 shafting system bearing frictional losses

Fleet energy loss	Daily		Annual	
	GWh	TJ	GWh	TJ
Aft stern tube bearing	1.095	3.941	295.538	1063.936
Forward stern tube bearing	0.305	1.099	82.419	296.710
Intermediate bearing	0.423	1.522	114.140	410.904

Table 4.44Simulation 9 main engine components frictional losses

Fleet energy loss	Daily		Annual	
	GWh	TJ	GWh	TJ
Guide shoe	19.369	69.728	5229.589	18826.52
Piston	16.245	58.481	4386.107	15789.97
Main bearing	14.370	51.734	3880.018	13968.06
Connecting rod	6.248	22.493	1686.964	6073.071
Stuffing box	3.124	11.246	843.482	3036.536
Thrust bearing	3.124	11.246	843.482	3036.536

Table 4.45 Simulation 9 fuel consumption

Fuel amount	Daily	Annual
	$t.10^3$	$t.10^3$
Fuel consumed due to friction	11.115	3000.915
Fuel consumed due to main engine operation	234.628	33075

4.3 Simulation results

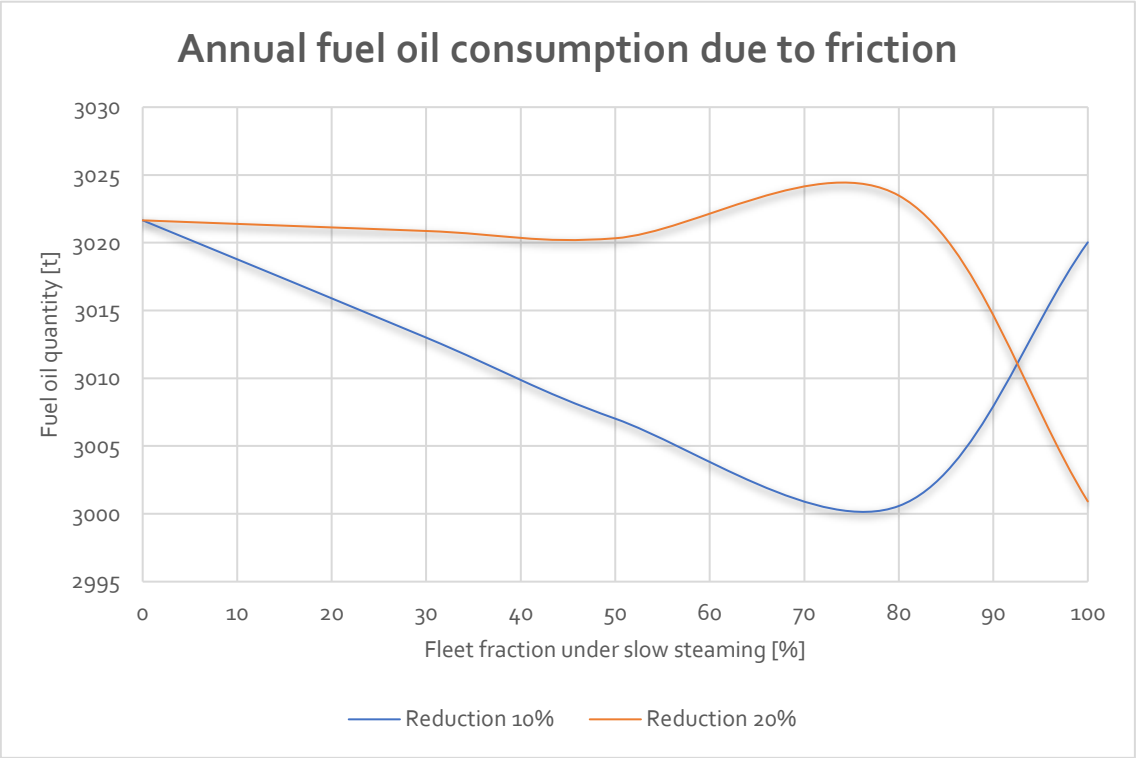

Figure 4.1 Annual fuel consumption due to friction

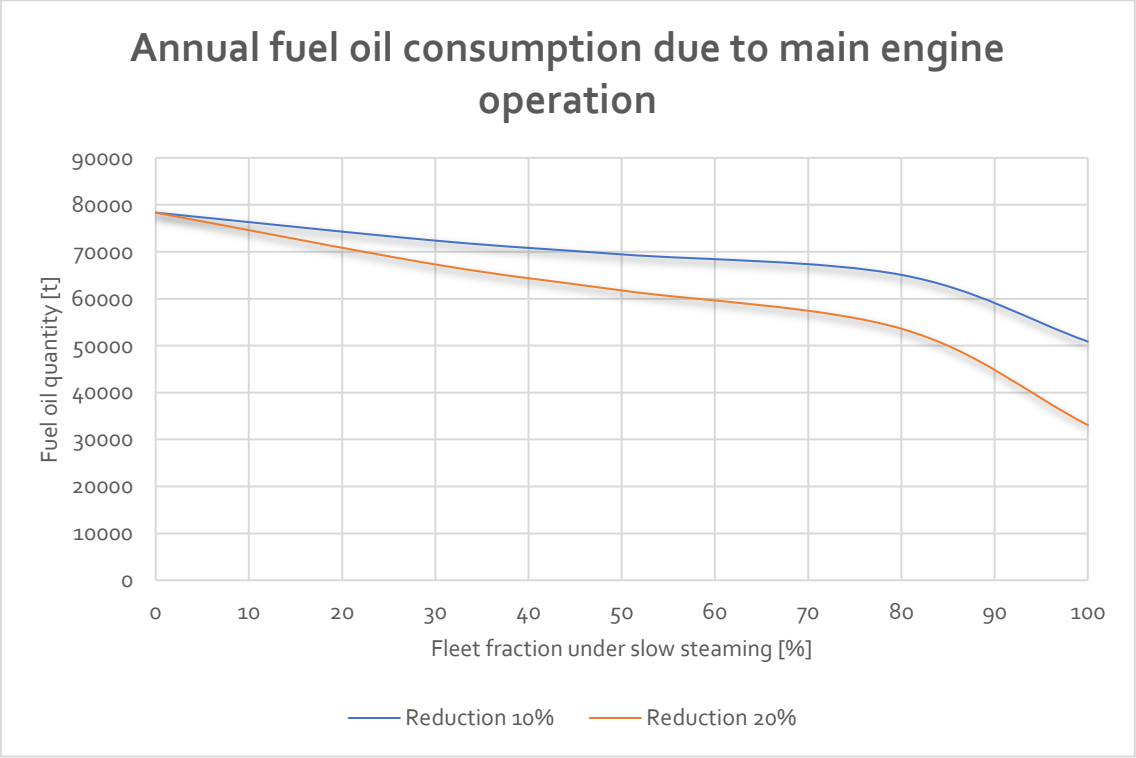

Figure 4.2 Annual fuel consumption due to main engine operation

Friction fuel consumption depends both on the magnitude of speed reduction and the fleet fraction that applies slow steaming operation. There is a limit in speed reduction, imposed by the operation of the main engine, so crankshaft speed cannot be reduced boundlessly. For simplicity, in this study, 10% and 20% service speed reduction were considered.

From the above figures, consumption due to friction losses are minimized when the fraction of global fleet applying slow steaming strategies ranges between 50-80%. Both speed reduction cases attribute in the same manner. By increasing fleet fraction operating under slow steaming, fuel consumption due to operation of main engine is reduced. For both cases, fuel consumption is minimized when the total fleet reduces speed.

By comparing these two curves, for slow steaming operation, some key points are concluded:

- For the case of speed reduction 10%, fuel consumption is minimum when the fraction of fleet applying slow steaming ranges between 70-80%.
- For the case of speed reduction 20%, fuel consumption is minimum when the total fraction of fleet applying slow steaming.
- If no vessel applies slow steaming operation, the annual consumption of fuel, both due to friction and due to main engine operation are increased.
- In economic terms, the study proposes that, in order to reduce the amount of fuel consumed due to friction from main engine operation, the 80% of the bulk carrier fleet should operate under slow steaming conditions.

However, these key points need to be further more investigated, since:

- The maximum increase in resistance was considered 25%. Larger values would lead to different engine installations and therefore, different specific oil consumptions and frictional losses.
- The maximum service resistance was no more than 15 knots, according to MAN technical papers [23]**.** Higher speeds lead to larger propulsion installations and therefore again, different oil consumptions and frictional losses.
- The slow steaming model was regarded as a fraction of the bulk carrier fleet reducing maximum speed by 10 or 20%. A more complex slow steaming model may lead to significantly different results, since the reduction processes differs among vessels (since turbocharger operation and shafting resonance frequencies are not the same for each vessel).
- Vessels were considered to burn Heavy fuel oil. Different fuel, which implies different lower calorific value affects the specific fuel oil consumption; thus, energy lost.
- 270 days of main engine operation were considered and the annual results were the product of a certain voyage times the number of these days. So annual results were produced from a certain timeframe, integrated in an annual period. Different results may occur, if annual results were the integration of different timeframes.
- Friction losses were calculated based on the selected random variables regarding added resistance, draft and speed. By changing the ranges of these variables, friction losses would differ and as a consequence, annual amount of energy consumed.

Summarization of results:

- Annual shafting friction losses ranged between 1771.450 to 1771.670 **TJ**
- Annual engine friction losses ranged between: 60857.06 to 61306.20 **TJ**
- Annual total friction losses ranged between: 62628.509 to 63077.909 **TJ**
- Annual stern tube aft bearing friction losses ranged between: 1063.876 to 1064.005 **TJ**
- Annual stern tube forward bearing friction losses ranged between: 296.693 to 296.730 **TJ**
- Annual intermediate bearing friction losses ranged between: 410.,881 to 410.931 **TJ**
- Annual guide shoe friction losses ranged between: 18865.69 to 19004.940 **TJ**

- Annual piston friction losses ranged between: 15822.840 to 15939.624 **TJ**
- Annual main bearing friction losses ranged between: 13997.124 to 14100.436 **TJ**
- Annual connecting rod friction losses ranged between: 6085.706 to 6130.625 **TJ**
- Annual stuffing box and thrust bearing friction losses, each ranged between: 3042.853 to 3065.312 **TJ**
- Annual amount of fuel consumed due to friction, ranged between: 3000.578 to 3023.478 thousand tones.

4.4 Comparison of energy consumption between parametric study and global fleet study

From the global fleet study, among 10347 ships, 97953.3 **TJ** of energy were lost due to friction in 270 days. By subtracting a 30% factor (which applies to the number of vessels not included in the simulations due to the lack of the necessary criteria), the total amount energy lost is 68567.8 **TJ**. On average, 7921 ships from the fleet-scale simulations account for 62853.2 **TJ**. The difference between the two studies is of the order of 9.1%. Since the parametric study is based on 100 vessels of fixed resistance, draft and speed conditions and the fleet-scale study is the integration of a timeframe of 7921 ships, the difference of 9.1% is quite reasonable.

In the following figure, the regression model suggested in paragraph 3.2.3, is compared to the measurements of the calculation procedure.

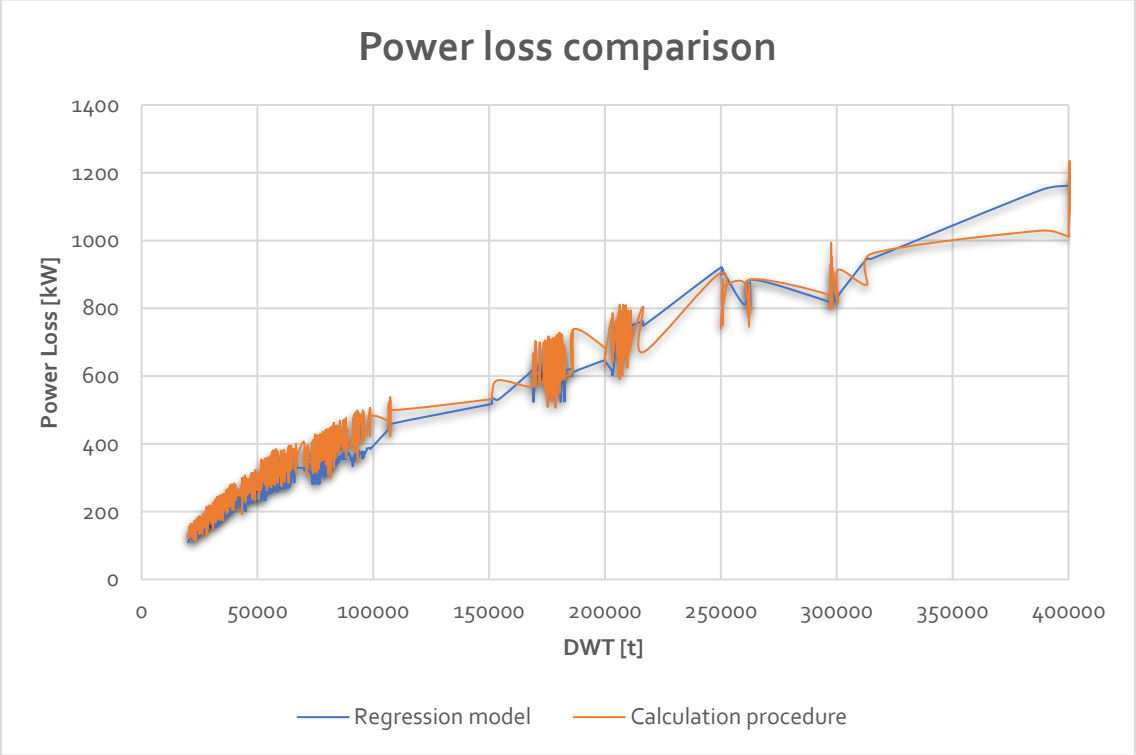

Figure 4.3 Regression model comparison to calculation procedure

5.Conclusions and future work

5.1 Conclusions

In the present study, the annual energy losses and fuel oil consumption due to friction in the propulsion system of the global bulk carrier fleet have been investigated. At first, empirical relations, formulae and methods have been reviewed in order to calculate all geometrical, hydrodynamic and mechanical parameters of each vessel of the fleet. To this end, proper software has been developed, which performs all the necessary calculations per vessel. The SeaWeb database has been used as the main source to determine the population of the worlds' bulk carrier fleet. To illustrate all the calculation steps, a single vessel example has been thoroughly analyzed and presented.

Next, a parametric study of frictional losses as a function of changing vessel size (dwt) has been performed. For each bulk carrier class, frictional losses were calculated for three cases of added resistance (clean hull, 50% fouled hull and 100% fouled hull), three cases of draft (summer load, partially laden 50% and full ballast) and two service speed conditions (maximum service speed and 20% reduced speed). A regression model has been extrapolated, based on the results of these scenarios, combining friction power loss to certain geometrical and propulsion parameters of a bulk carrier vessel.

Finally, nine simulations were performed on 10347 bulk carriers, calculating the friction power loss and the amount of fuel consumed due to friction annually, by setting random operational main engine points. The parameters changed in these simulations were the bulk carrier fleet fraction under slow steaming operation and the magnitude of vessel speed reduction (10% or 20%). The draft condition of these vessels was randomly chosen and the maximum total resistance increase that a ship could have, was assumed to be 25% of that corresponding to the case of clean vessel hull. The fuel consumed due to friction was calculated for each vessel and summarized over 270 days per year.

Specifically:

- Friction losses both at the shafting system and at the engine, as a quantity increase by vessel size, added resistance due to hull fouling and weather adverse conditions, increase of service speed and by decrease of vessel draft.
- As a percentage of power, friction behavior is the opposite of the quantitative case. This is explained by the fact that, as the engine load drops, mean effective pressure and mean friction pressure decrease in an uneven manner; with the effective pressure reduction being more significant.
- Engine losses were found varying between 4-6% of the operational brake power, an estimate that is in agreement with the existing literature.
- Shafting friction losses were found to receive values of the order of 0.1-0.25% of the operational brake power. This result implies that in literature, shafting friction losses are overestimated since they are usually considered to be 0.5-2% of the operational brake power.
- Frictional losses also depend on the geometrical characteristics of the ship (L, B, D), in addition to the above-mentioned parameters. Shafting weight, brake power and revolutions of the propeller affect the friction power loss.
- The most energy consuming bulk carrier class, in terms of friction, is the Capesize class followed by the Panamax class. Less losses occur at Handymax vessels. VLBCs and Handysize vessel seem to be the more efficient classes of the bulk carrier fleet, regarding their level of losses, size and vessel number.
- A regression model of estimation of power loss due to friction in main engine, line and propeller bearings was suggested. This model can be used in the preliminary stage of design

of a bulk carrier, based on the knowledge of principal vessel dimensions and engine operating point. The accuracy of the model was estimated 0.23%.

- Annually, on average, 62602 TJ of energy are consumed due to friction in the main engine components, bearings of the shafting system and propeller shaft bearings.
- Based on the above figure, annually, on average 3 million tons of fuel are consumed due to friction.
- The effect of slow steaming strategy varies according to the fraction of fleet applying, the amount of speed cut down and the engine load.
- The annual amount of fuel consumed due to friction decreases when slow-steaming operation is applied. By averaging all possible cases, 1.6 million tons of fuel are consumed due to friction annually.
- The annual amount of fuel consumed due to operation of main engine, decreases as more and more vessels apply slow steaming strategy. As anticipated, this is affected by the number of vessels of each bulk carrier class, since larger vessel sizes, demand more power thus increasing fuel oil consumption.
- However, conclusions or a universal model of predicting the effect of slow steaming in the global economy and the environment cannot be derived, since more simulations are needed. The complexity of the problem depends not only on the number of vessels applying this strategy, but also on the draft and hull condition each vessel operates under. In addition, no conclusion can be objective if other vessel types (tankers and containerships) are included in the calculation procedure. Another operating profile should be adopted if these vessels are included.
- Each vessel voyage scenario was based on three random variables, regarding draft, hull condition and vessel service speed. If these variables' margins were changed, friction losses would differ and so would annual quantity of fuel have been consumed.
- As mentioned, friction loss is not proportional to the engine load, and, as the latter is reduced, mean effective pressure drops in a more intensive manner than friction pressure loss. In this study, friction losses were estimated with the use of empirical relations. If a more sophisticated model, integrating pressure during an engine cycle, then the results might be affected in a different manner.

5.2 Future work

As a result of this work/thesis the following case studies can be investigated:

- Energy consumption due to friction in:
  - Tankers
  - Containerships
  - Passenger and Cruise vessels.
- A study on a more complex slow steaming model applied to the global fleet in order to better understand the benefit of this strategy.
- Evaluation of energy losses from auxiliary engines and machinery.
- Investigation of the effect of applying different propulsion solutions (for instance electric propulsion) and energy-saving systems.
- Investigation of an expanded model to calculate friction losses in all vessel types.
- Conduct simulations for the implementation of different energy consumption reduction strategies, by application of various technologies to the global fleet, and investigate the effect of each strategy on the shipping industry by evaluation of the market and freight rate changes.

Bibliography

1. Holmberg K, Andersson P, Erdemir A, (2011), Global energy consumption due to friction in passenger cars
2. Holmberg K, Andersson P, Erdemir A, Nylund N, Makela K, (2014), Global energy consumption due to friction in trucks and buses
3. Holmberg K, Erdemir A, (2017), Influence of tribology on global energy consumption, costs and emissions
4. Anders V, Peder K, (2003), Measurement and calculation of frictional loss in large two-stroke engines
5. Ciulli E, A review of internal combustion engine losses, part 2: studies for global evaluations
6. Ρακόπουλος Κ, Μηχανές εσωτερικής καύσης 1
7. Livanos G, Kyrtatos N, Friction model of a marine Diesel engine piston assembly
8. Rakopoulos C, Giakoumis E, Prediction of friction development during transient Diesel engine operation using a detailed model
9. Takata R, (2001) Effects of lubricant viscosity and surface texturing on ring pack performance in internal combustion engine.
10. Koukoulopoulos E, (2014), Software development for the solution of the hydrodynamic lubrication problems in piston rings of two-stroke marine Diesel engines
11. Delprete C, Razavykia A, (2017), Piston ring/liner lubrication and tribological performance evaluation: a review
12. Clausen N, Marine Diesel Engines-How efficient can they be?
13. Mrzljak V, (2018), Mean pressure of mechanical losses equation for marine slow speed two stroke Diesel engine
14. Petrovsky N, Marine internal combustion engines
15. Safar Z, Energy loss due to misalignment of journal bearings
16. Vlachos O, Effects of hull deformations, bearing foundation stiffness and oil film thickness on the shaft alignment characteristics of VLCC vessels
17. Siamantas S, (2019), Elastic Shaft Alignment of a Container Vessel
18. Khonsari, Booser, (2008), Applied Tribology-Bearing design and lubrication
19. Ιωαννίδης Ι, (1996), Ναυτικές μηχανές, τεύχος 1
20. Φραγκόπουλος Χ, (2008), Μέθοδος προμελέτης ναυτικών συστημάτων με κινητήρες Diesel
21. Man, technical papers, (2014), Waste heat recovery system for reduction of fuel consumption, emissions and EEDI
22. Man, technical papers, (2013/2018), Basic principles of ship propulsion
23. Man, technical papers, (2019), Propulsion trends in bulk carriers
24. Papanikolaou A, (2009), Μελέτη πλοίου, μεθοδολογίες προμελέτης, τεύχος 1
25. Papanikolaou A, (2009), Μελέτη πλοίου, μεθοδολογίες προμελέτης, τεύχος 2
26. Papanikolaou A, Anastasopoulos K, (2007), Μελέτη πλοίου, συλλογή βοηθημάτων
27. Γεωργάκης Π, (2012), Εκτίμηση παραμέτρων σχεδιασμού και λειτουργίας μηχανοστασίου σύγρονων πλοίων μεταφοράς φορτίου χύδην (bulk carriers) και δεξαμενοπλοίων (tanker)
28. Schneekluth, (1998), Ship design for efficiency and economy
29. Carlton J, (2012), Marine propellers and propulsion
30. Volker B, Practical ship hydrodynamics
31. Misra S, Design principles of ships and marine structures
32. Molland A, (2011), Ship resistance and propulsion
33. Kristensen H, (2013), Prediction of resistance and propulsion power of ships

34. Πολίτης Γ, (2018), Αντίσταση και πρόωση πλοίου
35. Christopoulos N, Lyridis D, Mitrou P, Papaleonidas C, Evangelou P, (2019), Quantitative analysis of the world merchant fleet greenhouse gas emission profile
36. Iosifidi M, (2020), Study of exhaust gas emissions from conventional merchant vessels
37. MAN, technical papers (2018)-Marine engine IMO TIER II and TIER III program
38. GL (2008) Main shafting Section 4

List of tables

List of figures

Nomenclature

A_E/A_O	Expanded area ratio	-
A_{bk}	Bilge keel wetted surface	[m²]
A_{rud}	Rudder wetted surface	[m²]
b	Engine Bore	[m]
B	Breadth	[m]
C	Bearing radial clearance	[m]
C_B	Block coefficient	-
C_M	Midship coefficient	-
C_P	Prismatic coefficient	-
C_{WP}	Waterplane area coefficient	-
d_b	Double bottom height	[m]
d	Shaft diameter	[m]
d_f	Shaft flange diameter	[m]
D	Depth	[m]
Db	Bearing diameter	[m]
D_{en}	Engine bore	[m]
D_p	Propeller diameter	[m]
DWT	Deadweight of vessel	[t]
F_N	Froude number	-
h_p	Port depth	[m]
l	Shaft length	[m]
L	Length between perpendiculars	[m]
L_b	Bearing length	[m]
LCB	Longitudinal center of buoyancy	[m]
LCF	Longitudinal center of floaticity	[m]
LS	Lightship weight	[t]
J_A	Advance coefficient	-
n_h	Hull efficiency	-
n_d	Quasi propulsive coefficient	-
n_o	Open water propeller efficiency	-
n_p	Propulsion efficiency	-
n_R	Relative rotative efficiency	-
N	Propeller revolutions	[Rpm]
p_e (mep)	Mean effective pressure	[Pa]
p_i	Mean indicative pressure	[Pa]
p_f	Friction mean effective pressure	[Pa]
p_o	Total static pressure at the shaft center line	[Pa]

p_v	Water vapor pressure	[Pa]
P_B	Brake horse power	[W]
P_D	Dead horse power	[W]
P_E	Effective power	[W]
P_S	Shaft horse power	[W]
r_{cargo}	Loading condition random variable	%
r_{fl}	Fouling resistance margin	%
r_{period}	Period between drydocks	%
r_{prop}	Propeller diameter random value	%
r_{rd}	Added resistance for regression model	%
r_{sl}	Fleet slow speed fraction	%
r_w	Weather resistance margin	%
R	Resistance	[N]
R_b	Bearing radius	[m]
R_a	Correlation resistance	[N]
R_{air}	Air resistance	[N]
R_f	Friction resistance	[N]
R_n	Reynolds number	-
R_{vp}	Viscous pressure resistance	[N]
R_t	Total resistance	[N]
R_w	Wave-making resistance	[N]
s	Engine stroke	[m]
S	Sommerfeld Number	-
S_{app}	Appendages wetted surface	[m²]
S_{en}	Engine stroke	[m]
S_{hull}	Naked hull wetted surface	[m²]
S_{tot}	Total wetted surface	[m²]
t	Thrust deduction	-
T	Draft	[m]
T_A	Aft draft	[m]
T_F	Fore draft	[m]
T_H	Thrust force	[m]
T_M	Draft amidships	[m]
V_S	Slow steaming speed	[kn]
V	Service speed	[kn]
w	Wake field deduction	-
w_{int}, w_{pr}, w_f	Intermediate shaft weight, propeller shaft weight, flanges weights	[kg]
W_{pr}	Propeller weight (in water)	[kg]

z	Propeller blade number	-
Z_{cyl}	Engine cylinder number	-
Δ	Displacement of vessel	[t]
μ	Shafting oil dynamic viscosity	[Pa.s]
ν	Water kinematic viscosity	[m^2/s]
ρ	Water density	[kg/m^3]
ρ_α	Air density	[kg/m^3]
ρ_{mb}	Manganese bronze density	[kg/m^3]
ρ_s	Steel density	[kg/m^3]
$\rho_{s,st}$	Stainless steel density	[kg/m^3]
$\sigma_{Y,st}$	Steel yield stress	[Mpa]